TAMPEREEN TEKNILLINEN YLIOPISTO
TAMPERE UNIVERSITY OF TECHNOLOGY

Essi Sariola-Leikas

Organic Chromophores in Self-Assembled Monolayers and Supramolecular Arrays

Julkaisu 1334 • Publication 1334

Tampere 2015

Tampereen teknillinen yliopisto. Julkaisu 1334
Tampere University of Technology. Publication 1334

Essi Sariola-Leikas

Organic Chromophores in Self-Assembled Monolayers and Supramolecular Arrays

Thesis for the degree of Doctor of Science in Technology to be presented with due permission for public examination and criticism in Festia Building, Auditorium Pieni Sali 1, at Tampere University of Technology, on the 20th of November 2015, at 12 noon.

Tampereen teknillinen yliopisto - Tampere University of Technology
Tampere 2015

ISBN 978-952-15-3600-7 (printed)
ISBN 978-952-15-3623-6 (PDF)
ISSN 1459-2045

Abstract

Large aromatic chromophores, e.g. phthalocyanines or perylene derivatives are widely used in modern photonic applications. For these systems, well-organized films of the chromophores are very important. One of the ways to ensure the order on molecular level is to bind the organic dyes covalently to a solid substrate with a suitable anchor group. Expanding the concept, multilayered supramolecular assemblies can be built on surfaces as well.

In the present Thesis various chromophores with a capability to anchor onto a solid surface were prepared. Synthesized molecules were porphyrins, phthalocyanines, and perylene mono- and diimides with different substituents. The anchor-surface pairs were of several types, and the chromophores were attached to a surface by one- or two-step methods.

Two of the perylene monoimide derivatives were found to be a perfect basement for construction of multilayered films. Using a metal-ligand interaction it was possible to prepare stable double layers, as well ten molecules thick stable deeply colored multi-layer films. The developed approach is versatile and will allow in future to expand the capabilities of molecular film architecture.

Preface

The research work reported in this Thesis has been carried out in the Department of Chemistry and Bioengineering at Tampere University of Technology during years 2009-2015. The Graduate School of Tampere University of Technology and the Academy of Finland are gratefully acknowledged for financial support.

First of all I want to express my gratitude to my supervisor Prof. Helge Lemmetyinen for giving me the opportunity to work in his excellent research group. I appreciate all his support during the years, also when I became a mom. Combining work and family life was not easy, but as Helge says: children are more important than science. My deepest compliment goes to my other supervisor Dr. Alexander Efimov. We have always been a good twosome and our teamwork has been fluent and pleasant. I hope that our growing friendship will continue. To Prof. Nikolai Tkachenko I am grateful for all his help and guidance with spectroscopic issues. I also want to express my appreciation to all the co-authors of the publications.

For the pleasant work atmosphere I am grateful to all my colleagues in the Supramolecular Photochemistry group and to people at the Department. Especially, I want to thank the people in our synthetic Team2 during the years: Dr. Kalle Lintinen, Dr. Somnath Dey, Dr. Rajeev Dubey, Dr. Jenni Ranta, Dr. Zafar Ahmed, Dr. Elena Efimova and Mr. Lijo George. My office mates, Dr. Marja Niemi, Dr. Anne Kotiaho, Dr. Paola Vivo and Mrs. Hanna Hakola, I owe most; all nice moments, conversations and hard times, not forgetting ongoing friendships. My long-term friends in and outside of the work, Dr. Kimmo Kaunisto and Dr. Riikka Lahtinen, I am also thankful.

I thank my family, mom, dad, my sister Eeva and grandparents, my friends, especially my diamond girls ♥. You have been great help and support during these years. My dear husband, Pekka, receive the greatest compliments. I love you! The love of my life, my children Enna and Peetu, now we have a new book for bedtime stories!

I dedicate this work to the memory of my dear grandfather Tapani. I miss you.

Tampere, September 2015

Essi Sariola-Leikas

Contents

List of Symbols and Abbreviations

A	absorbance
ALD	atomic layer deposition
AZO	aluminum doped zinc oxide
COSY	correlation spectroscopy
DBN	1,5-diazabicyclo[4.3.0]non-5-ene
DBU	1,8-diazabicyclo[5.4.0]undec-7-ene
DCC	1,3-dicyclohexylcarbodiimide
DCM	dichloromethane
DMAP	4-dimethylaminopyridine
DMF	dimethylformamide
DMSO	dimethylsulfoxide
dppf	1,1′-bis(diphenylphosphanyl)ferrocene
DSSC	dye-sensitized solar cell
ESI-TOF MS	electrospray ionization time-of-flight mass spectrometer
gHSQC	gradient-selected heteronuclear single quantum coherence spectroscopy
gHMBC	gradient-selected heteronuclear multiple bond correlation spectroscopy
HPLC	high-performance liquid chromatography
ITO	indium tin oxide
KSAc	potassium thioacetate
mma	mean molecular area

NMR	nuclear magnetic resonance
OTf	trifuoromethane sulfonate
Pc	phthalocyanine
PcM	phthalocyanine metal complex
PDI	perylene-3,4,9,10-tetracarboxylic acid diimide
PFP	pentafluorophenyl
PMI	perylene-3,4,9,10-tetracarboxylic acid-3,4-monoimide
ppm	parts per million
PTCDA	perylene-3,4,9,10-tetracarboxylic dianhydride
p-TsOH	*para*-toluenesulfonic acid
SAM	self-assembled monolayer
TBACl	tetrabutylammonium chloride
TFA	trifluoroacetic acid
THF	tetrahydrofuran
TLC	thin layer chromatography
TMS	tetramethylsilane
TPP	tetraphenylporphyrin
tpy	2,2':6'2''-terpyridine
ε	molar extinction coefficient (molar absorptivity)

List of Publications

The Thesis is based on the work contained in the following publications, which will hereafter be referred to by their Roman numerals:

I. **Mono-, bis- and tetrahydroxy phthalocyanines as building blocks for monomolecular layer assemblies**
Essi Sariola, Anne Kotiaho, Nikolai V. Tkachenko, Helge Lemmetyinen and Alexander Efimov, *J. Porphyrins Phthalocyanines* **2010**, *14*, 397-411.

II. **Synthesis of porphyrinoids with silane anchors and their covalent self-assembling and metallation on solid surface**
Essi Sariola-Leikas, Matti Hietala, Alexey Veselov, Oleg Okhotnikov, Sergei L. Semjonov, Nikolai V. Tkachenko, Helge Lemmetyinen and Alexander Efimov, *J. Colloid Interface Sci.* **2012**, *369*, 58-70.

III. **Supramolecular assemblies of bay-substituted perylene diimides in solution and on a solid substrate**
Essi Sariola-Leikas, Marja Niemi, Helge Lemmetyinen and Alexander Efimov, *Org. Biomol. Chem.* **2013**, *11*, 6397-6406.

IV. **Color bricks: building of highly organized and strongly absorbing multi-component arrays of terpyridyl-perylenes on metal oxide surfaces**
Essi Sariola-Leikas, Zafar Ahmed, Paola Vivo, Anniina Ojanperä, Kimmo Lahtonen, Jesse Saari, Mika Valden, Helge Lemmetyinen and Alexander Efimov, *Chem. Eur. J.*, *submitted*

Author's contribution

Strong teamwork has been an essential part of all the publications. Essi Sariola-Leikas (Sariola) has been the corresponding author in all the publications. She planned and performed most of the experimental work. She carried out the syntheses and analyses of substances. She developed methods for SAM deposition, and measured all the steady state measurements. All publications were written by author and discussed in collaboration with the co-authors.

In publication II Dr. A. Veselov performed all solid-core photonic crystal fiber studies and fluorescence lifetime microscope measurements. Dr. M. Niemi carried out the time-correlated single photon counting measurements and analyzed the results in publication III. In publication IV Dr. P. Vivo carried out all the solar cell studies and Dr. K. Lahtonen did the ALD experiments.

1 Introduction

Colored organic substances were used for centuries as pigments due to their strong and deep colors.[1] Nowadays these compounds are commonly employed for solar energy conversion[2] and various optical applications like organic light-emitting diodes[3]. Among others, the choice of chromophores includes porphyrins, phthalocyanines, and perylene derivatives, all of these being highly conjugated macromolecules. Porphyrins and phthalocyanines are structural analogues of natural chlorophyll pigments and because of that are largely studied in artificial photosynthetic systems.[4,5,6]

Most of these advanced applications need chromophores as uniform and well-organized films. One solution for manufacturing those is a covalent arrangement of the chromophores on surfaces in a controlled manner. The method is called “self-assembling” when molecules are spontaneously binding as regular structure.[7] To ensure the formation of proper self-assembled monolayers (SAMs), chromophores need to have an appropriate anchor moiety, which binds to the surface. The choice of such a “hook” is essential, since different surfaces need different anchors.[8,9]

Monolayer assemblies of functional molecules are important working units indeed. However, having a possibility to cover a base layer with an array of subsequent well-organized layers thus making a structurally-controlled thicker film would be a great advantage. Such a deposition requires an intermolecular lock, which can hold the two successive substances together thus allowing a layer-over-layer deposition, ideally as many times as needed. A good example of such a lock is the terpyridine moiety, which has strong chelating ability to a variety of transition metal ions, and can form linear ligand-metal-ligand arrangements.[10] In the field of supramolecular chemistry, the terpyridine (tpy) unit is one of the most versatile ligand for building supramolecular assemblies. The ligand is highly used in polymer chemistry, but its application in surface-bound structures is limited.[11] Nevertheless, a set of various geometrically matching chromophores decorated with a tpy substituent as the arrays component would allow to build multilayer arrays and films with many attractive properties.[12]

In the present study, we have undertaken an attempt to elaborate the methods and systematize our knowledge about building of different surface-anchor-chromophore-lock-chromophore combinations. We were aiming to: (1) synthesize various novel photo-active compounds, which can be further decorated with functional groups; (2) modify the chromophores to have anchor moieties and intermolecular locks at different positions of their macrocores; (3) find proper combinations of anchored chromophores and substrate surfaces to bind them to; (4) study the

possibilities to assemble chromophores into surface-bonded arrays, and (5) build a highly ordered, stable and reproducible, deeply colored multilayered film in a well controlled manner of molecule-by-molecule deposition.

As an ultimate goal, we were striving to create a toolbox of “color bricks” – substances, from which a desirable combination of absorption bands, oxidation potentials, and interchromophore distances with degrees of interactions between the substrates and light-capturing units could be deliberately built up and would be tuned according specific application. Certainly, it was expected that only a few possibilities would remain at the end of the study, thus the initial choice of substances and fragments would be as broad as possible.

On the following pages the results of the present work are presented. The Thesis compiles the materials from the three articles published (I, II, III), and the one recently submitted for publication (IV) in the following order:

- Syntheses of the compounds are presented in Chapter 5.1. Three different kinds of chromophore families, phthalocyanines, porhyrins, and perylene imides, were synthesized and decorated with appropriate side substituents, anchors, and chelating linker groups.

- Assembling of mono- and multilayers is described in Chapter 5.2. The fabrication of monomolecular films by different surface chemistries is given in Chapter 5.2.1 and 5.2.2.

- Chapter 5.2.3 presents the most important observations of the Thesis. It describes the preparation of surface-bonded arrays of chromophores forming highly absorptive stable multilayer films by molecule-by-molecule deposition. To the best of our knowledge, the prepared multilayers are the only example of such structures having that high intensities and distinctive characters of their absorption profiles.

2 Background

Organic chromophores are widely used in pigment industry, catalysis, opto-electronics, flat-panel displays, and organic light-emitting diodes.[1,4,13] Future applications of these versatile molecules comprise, for example, organic solar cells, nanophotonics, and laser technology.[14,15,16] One of the key issues for such applications is a specific and controlled organization of the compounds on molecular level. One solution for that is a covalent self-assembly of the chromophores on the surfaces of semiconductors and electrodes. Clearly, the ability of molecules for self-organization is determined by the structure of the macrocore and by the side substituents. An intense research is going on in recent years on that topic, however, the synthetic approaches towards predictably self-assembled chromophores are still a challenging and demanding field.[4,13,17]

2.1 Chromophores

Chromophores are groupings in the molecule that are responsible for the dye's color. In a broad sense, the term is also used to name colored chemical compounds.[18] An example from nature known to everyone is a molecule called chlorophyll (Fig. 2.1). Chlorophyll is a green pigment present in all plants and can be found anywhere on Earth. Although chlorophyll has the most important role in natural systems and gives life to our planet, its use in artificial photosynthetic systems remains very limited (for many reasons, e.g. instability, difficult purification, etc.).[19] Thus, the structural analogues, like porphyrins and phthalocyanines, have been largely studied for that purpose. These chromophores are commonly used as industrial dyes, in anticancer therapy, nonlinear optics, catalysis, and as sensitizers in photovoltaic devices.[1,4,6,13]

2.1.1 Porphyrin

Porphyrins are present everywhere in nature. The porphine macrocycle can be found in systems such as hemoglobin, myoglobin, cytochromes, and cofactors in methanogenic bacteria. The remarkable stability of porphyrin and the wide distribution in nature have indicated to some researchers that porphyrins might be prebiotic. In view of their chemical and photophysical similarities to the hemes and chlorophylls, porphyrins can be considered as ideal molecules for the construction of photonic systems.[14,20] Figure 2.1 shows examples of natural compounds and porphyrin with its numbering system.

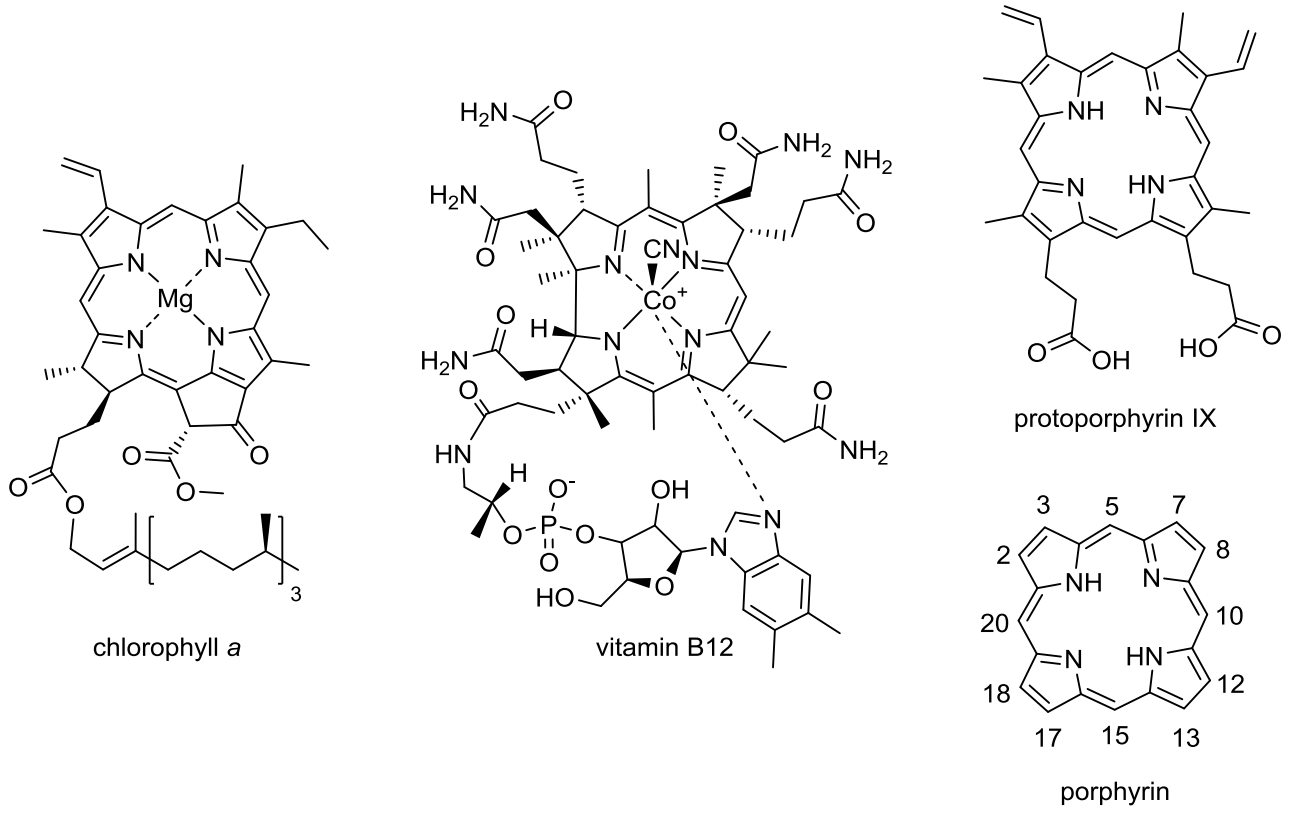

FIGURE 2.1 Structures of chlorophyll *a*, cyanocobalamin (vitamin B12), protoporphyrin IX, and porphyrin with its systematic numbering.

Porphyrins are highly conjugated macromolecules, which contain four pyrrole units linked together *via* methine bridges. Positions 2, 3, 7, 8, 12, 13, 17, and 18 on the ring are called β-positions and positions by numbers 5, 10, 15, and 20 are called *meso*-positions. During last few decades the most studied porphyrins are tetraphenylporphyrin (TPP) derivatives, which have four aryl groups at the *meso*-positions.[21,22]

2.1.1.1 Synthesis of *meso*-substituted porphyrins

A few tens of thousands of different porphyrins (48 000 according to Reaxys database, over 120 000 according to CAS index) have been synthesized or described so far. The basis of porphyrin chemistry has been created by Hans Fischer in the beginning of 20th century, and was based on synthesis of substituted pyrrols and their further cyclization into porphyrin macrocycles.[23] In 1935, Paul Rothemund reported a synthesis in which pyrrole and formaldehyde were used, and a porphine molecule was obtained (porphyrin containing only hydrogens as substituents) with 0.03 % yield.[24] Also *meso*-substituted tetraphenylporphyrin (TPP) was synthesized from benzaldehyde and pyrrole by Rothemund.[25] However, in Rothemund's synthesis the reaction conditions were harsh, temperature was high (90-155 °C) and the reaction time was long. Later Adler and Longo modified the reaction by heating at reflux benzaldehyde and pyrrole in propionic acid only for half an hour. Still that time yields were moderate, around 20 %, however the overall method was relatively simple and convenient.[26]

The reaction of pyrrole with benzaldehyde is reversible at room temperature and produces the thermodynamically favored porphyrinogen (**1**). Porphyrinogen needs to be oxidized into a stable porphyrin (**2**) (Fig. 2.2). These reactions were studied by Lindsey *et al.*[27] In 1984, Lindsey developed a two-step procedure, which included formation of intermediate **1**, followed by a treatment with an oxidant (2,3-dichloro-5,6-dicyanobenzoquinone or *p*-chloranil) to produce the porphyrin molecule. Practically, a solution of dry DCM was charged with benzaldehyde, pyrrole, and triethyl orthoacetate at equimolar concentrations under N_2. Boron trifluoride etherate was used as a catalyst. After one hour at room temperature in dark, the oxidant *p*-chloranil was added and the solution was heated at reflux for an hour.[21,27] With this method, TPP was obtained with up to 50 % yield after simple chromatographic purification.

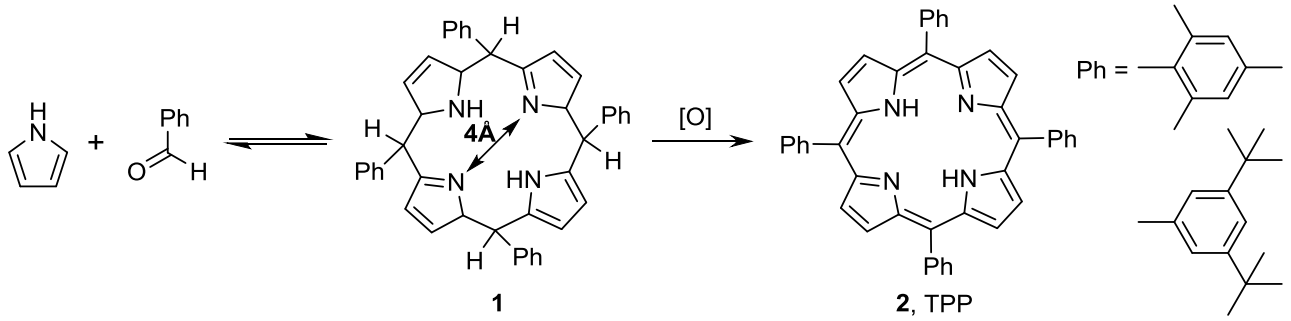

FIGURE 2.2 Procedure for synthesizing TPP by Lindsey *et al.*[27], and few other phenyl substituents, as example.

One can say that Lindsey's publication has opened the door for modern porphyrin chemistry. Formally cited about 1000 times, with a very rare exception, the Lindsey's method is used ever since researchers worldwide. The main advantage of this protocol is a huge number of sensitive or bulky groups, which can be introduced to porphyrins, inaccessible otherwise. For example, none of *tert*-butyl or mesityl substituted TPP can be made by Adler-Longo method.[28]

2.1.1.2 Coordination and optical properties

Porphyrins have a central cavity of sufficient size for various metal ions to accommodate. This cavity is approximately 4 Å wide by diagonal from nitrogen to nitrogen (Fig. 2.2).[29] Porphyrin molecules having just two imine hydrogens inside the cavity are known as free base porphyrins and when these are replaced with metal, structures are called metalloporphyrins.[21] In natural compounds, porphyrins always contain a chelated metal atom. For example hemoglobin and vitamin B_{12} (Fig. 2.1) contain iron and cobalt ions, respectively.[19]

Porphyrins are red by color and show a strong absorption in the visible region with a few distinct bands. The strong and sharp band around 400-430 nm is called the Soret band and several absorbance bands between 500 and 650 nm are known as the Q-bands. The photophysical as well as the redox properties of porphyrins can be altered readily by the choice of the metal center and the peripheral substituents.[21,30] Figure 2.3 presents absorption spectra of porphyrin and phthalocyanine compounds used in this study.

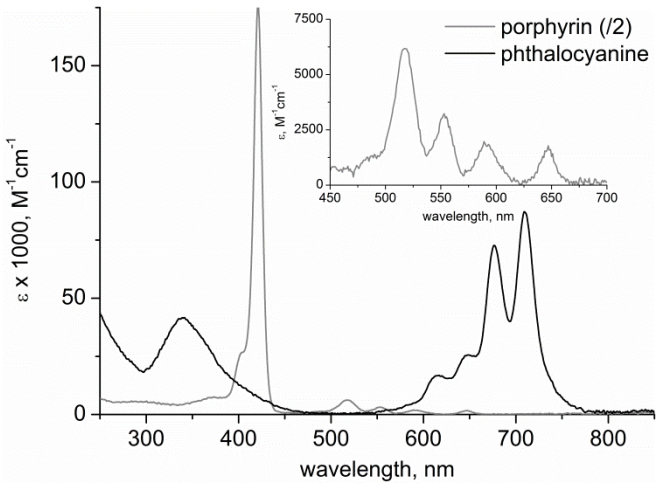

FIGURE 2.3 Absorption spectra in $CHCl_3$ for free base porphyrin and phthalocyanine [II]. The Q-band of the porphyrin spectrum is presented in the inset of the figure. The spectra are on molar absorptivity (***ε***) scale (porphyrin spectrum is divided by 2).

2.1.2 Phthalocyanine

Phthalocyanines (Pcs) are highly colored substances, broadly used as industrial dyes. Phthalocyanines are 40-membered, 18 π-electron aromatic macrocyclic molecules, whose π-electron system provides their unique physical properties. Pcs are composed of four isoindole units, which are linked together by aza bridges through 1,3-positions of isoindole.[31] The basic structure of Pc resembles that of tetrabenzoporphyrin and porphyrazine. Figure 2.4 presents the structures of porphyrin, tetrabenzoporphyrin, porphyrazine, and phthalocyanine, and the systematic numbering of the Pc substituents.

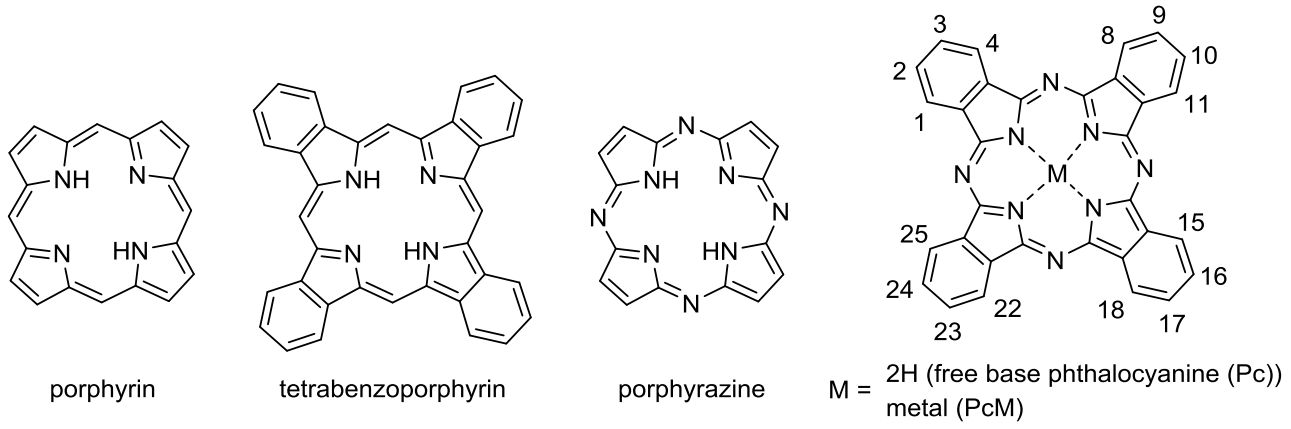

FIGURE 2.4 Structures of porphyrin, tetrabenzoporphyrin, porphyrazine, and phthalocyanine macrocycles. Numbers around phthalocyanine represents potential substitution sites of Pc.

Porphyrazines and phthalocyanines are purely synthetic compounds, and they are thermodynamically and chemically stable. In fact, Pcs are probably the most stable synthetic organic colorants.[18] The two hydrogen atoms in the center of phthalocyanine (free base Pc) have been replaced with more than 70 different elements, including virtually all the metals in the periodic table forming various types of metal phthalocyanines (PcM) (Fig. 2.4). Another way for chemical modification and changing the properties of phthalocyanine is to introduce different kinds of substituents onto the peripheral positions of phthalocyanine ring (positions 1-25 in Fig. 2.4).[13,31,32,33]

2.1.2.1 Methods of preparation

Phthalocyanines are commonly synthesized by a cyclotetramerization reaction in high-boiling solvents with phthalyl derivatives. In fact, phthalocyanines were accidentally discovered in the attempts of copper-catalyzed basic hydrolysis of phthalonitrile. Quite a large variety of monomeric precursors is used for the Pc preparation nowadays, namely phthalonitriles, phthalic anhydrides, phthalimides, 1,3-diiminoisoindolines, and phthalamides (Fig. 2.5). The precursors are mostly derivatives of phthalic acid. Usually the reactions are performed in non-aqueous solvents with high

boiling points at elevated temperatures in the presence of activators, catalysts, and/or promoters. The activators, such as 1,8-diazabicyclo[5.4.0]undec-7-ene (DBU) and 1,5-diazabicyclo[4.3.0]non-5-ene (DBN), are strong organic bases that act as proton acceptors.[4,34]

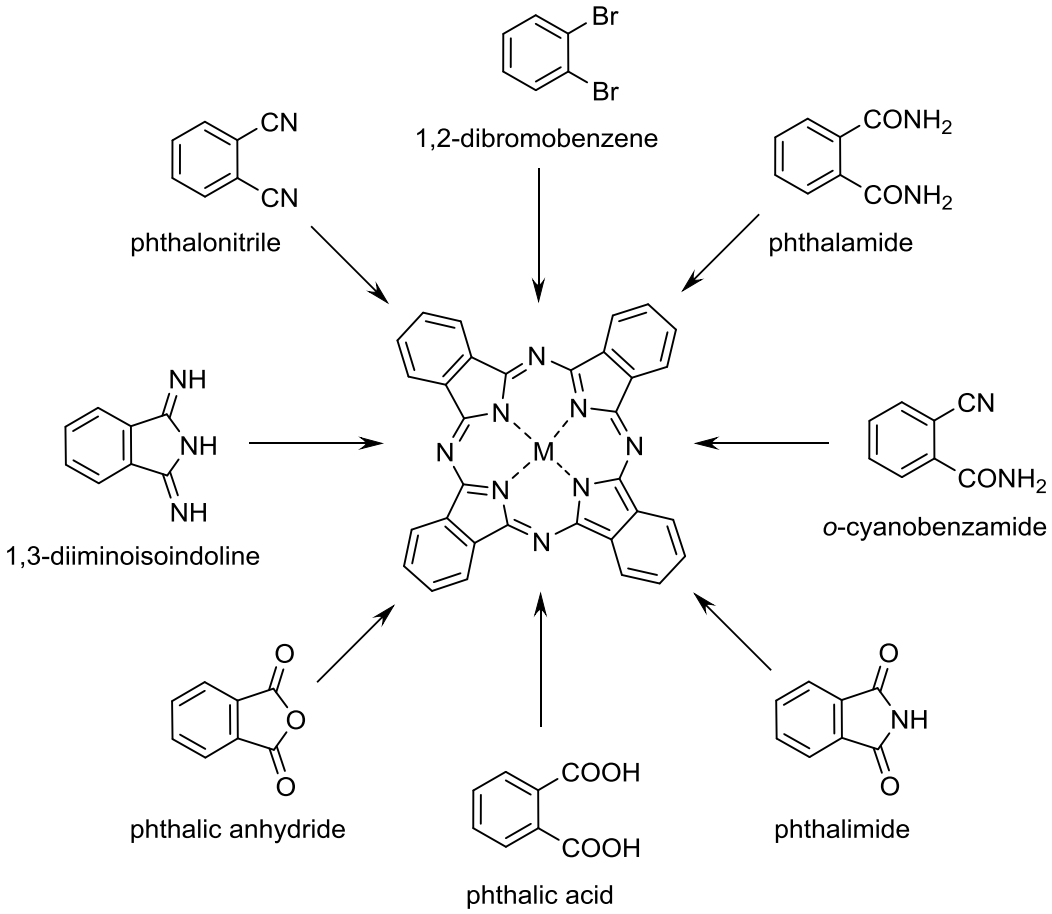

FIGURE 2.5 Main precursors of phthalocyanine.

The most studied starting materials for Pc syntheses are phthalonitriles and 1,3-diiminoisoindoline. However, these compounds are mainly used for research purposes because of their relatively high cost. In the dye industry, urea and phthalic anhydride, with molybdenum compounds as a catalyst and tetramethylurea as a promoter, are applied for the production of free base Pc and its metal complexes (mostly for PcCu).[34]

A tentative mechanism of phthalonitrile cyclization to phthalocyanine is presented in Figure 2.6.[35] In the reaction of phthalonitrile cyclization, an organic base perform a nucleophilic attack to the cyano group of phthalonitrile. The nucleophile ($Nucl^-$) is usually associated with a metal ion (M^+), which activates one of the cyano group (-CN) by coordinating with it. In the next step, a cyclization

reaction to an isoindoline derivative takes place, and these steps are repeated. Finally, the tetrameric intermediate undergoes a ring cyclization thus forming the phthalocyanine macrocycle.[1,18]

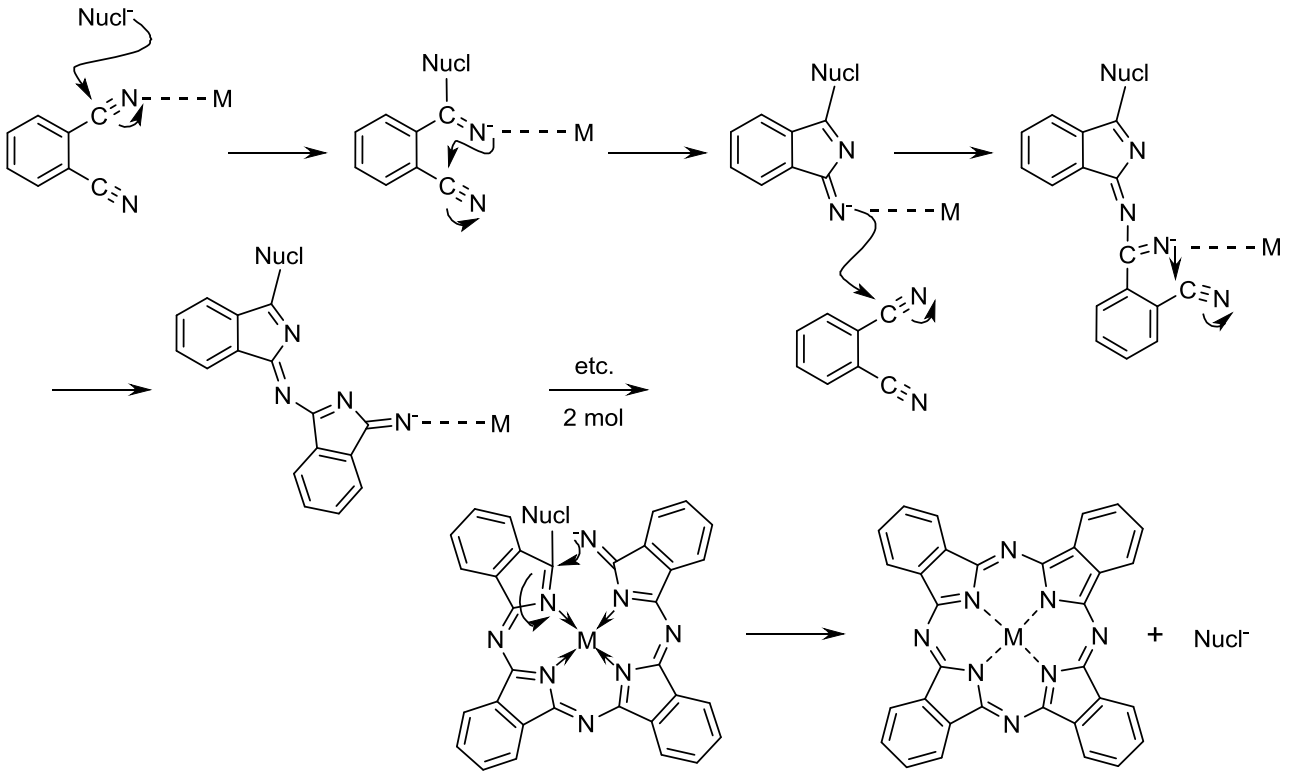

FIGURE 2.6 Proposed mechanism for phthalonitrile cyclotetramerization.

Free base phthalocyanine is easy to prepare from phthalonitrile using lithium alkoxide as a base. The method was first described by Oliver and Smith in 1987.[36] Lithium alkoxide induces cyclotetramerization of phthalonitrile (see Fig. 2.6, $Nucl^-$ = alkoxide anion). Usual procedure is to dissolve lithium metal shots in an alcohol by heating at reflux obtaining this way a lithium alkoxide solution. After addition of the precursor, lithium-metallated macrocycle (PcLi) is prepared by heating the solution for appropriate time. Upon acidic work-up (e.g. treatment with acetic acid), lithium ion in the central cavity of Pc is replaced by two protons.[37,38]

2.1.2.2 Modifications

Phthalocyanines are naturally rather insoluble or extremely insoluble, which makes modification of the macrocycle needed for practical use. A wide variety of substituents can be attached to the sixteen reactive sites on the four benzene units in the Pc macrocycle at the α- and β-positions (so called *phthalo*-positions, Fig. 2.7). When these substituents are bulky or long-chain hydrophobic moieties, the solubility of Pc in common organic solvents increases. Increasing solubility makes

purification and separation of crude products easier. Substitutions also prevent aggregation of the molecules, which is very common for Pcs.[39,40]

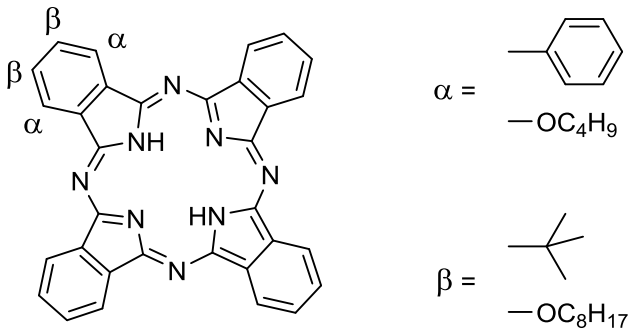

FIGURE 2.7 α- and β-positions of phthalocyanine and some examples of substituents.[39,40]

Modification in the Pc structure can be also made by adding a metal in the central cavity of the Pc core. Metal phthalocyanines can be directly synthesized from metals (or their salts) and a phthalic precursor in non-aqueous solvents. Phthalocyanine gives stable metal complexes for example with Fe, Cu, and Ni, and less stable complexes with Mg and Sb, according to metals resistance to eliminate from the product without destruction of the Pc structure.[34,39,40]

Unlike red porphyrins, Pcs are blue-green pigments, which strongly absorb light also in the visible wavelengths. Typical regions in their absorption are the Q-bands located at longer wavelengths 600-800 nm, and the Soret band at roughly 350 nm (see Fig. 2.3). Bands position and width varies depending on the peripheral substituents, their nature, amount and location, and also depending on the central metal atom in phthalocyanine. Usually, it is the Q-band, which is particularly sensitive to substitution and environment of the Pc macrocycle.[13,40]

The substituents can in principle be divided to electron withdrawing and electron donating groups. The electron withdrawing groups are for example carboxyl, fluorine, and sulfonyl, and electron releasing groups includes alkyl, alkoxy, and amino groups.[41] These groups have different effects on the optical properties of Pc when they are in the α- and β-positions. The general trend for β-substituted Pcs is that the electron withdrawing groups cause a shift of the Q-band to the red region. Nevertheless, usually substitution at the α-position in Pc leads to stronger effect in the absorption spectrum than in β-substituted Pcs.[39,40]

2.1.3 Perylene derivatives

Perylene-3,4,9,10-tetracarboxylic acid diimides (commonly called perylene diimides, PDIs) are stable and versatile organic chromophores.[42] They are known for over 100 years, when Kardos

found their synthetic method.[43] Highly fluorescent PDIs are widely used as dyes and pigments due to their outstanding chemical, thermal, and photochemical stability.[1,17]

The most common starting material to synthesize the perylene diimides is commercial perylene tetracarboxydianhydride PTCDA (Fig. 2.8). By simple imidization reactions with aliphatic or aromatic amines, PTCDA converts into perylene diimide derivatives. The solubility of resulting PDIs varies greatly depending on the substituents at the imide nitrogen. Two examples of commercially important perylene pigments, Pigment Red 179 and 149, are presented in Figure 2.8. Both pigments are used in the coating industry and plastic coloring.[17,44,45]

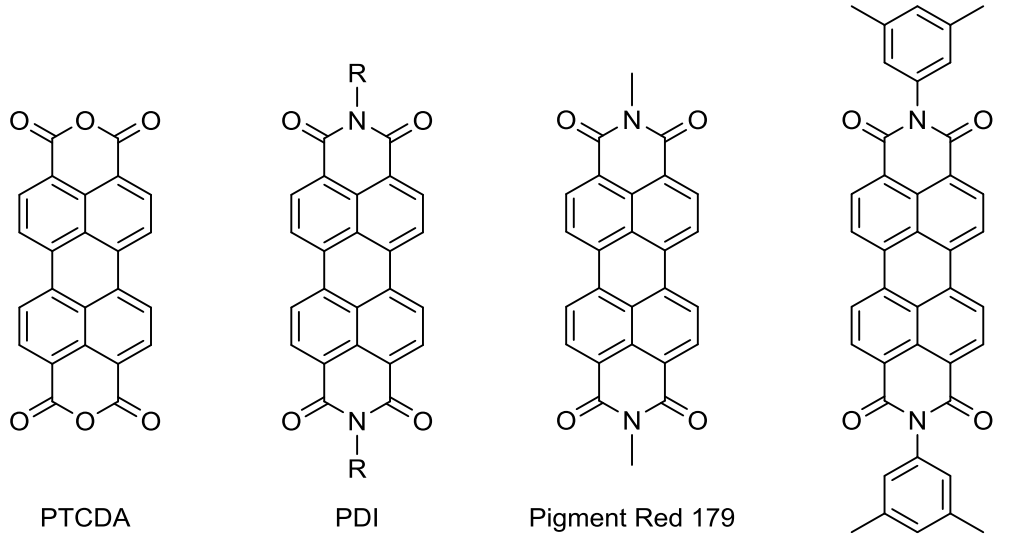

FIGURE 2.8 The chemical structures of PTCDA, PDI and two commercial red pigments.

2.1.3.1 Substitution

The perylene core has twelve functional positions. These are presented by numbers in Figure 2.9. The *peri*-positions are 3, 4, 9, and 10 positions of the perylene core. The 1, 6, 7, and 12 are known as the *bay*-positions, and the 2, 5, 8, and 11 are the *ortho*-positions. In regard to these functionalizing positions, the development of PDIs can be divided in three stages. In the beginning, PDI derivatives have been prepared mainly by the variations of the *peri*-positions.[46] Nowadays, the *bay*-positions as well as the asymmetric perylene monoimides or monoanhydrides are being increasingly investigated. Recent discoveries has been focusing on *ortho*-positions, and this will be an interesting direction for research in future.[17,47]

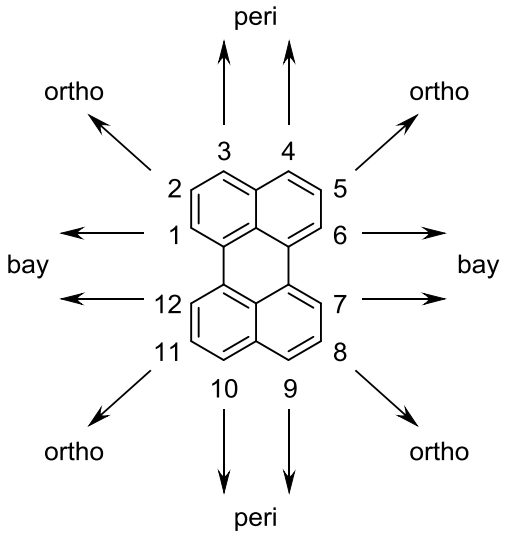

FIGURE 2.9 The structure of the perylene molecule along with the numbering of the various positions.

As mention earlier, the solubility of PDI depends on the substituent at imide nitrogen. Small or linear alkyl chains lead to quite insoluble PDIs in organic solvents. Thus to make PDIs highly soluble, bulky alkyl or aryl substituents can be introduced. However, the optical and redox properties of perylene materials are not affected much by the imide substituents. If such a tuning of the substances is required, the functionalization of the *bay*-positions has to be done. Substituents in this region not only increase the solubility but also alter the PDIs' optical and electronic properties and geometry.[17,48] Modifications in the *ortho*-positions also change the spectral properties but at the same time also help retaining the planarity of the PDI core.[47]

A milestone in the PDI chemistry was a BASF patent from 1997 describing a handy way to halogenate PTCDA at the *bay*-positions.[49] The following exchange of the *bay*-bromine with functional groups is quite straightforward, and up to this day a large number of differently *bay*-substituted PDIs has been prepared.[17,50] An interesting twist the story underwent in 2004 when Würthner's group demonstrated that the bi-functionalized PDIs prepared so far were mixtures of 1,7- and 1,6-substituted regioisomers, and proposed the separation of pure 1,7-dibrominated PDI by repetitive recrystallization.[51] A significant number of papers addressing the problem has emerged since, but the question of regiospecific synthesis of PDIs remains open.[52,53]

2.2 Self-assembled monolayers

Molecules, which have a surface-active head-group e.g. siloxane fragment, can adsorb spontaneously onto a solid surface and covalently anchor to it. If, upon the spontaneous binding a well-

ordered molecule-thick regular structure is formed, the process is called a self-assembling (Fig. 2.10), and the molecular assemblies are called self-assembled monolayers (SAMs).[7]

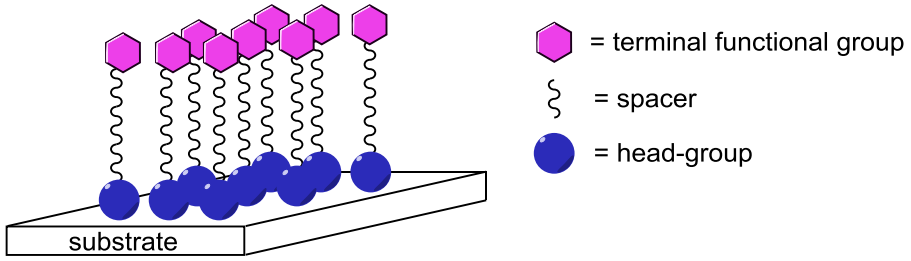

FIGURE 2.10 Schematic representation of a self-assembled monolayer structure.

SAMs are nanostructures with a number of useful properties. Remarkably, they are simple to fabricate. They do not require ultrahigh vacuum or other specialized equipment (e.g. Langmuir-Blodgett troughs) in their preparation. Monolayers can be formed on surfaces with various geometries, from planar substrates, to nanoparticles and porous networks. The thickness of a SAM is typically 1-3 nm which makes them a very good nanometer-scale material. They have high stability and reproducibility, and they are more robust than unbounded coatings, e.g. Langmuir-Blodgett films. However, a full control over the SAM formation process is tricky to achieve. Apart from the molecular structure itself, the choice of solvent, solution temperature, concentration, and immersion time are among the various factors affecting the structure of the resulting SAM.[8]

2.2.1 Anchors and substrates

The chromophores can be customized to have one or more anchor groups as side substituents. Through these anchors, the chromophores can form SAMs. The number and relative orientation of the anchor groups on the macrocycle can dictate the relative orientation of the molecule to the planar surface; from nearly perpendicular to nearly parallel (Fig. 2.11). For example, when all the four *meta*-positions on tetraarylporphyrins bear carboxylate moieties, the porphyrin results in a roughly parallel binding to a metal oxide surface (Fig. 2.11 C). If the porphyrin has a carboxyl group as *para*-substituent the result is a nonparallel orientation in SAM (Fig. 2.11 A).[54]

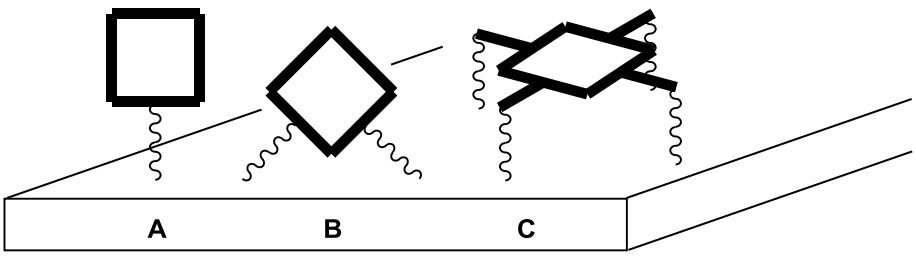

FIGURE 2.11 Different orientations of the macrocycles on surface, example of porphyrins.

An attachment of molecules onto the substrate can occur by chemisorption, which includes the formation of a covalent bond between the active surfactant and solid surface. Adsorbed species, once bonded, are stable because of the strong bonds. The deposition of the molecules can be either a direct adsorption of the functional component that carries a surface-active anchor (Fig. 2.12) or a reaction of the functional components with existing active moieties (e.g. -COOH, -NH_2), which are in turn covalently bonded to the surface (Fig. 2.13).[55]

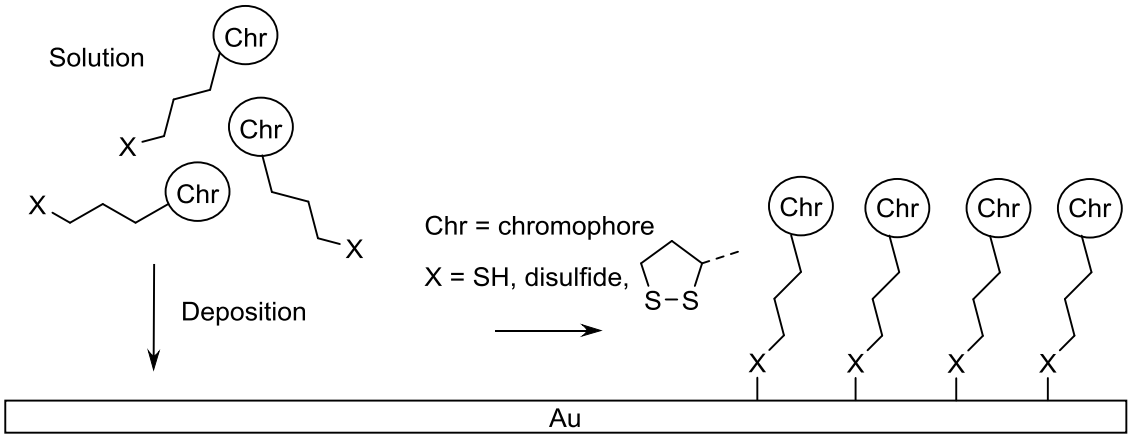

FIGURE 2.12 Direct adsorption method, example of thiol compounds binding onto a gold surface.

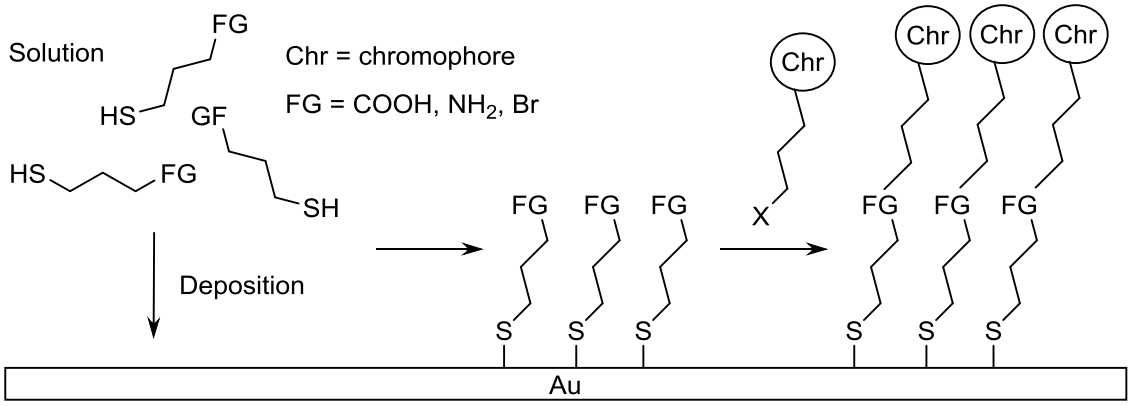

FIGURE 2.13 Covalent attachment of chromophores to a preformed layer of alkanethiols terminated with functional groups (FG).

Types of SAMs are numerous. The most common includes alkanethiolates on gold, silver, or copper, alcohols and amines on platinum, and carboxylic acids on glass, aluminum oxide (Al_2O_3), and silver oxide. The immobilization of organosilicon ligands on hydroxylated surfaces like silica (SiO_2), glass, mica, and indium tin oxide (ITO) is also a known self-assembly method.[8,55] Some examples of these anchor-substrate pairs are more discussed in next chapters.

2.2.1.1 Thiols on gold surface

Organosulfur compounds react readily with a gold surface. The coating process is as simple as to immerse a gilded substrate into a diluted solution of thiol. The sulfur group can also be a disulfide, an acetyl protected thiol or 1,2-dithiolane. In the case of thiol, an oxidative addition of the S-H bond occurs to the gold surface followed by a reductive elimination of hydrogen. In a high-humidity environment, thiolates on gold slowly oxidize to sulfoxides.[7,55]

The self-assembling behavior of small sulfur-containing molecules has been studied extensively, but only limited work has been done with the chromophores bearing sulfur-containing substituents, especially phthalocyanines.[56] Recently, Zhao *et al.*[57] published the synthesis of asymmetrically substituted phthalocyanines bearing a disulfide group and thioacetate. The synthetic scheme for the latter is presented in Figure 2.14. The Pcs self-assembling behavior on gold substrates was studied by UV-vis spectroscopy. Spectra show that the Q-bands of the SAMs were broadened and blue-shifted compared to their corresponding spectra in solutions. Reason for that is aggregation of Pcs in films.

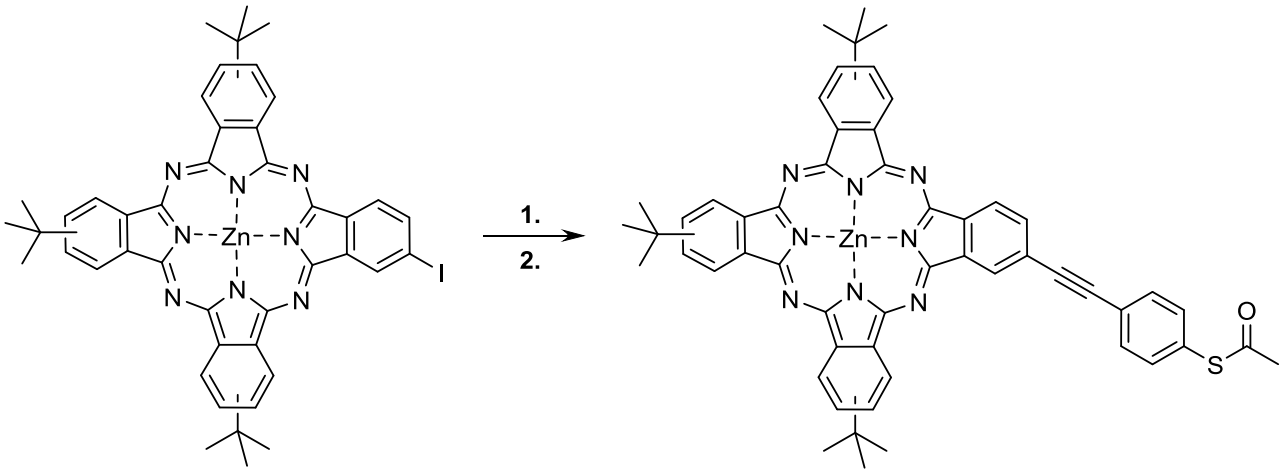

FIGURE 2.14 Synthesis of an acetyl protected thiol Pc (1. a) $(Ph_3P)_2PdCl_2$, CuI, Et_3N, trimethylsilylacetylene, b) NaOH; 2. $(Ph_3P)_2PdCl_2$, CuI, Et_3N, *S*-(4-iodophenyl)ethanethioate).

2.2.1.2 Siloxanes on glass

Attachment of organosilicon compounds to an appropriate substrate is one of the several self-assembly methods. It has gained a huge kick due to the development of reversed-phase sorbents for HPLC and their large-scale production.[58,59] Trialkoxysilanes, with the general formula $RSi(OR')_3$, where R is a terminal functional group and R' is a hydrocarbon radical (usually methyl or ethyl), are generally used in these reactions. One of the advantages of this method is a number of silica-like surfaces, which can be used for immobilization (e.g. glass and various metallic oxides).[60]

In the case of organosilicon compounds, temperature and moisture control are the crucial factors in the self-assembly process. However, water is essential for the silanation reaction since the formation of robust monolayers depends heavily on the hydrolysis of the silane. If the modification conditions are such that the amount of hydrolysis is not sufficient, an incomplete monolayer will be formed (Fig. 2.15). Thus the quality of SAMs is very sensitive to the amount of water in the solvent or adsorbed on the surface of the oxide. Still siloxanes need to be stored in anhydrous conditions as they may self-condense over time.[61]

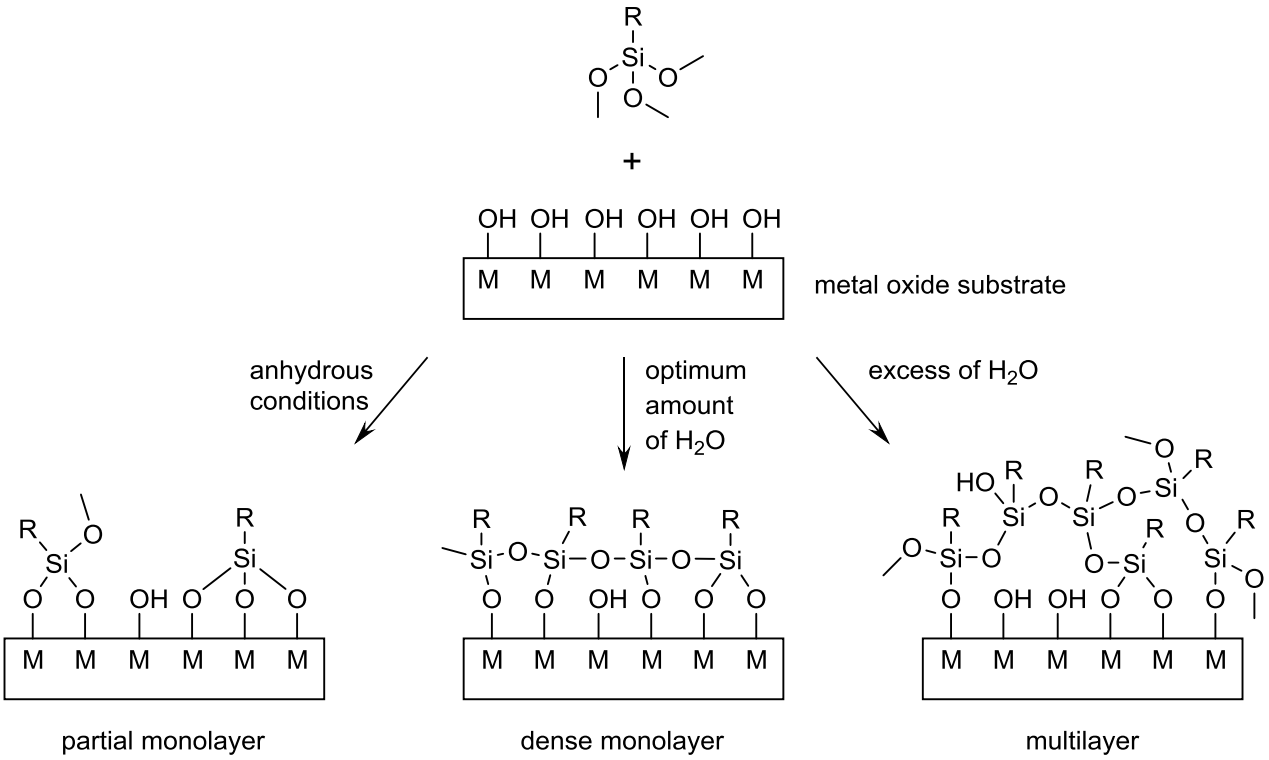

FIGURE 2.15 Schematic representation of the influence of residual water on the layer formation process: an oxide surface and organotrimethoxysilane ligand as example.

The list of chromophores attached to a surface via siloxane bonding is not large, chiefly due to synthetic obstacles. Yamada *et al.*[62] reported the studies of ITO surfaces, which were chemically modified with porphyrins and porphyrin-fullerene dyads. ITO electrodes were treated with aminopropyltrimethoxysilane and chromophores were coupled to aminopropylsilylated ITO. This was done through amide bond reaction between pentafluorophenyl ester group on chromophore and amino group on silylated ITO (i.e. covalent attachment of the functional components onto preformed tails). Using the same reaction, different kinds of porphyrin-fullerene dyads were attached to ITO electrode by Chukharev *et al.*[63] Dyads were either ITO-porphyrin-fullerene or ITO-fullerene-porphyrin orientation. Latter structure is shown in Figure 2.16.

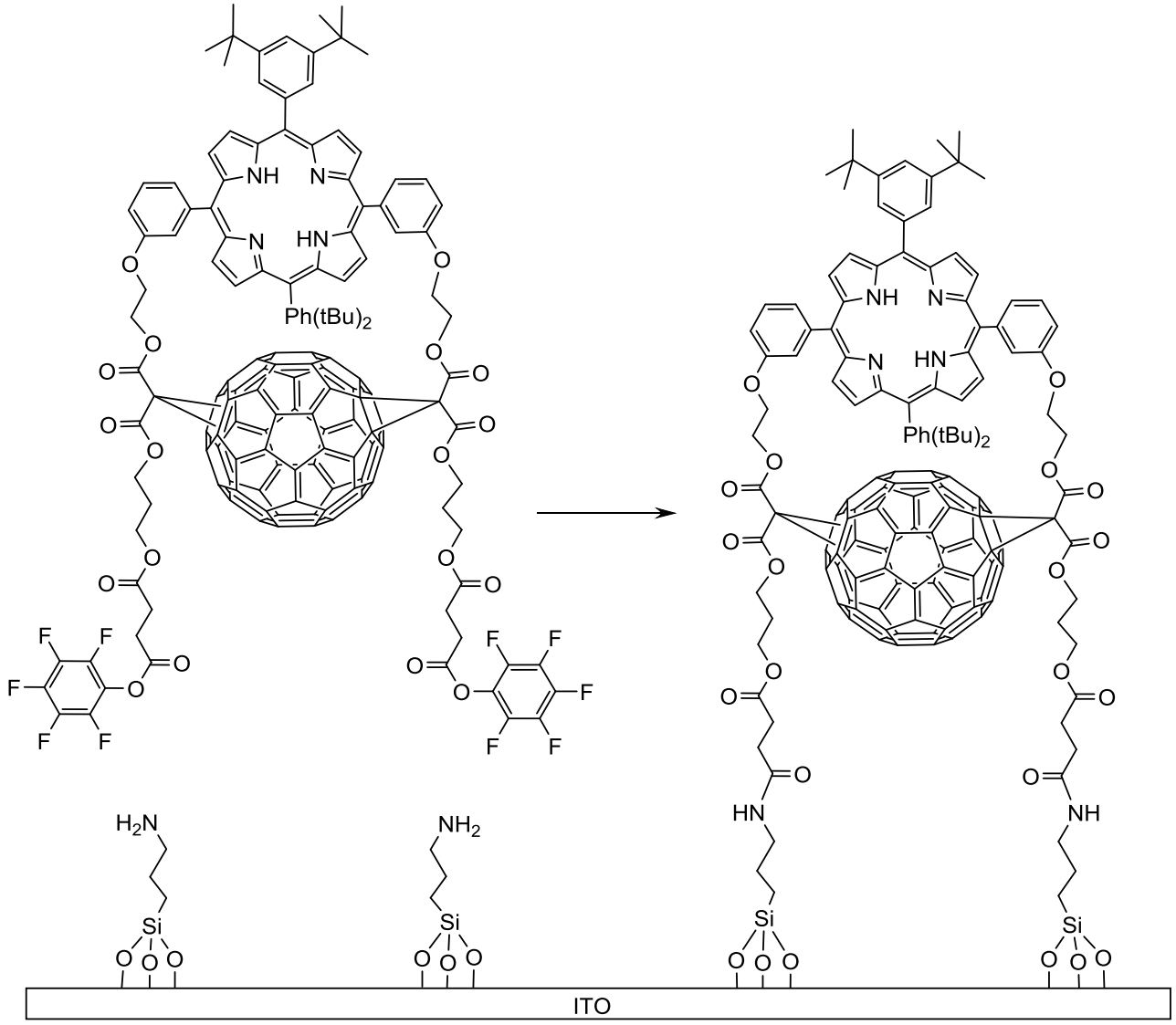

FIGURE 2.16 Formation of porphyrin-fullerene dyad on ITO.

2.2.1.3 Carboxyl on metal oxides

One of the most commonly used anchoring group for metal oxide surfaces is the carboxyl group (-COOH). Carboxy-function is able to coordinate to the surface by three different binding modes, namely by an unidentate ester-type, a chelating linkage, and bidentate bridging linkage (Fig. 2.17). The bidentate structures are more stable than the unidentate structure.[5] This combination of binding modes and their relative weakness often makes monolayers, which are not strongly bounded to the surface. Sometimes they can be easily removed, even by simple rinsing in solvents.[64] However, the stability of a sorbed layer strongly depends on the nature of surface.

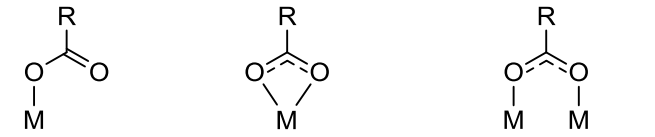

FIGURE 2.17 The three main binding modes between a COOH group and a metal oxide surface.

Titanium dioxide (TiO_2) is the substrate used in dye-sensitized solar cells (DSSC). In these systems, the carboxyl group of the dye acts as an electron-withdrawing anchoring group on the titania surface. [65,66] A vast number of organic dyes functionalized with carboxyl groups has been tested in DSSC applications, and in most of the cases bonding was strong enough.[9] For example, three unsymmetrical PDI dyes containing 6-undecanoxy as donor group were utilized in dye-sensitized solar cells by Dinçalp *et al.*[67] The structure of the acceptor side of the molecules were improved by adding different aryl substituents with carboxylic acid to one of the imide-side of the dye, and these were immobilized to nanocrystalline TiO_2 surface. Figure 2.18 presents these PDI structures.

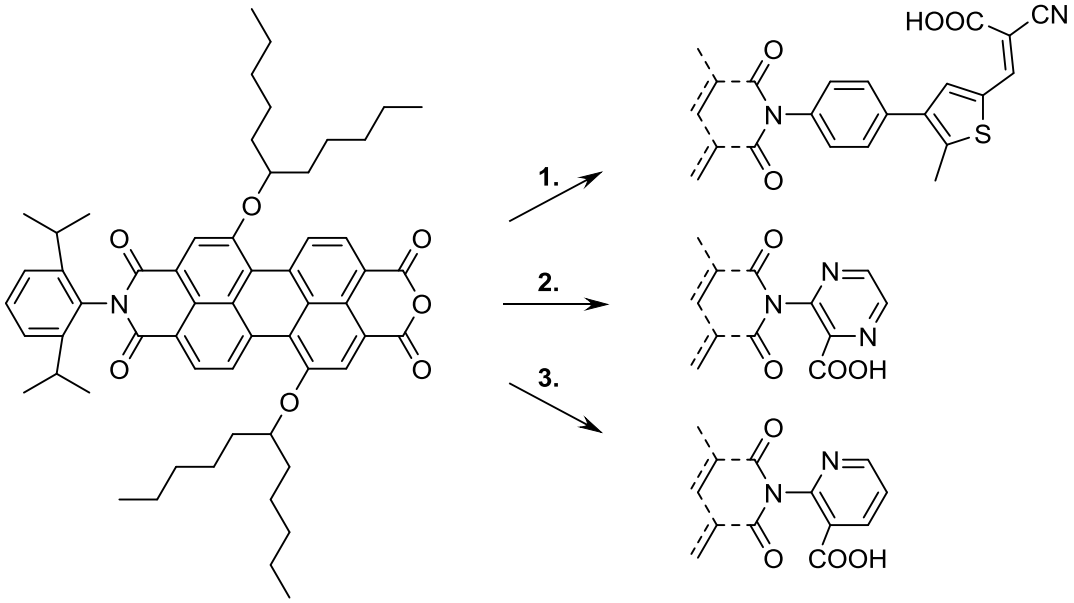

FIGURE 2.18 Carboxyl-containing PDIs (1. 3-[4-(4-aminophenyl)-5-methyl-thien-2-yl]-2-cyanoacrylic acid, imidazole; 2. 3-aminopyrazine-2-carboxylic acid, imidazole; 3. 2-aminonicotinic acid, imidazole) used for immobilization on TiO_2.

2.2.2 Multicomponent arrays on surface

Highly ordered thin molecular films, from monolayer to multilayer assemblies, promise considerable development for micro- and nanotechnology. Multicomponent molecules and supramolecular aggregates are synthesized by the ‘‘bottom-up’’ approach that builds nanoscale structures from the molecular level. In particular, the application of supramolecular chemistry to the direct assembling of functional layers at surfaces added a new and highly diverse class of materials to modern material science. Multicomponent arrays are attractive materials for application in many different fields such as optics, biotechnology, photo- and electrochemistry; i.e. nonlinear optical materials, enzyme sensors, solar energy storage devices, and molecular rectifiers.[68]

Fabrication of chromophores’ arrays on surfaces can be done by so called layer-by-layer technique where a film grows as a single monolayer at each step. The primary advantage of this technique is that single monolayer formation can be achieved by simply immersing the sample in solutions of the various components sequentially, thus avoiding long and difficult synthesis and tedious purification steps. Formation of such multilayers on surfaces has been achieved by a number of different interlayer coupling methods, including transition metal coordination chemistry (see Fig. 2.20).[68,69]

In the field of supramolecular chemistry, the 2,2’:6’2’’-terpyridine (tpy) unit is one of the most versatile and widely used chelating ligand for building supramolecular assemblies (Fig. 2.19). Terpyridine derivatives are not only important light-harvesting units, but they also have strong coordinative ability to a variety of transition metal ions, thus leading to diverse metal-complexes and metallo-supramolecular architectures (Fig. 2.19). Tpy-derivatives can form arrays with a large number of different metal complexes, e.g. Ru, Fe, Zn, and Cu ions of different oxidations states, which are characterized by a broad range of physico-chemical properties and different stabilities. Although the terpyridine unit was introduced to the synthetic world as early as 1931, it was only after it combined with supramolecular chemistry that its importance was properly realized.[11,70]

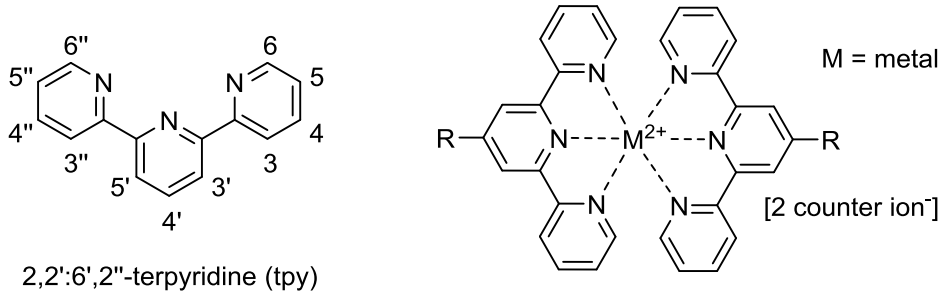

FIGURE 2.19 Structure of 2,2’:6’,2’’-terpyridine and its metal complex.

Even though the solution-state polymers with tpy linker are quite common,[71,72] examples of surface-bound structures incorporating tpy groups are limited.[73,74] Terpyridines with anchors can be found for example with silyl[75,76] and thiol[77,78] groups. Nevertheless, more interesting form the practical point of view would be the chromophores decorated with tpy substituent, which would have attractive electronic, magnetic, catalytic, and photonic properties.[12] Some examples are ZnPc with Ru-tpy[79,80], tetra-aryl porphyrin[81], and tpy-PDIs[82,83], but these supramolecular arrays are not bonded to surface. Very few multilayers with PDIs having terpyridines as coordination blocks have been prepared on solid substrate to date.[84,85,86] Some of these supramolecular structures are illustrated in Figure 2.20. Remarkably, as many as 25 subsequent layers of PDI were deposited by chelating the iron(II) sulfate between the tpy units. Absorbance per layer of PDI was 0.001, which is somewhat low value considering the high extinction coefficient of PDI. This probably indicates that the surface density of the chromophores was not high enough. One can suggest that the formed film was not a densely packed monolayer, but a rather loose structure. Nevertheless, the AFM measurements revealed the film thickness corresponding to 25 subsequent PDIs arranged atop each other and gave evidence for a vertical orientation of the arrays.[85]

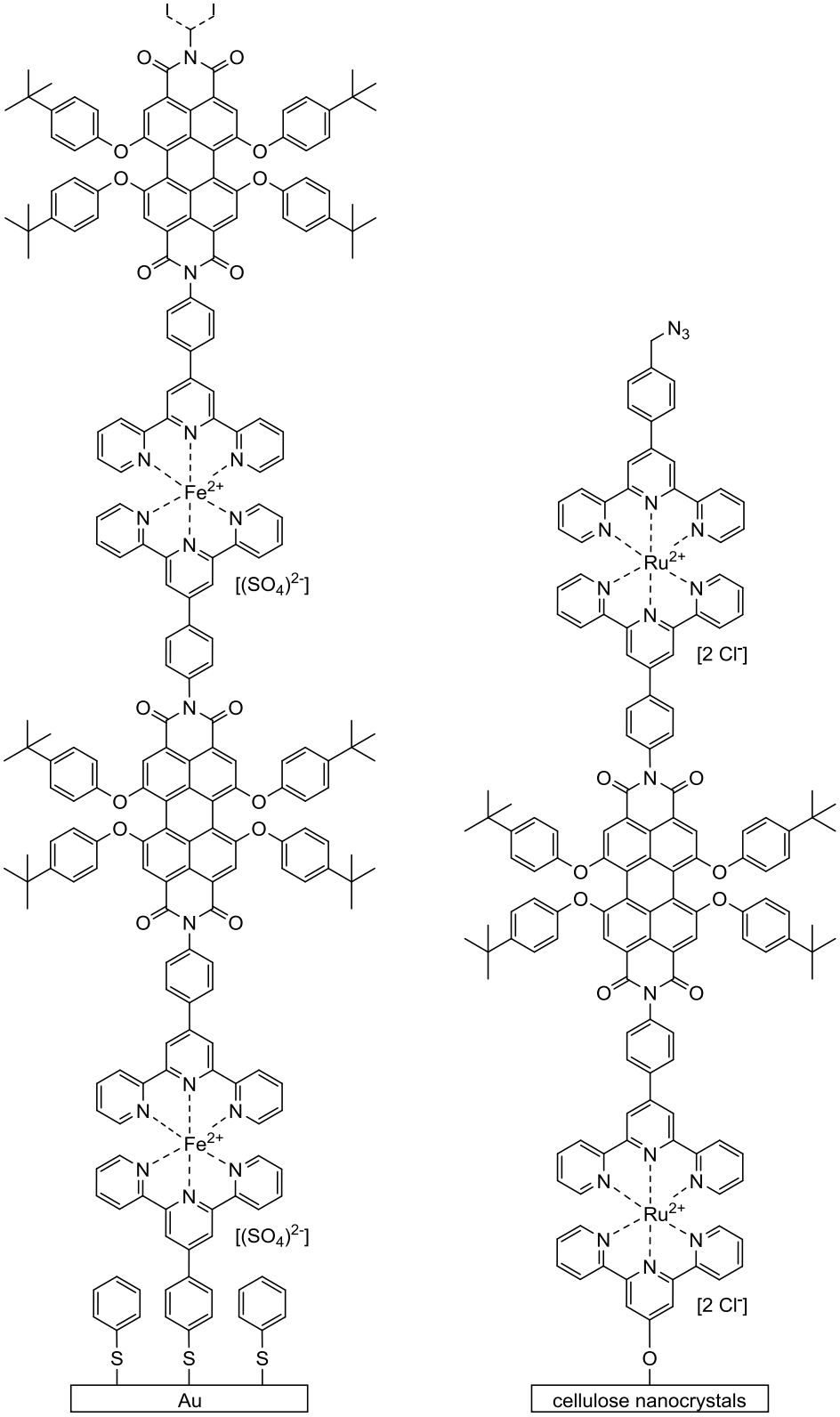

FIGURE 2.20 Schematic representation of self-assembled multilayers via metal coordination.

3 Aims of the study

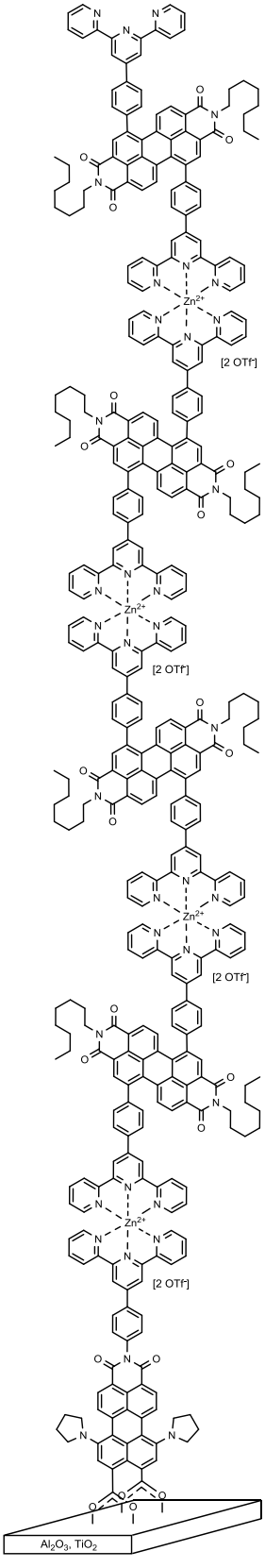

An ultimate goal of the present work was to prepare a set of photo-active compounds, from which monomolecular layers and well-ordered multi-layered molecular films of different thickness, color, and internal structure can be built at will in a controllable manner.

First of all, the chromophore molecules with appropriate modification sites should be synthesized. The molecules needed to have an anchor moiety to fasten onto surface covalently. Different anchors should be tested. Then optimum conditions for every anchor-surface pairs should be found to prepare self-assembled monolayers.

The fabrication of multilayered structures should be done by a simple and inexpensive metal coordination. Appropriate ligands, chelated ions, and counter ions as well as reaction conditions should be found.

The final goal was to build the supramolecular assemblies of chromophores on solid substrates. Deposition methods should be reliable, scalable, and versatile, and should provide stable and high quality films.

4 Materials and methods

Commercial reagents and solvents (HPLC grade) were purchased from standard suppliers (Acros Organics, Sigma-Aldrich Co., Tokyo Chemical Industry Co., VWR International) and used without further purification. If needed, chloroform was distilled over K_2CO_3, dichloromethane over P_2O_5, and toluene was distilled over sodium shots. Triethylamine was distilled over KOH and tetrahydrofurane over $LiAlH_4$. Hellmanex III, special alkaline concentrate for cleaning plates, was purchased from VWR International.

The monitoring of reactions was carried out by thin layer chromatography (TLC), employing aluminum sheets precoated with silica gel 60 F_{254} or aluminum oxide 60 F_{254} neutral (Merck). The purification and isolation of the products were performed by column chromatography on silica gel 60 (mesh size 40-63 µm), silica gel 100 (mesh size 63-200 µm) or by flash chromatography using CombiFlash Companion (Teledyne ISCO).

4.1 Characterization

4.1.1 NMR

The structural characterization of molecules was done with NMR, Varian Mercury 300 MHz spectrometer (Varian Inc.). All chemical shifts were given in ppm relative to TMS as internal standard. Most of the products had good solubility allowing the measurements of highly concentrated samples in $CDCl_3$. The signal assignments in ^1H and ^{13}C NMR spectra were based on two-dimensional NMR spectroscopy: the gradient-selected heteronuclear single quantum coherence (gHSQC) with multiplicity editing, the gradient-selected heteronuclear multiple bond correlation (gHMBC), and the homonuclear correlation spectroscopy (COSY).

The NMR spectra of synthesized chromophores were informative though crowded. Therefore, full assignment of the peaks for the starting materials was needed for correct interpretation of the spectra of the final compounds. The structural characterization of phthalocyanines is often challenging due to their poor solubility and a number of regioisomers. In contrast, our specifically designed porphyrinoids had good solubility, relatively easy NMR analysis, and a reduced number of regioisomers.[I,II] In case of perylene compounds, the assignment of ^{1}H NMR peaks was complicated due to the overlapping of the peaks and crowded aromatic and aliphatic regions. Most of the signals were visible as multiplets. However, the assignment for all the proton signals was done successfully. The NMR spectroscopy proved to be a very powerful tool also in characterization of PDI zinc complexes.[III]

4.1.2 Mass spectrometry

The structures of the synthesized compound were proved by high resolution ESI-TOF mass spectrometry (ESI-TOF LCT Permier XE mass spectrometer, Waters Corp.). For the MS measurements, the sample of an analyte was dissolved in an appropriate solvent at concentration approximately 0.01 mg/mL and infused at a rate of 15 µL/min. To obtain an accurate mass, a solution of reference compound (Leucine Enkephaline 50 pg/mL) was infused simultaneously. The experimental spectra were processed with peak centering and lock mass TOF correction. The solvent used for infusion was typically a mixture of $CHCl_3$/MeOH 2:3 v/v, and positive ion mode was used.

4.1.3 Steady state absorption and emission

Steady state absorption spectra were recorded with a Shimadzu UV-2501PC UV-Vis Recording spectrometer. The measurements indicate the ground state absorption spectra of the compounds in the range 250-850 nm. Mostly chloroform was used as a solvent in the solution studies. The emission spectra were recorded by Fluorolog Yobin Yvon-SPEX spectrofluorometer.

Absorption spectra of the SAMs were obtained by subtracting the absorbance of the clean substrate from the absorbance of the plate with the SAM. Considering the absorption spectrum of the monolayer on glass and quartz, the observed optical densities should be divided by two, because layers are formed on both sides of the substrate.[I,II,III]

Emission spectra from the plates with SAMs were also measured. For the metallation process (on-surface reactions from free base chromophores to Zn(II) and Mg(II) metal complexes), the steady state emission was the best mean for seeing progress of the reaction. The metal ion which is chelated in porphyrinoid cavity alters the fluorescence properties dramatically, thus the peak shifts and intensity quenching were more visible in the emission spectra than in absorption.[II]

4.2 SAM preparation

First step towards successful SAMs was a proper cleaning of substrates. In the beginning of the studies glass and quartz plates were cleaned first manually with a cotton stick and $CHCl_3$, and then by a sonication in a set of solvents ($CHCl_3$, acetone, chromosulfuric acid, NaOH (aq), conc. HNO_3, EtOH) on ultrasonic bath.[I,II,III] Within time, the procedure was simplified without sacrificing the performance. Thus lately, the plates were first kept overnight in Hellmanex III solution (2 %), rinsed with MilliQ water, then sonicated in acetone and isopropanol, 30 min in each solvent.[IV] The cleaned plates were dried in the oven at 150 °C for 1 h. Glass plates with ITO layer on one side were cleaned by sonication in acetone/water 1:1, 2-propanol, and CH_2Cl_2, 5 min in each solvent, and dried in the oven at 150 °C.[I,II]

The gold substrates were prepared by thermal evaporation under vacuum of a layer of gold onto cleaned glass plates that had been precoated with a titanium layer. Titanium layer improves the adhesion of gold that do not form oxides readily.[8] Titanium and gold layers were 2 nm and 3 nm thick, respectively.[I] Glass plates with aluminum doped zinc oxide (AZO) layer on one side were used as received after atomic layer deposition (ALD).[87][II] Quartz plates with Al_2O_3 layer (20 nm) on one side were also used as received after ALD.[IV]

Before deposition of SAMs, the reaction vessel and the plates were kept in oven (150 °C) for an hour to remove the residual moisture. This operation was mostly essential when working with siloxane compounds but is a good practice for all types of anchors.

SAMs with 2-step process. At the Step 1 the plates were activated with 3-aminopropyltrimethoxysilane in dry toluene at 105 °C for 1 h. The activated plates right from the reactor were rinsed for 15 s in toluene and toluene/acetone 1:1 v/v mixture on ultrasonic bath and dried in an argon flow (30 min). Phthalocyanines were then covalently attached to the aminosilane-modified surface by immersing the plates into a Pc solution in dry toluene at the Step 2. Phthalocyanine's bonding occurred through amidation reaction between pentafluorophenyl ester group on Pcs and amino group on silylated substrates (see Fig. 2.16). This second step was completed in 2 h at 105 °C. Both the silylation and amidation were done under argon. To remove residual physisorbed Pc, the samples were sonicated in toluene and CH_2Cl_2 after the second step.[I]

SAMs with 1-step process. The reaction vessel was loaded with a solution of a siloxane chromophore in the mixture of distilled toluene and isopropyl amine under argon. The cleaned plates (quartz, ITO, AZO) were immersed in the solution and the reaction vessel was heated at 105 °C for 2 h. After appropriate time the plates were sonicated twice in toluene and once in CH_2Cl_2, and dried in an argon flow (30 min).[II,III]

SAMs of phthalocyanine with thioacetate anchors were prepared by immersing the gold-coated glass plates in the Pc solutions in CH_2Cl_2 for 30 min at room temperature. After that the plates were rinsed with CH_2Cl_2 and $CHCl_3$, and dried in air.[I]

SAMs from PMI anhydrides were done by dissolving an anhydride compound in toluene/EtOH 9:1 v/v. Solutions were stirred at 80 °C at least 30 min to ensure complete disappearance of solid particles; for some compounds a 30 min treatment on ultrasonic bath was also needed. The cleaned plates (quartz+Al_2O_3) were immersed in the solution and the reaction vessel was heated at 80 °C. After overnight incubation, the plates were washed by soaking twice in toluene for 30 s. Finally, the plates were dried in an argon flow.[IV]

Multilayer preparation. Multilayers were prepared by successive repetition of the two steps: (A) complexation of the PMI SAMs; and (B) attachment of a tpy-PDI layer.[IV]

Step (A) was done by immersing the substrates into solutions of the zinc metal ions. Zinc(II) trifluoromethanesulfonate ($Zn(OTf)_2$) (36 mg, 0.1 mmol) was dissolved in toluene/EtOH 9:1 v/v by sonication. For complexation the stock solution (3.6 ml) was diluted with toluene/EtOH 9:1 (20 ml). The plates with SAMs were immersed in the zinc solution at room temperature for 1 h. The plates were washed with toluene, and the samples were dried under an argon flow.

Step (B) was done by immersing the complexed SAM plate in the PDI linker solution, which was dissolved in toluene/EtOH 9:1 v/v. The plates were kept at 80 °C overnight for the first layer, but only 1 h for the next ones. After immobilization, the plates were washed with toluene and dried in an argon flow. Steps 1 and 2 were repeated iteratively up to the desired number of layers.

5 Results and discussion

This chapter summarizes the essential work presented in the publications I-IV. Syntheses of chromophores will be discussed in the first part of the chapter. The synthetic schemes are divided in two groups: dyes for 2-step SAMs and dyes for 1-step SAMs, with a subdivision by the type of anchor. Self-assembling procedures and layers of chromophores on solid surfaces are discussed in the second part of the chapter.

Because of the large number of synthesized compounds it is recommended to refer to the Table 5.1 on page 43, where all the essential substances are collected for reader's convenience.

5.1 Synthesis

5.1.1 Chromophores for 2-step SAMs [I]

As it was discussed earlier, monolayers can be formed by covalent attachment of the functional components onto preformed tails immobilized on the surface. In that case, one needs to prepare compounds with a functional group, which react with the terminal groups of the tails. A useful example of such reacting pair is the pentafluorophenyl (PFP) ester and amine. PFP-esters are reactive yet stable, and, importantly, relatively easy to introduce into large aromatic structures such as porphyrinoids. The amino terminus is a convenient surface modifier, and can be implemented by a treatment of surface with a choice of aminoalkylsilanes. Following this route, three different phthalocyanines with one, two or four pentafluorophenyl ester groups were synthesized, as discussed below and their 2-step SAMs were made and studied as described in Chapter 5.2.1.

The aim of our studies was not only to find a method of attachment of certain chromophores to certain surfaces. We wanted to compare the surface coverage and quality of the films, interactions

between chromophores and substrates, as well as the influence of the number of anchors and overall geometry of the molecule. We also wanted to compare the one- and two-step binding methods in terms of effectiveness, simplicity and time consumption. To optimize the synthetic efforts and to make the SAMs comparable to each other, we have prepared the three key intermediates **3**, **9**, and **14**, phthalocyanines with one, two, and four hydroxy groups (Schemes 5.1, 5.2, 5.3). These phthalocyanines were later decorated with PFP, thiol, and siloxane anchors and used for film preparation.

Phthalocyanines were synthesized from commercial phthalonitriles **1** and **8**, and from phthalonitriles **2** and **13**, which were prepared by known methods.[88] Commercially available 3,6-dihydroxyphthalonitrile and 1-bromopropanol were used to synthesize phthalonitrile **7**.[37] In synthesis of Pc **3** (Scheme 5.1) and **9** (Scheme 5.2), an excess of phthalonitriles **1** and **8**, respectively, was used to favor the formation of A_3B type Pc.[31] Indeed, the compounds **9** and **14** formed as a set of regioisomers, however in Schemes 5.2 and 5.3 only one isomer of target Pcs is shown for clarity.

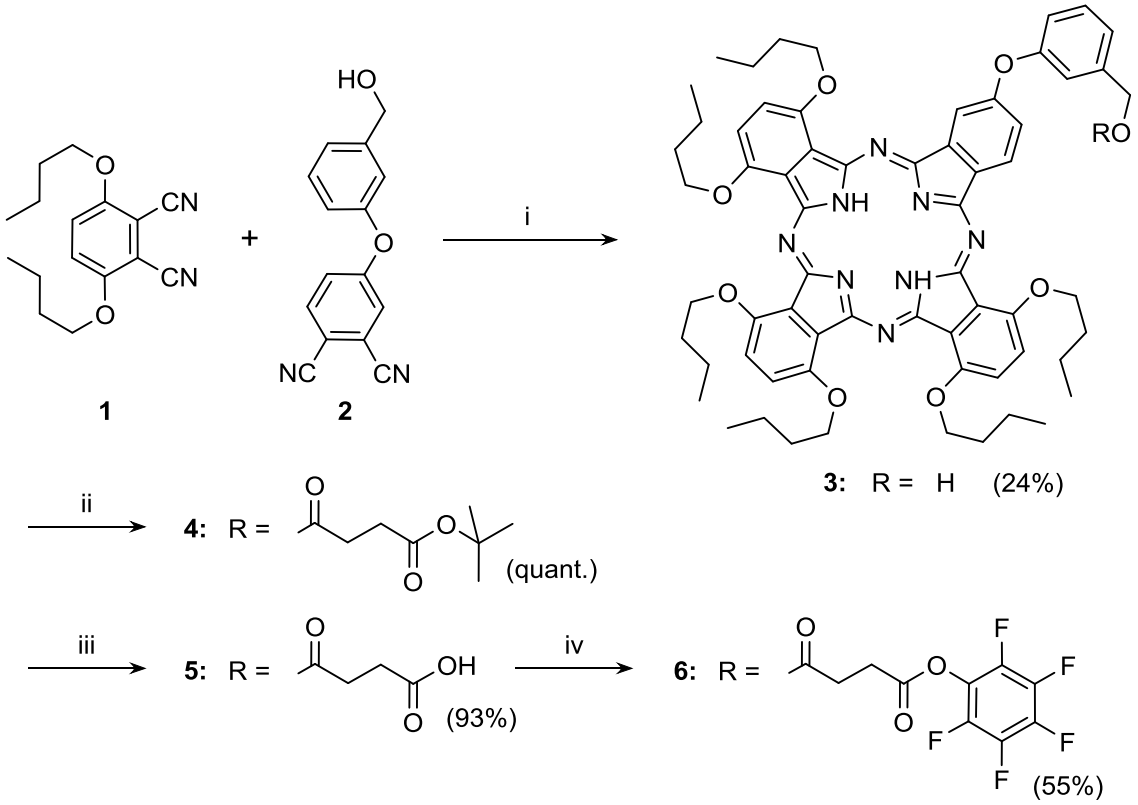

SCHEME 5.1 Synthetic route to monohydroxy phthalocyanine **3**, and its derivatives. Reagents and conditions: (i) Li, 1-butanol, reflux, 4 h; (ii) mono-*tert*-butyl succinate, DCC, DMAP, CH_2Cl_2, rt, 48 h; (iii) TFA, dry CH_2Cl_2, rt, 3 h; (iv) pentafluorophenol, DCC, EtOAc, rt, 120 h.

Synthesis of pentafluorophenyl ester **6**, **12**, and **17** included three steps. At first mono-*tert*-butyl succinate was attached to hydroxy-substituted Pc under DCC/DMAP conditions. The succinic acid was deprotected with trifluoroacetic acid (TFA). The acid was converted into pentafluorophenyl in the last step.[63] Conversion of monohydroxy Pc **3** and bishydroxy Pc **9** to the corresponding *tert*-butyl succinates **4** and **10** required two days stirring in dichloromethane, and the products were obtained with quantitative yields. In the synthesis of tetrakis(*tert*-butyl succinate) Pc **15** (Scheme 5.3), tetrahydroxy phthalocyanine **14** was dissolved in THF. Compared to others, the reaction was slow – the reaction mixture was stirred at room temperature for seven days. The long reaction time is due to the poor solubility of Pc **14**. However, the product was obtained again with quantitative yield.

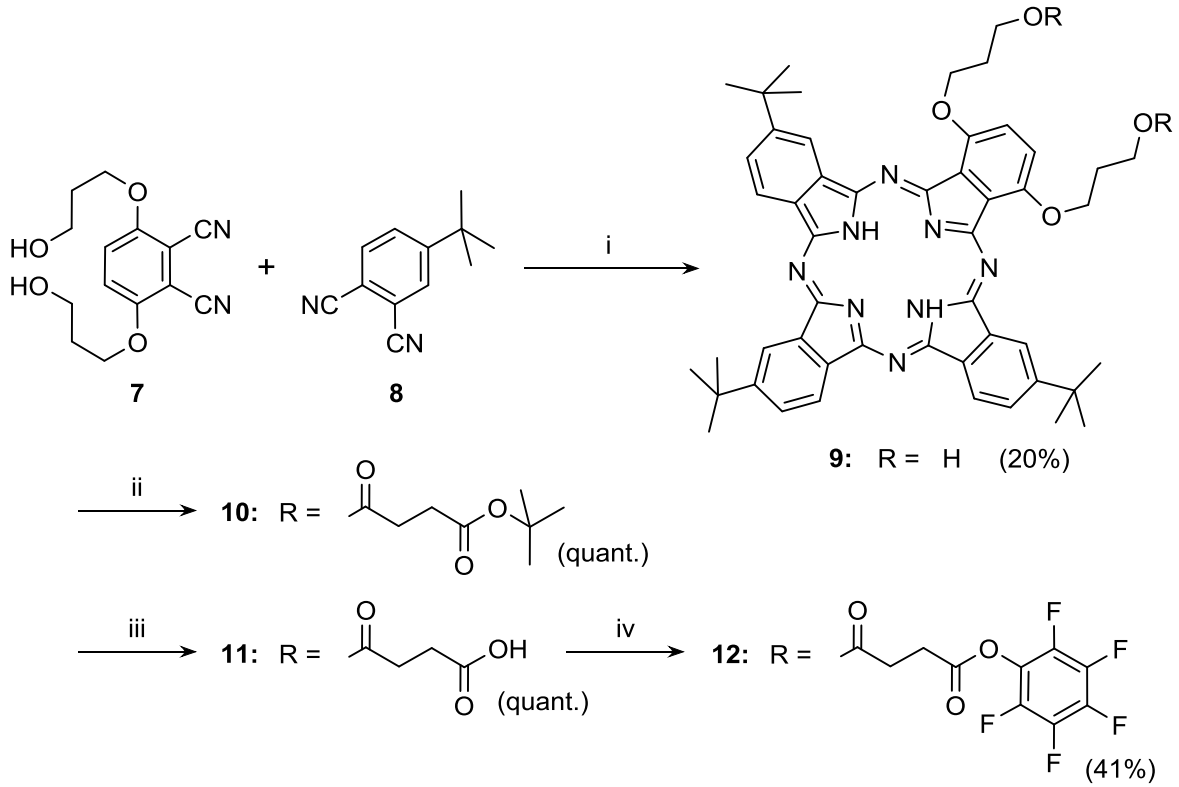

SCHEME 5.2 Synthetic route to bishydroxy phthalocyanine **9**, and its derivatives. Reagents and conditions: (i) Li, 1-pentanol, reflux, Ar, 2.5 h; (ii) mono-*tert*-butyl succinate, DCC, DMAP, CH_2Cl_2, rt, 48 h; (iii) TFA, dry CH_2Cl_2, rt, 4.5 h; (iv) pentafluorophenol, DCC, EtOAc, rt, 96 h.

The deprotection of phthalocyanines **4**, **10**, and **15** was done by treatment with TFA. Yields were almost quantitative in every case. Finally, the pentafluorophenyl esters **6** and **12** were prepared by stirring the reaction mixtures for a few days at room temperature. Yields of esterification reactions were moderate (40-50 %). Because of the very poor solubility of compound **16** preparation of tetrakis(pentafluorophenyl ester) **17** started by dissolving intermediate product **16** in ethyl acetate

on ultrasonic bath. After that the reaction mixture was stirred in cold for three days. Purification of the product needed both the flash chromatography and preparative TLC, and thus pure product **17** was obtained with a 25 % yield only.

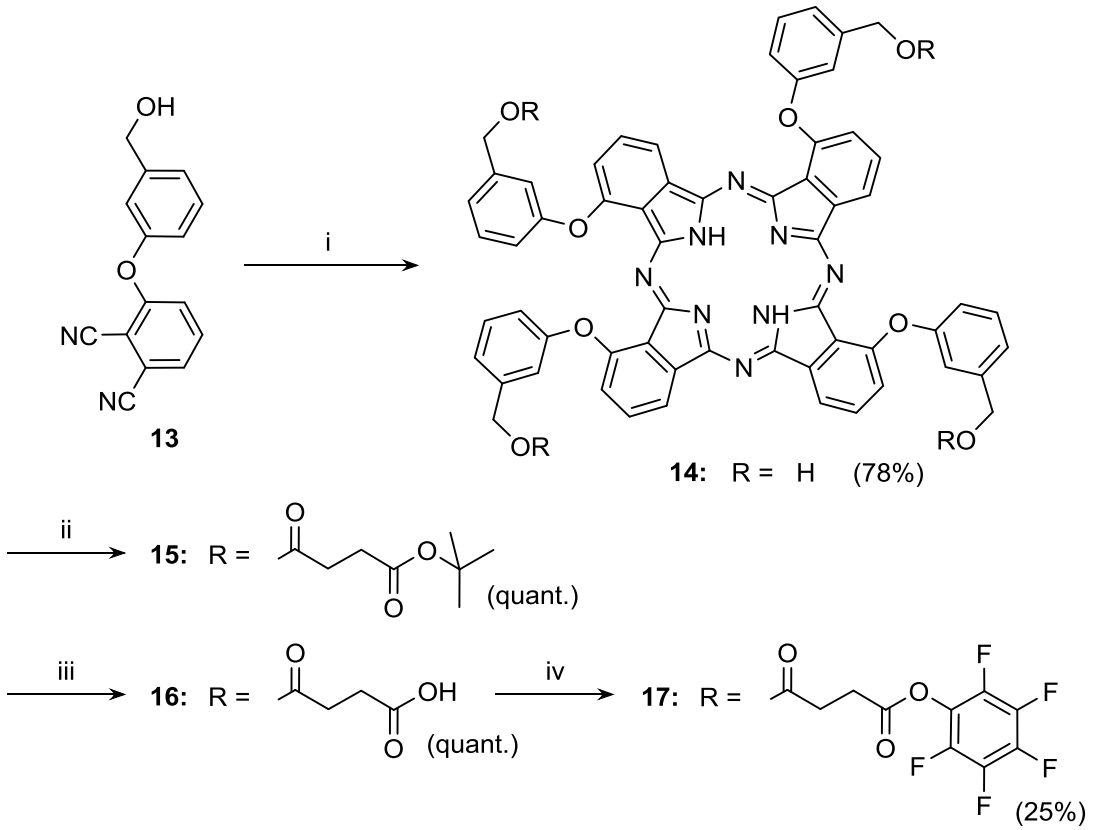

SCHEME 5.3 Synthetic route to tetrahydroxy phthalocyanine **14**, and its derivatives. Reagents and conditions: (i) lithium octoxide, THF, 80 °C, Ar, 72 h; (ii) mono-*tert*-butyl succinate, DCC, DMAP, THF/CH_2Cl_2, rt, 168 h; (iii) TFA, dry CH_2Cl_2, rt, 4.5 h; (iv) pentafluorophenol, DCC, EtOAc, 0 °C 48 h, rt 24 h.

5.1.2 Chromophores for 1-step SAMs [I,II,III]

Making monolayers by a one-step immersion requires molecules with surface-reactive anchor groups. These kinds of chromophores were prepared with thioacetate (phthalocyanines), triethoxysilane and dimethylmethoxysilane moieties (phthalocyanines, porphyrins, PDIs), and carboxylic groups (anhydride cycles in perylene monoimides).

Hydroxy-phthalocyanines introduced in the previous chapter were used as starting materials in synthesis of thioacetyl-substituted Pcs. The synthesis included two steps: (a) an acylation of hydroxy Pc with bromopropionic acid, and (b) an exchange of the terminal bromine to a thioacetate group. 3-Bromopropionyl chloride, which was used in the acylation, was prepared by a known

method just before use.[89] A six-fold excess of bromopropionyl chloride per hydroxy group was added into the reactions to form Pcs **18** (Scheme 5.4) and **20** (Scheme 5.5). For tetra-substituted Pc **22** (Scheme 5.6), overall 30-fold excess of bromopropionyl chloride was needed. Attempts to promote the reaction conditions by addition of an amine base resulted in a rapid dehydrobromination and formation of a terminal double bond.

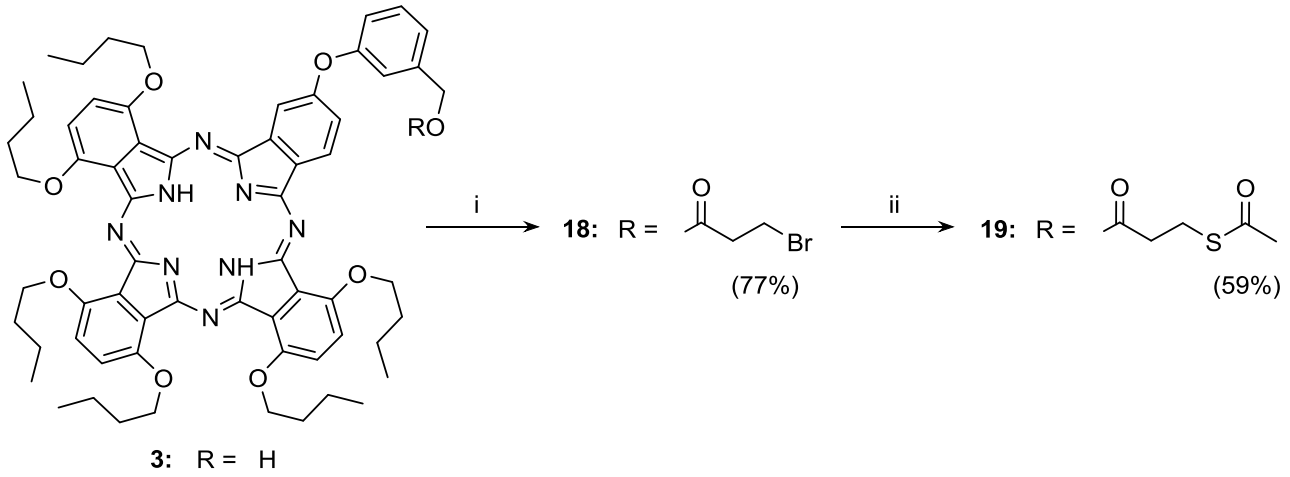

SCHEME 5.4 Synthetic route to monothioacetate phthalocyanine **19**. Reagents and conditions: (i) 3-bromopropionyl chloride, CH_2Cl_2, rt, 24 h; (ii) KSAc, acetone, reflux, 72 h.

The exchange of the terminal bromine to thioacetate was done in acetone using potassium thioacetate (KSAc). An elevated temperature was required in synthesis of Pc **19**, because of the poor solubility of compound **18** in acetone. Changing the solvent did not help; actually, no reaction was observed in DMF at 60 °C or in THF at reflux. Preparation of bisthioacetyl Pc **21** was easier and was done by stirring Pc **20** and a four-fold excess of KSAc at room temperature for 4 days (Scheme 5.5). Besides the higher yield this reaction proceeded faster than monothioacetyl synthesis. In fact, after 16 h of stirring, the yield of bisthioacetate was as high as 67 %.

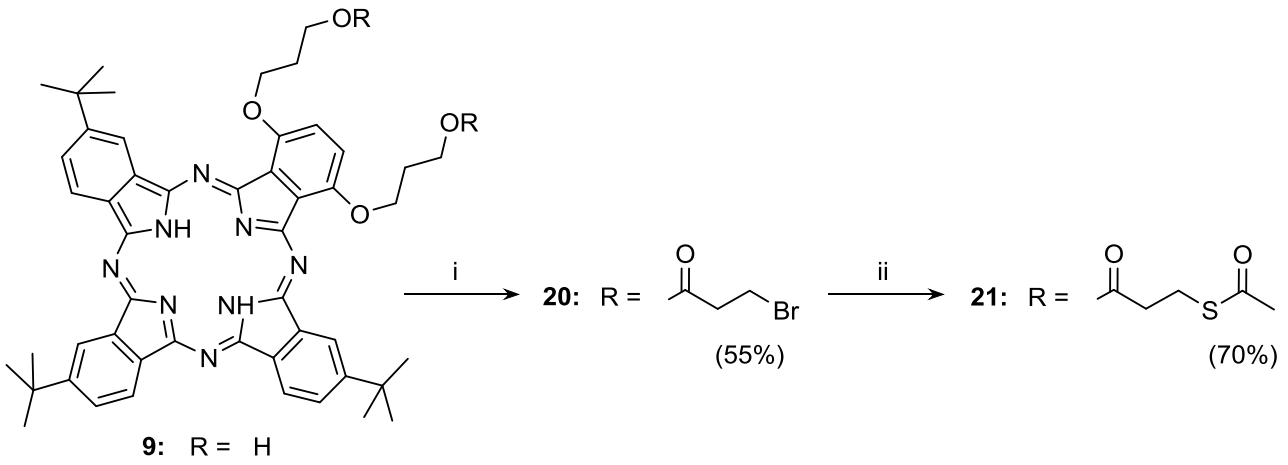

SCHEME 5.5 Synthetic route to bisthioacetate phthalocyanine **21**. Reagents and conditions: (i) 3-bromopropionyl chloride, CH_2Cl_2, rt, 72 h; (ii) KSAc, acetone, rt, 96 h.

The formation of tetrathioacetyl phthalocyanine **23** at room temperature was slow, and heating for one day at 60 °C did not promote the reaction any further. However, when a double excess of KSAc was added and the solution was stirred at 60 °C for another day, Pc **23** was obtained with 70 % yield.

Tetrahydroxy Pc was also used for the initial experiment to prepare a silane-anchored chromophore. Pc **14** was acylated with bromopropionic acid and dehydrobrominated by the triethylamine treatment (Scheme 5.6). Tetraacrylate Pc **24** thus obtained was hydrosilylated with commercial Speier catalyst (hexachloroplatinic(IV) acid hydrate, $H_2PtCl_6 \cdot nH_2O$) and triethoxysilane.[59] Unfortunately, the reaction product was a mixture of partly silylated and reduced compounds (**25**), as revealed by the mass-spectrometry and NMR. The mixture was not possible to separate, and the target tetrasilane Pc (**25** n=0, m=4) was never isolated in pure form.

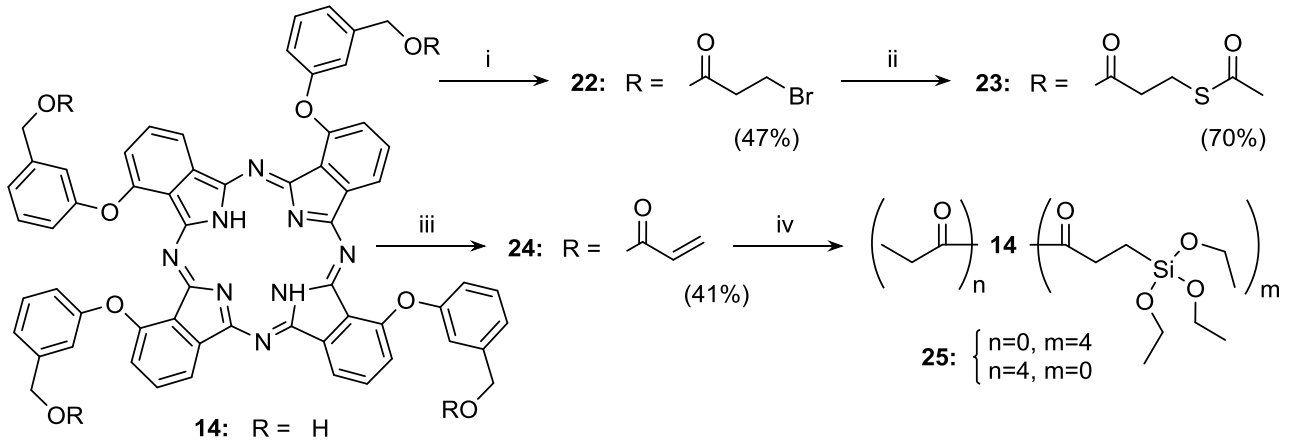

SCHEME 5.6 Synthetic routes to tetrathioacetate phthalocyanine **23** and silane derivative **25**. Reagents and conditions: (i) 3-bromopropionyl chloride, THF/CH_2Cl_2, rt, 72 h; (ii) KSAc, acetone, rt 24 h, 60 °C 48 h; (iii) 3-bromopropionyl chloride, Et_3N, THF/CH_2Cl_2, rt, 24 h; (iv) $HSi(OEt)_3$, H_2PtCl_6, dry THF, rt, Ar, 48 h.

Thus, the approach was changed. Firstly, acrylic acid was replaced with the next shortest possible linkers, 3-butenoic and 4-pentenoic acids. Secondly, the reaction conditions were optimized using monohydroxy porphyrin **26** as a basic structure. Porphyrin was selected because of the simple synthesis and good solubility that greatly facilitated the purification and analysis. Porphyrins **27** and **29** with a terminal double bond were synthesized starting from compound **26** and either 3-butenoic acid or 4-pentenoic acid, respectively, by DCC-DMAP method (Scheme 5.7). The products were obtained with good yields, over 80 %.

From the literature it is evident that the catalyst plays a crucial role in hydrosilylations.[90,91,92] In most of the cases an unwanted side process, the reduction of a double bond, competes with the hydrosilylation reaction. Chromophores with silane anchors isolated in pure form are rare, and the compounds used for immobilization are usually mixtures of products.

Sometimes the reduction problem can be solved by a proper treatment of catalyst[90], thus we decided to use three different catalytic systems. **Cat1** was the commercial Speier catalyst dissolved in dry THF. Without the pretreatment it gave mostly the reduced compound as the reaction product. Therefore, a catalyst portion of commercial Speier powder was dried in a vacuum oven at 150 °C for 4 h before use, dissolved in 2-propanol and sealed under argon, thus making the system **Cat2**. Third catalyst (**Cat3**) was the commercial Karstedt catalyst (platinum(0)-1,3-divinyl-1,1,3,3-tetramethyldisiloxane complex solution (Pt ~2 %) in xylene), which was diluted in sodium-distilled toluene and stored under argon.

Considering the balance between the reactivity and stability of silane-decorated compounds, two hydrosilanes were selected for experiments, namely triethoxysilane $HSi(OEt)_3$ and chlorodimethylsilane $HSiMe_2Cl$. Since we were aiming at the pure individual compounds, stability of the silylated products during purification had to be taken into account. Chromatographic isolation of trialkoxysilanes is possible[59,93], but chlorodimethylsilane is far too reactive for separation on Silica. Therefore, a chlorodimethylsilane anchor was converted into a dimethylmethoxysilane group[94], thus making it suitable for the purification by conventional methods. Compound **27** and **Cat2** were used to prepare porphyrin **28**, and compound **29** and **Cat3** were used to produce product **30** (Scheme 5.7). Hydrogenated products (reduced double bond) were still observed in reactions, but only in minor amounts. Products **28** and **30** were isolated with 39 % and 67 % yields, respectively, which indicated that Karstedt catalyst (**Cat3**) worked better with triethoxysilane.

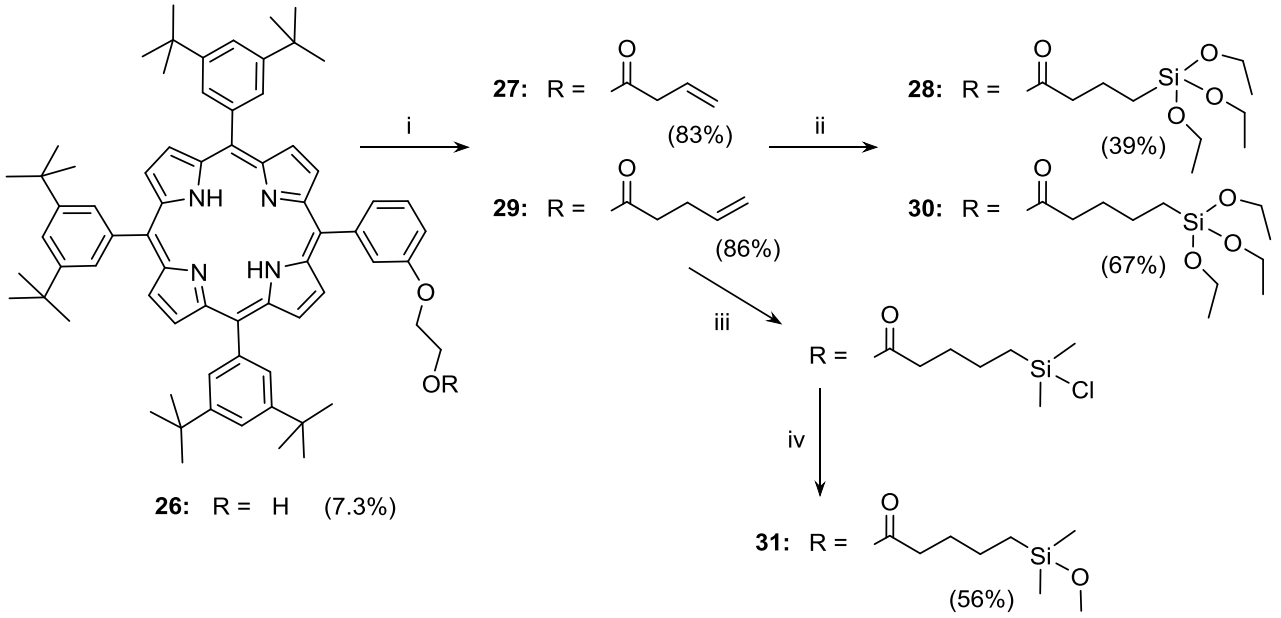

SCHEME 5.7 Synthetic route to mono(triethoxysilane) porphyrins **28** and **30**, and mono(dimethylmethoxysilane) porphyrin **31**. Reagents and conditions: (i) 3-butenoic acid/4-pentenoic acid, DCC, DMAP, CH_2Cl_2, rt, 72 h; (ii) $HSi(OEt)_3$, **Cat2**/**Cat3**, dist. toluene, Ar, 0 °C/rt, 2 h; (iii) $HSiMe_2Cl$, **Cat2**, dist. toluene, Ar, 0 °C/rt, 2 h; (iv) MeOH, dry Et_3N, rt, 2 h.

Porphyrin **29** was also used for synthesis of dimethylmethoxysilane porphyrin **31** (Scheme 5.7). At first, chlorodimethylsilane anchor was attached on a terminal double bond of porphyrin. The chlorine atom in the anchor was replaced by methoxy group in the second step. Substitution of chlorine was necessary not only to make the purification possible but also to simplify the product's handling and extend its shelf life. Synthesis of porphyrin **31** was carried out using **Cat2**. Again, hydrogenated compound was found in the reaction mixture, but it could be separated chromatographically, and the target product **31** was obtained with 56 % yield.

Same reaction was also repeated using **Cat3**. After 2 h of stirring at room temperature, starting material was still left. Reaction time was extended to 3 days, but the full conversion of starting material was not achieved. After a MeOH/Et_3N treatment, the obtained product was a mixture of unreacted starting material **29** and a hydrogenated compound.

After optimizing the hydrosilylation with porphyrin, the same reaction conditions were applied to prepare the phthalocyanine derivatives. As we have already learned, Karstedt catalyst (**Cat3**) worked better with triethoxysilane. Therefore, Pc **34** was prepared using a similar method (Scheme 5.8), and the yield was just as high as in porphyrin reaction.

Dimethylmethoxysilane porphyrin **31** could only be prepared using dried Speier catalyst (**Cat2**), so phthalocyanine **35** was synthesized the same way. At room temperature the reaction did not proceed and only starting material was recovered. Therefore, the reaction mixture was stirred at 80 °C for 6 h. The second step of the synthesis was over after 1 h, yielding dimethylmethoxysilyl Pc (Scheme 5.8).

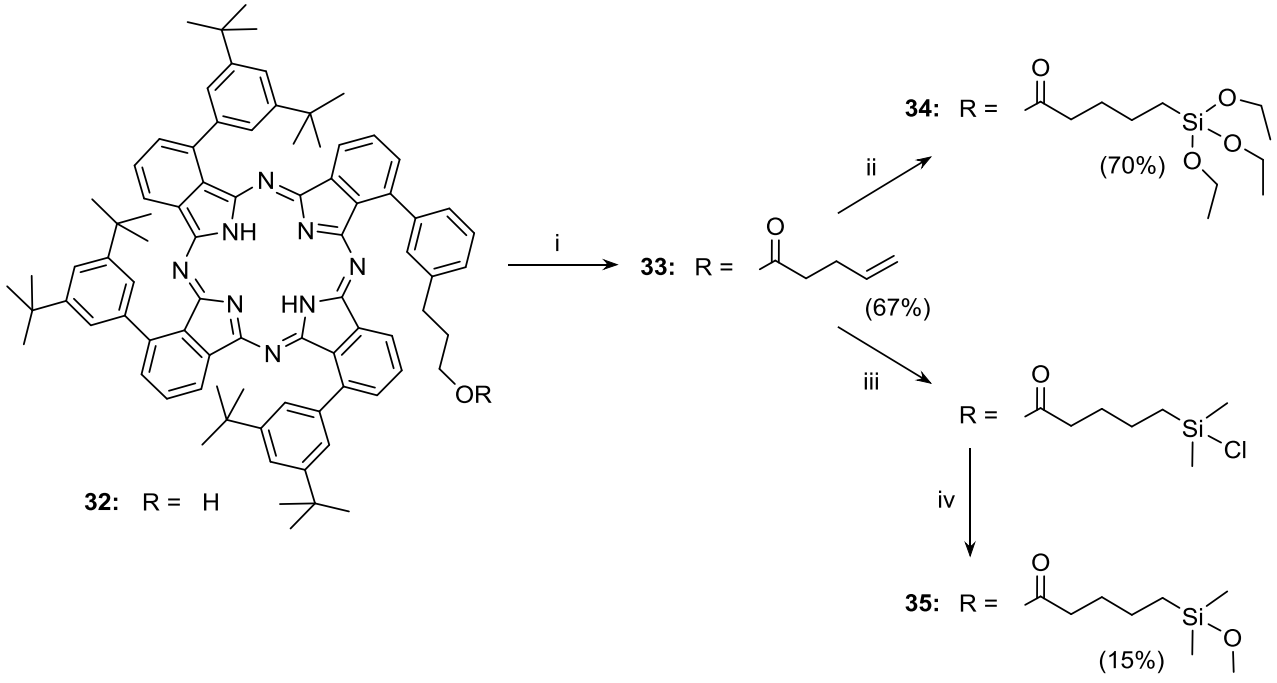

SCHEME 5.8 Synthetic route to mono(triethoxysilane) phthalocyanine **34** and mono(dimethylmethoxysilane) phthalocyanine **35**. Reagents and conditions: (i) 4-pentenoic acid, DCC, DMAP, CH_2Cl_2, rt, 24 h; (ii) $HSi(OEt)_3$, **Cat3**, dist. toluene, Ar, 0 °C /rt, 2 h; (iii) $HSiMe_2Cl$, **Cat2**, dist. toluene, Ar, 80 °C, 6 h; (iv) dist. toluene, MeOH, dry Et_3N, rt, 1 h.

A siloxane-anchor was also introduced in PDI molecule. Hydroxy-PDI **36** was prepared according to a literature procedure.[95] A shorter linker, 3-butenoic acid, and Karstedt catalyst (**Cat3**), were used to make a siloxane-PDI **38**, as presented in Scheme 5.9.

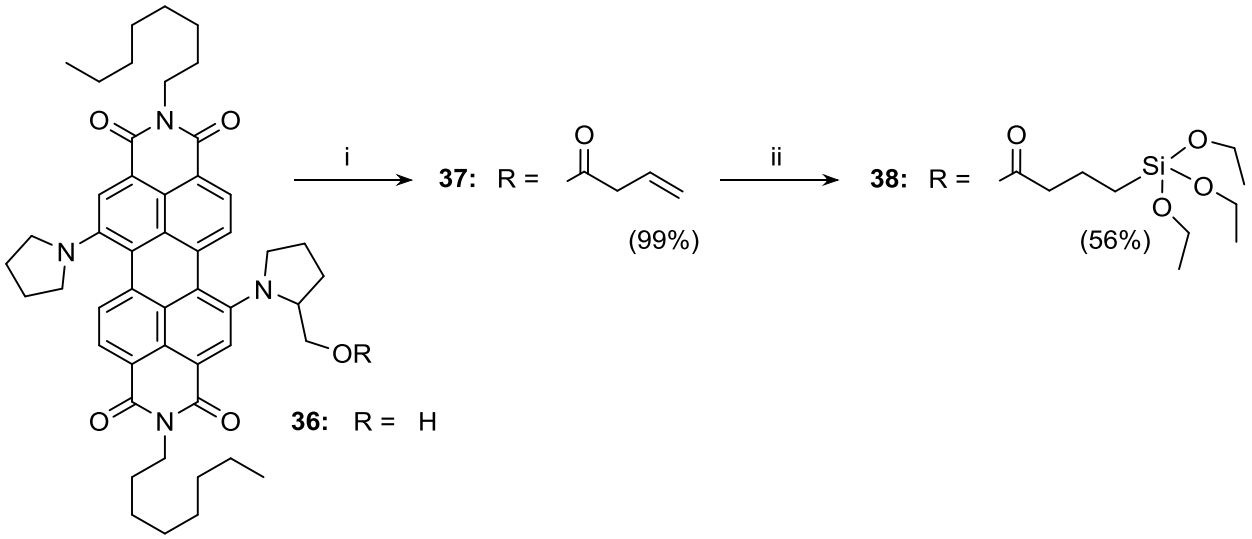

SCHEME 5.9 Synthetic route to pyr-PDI-Si(OEt)$_3$ **38**. Reagents and conditions: (i) 3-butenoic acid, DCC, DMAP, CH_2Cl_2, rt, 20 h; (ii) $HSi(OEt)_3$, **Cat3**, dist. toluene, Ar, 0 °C /rt, 2 h.

5.1.3 Chromophores for multicomponent assemblies [III,IV]

The use of monomolecular layers as coatings has certain disadvantages. Layers are sensitive to the surface defects, and therefore a full and uniform coverage is difficult to achieve and control. Single molecule thick films are easy to damage, and their optical density is low. Thickening the film solves most of these problems, but the regular arrangement of the layers remains a big question mark, unless a special deposition method is used.

In our studies we decided to build off-surface growing multicomponent assemblies using perylene imides decorated with terpyridine moieties. We selected perylene imide as a core dye, chiefly due to its superior stability and synthetic accessibility. To make the geometry of supramolecular arrays more predictable and close to linear, we planned to connect the terpyridyl ligands to PDIs either at the imide positions (PMIs **53**, **55**, **63**) or at the 1,7-positions of the *bay*-region by a direct aryl-aryl bonding (PDIs **50**, **65**).

The synthetic route towards terpyridyl building blocks **41** and **43** is shown on Scheme 5.10. Aniline-tpy **45** was synthesized starting from acetyl pyridine (**42**) and 4-nitrobenzaldehyde (**43**). The synthesis was done according to the literature procedure,[96] but the purification was performed by column chromatography on alumina instead of recrystallization.

The borylation of commercial bromophenylterpyridine **39** was done with a moderate yield of 50 % producing tpy-boronic derivative **41**. Attempts to improve the reaction efficiency by changing the base from KOAc to NaOAc and by using the catalyst $PdCl_2$ and the ligand [dppf = 1,1'-bis(diphenylphosphanyl)ferrocene] as separate reagents did not increase the yield.

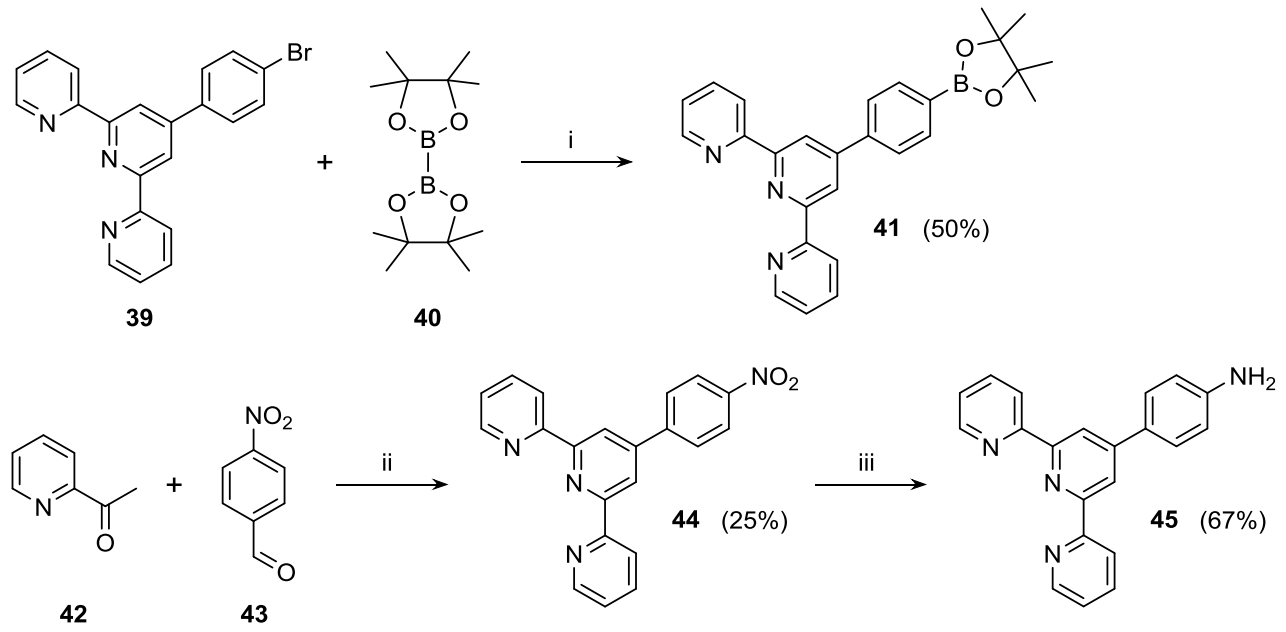

SCHEME 5.10 Synthetic routes to boron-tpy **41** and aniline-tpy **45**. Reagents and conditions: (i) KOAc, $Pd(dppf)Cl_2 \cdot Cl_2CH_2$, DMSO, Ar, 80 °C, 45 min; (ii) KOH (aq), conc. NH_4OH, MeOH, rt, 5 days; (iii) $SnCl_2 \cdot 2H_2O$, conc. HCl, 80 °C, 8 h.

Boron-tpy **41** was used in a Suzuki coupling reaction with 2-(benzyloxymethyl)pyrrolidine substituted PDI **46**[95], which was a pure 1,7-dibromo isomer (Scheme 5.11).[51] The reaction was done in a toluene-water biphase system with Pd catalyst. Product **47** was purified using automated low-pressure Combiflash chromatography on an alumina column. Silica could not be used for the purification because of its excessive retention of terpyridyl-containing compounds. In the next few steps a siloxane anchor, which provides a reliable and strong connection to the surface, was introduced to the molecule. As shown on Scheme 5.11, removal of a benzyl group of **47** was performed using boron tribromide, and the hydroxy-PDI **48** was subjected to acylation and hydrosilylation according to the procedures established earlier. Following the route optimized on phthalocyanines and porphyrins as described in the previous chapter, siloxane-anchored tpy-PDI **50** was obtained with a relatively high yield.

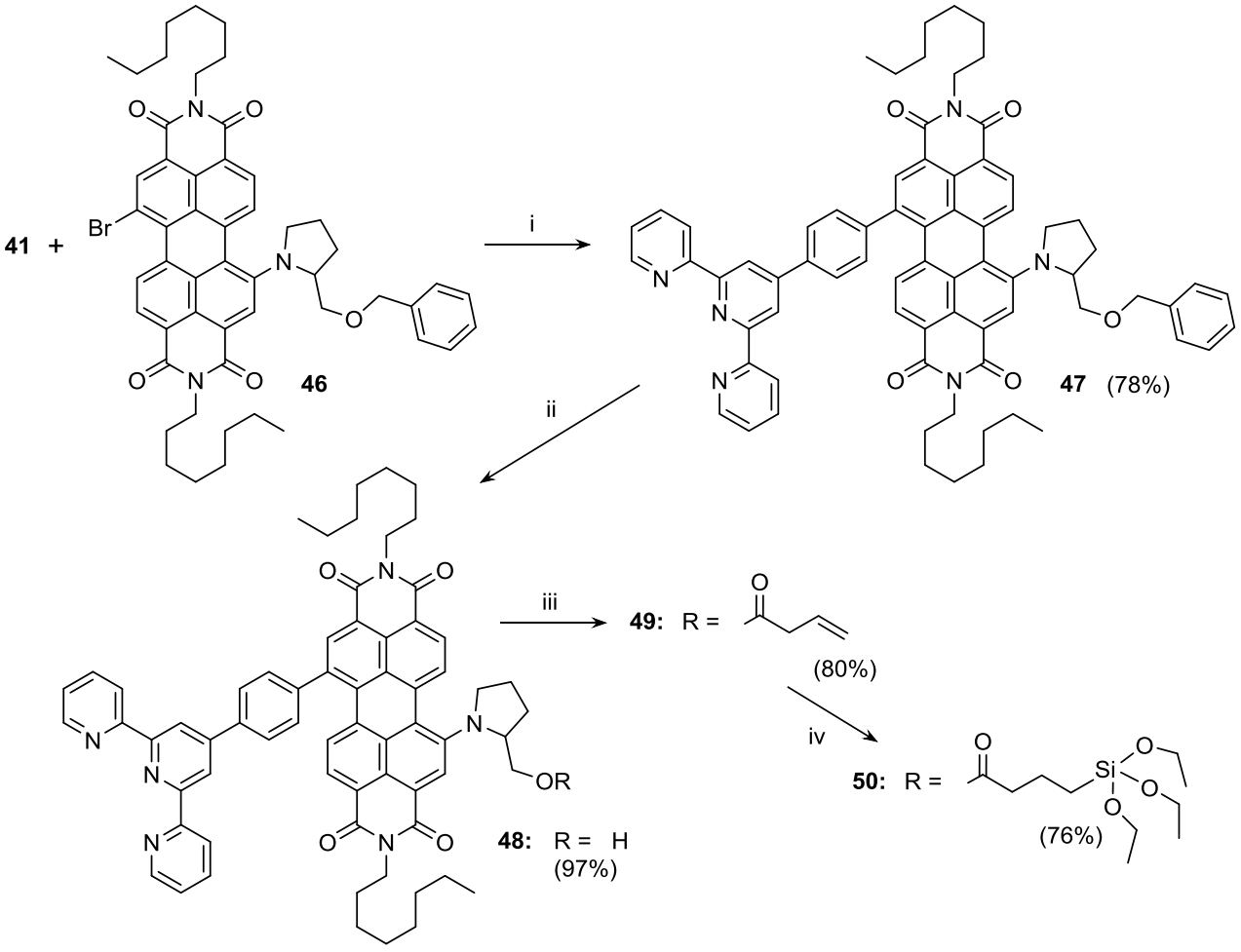

SCHEME 5.11 Synthetic route to tpy-PDI **47** and tpy-PDI-Si(OEt)$_3$ **50**. Reagents and conditions: (i) TBACl, Pd(dppf)$Cl_2 \cdot Cl_2CH_2$, K_2CO_3 (aq), toluene, 90 °C, 19 h; (ii) BBr_3, dry CH_2Cl_2, 0 °C, 4 h; (iii) 3-butenoic acid, DCC, DMAP, CH_2Cl_2, rt, 3.5 h; (iv) $HSi(OEt)_3$, **Cat3**, dist. toluene, Ar, 0 °C /rt, 4 h.

The siloxane anchor provides a stable and reliable bonding to inorganic oxides. However, it does not allow the chromophore core to go into a close proximity to the surface, neither does it ensure the orthogonal orientation of the dye relative to substrate. In that sense, the carboxylic group might be a better choice, or, in the case of perylene derivatives, an anhydride cycle. The anhydride fragment makes an anchor via a ring opening and the resultant dicarboxylates groups bind to the substrate surface.[97]

The anhydride cycle as an anchor group let us to select the *bay*-region substituents' at will. In order to have a choice of absorption profiles and redox potentials of the immobilized layers, we have prepared three different perylene monoimide (PMI) monoanhydrides **53**, **55**, and **63** with different *bay*-substituents.

Perylene monoanhydride-diester **51** was prepared by a known method.[98] Aniline-terpyridine **45** was connected to the PMI unit (Scheme 5.12) by an imidization. An acid hydrolysis of tpy-PMI diester **52** with *p*-toluenesulfonic acid (*p*-TsOH) in toluene at elevated temperature yielded tpy-PMI monoanhydride **53** in 94 % yield. Purification of product **53** was not that straightforward because of its poor solubility in common organic solvents. Extraction proved to be inefficient, and finally the remaining of sulfonic acid was removed by suspending the dry substance in water, with a subsequent centrifugation. Product **53** was treated this way several times, and disappearance of *p*-TsOH was controlled by pH.

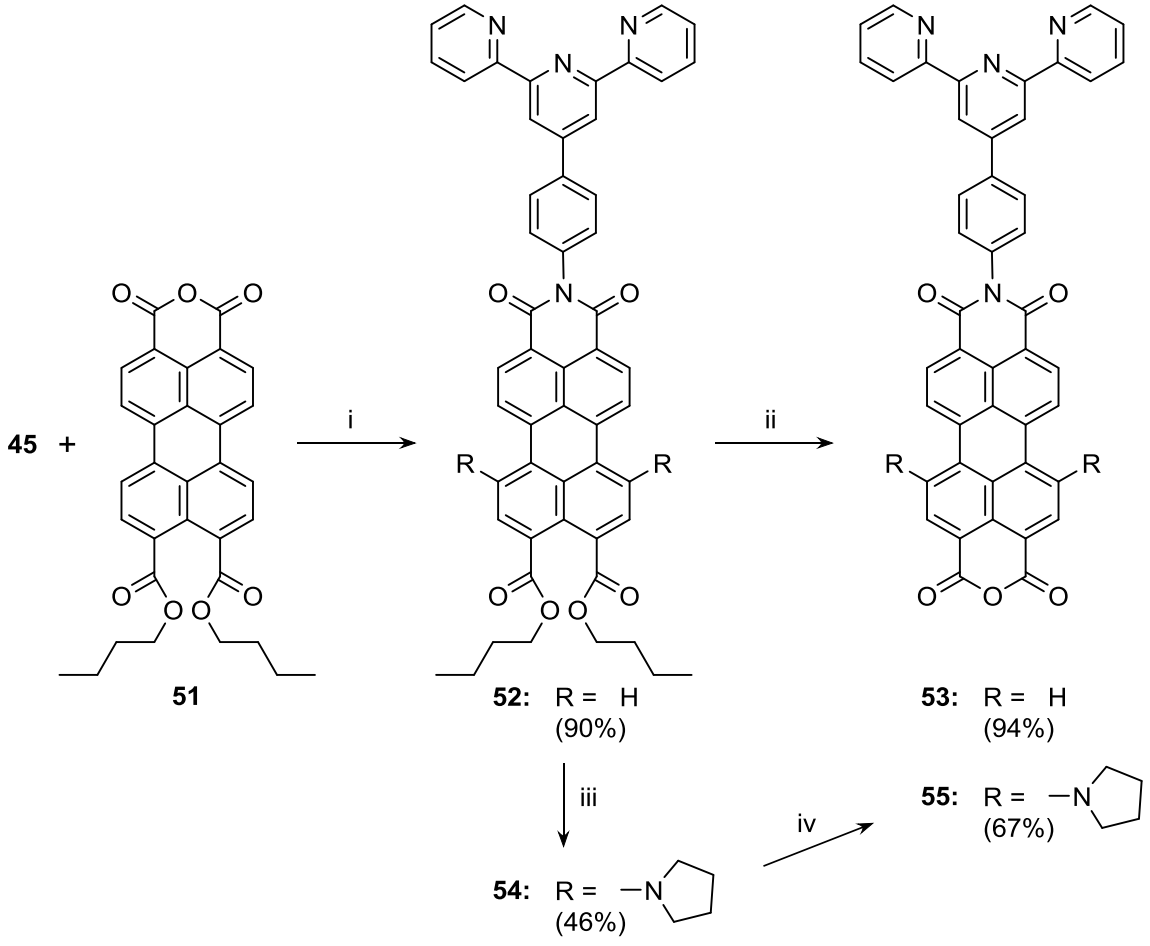

SCHEME 5.12 Synthetic route to tpy-PMI anhydride **53** and tpy-PMI-$(pyr)_2$ anhydride **55**. Reagents and conditions: (i) imidazole, toluene, 140 °C, 4 h; (ii) *p*-TsOH·H_2O, toluene, 100 °C, 23 h; (iii) pyrrolidine, $CuCl_2$ (anhydr.), drying tube, rt, 44 h; (iv) *p*-TsOH·H_2O, toluene, 100 °C, 5 days.

Bay-substituted PMI anhydride was prepared as shown on Scheme 5.12. 1,6-Bis(pyrrolidine)-PMI diester **54** was synthesized from PMI **52** by a direct amination with pyrrolidine catalyzed by $CuCl_2$. The reaction progress could be monitored by its color. After dissolving compound **52** in pyrrolidine and addition of copper chloride, the reaction mixture changed rapidly from dark red to green. After

15 min it was already blue, but the reaction time was extended for another hour to allow disubstitution to occur completely. In fact, mono-substituted pyrrolidine PMI was not observed in the reaction products at all. Purification of product **54** with column chromatography was not successful, thus the preparative TLC plates had to use. An acid hydrolysis of tpy-PMI-$(pyr)_2$ diester **54** was done similarly as for unsubstituted PMI **52**, though longer reaction time, larger excess of *p*-TsOH, and elevated temperature were needed to complete the reaction. 1,6-Bis(pyrrolidine)-PMI anhydride **55** was obtained as a dark blue solid with 67 % yield.

1,7-*Bay*-substituted PMI with terpyridine moiety was also prepared (Scheme 5.13). Perylene tetraester (PTE) **57** was obtained via esterification of commercially available PTCDA **56** with an alkanol and alkyl halide in homogeneous solution in 84 % yield by following the literature procedure.[99] PTE **57** was brominated in the presence of a base and molecular bromine in CH_2Cl_2 at room temperature. Dibromo PTE was obtained in 91 % yield as a mixture of 1,7- and 1,6-regioisomers (4:1). A repeated recrystallization afforded pure 1,7-dibromo PTE **58**.[100] Coupling of 4-nitrophenylboronic acid with compound **58** was carried out under Suzuki conditions and we obtained desired *bay*-substituted product **59**. Substituted PTE **59** was then selectively hydrolyzed by *p*-TsOH to yield monoanhydride-diester **60** as a precipitate, which upon imidization with tpy **45** and imidazole produced PMI diester **61** and PDI **62** as dark red solids in 57 and 10 % yields, respectively. The crucial step in the synthesis of **60** was the selective hydrolysis with *p*-TsOH, as even a slight excess of *p*-TsOH, wrong reaction temperature or inappropriate solvent, resulted in the formation of bisanhydride. A mixture of toluene and heptane (5:1 v/v), 1.2 eq. of *p*-TsOH and heating at 95 °C turned out to be the optimal conditions, which prevented the second hydrolysis. The second diester moiety of PMI **61** was later hydrolyzed to an anhydride by using excess of *p*-TsOH in toluene. The target compound **63** was obtained as red solid in 84 % yield.

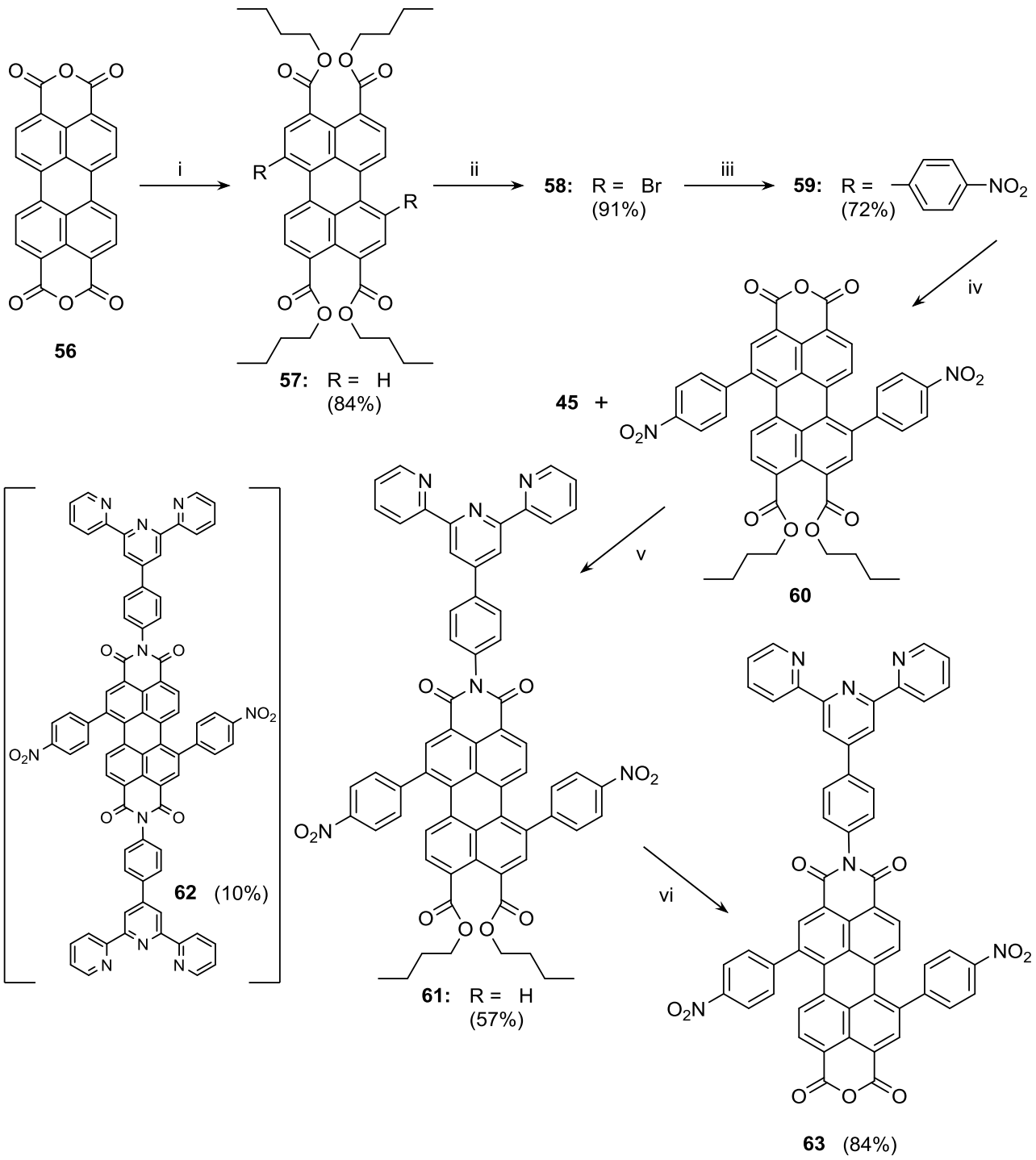

SCHEME 5.13 Synthetic route to tpy-PMI-$(NO_2)_2$ anhydride **63**. Reagents and conditions: (i) *n*-BuOH, DBU, 1-bromobutane, DMF, 60 °C, 3 h; (ii) Br_2, K_2CO_3, CH_2Cl_2, rt, 24 h; (iii) 4-nitrophenylboronic acid, TBACl, Pd(dppf)Cl_2·Cl_2CH_2, K_2CO_3 (aq), toluene, Ar, 90 °C, 3 h; (iv) *p*-TsOH·H_2O, toluene/heptane 5:1, 95 °C, 5 h; (v) imidazole, toluene, 140 °C, 4 h; (vi) *p*-TsOH·H_2O, toluene, 90 °C, 18 h.

Having four terpyridyl-substituted perylene imides with anchors as initial sockets on a surface, we were still missing the linkers, which can be bound to it. These middle-layer components of our multicomponent assemblies required compounds with two terpyridine moieties located at the opposite sides of the chromophore core. Unlike the published molecules with tpy unit at the imide position, we prepared PDI with double terpyridine units at the *bay*-region. Bis(substituted) tpy-PDI **65** (Scheme 5.14) was synthesized from dibromo-PDI **64**, which was a pure 1,7-regioisomer.[51] The reaction conditions were similar to those described for PDI **47**. However, the purification was not that straightforward because of the minor amount of mono-tpy-substituted PDI. The column separation did not provide enough resolution, and the complete separation was achieved only using preparative TLC on the alumina plates. The modest yield of the target compound can be explained by its limited solubility and significant losses during separation. However, with more careful purification procedure, the yield could be pushed up to 35 %.

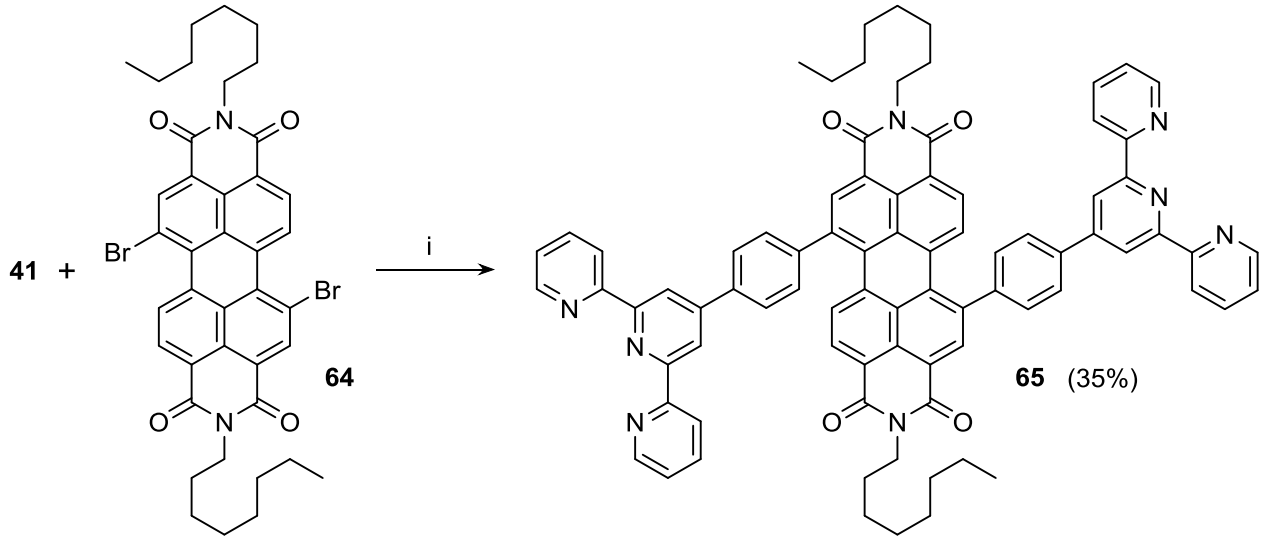

SCHEME 5.14 Synthetic route to $(tpy)_2$-PDI **65**. Reagents and conditions: (i) TBACl, $Pd(dppf)Cl_2 \cdot Cl_2CH_2$, K_2CO_3 (aq), toluene, 90 °C, 18 h.

All in all, we have synthesized 16 chromophores with the anchor groups suitable for the SAM deposition. These are summarized in Table 5.1.

TABLE 5.1 Basic structures of synthesized products and their anchors.

	-OPFP	-SAc	-Si(OEt)$_3$	-SiOMe	-anhydride
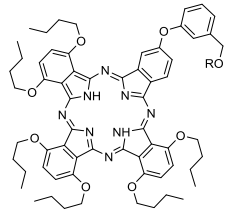	**6**	**19**			
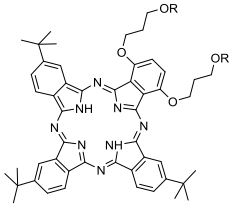	**12**	**21**			
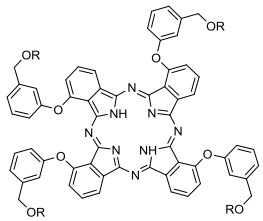	**17**	**23**	**25**		
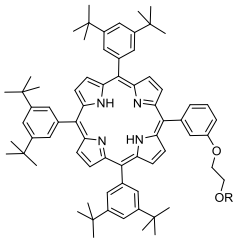			**28 / 30**	**31**	
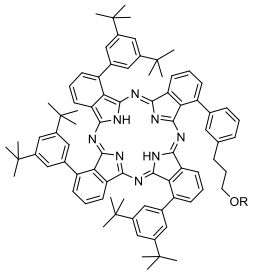			**34**	**35**	
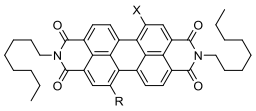			**38 / 50**	**38**: X = pyrrolidyl **50**: X = terpyridyl	
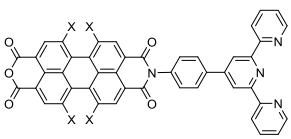			**53**: X = hydrogen **55**: X = 1,6-dipyrrolidyl **63**: X =1,7-di(nitrophenyl)		**53 / 55 / 63**

5.2 Self-assembling on solid surface

This chapter describes the preparations of various SAMs. The fabrication of molecular layers was initially done with phthalocyanines via two-step procedure, as it followed the most established protocol. After gaining enough experience we proceeded to one-step SAM fabrications and multilayer assembling.

The analysis of the quality of the prepared films relied chiefly on the measurements of the absorption spectra. The estimation of the area per single molecule of the chromophores in the layer was based on the optical density of the films and the substance's extinction coefficients. The obtained mean molecular area (mma) values were compared with the estimated dimensions of the molecules, thus giving a rough idea of how tightly or loosely the molecules were packed within the layer.

5.2.1 2-step SAMs [I]

Phthalocyanines decorated with pentafluorophenyl ester moieties were immobilized on glass and ITO substrates. SAMs were done with a two-step process, where the plates were first activated with 3-aminopropyltrimethoxysilane in dry toluene at 105 °C for 1 h. Pcs were then covalently attached to the aminopropylsilylated surface by immersing the plates into a solution of PFP-esters **6**, **12**, or **17** in dry toluene. This second step was completed in 2 h at 105 °C. Both steps were done under argon. To remove residual physisorbed Pc, the samples were sonicated in toluene and CH_2Cl_2 after the second step. After drying in argon, the UV-vis spectra of the plates with SAMs were measured to reveal the presence and amount of immobilized chromophore. Since both sides of the substrates were activated, the monolayers were formed on each side of the plates. Thus the absorption spectra in Figures 5.15 and 5.16 are of double intensity.

The absorbance of SAM was obtained by subtracting the absorbance of a clean substrate from that of the plate with SAM. The absorption spectrum of the SAM of hexabutoxy single-linked Pc **6** on glass substrate showed clear Q- and Soret bands (Fig. 5.15), which both were shifted towards shorter wavelengths compared to absorption maxima of Pc **6** in $CHCl_3$. For unknown reasons, the absorption of SAM **6** on ITO was five times smaller than on glass. Results were the same with an extended reaction time of both steps, so it seems that the compound **6** bonded very weakly onto ITO. However, the shapes of the absorption spectra of SAM **6** on glass and ITO were the same and very similar to the spectrum in solution.

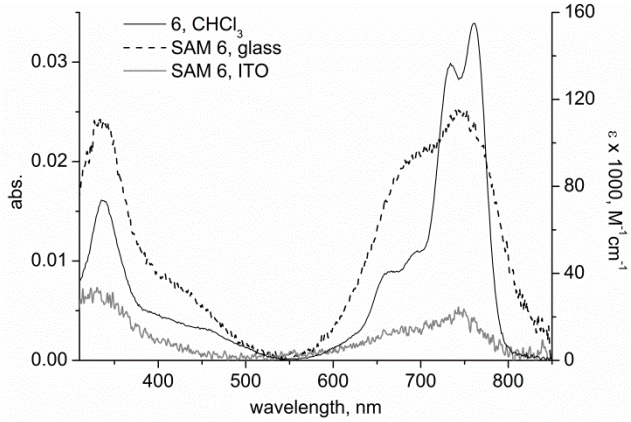

FIGURE 5.15 Absorption spectra of mono(pentafluorophenyl ester) Pc **6** in solution on molar absorptivity (***ε***) scale, and SAM **6** on glass and ITO.

In the absorption spectrum of SAM of tris(*tert*-butyl) double-linked Pc **12** on glass and ITO (Fig. 5.16a), the Q-band was blue-shifted by almost 50 nm compared to the absorption spectrum of Pc **12** in $CHCl_3$. The spectra of SAM **12** on glass and on ITO were perfectly same on both substrates. Also the absorption spectra of SAM of tetra-linked Pc **17** on glass and ITO were almost identical (Fig. 5.16b). The spectra showed the Q-band maxima around 695 nm, which was between the two maxima in the absorption spectrum of compound **17** in $CHCl_3$.

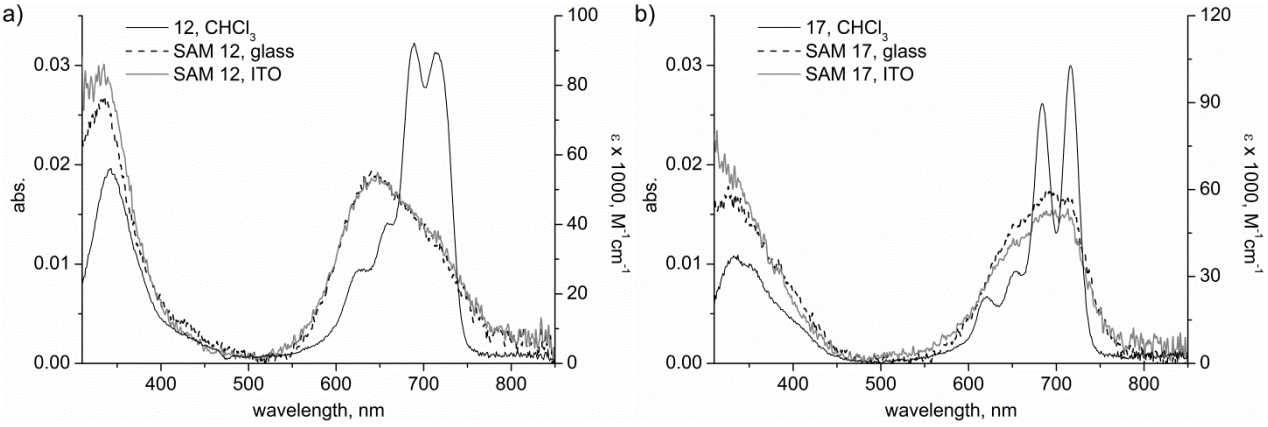

FIGURE 5.16 Absorption spectra of a) bis(pentafluorophenyl ester) Pc **12** in solution and SAM **12** on glass and ITO, b) tetra(pentafluorophenyl ester) Pc **17** in solution and SAM **17** on glass and ITO. Solution spectra are on molar absorptivity (***ε***) scale.

All phthalocyanines immobilized via the two-step process demonstrated significant broadening of their absorption bands, which can be attributed to the aggregation of chromophores within the layer.

5.2.2 1-step SAMs [I,II,III]

In a one-step process, the reaction vessel is loaded with a solution of a chromophore in a proper solvent, and an appropriate substrate is immersed into it. In some cases an inert atmosphere, heating, or an auxiliary substance is needed. As discussed previously, compound with a certain anchor should be chosen to bind to a specific surface.

Thiol anchor, gold surface [I]

In the case of the thioacetyl group, an oxidative addition of the S-Ac bond occurs on a gold surface, followed by a reductive elimination of the acetyl group (Ac).[7] For spectral measurements, a robust and optically transparent substrate is required. These were prepared by evaporation of a very thin (3 nm) gold layer onto glass plates. Gold substrates were immersed into solutions of Pcs **19**, **21**, and **23** in CH_2Cl_2. The plates were kept at room temperature for 30 min, and after that rinsed several times with CH_2Cl_2 and $CHCl_3$ to remove unbound Pc molecules.

Absorption spectra of the SAMs **19**, **21**, and **23** on gold surface showed a broad Q-band between 600-800 nm (Fig. 5.17). Compared to the spectra of solutions, the absorption maxima of SAM **19** (single linker) and **21** (two linkers) were shifted to shorter wavelengths, even though defining the maxima of the spectra was difficult because of their low intensity and broad shape. The shift of the band maxima of SAM of bis-linked Pc **21** on gold was as high as 40 nm. This huge shift was also seen in the spectrum of SAM of bis-linked phthalocyanine on glass/ITO (compound **12**).

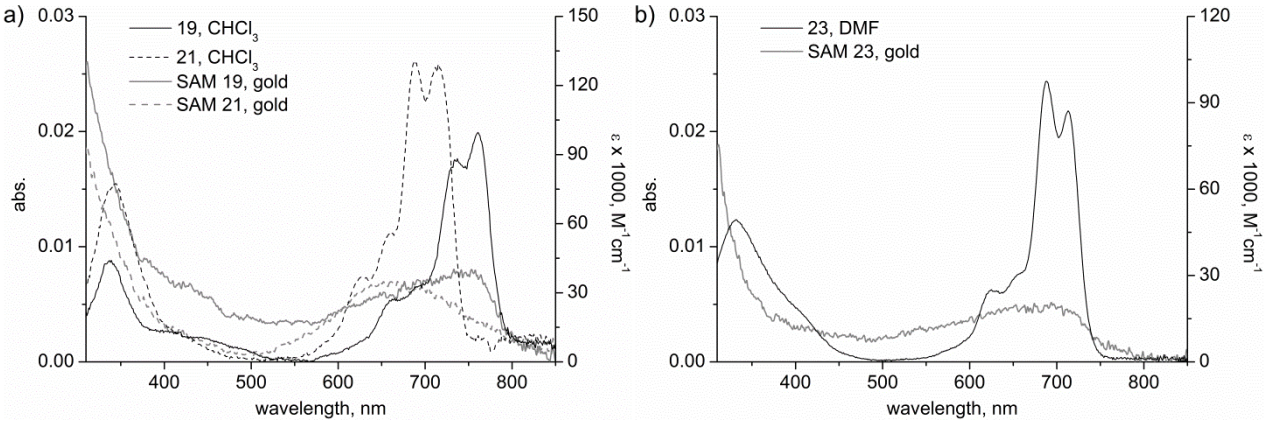

FIGURE 5.17 Absorption spectra of a) monothioacetate Pc **19** and bisthioacetate Pc **21** in solution, and SAM **19** and **21** on gold, b) tetrathioacetate Pc **23** in solution and SAM **23** on gold. Solution spectra are on molar absorptivity (***ε***) scale.

Siloxane anchor, inorganic oxide surfaces [II,III]

The silane-anchored chromophores (porphyrins **28**, **30**, **31**; phthalocyanines **34**, **35**) were assembled as monomolecular layers on metal oxides surfaces of ITO and aluminum-doped zinc oxide (AZO), and on quartz substrates (also PDI **38**). At first, an oven-dried reaction vessel was charged with a solution of the chromophore in distilled toluene and isopropyl amine under argon. SAMs were deposited by immersing the cleaned plates into solution, and keeping the reaction vessel at 105 °C for 2 h. After the deposition the plates were washed from unbound substances by sonication in toluene and CH_2Cl_2.

Considering the absorption spectra of monolayers on quartz, ITO, and AZO surfaces, one has to take into account that layers are formed on both sides of the substrates. To estimate the absorbances of single layers, the absorbances in Figures 5.18 and 5.19 should be divided by two. The absorption of free base porphyrin in solution shows the narrow Soret band and four small peaks of the Q-band (see Fig. 2.3). Same features were found also in the absorption spectra of SAMs, but both the Soret and Q-bands of SAMs were broadened. The absorption of SAM **28** (porphyrin with a C_4-triethoxysilane terminus) on quartz had the Soret band at 426 nm and at least two well visible peaks (514 nm and 553 nm) of the Q-band (Fig. 5.18a). Two other peaks of the Q-band were also present, but not so well resolved due to spectrophotometer sensitivity limit. The Soret band was red-shifted by 5 nm compare to the compound **29** in $CHCl_3$.

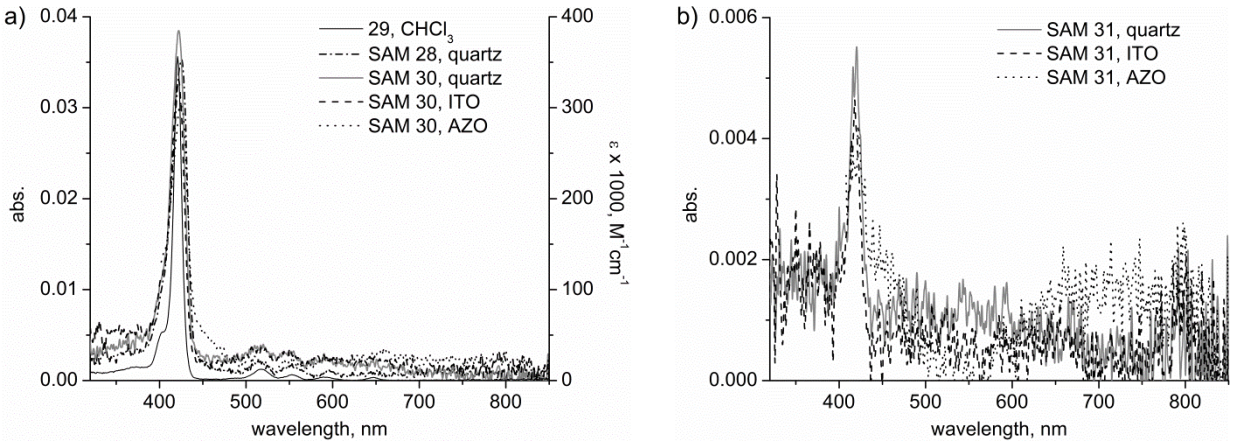

FIGURE 5.18 Absorption spectra of a) porphyrin **29** in solution on molar absorptivity (***ε***) scale, and SAM **28** and **30** on different substrates, b) SAM **31** on different substrates.

The spectrum of SAM **30** (porphyrin with C_5-triethoxysilane linker) on quartz and ITO corresponded well to the spectrum of porphyrin **29** in $CHCl_3$. SAM **30** on quartz and ITO had the Soret band at 422 nm and two peaks of the Q-band around 520 nm and 550 nm. SAM **30** on AZO had the Soret band at 424 nm. Surprisingly, SAM **31** with dimethylmethoxysilyl anchor had almost ten times lower absorbance than SAM **30**. Even though the absorbances were low, the Soret band was clearly

distinguishable in the spectra of SAM **31** around 420 nm (Fig. 5.18b). The spectra on the AZO substrates were plotted only till 400 nm because at lower wavelength ZnO layer starts to absorb.

Absorption spectra of SAMs of triethoxysilane-Pc **34** on quartz, ITO, and AZO had similar shape as Pc **33** in $CHCl_3$ (Fig. 5.19a). SAM **34** on quartz had two Q-band maxima at 713 nm and 679 nm, and in solution, these bands were few nanometers at lower wavelength. The Soret band was found in both spectra close to 340 nm. SAM **34** on ITO and AZO showed quite same maxima of the Q-band as in the absorption spectrum on quartz. The absorption of SAM **35** was so low that it was not visible from the noise. This correlated well with the result gained from porphyrins that dimethylmethoxysilyl-porphyrin SAM had ten times lower absorption than triethoxysilyl-porphyrin SAM. If the case is the same for Pcs, the absorption of SAM **35** would be, as it was, too low to be observed.

Bis-pyrrolidine PDI **38** was also attached on the quartz surface. The absorption spectrum of SAM **38** imitated nicely the spectrum of pyr-PDI **37** (Fig. 5.19b). The absorption bands were broadened for the SAM compared to solution but the band maxima corresponded quite well with PDI **37** in $CHCl_3$.

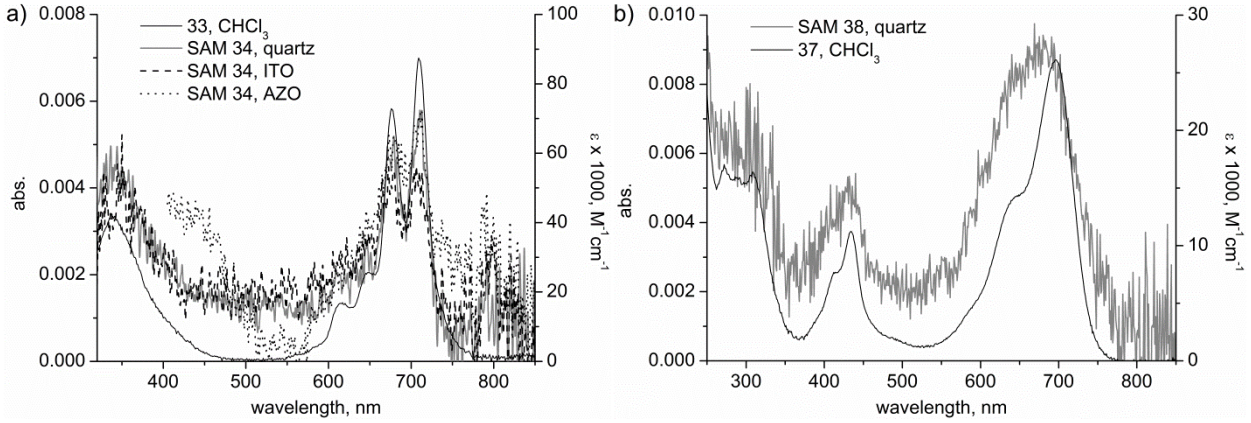

FIGURE 5.19 Absorption spectra of a) Pc **33** in solution and SAM **34** on different substrates, b) pyr-PDI **37** in solution and SAM **38** on quartz. Solution spectra are on molar absorptivity (***ε***) scale.

5.2.3 Multilayer arrays [III,IV]

The results of immobilization of porphyrinoids on solid substrates were encouraging. However, the preparation of terpyridyl-substituted porphyrins or phthalocyanines, especially asymmetric ones, looked so challenging that the core macrocycle was changed to a compound with higher stability and better synthetic yield, perylene imide. The molecules with the anchor groups (PDI **50**, PMIs **53**, **55**, **63**) were synthesized as described before and were immobilized on substrates. These compounds, when bound to the surface, would serve as sockets for further complexation of zinc ions

and attachment of another bis(terpyridyl)-substituted linkers, thus making possible a multilayer deposition. The four compounds represented two different orientations in the film, even though their terpyridine moiety expected to be pointed out from the surface. That is, perylene **50** was bound by a relatively long and flexible linker terminated by a siloxane group, which allowed a variety of orientations, while three PMIs **53**, **55**, and **63** were bound close to surface by the two carboxyls in a direction perpendicular to the substrate. Absorption spectra (Figures 5.20-5.22) showed optical densities ca. 0.01-0.005 in all cases, which evidenced that a layer of a reasonably good quality had formed. Next step would be an addition of zinc ion and further complexation of a second perylene layer.

According to the literature, zinc ions form complexes with terpyridines under very mild conditions and the complexation can be detected from their absorption spectra.[82,101] In our experiments, zinc acetate did not give stable complexes. Therefore, the counter ion was changed to zinc triflate $Zn(OTf)_2$. Complexation on the surface was done by immersing the substrate with the SAM in the $Zn(OTf)_2$ solution at room temperature for 1 h. Steady state absorption was used as a quick method to prove the formation of the complexes, and distinct changes in absorption were observed after complexation with zinc: an increase of the absorption intensity between 300 and 350 nm, and a decrease and sharpening around 270 nm. These correspond to the changes in the tpy unit absorption and thus indicate the formation of a zinc complex.[82]

First attempts to build the multilayer assembly on the surface were done with siloxane-anchored PDI **50**. The absorption spectrum of SAM **50** showed similar shapes as PDI **49** in $CHCl_3$ (Fig. 5.20). Even though the absorptions of the SAMs were low, the complexation with zinc triflate was nicely observed from the spectrum of the plate. The same changes in the absorption spectrum were seen as with complexation in chloroform: an increase of absorption between 300 and 350 nm and a decrease around 270 nm. An expected increase at 400 nm and 440 nm was also noticeable as these bands were more intense in the Zn-complex form of PDI (**47**+$Zn(OTf)_2$). The absorption of PDI SAMs around 640 nm was slightly red-shifted upon complexation as it was visible also in the solution studies.

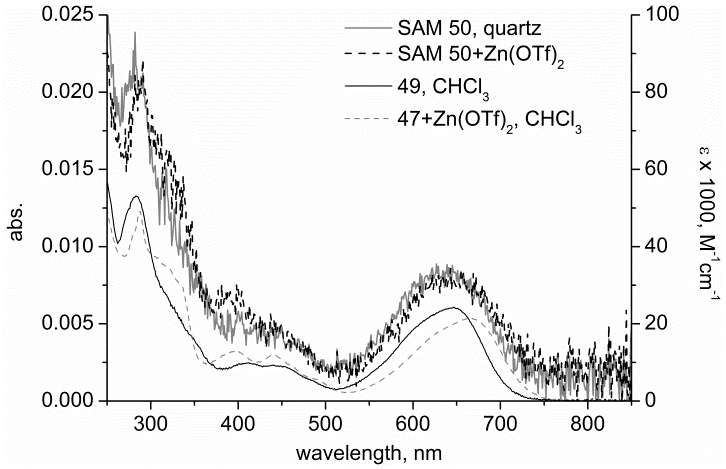

FIGURE 5.20 Absorption spectra of butenoic-PDI **49** and tpy-PDI **47** Zn-complex in solution on molar absorptivity (***ε***) scale, and SAM **50** and its Zn-complex on quartz.

Unfortunately, even though the dimer and trimer complexes were formed in solution, we were not able to build these on the surface. Most probably, this was due to a cramped geometry of the first layer initiated by the siloxane-terminated acyloxypyrrolidine linker. As seen with mma values (Chapter 5.2.4, Table 5.2), the film was too dense for a well-aligned monolayer. Obviously, a more rigid tether was needed to improve the orientation of the socket molecules in films. This task was successfully accomplished by using the PMI anhydrides, as described below.

Carboxyl anchor, aluminum oxide surface [IV]

It is known that the anhydride moiety can open up on the adsorption over TiO_2, providing strong chemical interactions with TiO_2 surfaces and effective electronic coupling by the carboxyl anchor.[102] The same phenomenon is also observed with the Al_2O_3 surface. Aluminum oxide is optically transparent down to 250 nm, and therefore quartz plates covered with a thin layer of Al_2O_3 were used as a substrate for multilayer formation studies. PMI anhydrides **53** and **55** (*bay*-unsubstituted and 1,6-di-pyrrolidyl derivatives, respectively) were immobilized on the Al_2O_3 surface by dissolving anhydride compounds in toluene/EtOH 9:1 mixture and by immersing the plates in the solution at 80 °C overnight. Ethanol is often reported to help in SAM formation, particularly with the carboxyl anchor.[8] However, the solubility of the anhydrides in neat EtOH was poor and addition of $CHCl_3$ or toluene was necessary. An excess of toluene was proved to be the best, as it also helped to increase the temperature of the reaction.

After washing, drying, and checking the UV-Vis absorption the plates with the socket layer were immersed into zinc triflate solution. Zinc triflate was dissolved in first attempts in $CHCl_3$/CH_3CN 4:1, but the absorption of anhydride had decreased extensively after the complexation (Fig. 5.21). This showed that a part of the anhydride was bonded weakly to the surface and the solvent system was

too strong to keep it intact. Therefore, further complexation with zinc triflate was done in toluene/EtOH 9:1 mixture, which provided good quality layers with little deterioration.

To our delight, the addition of a second layer over the first PMI sockets was much efficient. Bilayer films were prepared easily by immersing the Zn-complexed plates into solutions of PMI esters (**52** and **54**) at room temperature and incubating them overnight. As shown in Figure 5.21, double layers were formed nicely and the bands positions corresponded well with absorption of the PMI components (Fig. 5.22b). It should be noted that absorption of the bonded anhydrides must be compared with PMI diesters, as the anhydride cycle opens up upon immobilization.

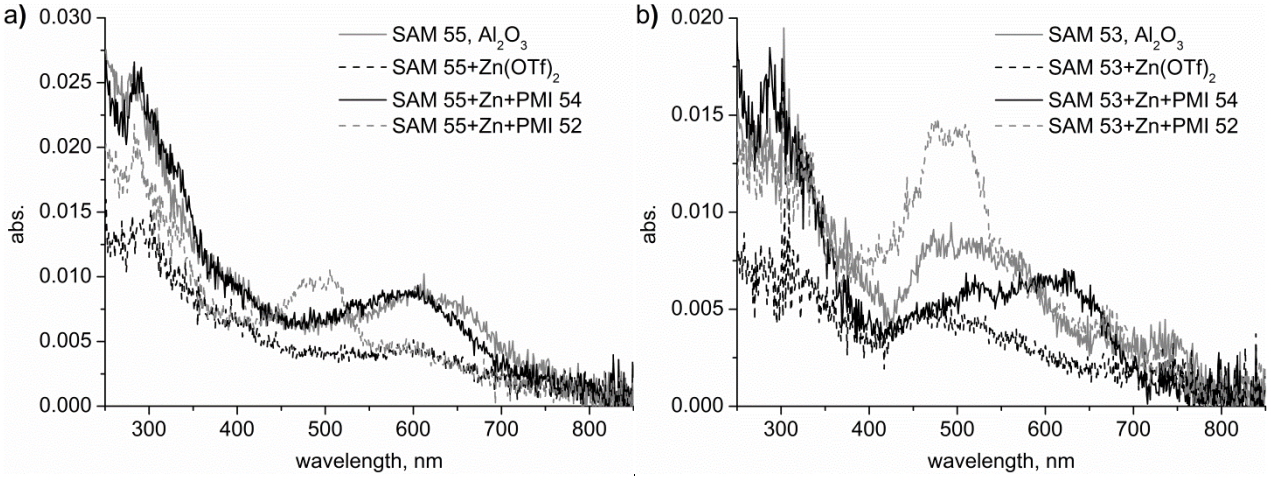

FIGURE 5.21 Absorption spectra of a) tpy-PMI-$(pyr)_2$ anhydride **55** on Al_2O_3 and b) tpy-PMI anhydride **53** on Al_2O_3, and their bilayers with PMI **52** and **54**.

Nitrophenyl-substituted PMI **63** was immobilized on the Al_2O_3 surface as well and proved to be an efficient socket. Bilayers with PMI diesters **52** and **54** were prepared with ease. Right from the deposition solution, SAM **63** with diester **52** gave too high absorption (Fig. 5.22a). However, after the plate was sonicated for 30 min and kept in neat toluene at 80 °C overnight, the absorption decreased to a reasonable value. It should be noted that a previously prepared bilayer of PMI **53** with tpy-PMI diester **52** atop also gave somewhat higher absorption than expected (Fig. 5.21b). Probably, it means that diester **52** intercalates easily into the base layer in addition to the coordinate bonding.

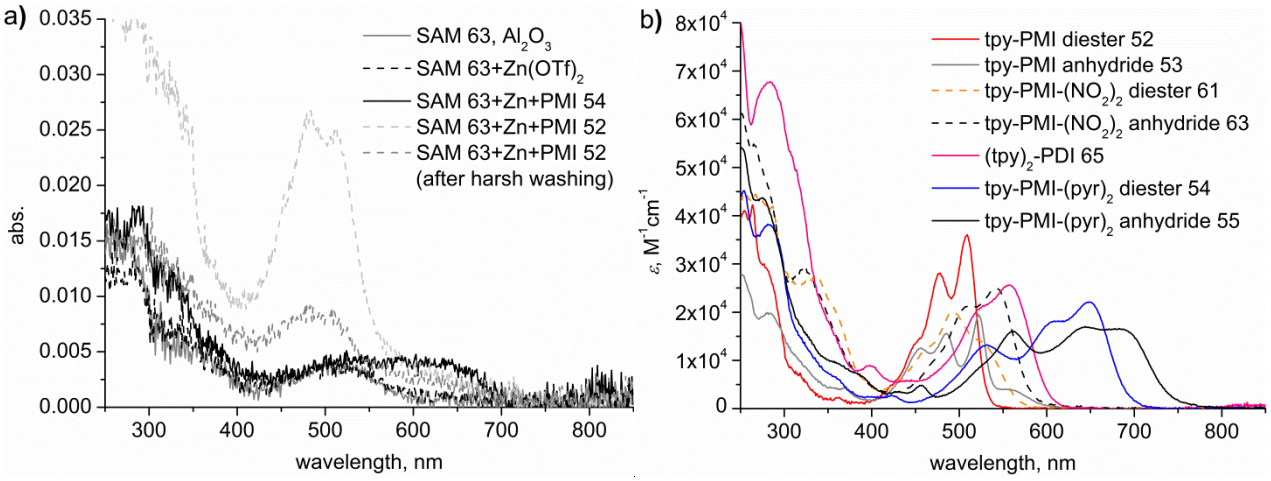

FIGURE 5.22 Absorption spectra of a) tpy-PMI-$(NO_2)_2$ anhydride **63** on Al_2O_3 and its bilayers with PMI **52** and **54**, and b) PMIs **52**-**55**, **61**, **63**, and PDI **65** in $CHCl_3$ on molar absorptivity (***ε***) scale.

The main drawback of tpy-PMI anhydride **53** was its poor solubility. It was not possible to prepare a proper solution of it, and the SAMs prepared from it were too weak in absorbance. In a drastic contrast, PMI anchors **55** and **63** were perfectly suitable as sockets and were largely employed for preparing the multilayer assemblies. Upon selection of appropriate components the procedure of multilayers' deposition was fairly straightforward. After bonding the initial PMI layer, zinc triflate was complexed on it. Second layer was added by immersing the substrate with Zn-PMI layer in to solution of bis-terpyridyl PDI **65**. The two last steps were repeated and ten layer assemblies were prepared.

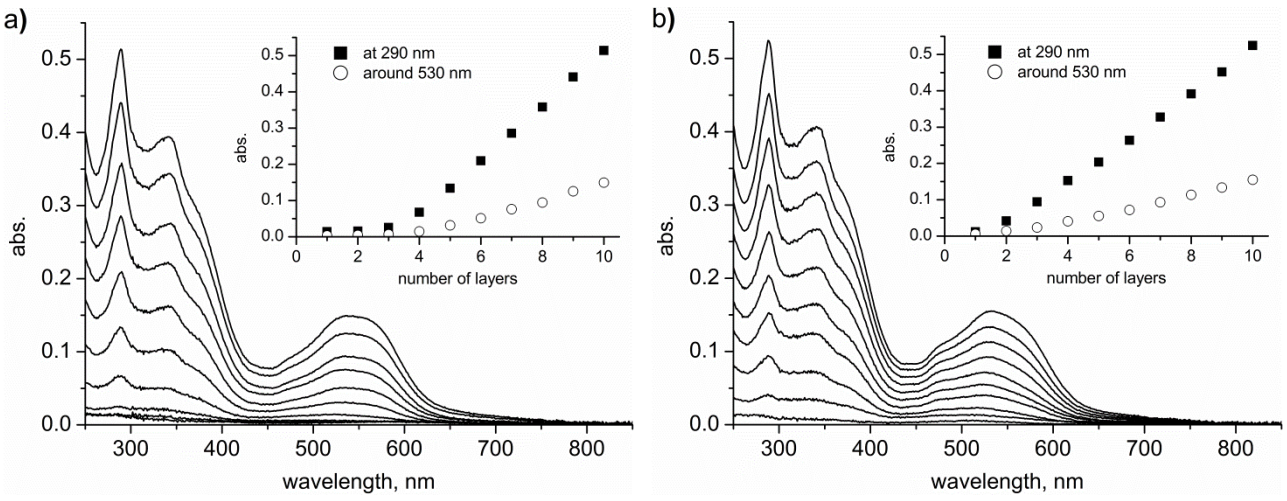

FIGURE 5.23 Absorption spectra of a) tpy-PMI-$(pyr)_2$ anhydride **55** on Al_2O_3, b) tpy-PMI-$(NO_2)_2$ anhydride **63** on Al_2O_3, and $(tpy)_2$-PDI **65** multilayers. The inset shows the absorbance at the absorption peaks at 290 nm (■) and the highest point around 530 nm (○) as a function of the number of layers.

Layer growth was monitored by the steady state absorption measurements (Fig. 5.23). These are presented in inset figures in Figure 5.23 at two different positions: at 290 nm and at the maximum around 530 nm. With PMI **55** anchor (Fig. 5.23a), the growth of layers of PDI **65** started slowly when compared with PMI **63** as socket (Fig. 5.23b). However, after ten layers intensities of absorption spectra were practically the same. Obviously, the base layer of PMIs **55** or **63** is not an ideally perfect monolayer, and some rearrangement is needed for the subsequent layers to accommodate in a regular structure. However, after few initial depositions the layers of PDI **63** began to grow steadily and with even increase in absorbance. This was in a drastic contrast with bis(nitrophenyl)-bis(terpyridyl) PDI **62** which have not produced any multilayer structures at all. Evidently, for building multilayered arrays the structure of the linker, bis(terpyridyl)-PDI, plays as crucial role as the nature of PMI socket. Indeed, we have done a very successful attempt and managed to prepare very stable, well absorbing multilayers. However, there is still much to study about the effect of geometry of the linkers and influence of various substituents on the film formation properties.

5.2.4 Comparison of the bonding densities [I-IV]

The absorption data of the films provides a possibility to estimate and compare the bonding densities of chromophores in SAMs. The space, which a molecule occupies in a layer, so-called mean molecular area (mma), can be calculated by the following formula:

$$mma = \frac{\varepsilon}{(N_A A)} \quad , \tag{1}$$

where ε is the molar absorptivity, N_A is the Avogadro constant and A is the absorbance of the layer. This is a rough estimation, as it assumes that the molar absorptivity of compounds in SAMs and in solution is the same. This is true only if the molecules are randomly oriented on the surface and if the chromophore-chromophore or chromophore-surface interactions are disregarded.[103] Thus the values are just approximate.

Reference values for the areas can be gained from a 3D structure, optimized with a standard method, in this case by MM2 calculations with Chem3D Pro (CambridgeSoft). As an example, in Figure 5.24 (right) a top view of the model of tpy-PMI is shown. Approximate dimensions are given by blue arrows. One also has to take into account van der Walls radii, thus 1.5 Å is added on all edges. This value is an average of hydrogen and carbon van der Walls radii, which also depends on the bond type, etc.[104] The mma value estimated this way is marked with a gray rectangle. These very rough approximations of molecular areas will be compared with the data calculated according to Equation 1.

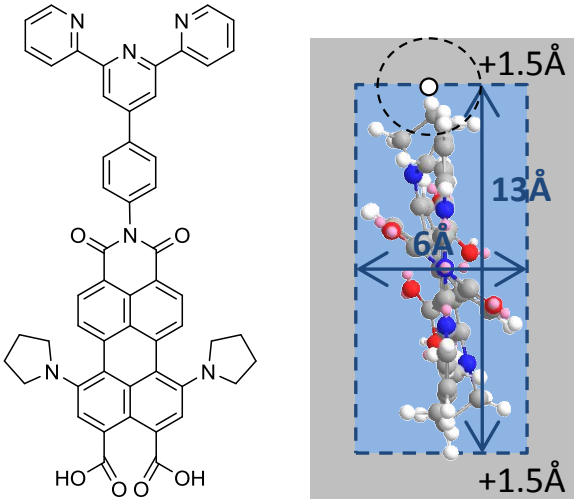

FIGURE 5.24 Left: structure of tpy-PMI; right: Chem3D model of tpy-PMI, top view, interatomic dimensions (blue arrows) and approximate size with van der Walls radii (grey rectangle).

The data are collected in Table 5.2. For reader's convenience it is recommended to refer to the Table 5.1 on page 43 to see the chemical structures.

The mma values of phthalocyanines **6** on glass, **12** and **17** on glass and ITO are quite similar and match well the expected values for vertical orientation of the macrocycles with densely packed layers. On the other hand, comparing the molecular areas on glass and on gold (SAM **12** and **21**, and SAM **17** and **23**), a difference can be observed. Evidently, phthalocyanines on gold are packed quite loosely, which can be attributed to the different tilting angles of the molecules on different substrates. Comparing the molecular areas of mono-, di- and tetra-anchored Pcs **19**, **21**, and **23** on gold, the area increased towards larger chromophore and more linkers, as expected. Nevertheless, the mma value for tetrasubstituted phthalocyanine on gold is quite small for a flat orientation and probably evidences for more vertical arrangement of the macrocycles. The data must be treated with care, as this could be due to a gradual decrease of the molar absorption coefficient in SAMs compared to that in solution. Indeed, the Q-band peaks were 2-3 times broader for films, indicating that the molar absorption could be 2-3 times lower for SAMs. Therefore the mma values listed in Table 5.2 present the higher limits for actual area per molecule, but real bonding densities of molecules can be greater.

For porphyrin, the mma values of SAM **30** on quartz, ITO, and AZO were below 4 nm^2 (Table 5.2), which fits well its geometry with large *tert*-butyl substituents. Obviously, the Soret band was two times broader for films, thus making the apparent optical densities for SAMs two times lower. The mma values for SAM of porphyrin **31** on different substrates were over 20 nm^2, which are evidences for a loose packing of the molecules with dimethylmethoxysilane anchor on surface.

The mma values for SAM of phthalocyanine **34** were calculated from maximum of the Q-band, and the molecular areas were around 5 nm^2. Values were almost double compared with modeled molecular area (mma^{vdW}), which indicates loose packing of the molecules. The area per molecule for dimethylmethoxysilyl-Pc SAM **35** could not be calculated reliably because of too low absorbance of the sample.

In the case of PDI, the mma values (SAM **38** and **50**, Table 5.2) were smaller than expected for perfect monolayers. This might be due to the long linker, which allows chromophores to stack one over another instead of forming an ideal monomolecular film. This hypothesis was supported by the complete fluorescence quenching of the films, which can be attributed the aggregation of PDI units.

The experimental mma values of PMIs (SAM **53**, **55**, and **63**, Table 5.2) gave also smaller numbers than expected. These were calculated using molar absorptivity values of PMI esters (**52**, **54**, and **61**), the closest structural analogues of anhydrides bound on surface. Even though it seems that packing was tight, one should remember that double and multilayers were possible to make. Evidently, the quality of the layers for PMIs **55** and **63**, having either 1,6-dipyrrolidyl or 1,7-di(nitrophenyl) substituents was highest. These two PMI sockets allowed either to cap them with another mono(terpyridyl)-PDI, or extend the off-surface chain for at least ten links supposedly forming a layer which has a well-defined complex organized anisotropic 3D structure on the molecular level.

TABLE 5.2 Mean molecular areas (mma) of SAMs on different substrates. 3D top view of molecules and rectangles are drawn in scale 1 mm = 1 Å. Grey rectangle represents approximate size with van der Walls radii (mma^{vdW}) and color rectangles experimentally calculated values (exp. mma, Equation 1).

	molecule, substrate	**approx. size, Å**	**mma^{vdW}, nm^2**	**exp. mma, nm^2**
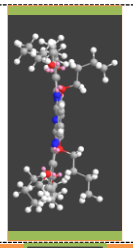	**6**, glass **19**, gold	16x7	1.90	2.06 2.07
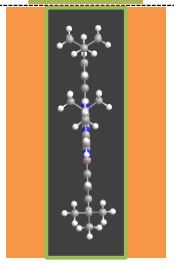	**12**, glass/ITO **21**, gold	19x4	1.54	1.61 3.10

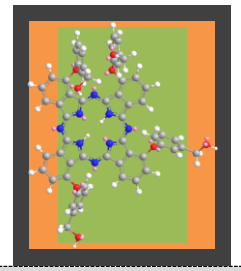	**17**, glass/ITO **23**, gold	20x16	4.37	1.90/2.13 3.24
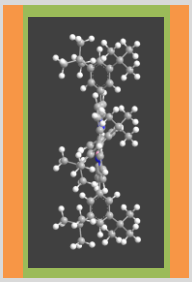	**30**, quartz/ITO/AZO **31**, quartz/ITO/AZO	19x9	2.64	3.11/3.48/3.94 20/25/27
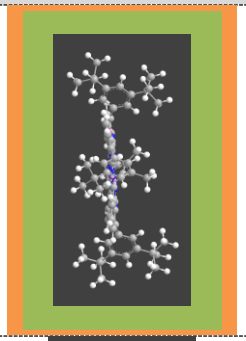	**34**, quartz/ITO/AZO	21x9	2.88	4.84/5.81/4.84
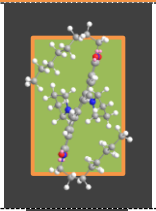	**38**, quartz **50**, quartz/+Zn	15x10	2.34	0.96 1.01/0.89
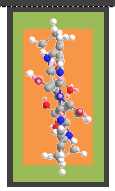	**53**, Al_2O_3 **55**, Al_2O_3 **63**, Al_2O_3	13x6	1.44	1.20 0.73 0.74

Conclusions

A library of phthalocyanine, porphyrin and perylene chromophores suitable for further functionalization was synthesized. These chromophores were modified to have anchors in a broad range of functionalities from thioacetate to siloxane. Altogether 16 different highly colored compounds suitable for immobilization on surface and building of multilayered assemblies were prepared.

Chromophores were immobilized as SAMs on a range of solid substrates by one- or two-step method depending on the anchor moiety. Bonding densities of the chromophores on different substrates depended quite much on the anchor. However, we were able to find a suitable combination for particular chromophore or substrate. It was noticed during the studies of SAM formation that the first layer would play a crucial role in further multilayer assembling.

We have found at least two perylene monoimides, which can serve as a basement for on-surface building of multilayered films. Using coordination chemistry and molecule-by-molecule technique we have prepared stable double layers and demonstrated that at least ten successive layers can be built on surface with rigid PMI anchors as sockets. Terpyridine substituents on perylene core were key elements of these structures.

This work is a continuous piece, starting from two-step monolayers, acrossing one-step monolayers to double layers, and ending up to multilayers (Fig. 5.25). Within growing knowledge after each step, molecules were modified and the final goal of supramolecular multicomponent assemblies has been reached.

The proposed approach is flexible and versatile. Evidently, not each and every perylene derivative would be suitable for building the maultilayers, but we expect that already a modification of the present core structures would allow to vary, for example, the absorbance, electrochemical potential or conductivity of the film, thus making it suitable for various photonic applications.

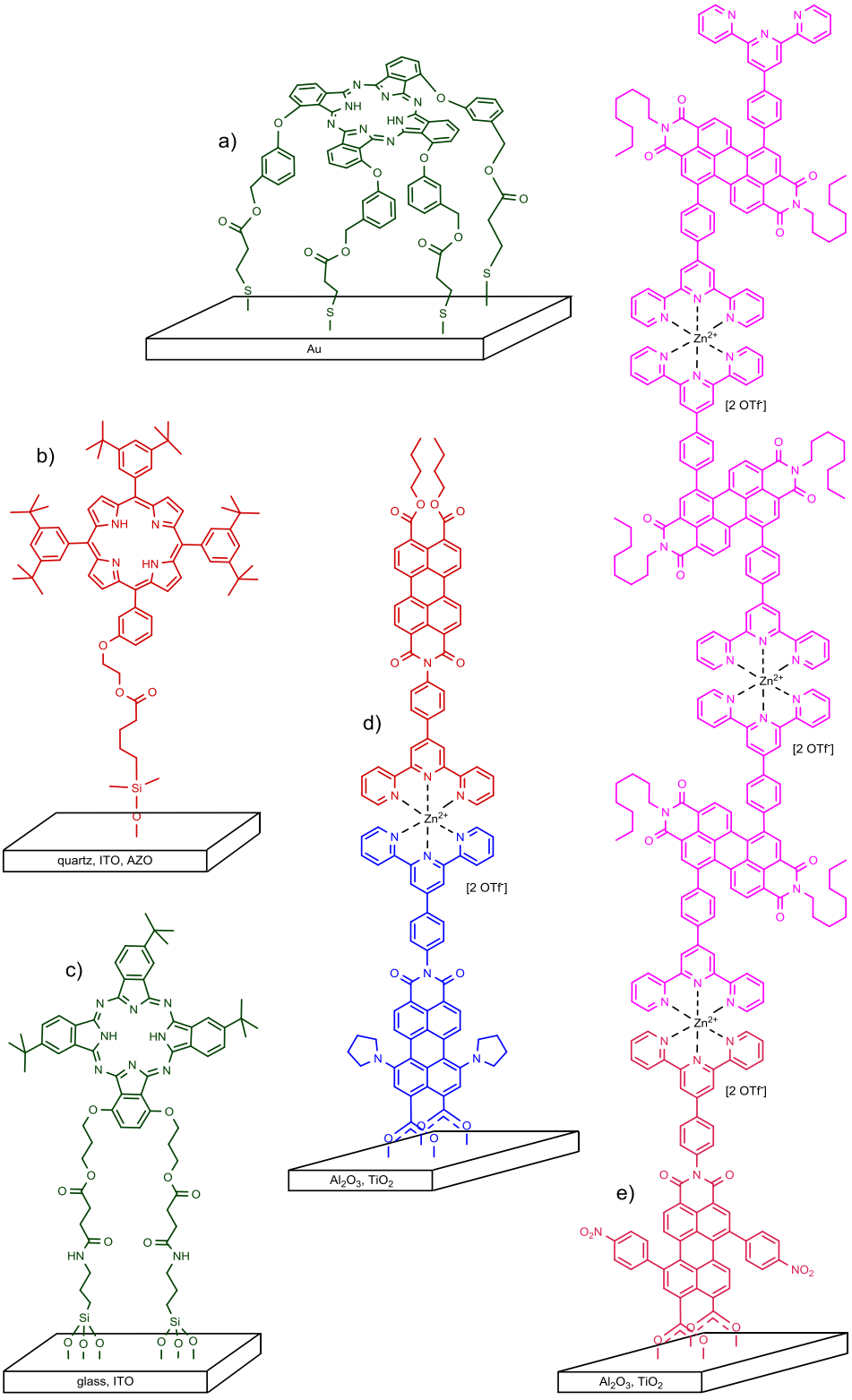

FIGURE 5.25 Examples of molecular layers prepared in this work.

References

[1] Herbst, W. & Hunger, K. Industrial organic pigments: production, properties, applications. 3rd. Weinheim 2004, Wiley-VCH. 660 p.

[2] Likhtenshtein, G.I. Solar energy conversion: chemical aspects. Weinheim 2012, Wiley-VCH. 286 p.

[3] Buckley, A. Organic light-emitting diodes (OLEDs): materials, devices and applications. Cambridge 2013, Woodhead Publishing Limited. 666 p.

[4] Nalwa, H.S. Supramolecular photosensitive and electroactive materials. San Diego 2001, Academic Press. 970 p.

[5] Hagfeldt, A., Boschloo, G., Sun, L., Kloo, L. & Pettersson, H. Dye-sensitized solar cells. *Chem. Rev.* **2010**, *110*, 6595-6663.

[6] Martínez-Díaz, M.V., De la Torre, G. & Torres, T. Lighting porphyrins and phthalocyanines for molecular photovoltaics. *Chem. Commun.* **2010**, *46*, 7090-7108.

[7] Ulman, A. Formation and structure of self-assembled monolayers. *Chem. Rev.* **1996**, *96*, 1533-1554.

[8] Love, J.C., Estroff, L.A., Kriebel, J.K., Nuzzo, R.G. & Whitesides, G.M. Self-assembled monolayers of thiolates on metals as a form of nanotechnology. *Chem. Rev.* **2005**, *105*, 1103-1169.

[9] Ladomenou, K., Kitsopoulos, T.N., Sharma, G.D. & Coutsolelos, A.G. The importance of various anchoring groups attached on porphyrins as potential dyes for DSSC applications. *RSC Adv.* **2014**, *4*, 21379-21404.

[10] Shunmugam, R., Gabriel, G.J., Aamer, K.A. & Tew, G.N. Metal–ligand-containing polymers: terpyridine as the supramolecular unit. *Macromol. Rapid Commun.* **2010**, *31*, 784-793.

[11] Schubert, U.S., Hofmeier, H. & Newkome, G.R. Modern terpyridine chemistry. Weinheim 2006, Wiley-VCH. 237 p.

[12] Miyachi, M., Ohta, M., Nakai, M., Kubota, Y., Yamanoi, Y., Yonezawa, T. & Nishihara, H. Surface bottom-up fabrication of porphyrin-terminated metal complex molecular wires with photo-electron conversion properties on ITO. *Chem. Lett.* **2008**, *37*, 404-405.

[13] McKeown, N.B. Phthalocyanine materials: synthesis, structure, and function. Cambridge 1998, Cambridge University Press. 193 p.

[14] Higashino, T. & Imahori, H. Porphyrins as excellent dyes for dye-sensitized solar cells: recent developments and insights. *Dalton Trans.* **2015**, *44*, 448-463.

[15] Ragoussi, M-E. & Torres, T. Modern synthetic tools toward the preparation of sophisticated phthalocyanine-based photoactive systems. *Chem-Asian J.* **2014**, *9*, 2676-2707.

[16] Kozma, E. & Catellani, M. Perylene diimides based materials for organic solar cells. *Dyes Pigments* **2013**, *98*, 160-179.

[17] Li, C. & Wonneberger, H. Perylene imides for organic photovoltaics: yesterday, today, and tomorrow. *Adv. Mater.* **2012**, *24*, 613-636.

[18] Christie, R. Colour chemistry. 2nd. Cambridge 2014, Royal Society of Chemistry. 360 p.

[19] Grimm, B., Porra, R.J., Rüdiger, W. & Scheer, H. Chlorophylls and bacteriochlorophylls: biochemistry, biophysics, functions and applications. Dordrecht 2006, Springer. 633 p.

[20] Mauzerall, D.C. Evolution of porphyrins. *Clin. Dermatol.* **1998**, *16*, 195-201.

[21] Kadish, K.M. The porphyrin handbook: synthesis and organic chemistry. San Diego 2000, Academic Press. 405 p.

[22] Urbani, M., Grätzel, M., Nazeeruddin, M.K. & Torres, T. Meso-substituted porphyrins for dye-sensitized solar cells. *Chem. Rev.* **2014**, *114*, 12330-12396.

[23] Fisher, H. & Orth, H. Die chemie des pyrrolls. Leipzig 1937, Akad. Verl. m.b.H. 764 p.

[24] Rothemund, P. Formation of porphyrins from pyrrole and aldehydes. *J. Am. Chem. Soc.* **1935**, *57*, 2010-2011.

[25] Rothemund, P. A new porphyrin synthesis. The study of porphin. *J. Am. Chem. Soc.* **1936**, *58*, 625-627.

[26] Adler, A.D., Longo, F.R. & Shergalis, W. Mechanistic investigations of porphyrin synthesis. I. Preliminary studies on *ms*-tetraphenylporphin. *J. Am. Chem. Soc.* **1964**, *86*, 3145-3149.

[27] Lindsey, J.S., Schreiman, I.C., Hsu, H.C., Kearney, P.C. & Marguerettaz, A.M. Rothemund and Adler-Longo reactions revisited: synthesis of tetraphenylporphyrins under equilibrium conditions. *J. Org. Chem.* **1987**, *52*, 827-836.

[28] Vicente, M.G.H. & Smith, K.M. Syntheses and functionalizations of porphyrin macrocycles. *Curr. Org. Synth.* **2014**, *11*, 3-28.

[29] Stuzhin, P.A. & Khelevina, O.G. Azaporphyrins: structure of the reaction centre and reactions of complex formation. *Coord. Chem. Rev.* **1996**, *147*, 41-86.

[30] Lo, P-C., Leng, X. & Ng, D.K.P. Hetero-arrays of porphyrins and phthalocyanines. *Coord. Chem. Rev.* **2007**, *251*, 2334-2353.

[31] De la Torre, G., Claessens, C.G. & Torres, T. Phthalocyanines: the need for selective synthetic approaches. *Eur. J. Org. Chem.* **2000**, 2821-2830.

[32] Bian, Y., Li, L., Dou, J., Cheng, D.Y.Y., Li, R., Ma, C., Ng, D.K.P., Kobayashi, N. & Jiang, J. Synthesis, structure, spectroscopic properties, and electrochemistry of (1,8,15,22-tetrasubstituted phthalocyaninato)lead complexes. *Inorg. Chem.* **2004**, *43*, 7539-7544.

[33] Sorokin, A.B. Phthalocyanine metal complexes in catalysis. *Chem. Rev.* **2013**, *113*, 8152-8191.

[34] Garnovskii, A.D. & Kharisov, B.I. Synthetic coordination and organometallic chemistry. New York 2003, CRC Press. 513 p.

[35] Christie, R.M. & Deans, D.D. An investigation into the mechanism of the phthalonitrile route to copper phthalocyanines using differential scanning calorimetry. *J. Chem. Soc., Perkin Trans. 2* **1989**, 193-198.

[36] Oliver, S.W. & Smith, T.D. Oligomeric cyclization of dinitriles in the synthesis of phthalocyanines and related compounds: the role of the alkoxide anion. *J. Chem. Soc., Perkin Trans. 2* **1987**, 1579-1582.

[37] Cook, M.J., Dunn, A.J., Howe, S.D., Thomson, A.J. & Harrison, K.J. Octa-alkoxy phthalocyanine and naphthalocyanine derivatives: dyes with Q-band absorption in the far red or near infrared. *J. Chem. Soc., Perkin Trans. 1* **1988**, 2453-2458.

[38] Cammidge, A.N., Cook, M.J., Hughes, D.L., Nekelson, F. & Rahman, M. A remarkable side-product from the synthesis of an octaalkylphthalocyanine: formation of a tetrabenzotriazaporphyrin. *Chem. Commun.* **2005**, 930-932.

[39] Mack, J. & Kobayashi, N. Low symmetry phthalocyanines and their analogues. *Chem. Rev.* **2011**, *111*, 281-321.

[40] Claessens, C.G., Hahn, U. & Torres, T. Phthalocyanines: from outstanding electronic properties to emerging applications. *Chem. Rec.* **2008**, *8*, 75-97.

[41] Singh, V.K., Kanaparthi, R.K. & Giribabu, L. Emerging molecular design strategies of unsymmetrical phthalocyanines for dye-sensitized solar cell applications. *RSC Adv.* **2014**, *4*, 6970-6984.

[42] Würthner, F., Saha-Möller, C.R., Fimmel, B., Ogi, S., Leowanawat, P. & Schmidt, D. Perylene bisimide dye assemblies as archetype functional supramolecular materials. *Chem. Rev.* **2015**, DOI: 10.1021/acs.chemrev.5b00188.

[43] Kardos, M. German Patent, DE 276956, 1913.

[44] Huang, C., Barlow, S. & Marder, S.R. Perylene-3,4,9,10-tetracarboxylic acid diimides: synthesis, physical properties, and use in organic electronics. *J. Org. Chem.* **2011**, *76*, 2386-2407.

[45] Faulkner, E.B. & Schwartz, R.J. High performance pigments. 2nd. Weinheim 2009, Wiley-VCH. 538 p.

[46] Kazmaier, P.M. & Hoffmann, R. A theoretical study of crystallochromy. Quantum interference effects in the spectra of perylene pigments. *J. Am. Chem. Soc.* **1994**, *116*, 9684-9691.

[47] Nakazono, S., Easwaramoorthi, S., Kim, D., Shinokubo, H. & Osuka, A. Synthesis of arylated perylene bisimides through C-H bond cleavage under ruthenium catalysis. *Org. Lett.* **2009**, *11*, 5426-5429.

[48] Zhao, Y. & Wasielewski, M.R. 3,4:9,10-Perylenebis(dicarboximide) chromophores that function as both electron donors and acceptors. *Tetrahedron Lett.* **1999**, *40*, 7047-7050.

[49] Böhm, A., Arms, H., Henning, G. & Blaschka, P. German Patent, DE 19547209 A1, 1997.

[50] Würthner, F. Perylene bisimide dyes as versatile building blocks for functional supramolecular architectures. *Chem. Commun.* **2004**, 1564-1579.

[51] Würthner, F., Stepanenko, V., Chen, Z., Saha-Möller, C.R., Kocher N. & Stalke, D. Preparation and characterization of regioisomerically pure 1,7-disubstituted perylene bisimide dyes. *J. Org. Chem.* **2004**, *69*, 7933-7939.

[52] Ma, J., Yin, L., Zou, G. & Zhang, Q. Regioisomerically pure 1,7-dibromo-substituted perylene bisimide dyes: efficient synthesis, separation, and characterization. *Eur. J. Org. Chem.* **2015**, 3296-3302.

[53] Liu, Y., Wang, Y., Ai, L., Liu, Z., Ouyang, X. & Ge, Z. Perylenebisimide regioisomers: effect of substituent position on their spectroscopic, electrochemical, and photovoltaic properties. *Dyes Pigments* **2015**, 121, 363-371.

[54] Drain, C.M., Varotto, A. & Radivojevic, I. Self-organized porphyrinic materials. *Chem. Rev.* **2009**, *109*, 1630-1658.

[55] Würthner, F. Supramolecular dye chemistry. Berlin 2005, Springer. 324 p.

[56] Grabowska, I., Maes, W., Ngo, T.H., Rohand, T., Dehaen, W., Radecki, J. & Radecka, H. Multiple redox-active sites in copper dipyrromethene-corrole self-assembled monolayers deposited onto gold electrodes. *Int. J. Electrochem. Sci.* **2014**, *9*, 1232-1249.

[57] Zhao, Y., Ding, J. & Huang, X-B. Synthesis and self-assembly of phthalocyanines bearing sulfur-containing substituents. *Chinese Chem. Lett.* **2014**, *25*, 46-50.

[58] Molíková, M. & Jandera, P. Characterization of stationary phases for reversed-phase chromatography. *J. Sep. Sci.* **2010**, *33*, 453-463.

[59] Görlach, B., Hellriegel, C., Steinbrecher, S., Yüksel, H., Albert, K., Plies, E. & Hanack, M. Synthesis, characterization and HPLC-applications of novel phthalocyanine modified silica gel materials. *J. Mater. Chem.* **2001**, *11*, 3317-3325.

[60] Aswal, D.K., Lenfant, S., Guerin, D., Yakhmi, J.V. & Vuillaume, D. Self assembled monolayers on silicon for molecular electronics. *Anal. Chim. Acta* **2006**, *568*, 84-108.

[61] Mutin, P.H., Guerrero, G. & Vioux, A. Organic-inorganic hybrid materials based on organophosphorus coupling molecules: from metal phosphonates to surface modification of oxides. *C. R. Chimie* **2003**, *6*, 1153-1164.

[62] Yamada, H., Imahori, H., Nishimura, Y., Yamazaki, I. & Fukuzumi, S. Enhancement of photocurrent generation by ITO electrodes modified chemically with self-assembled monolayers of porphyrin-fullerene dyads. *Adv. Mater.* **2002**, *14*, 892-895.

[63] Chukharev, V., Vuorinen, T., Efimov, A., Tkachenko, N.V., Kimura, M., Fukuzumi, S., Imahori, H. & Lemmetyinen, H. Photoinduced electron transfer in self-assembled monolayers of porphyrin-fullerene dyads on ITO. *Langmuir* **2005**, *21*, 6385-6391.

[64] Taylor, C.E. & Schwartz, D.K. Octadecanoic acid self-assembled monolayer growth at sapphire surfaces. *Langmuir* **2003**, *19*, 2665-2672.

[65] Kalyanasundaram, K. & Grätzel, M. Applications of functionalized transition metal complexes in photonic and optoelectronic devices. *Coord. Chem. Rev.* **1998**, *177*, 347-414.

[66] Ooyama, Y., Ohshita, J. & Harima, Y. Control of molecular arrangement and/or orientation of D-π-A fluorescent dyes for dye-sensitized solar cells. *Chem. Lett.* **2012**, *41*, 1384-1396.

[67] Dinçalp, H., Aşkar, Z., Zafer, C. & İçli, S. Effect of side chain substituents on the electron injection abilities of unsymmetrical perylene diimide dyes. *Dyes Pigments* **2011**, *91*, 182-191.

[68] Haga, M. Kobayashi, K. & Terada, K. Fabrication and functions of surface nanomaterials based on multilayered or nanoarrayed assembly of metal complexes. *Coord. Chem. Rev.* **2007**, *251*, 2688-2701.

[69] Beauvilliers, E.E., Topka, M.R. & Dinolfo, P.H. Synthesis and characterization of perylene diimide based molecular multilayers using CuAAC: towards panchromatic assemblies. *RSC Adv.* **2014**, *4*, 32866-32875.

[70] Haensch, C., Chiper, M., Ulbricht, C., Winter, A., Hoeppener, S. & Schubert, U.S. Reversible supramolecular functionalization of surfaces: terpyridine ligands as versatile building blocks for noncovalent architectures. *Langmuir* **2008**, *24*, 12981-12985.

[71] Gao, Y., Rajwar, D. & Grimsdale, A.C. Self-assembly of conjugated units using metal-terpyridine coordination. *Macromol. Rapid Commun.* **2014**, *35*, 1727-1740.

[72] Li, H., Yao, Z-J., Liu, D. & Jin, G-X. Multi-component coordination-driven self-assembly toward heterometallic macrocycles and cages. *Coord. Chem. Rev.* **2015**, *293-294*, 139-157.

[73] Maeda, H., Sakamoto, R. & Nishihara, H. Metal complex oligomer and polymer wires on electrodes: tactical constructions and versatile functionalities. *Polymer* **2013**, *54*, 4383-4403.

[74] Musumeci, C., Zappalà, G., Martsinovich, N., Orgiu, E., Schuster, S., Quici, S., Zharnikov, M., Troisi, A., Licciardello, A. & Samorì, P. Nanoscale electrical investigation of layer-by-layer grown molecular wires. *Adv. Mater.* **2014**, *26*, 1688-1693.

[75] Fernandes, A.E., Devillez, S., d'Haese, C., Deumer, G., Haufroid, V., Nysten, B., Riant, O. & Jonas, A.M. Grafting control of mainstay terpyridine self-assembled monolayers for the preparation of planar silicon surfaces with variable catalytic loadings. *Langmuir* **2012**, *28*, 14822-14828.

[76] Wu, W-J., Huang, H-X., Chen, M. & Qian, D-J. Synthesis and luminescent properties of a silylated-terpyridine derivative and its metalated complexes in solutions and self-assembled monolayers. *Chinese Chem. Lett.* **2015**, *26*, 343-347.

[77] Kosbar, L., Srinivasan, C., Afzali, A., Graham, T., Copel, M. & Krusin-Elbaum, L. Self-assembled multilayers of transition-metal-terpyridinyl complexes; formation, and characterization. *Langmuir* **2006**, *22*, 7631-7638.

[78] Liatard, S., Chauvin, J., Balestro, F., Jouvenot, D., Loiseau, F. & Deronzier, A. An original electrochemical method for assembling multilayers of terpyridine-based metallic complexes on a gold surface. *Langmuir* **2012**, *28*, 10916-10924.

[79] Kimura, M., Hamakawa, T., Muto, T., Hanabusa, K., Shirai, H. & Kobayashi, N. Five-nuclear complexes of zinc (II) phthalocyanine with directly linked terpyridine ligands. *Tetrahedron Lett.* **1998**, *39*, 8471-8474.

[80] Odobel, F. & Zabri, H. Preparations and characterizations of bichromophoric systems composed of a ruthenium polypyridine complex connected to a difluoroborazaindacene or a zinc phthalocyanine chromophore. *Inorg. Chem.* **2005**, *44*, 5600-5611.

[81] Flamigni, L., Barigelletti, F., Armaroli, N., Collin, J-P., Dixon, I.M., Sauvage, J-P. & Williams, J.A.G. Photoinduced processes in multicomponent arrays containing transition metal complexes. *Coord. Chem. Rev.* **1999**, *190-192*, 671-682.

[82] Dobrawa, R., Lysetska, M., Ballester, P., Grüne, M. & Würthner, F. Fluorescent supramolecular polymers: metal directed self-assembly of perylene bisimide building blocks. *Macromolecules* **2005**, *38*, 1315-1325.

[83] El-Batal, H., Guo, K., Li, X., Wesdemiotis, C., Moorefield, C.N. & Newkome, G.R. Perylene-based bis-, tetrakis-, and hexakis(terpyridine) ligands and their ruthenium(II)–bis(terpyridine) complexes: synthesis and photophysical properties. *Eur. J. Org. Chem.* **2013**, 3640-3644.

[84] Stepanenko, V., Stocker, M., Müller, P., Büchner, M. & Würthner, F. Self-assembly and layer-by-layer deposition of metallosupramolecular perylene bisimide polymers. *J. Mater. Chem.* **2009**, *19*, 6816-6826.

[85] Tuccitto, N., Delfanti, I., Torrisi, V., Scandola, F., Chiorboli, C., Stepanenko, V., Würthner, F. & Licciardello, A. Supramolecular self-assembled multilayers of terpyridine-functionalized perylene bisimide metal complexes. *Phys. Chem. Chem. Phys.* **2009**, *11*, 4033-4038.

[86] Hassan, M.L., Moorefield, C.M., Elbatal, H.S., Newkome, G.R., Modarelli, D.A. & Romano, N.C. Fluorescent cellulose nanocrystals via supramolecular assembly of terpyridine-modified cellulose nanocrystals and terpyridine-modified perylene. *Mat. Sci. Eng. B* **2012**, *177*, 350-358.

[87] Saarenpää, H., Niemi, T., Tukiainen, A., Lemmetyinen, H. & Tkachenko, N. Aluminum doped zinc oxide films grown by atomic layer deposition for organic photovoltaic devices. *Sol. Energy Mater. Sol. Cells* **2010**, *94*, 1379-1383.

[88] Cosimelli, B., Roncucci, G., Dei, D., Fantetti, L., Ferroni, F., Riccic, M. & Spinelli, D. Synthesis and antimycotic activity of new unsymmetrical substituted zinc phthalocyanines. *Tetrahedron* **2003**, *59*, 10025-10030.

[89] Tercel, M., Stribbling, S.M., Sheppard, H., Siim, B.G., Wu, K., Pullen, S.M., Botting, K.J., Wilson, W.R. & Denny, W.A. Unsymmetrical DNA cross-linking agents: combination of the CBI and PBD pharmacophores *J. Med. Chem.* **2003**, *46*, 2132-2151.

[90] Behr, A., Naendrup, F. & Obst, D. Platinum-catalysed hydrosilylation of unsaturated fatty acid esters. *Adv. Synth. Catal.* **2002**, *344*, 1142-1145.

[91] Markó, I.E., Stérin, S., Buisine, O., Mignani, G., Branlard, P., Tinant, B. & Declercq, J.-P. Selective and efficient platinum(0)-carbene complexes as hydrosilylation catalysts. *Science* **2002**, *298*, 204-206.

[92] Stegmaier, P., Alonso, J.M. & del Campo, A. Photoresponsive surfaces with two independent wavelength-selective functional levels. *Langmuir* **2008**, *24*, 11872-11879.

[93] Alonso, J.M., Reichel, A., Piehler, J. & del Campo, A. Photopatterned surfaces for site-specific and functional immobilization of proteins. *Langmuir* **2008**, *24*, 448-457.

[94] Kamieth, M., Burkert, U., Corbin, P.S., Dell, S.J., Zimmerman, S.C., & Klärner, F-G. Molecular tweezers as synthetic receptors: molecular recognition of electron-deficient

aromatic substrates by chemically bonded stationary phases. *Eur. J. Org. Chem.* **1999**, 2741-2749.

[95] Dubey, R.K., Niemi, M., Kaunisto, K., Efimov, A., Tkachenko, N.V. & Lemmetyinen, H. Direct evidence of significantly different chemical behavior and excited-state dynamics of 1,7- and 1,6-regioisomers of pyrrolidinyl-substituted perylene diimide. *Chem. Eur. J.* **2013**, *19*, 6791-6806.

[96] Zhang, X-C., Huo, Z-M., Wang, T-T. & Zeng, H-P. Facile synthesis and photochromic properties of diarylethene-containing terpyridine and its transition metal (Zn^{2+}/Co^{2+}/Ru^{2+}) complexes. *J. Phys. Org. Chem.* **2012**, *25*, 754-759.

[97] Ahmed, Z., George, L., Hiltunen, A., Lemmetyinen, H., Hukka, T. & Efimov, A. Synthesis and study of electrochemical and optical properties of substituted perylenemonoimides in solutions and on solid surfaces. *J. Mater. Chem. A* **2015**, *3*, 13332-13339.

[98] George, L., Ahmed, Z., Lemmetyinen, H. & Efimov, A. Controlled regioselective amination of peryleneimides. *Eur. J. Org. Chem.* **2015**, 584-590.

[99] Li, Y., Wang, C., Li, C., Di Motta, S., Negri, F. & Wang, Z. Synthesis and properties of ethylene-annulated di(perylene diimides). *Org. Lett.* **2012**, *14*, 5278-5281.

[100] Sengupta, S., Dubey, R.K., Hoek, R.W.M., van Eeden, S.P.P., Gunbas, D.D., Grozema, F.C., Sudhölter, E.J.R. & Jager, W.F. Synthesis of regioisomerically pure 1,7-dibromoperylene-3,4,9,10-tetracarboxylic acid derivatives. *J. Org. Chem.* **2014**, *79*, 6655-6662.

[101] Rabindranath, A. R., Maier, A., Schäfer M. & Tieke, B. Luminescent and ionochromic polyiminofluorene with conjugated terpyridine substituent groups. *Macromol. Chem. Phys.* **2009**, *210*, 659-668.

[102] Wang, S., Dössel, L., Mavrinskiy, A., Gao, P., Feng, X., Pisula W. & Muellen, K. Self-assembly and microstructural control of a hexa-peri-hexabenzocoronene–perylene diimide dyad by solvent vapor diffusion. *Small*, **2011**, *7*, 2841-2846.

[103] Bramblett, A.L., Boeckl, M.S., Hauch, K.D., Ratner, B.D., Sasaki, T. & Rogers Jr., J.W. Determination of surface coverage for tetraphenylporphyrin monolayers using ultraviolet visible absorption and x-ray photoelectron spectroscopies. *Surf. Interface Anal.* **2002**, *33*, 506-515.

[104] Batsanov, S.S. Van der Waals radii of elements. *Inorg. Mater.* **2001**, *37*, 871-885.

Paper I

Mono-, bis- and tetrahydroxy phthalocyanines as building blocks for monomolecular layer assemblies

Essi Sariola, Anne Kotiaho, Nikolai V. Tkachenko, Helge Lemmetyinen and Alexander Efimov

J. Porphyrins Phthalocyanines **2010**, *14*, 397-411.

Mono-, bis- and tetrahydroxy phthalocyanines as building blocks for monomolecular layer assemblies

Essi Sariola*, Anne Kotiaho, Nikolai V. Tkachenko, Helge Lemmetyinen and Alexander Efimov

Department of Chemistry and Bioengineering, Tampere University of Technology, P.O. Box 541, 33101 Tampere, Finland

Received date (to be automatically inserted after your manuscript is submitted)
Accepted date (to be automatically inserted after your manuscript is accepted)

ABSTRACT: We have developed three basic phthalocyanine structures, containing one, two, or four hydroxy groups, which are simple to synthesize and purify and which can be characterized well by NMR and MS. These building blocks can easily be further modified to have anchor groups, which make the molecules suitable for attachment to solid substrates. We have used thioacetate and pentafluorophenyl ester moieties giving target phthalocyanines the ability to self-assemble on gold, metal oxides, and glass. Bonding densities calculated from the absorbances of the layers suggest mean molecular area to be in range of 1-3 nm^2, which can be partially controlled by side substituents and the number of linkers.

KEYWORDS: phthalocyanine, self-assembly, pentafluorophenyl ester, thioacetate

*Correspondence to: E-mail: essi.sariola@tut.fi, Tel: +358 3 3115 3628, Fax: +358 3 3115 2108

INTRODUCTION

Phthalocyanines (Pcs) have been the subject of much study over the years. These materials are important industrial dyes and pigments and commonly used as catalysts [1-4]. More recently, they have been employed for advanced applications such as sensors and organic solar cells. In these future devices, Pcs are present often as thin films [5-8]. Therefore, part of modern research has been concentrated to developing chromophores containing anchors that could be attached to solid surfaces [9-13].

An evident advantage of covalent bonding is the stability of the formed layer [14]. The deposition of the molecules can be either one-step direct adsorption of the functional component that carries a surface-active group (*e.g.* thiol) or two-step procedure, where the functional components are bonded to preformed ω-functionalised (*e.g.* -COOH, -NH_2) tails, which are in turn covalently bonded to a solid surface [15]. The molecular assemblies thus formed are usually called self-assembled monolayers (SAMs). SAM is particularly attractive as a thin film preparation tehnique because it is simple to fabricate and has a high stability and reproducibility [16].

There are many examples of porphyrin monomolecular layer assemblies used in solar cells, organic light-emitting diodes (OLEDs) and sensors [17-20]. Examples of phthalocyanine monomolecular layer assemblies are rare, though the chromophores themselves are widely used in solar cells as evaporated and spin-coated layers [21-24]. Problems arise due to difficulties with Pc functionalization (chiefly low solubility) and characterization (as they usually have a large number of regioisomers). However, compared to porphyrins, Pcs offer a much wider absorbance in the visible part of the solar spectrum, which makes them better candidates as light/energy harvesting materials. Porphyrins and phthalocyanines also have different photophysical and redox properties despite the structural similarities of the molecules [25].

In this paper we report the preparation of three basic phthalocyanine structures containing one, two, and four hydroxy groups, which are soluble in common organic solvents, are easy to synthesize and can be well characterized by ^{1}H NMR, MS and UV-vis spectroscopies. The versatile building blocks are further used to add anchor groups, which gives Pcs the ability to self-assemble on various solid substrates. We have tested the attachment of our Pcs to gold, glass, and ITO, and we demonstrate that the bonding densities are similar for different substrates yielding mean molecular areas in the range of 1-3 nm^2.

RESULTS AND DISCUSSION

Synthesis

Preparation of hydroxy-substituted phthalocyanines

Mono-, bis-, and tetrahydroxy Pcs were synthesized using the well known Li method. 3,6-dibutoxyphthalonitrile (**1**) and 4-[3-(hydroxymethyl)phenoxy]phthalonitrile (**2**) were used to prepare the monohydroxy phthalocyanine **3** (Scheme 1). A five-fold excess of the phthalonitrile **1** over compound **2** was loaded into the reaction to decrease the amount of other Pcs that form statistically as side products [26]. 1-butanol was chosen as solvent to keep the structure of phthalonitrile **1** intact because lithium alkoxide, which is formed in the reaction, can exchange the alkoxy substituent of phthalonitrile. The reaction mixture was heated at reflux for 4 h under a drying tube, and after chromatographic purification the product **3** was obtained with the yield of 24%.

Synthesis of the bishydroxy phthalocyanine **6** was carried out using 3,6-di(hydroxypropyloxy)phthalonitrile (**4**) and 4-*tert*-butylphthalonitrile (**5**) (Scheme 2) [27]. The compound **5** was used in six-fold excess thus improving the formation of A_3B type Pc. A 2.5 h reaction under argon atmosphere was most efficient producing a 20% yield of Pc **6**.

When the reaction time was prolonged or the reaction was done in ambient air, the yield of the product **6** decreased significantly.

3-[3-(hydroxymethyl)phenoxy]phthalonitrile (**7**) and lithium octoxide was used for the synthesis of tetrahydroxy phthalocyanine **8** (Scheme 3). The reaction mixture was stirred at 80 °C under argon atmosphere for 3 days. After work-up and purification the yield of tetra-substituted Pc **8** was 78%. The starting materials **1** and **5** are commercially available, while the compounds **2**, **4** and **7** were prepared by known methods [27, 28]. Only one isomer is shown for clarity in Schemes 2 and 3.

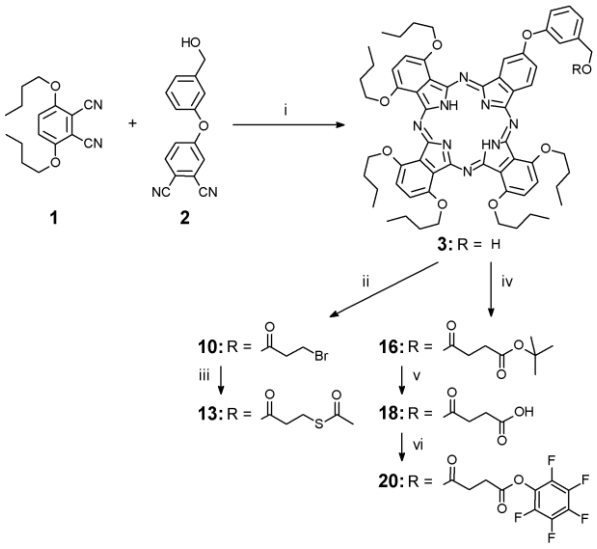

Scheme 1. Synthetic route to monohydroxy phthalocyanine **3**, and its derivatives. *Reagents and conditions:* **i)** Li, 1-butanol, reflux, 4 h; **ii)** 3-bromopropionyl chloride, CH_2Cl_2, rt, 24 h; **iii)** potassium thioacetate, acetone, reflux, 72 h; **iv)** mono-*tert*-butyl succinate, DCC, DMAP, CH_2Cl_2, rt, 48 h; **v)** TFA, dry CH_2Cl_2, rt, 3 h; **vi)** pentafluorophenol, DCC, EtOAc, rt, 120 h.

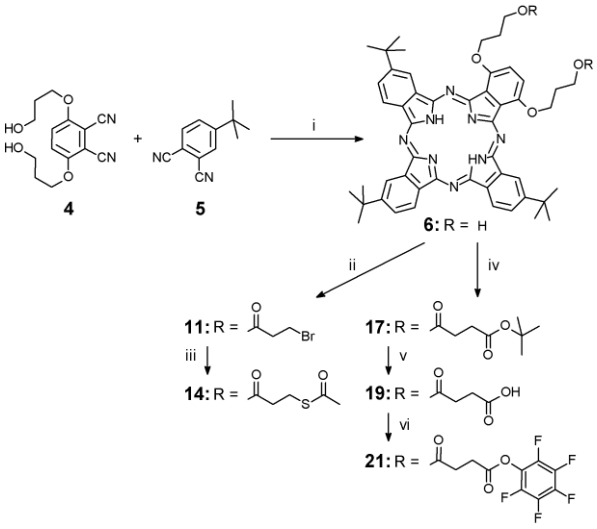

Scheme 2. Synthetic route to bishydroxy phthalocyanine **6**, and its derivatives. *Reagents and conditions:* **i)** Li, 1-pentanol, reflux, Ar, 2.5 h; **ii)** 3-bromopropionyl chloride, CH_2Cl_2, rt, 72 h; **iii)** potassium thioacetate, acetone, rt, 96 h; **iv)** mono-*tert*-butyl succinate, DCC, DMAP, CH_2Cl_2, rt, 48 h; **v)** TFA, dry CH_2Cl_2, rt, 4.5 h; **vi)** pentafluorophenol, DCC, EtOAc, rt, 96 h.

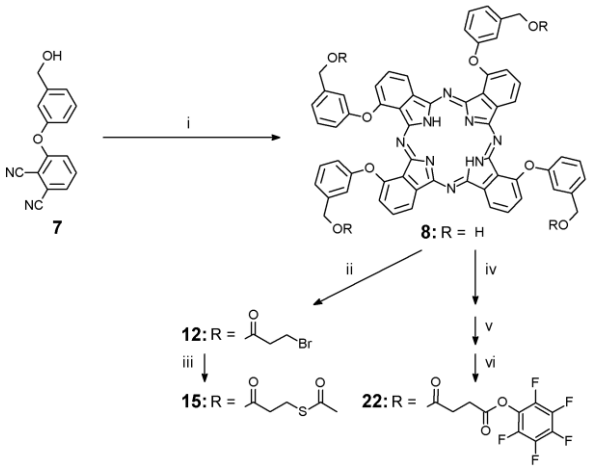

Scheme 3. Synthetic route to tetrahydroxy phthalocyanine **8**, and its derivatives. *Reagents and conditions:* **i)** lithium octoxide, THF, 80 °C, Ar, 72 h; **ii)** 3-bromopropionyl chloride, THF/CH_2Cl_2, rt, 72 h; **iii)** potassium thioacetate, acetone, rt 24 h, 60 °C 48 h; **iv)** mono-*tert*-butyl succinate, DCC, DMAP, THF/CH_2Cl_2, rt, 168 h; **v)** TFA, dry CH_2Cl_2, rt, 4.5 h; **vi)** pentafluorophenol, DCC, EtOAc, 0 °C 48 h, rt 24 h.

Preparation of thioacetyl-substituted phthalocyanines

Synthesis of thioacetyl-substituted phthalocyanine includes two steps. At first bromopropionic acid was attached to hydroxy Pc, and then the terminal bromine was exchanged to thioacetate group. 3-bromopropionyl chloride (**9**), which was used in acylation, was prepared by a known method just before use [29].

Hydroxy phthalocyanines **3** and **6** were dissolved in CH_2Cl_2 and a six-fold excess of bromopropionyl chloride per hydroxy group was added into the reaction. Tetrahydroxy Pc **8** should be first dissolved in THF/CH_2Cl_2 1:1 mixture and after that diluted with CH_2Cl_2. In this reaction the acid chloride **9** was used in 30-fold excess overall. Acylation of the bishydroxy Pc **6** and the tetrahydroxy Pc **8** requires stirring at room temperature for 3 days. For the monohydroxy phthalocyanine **3** sufficient reaction time was 1 day at room temperature, and during this time the color of the solution changed from dark green to dark purple due to the protonation of the macrocycle. Acylation cannot be promoted by adding organic base (*e.g.* triethylamine), as it leads immediately to dehydrobromination and formation of acrylic esters. Yields of the products **10**, **11** and **12** after straightforward purification were 77%, 55% and 47%, respectively.

Exchange of terminal bromine to thioacetate was done in acetone using potassium thioacetate (KSAc). The monobromo Pc **10** was heated at reflux under a drying tube for 3 days in acetone with five-fold excess of KSAc. The monothioacetate product **13** was obtained as dark green solid with a 59% yield. Elevated temperature was required because of poor solubility of the product **10** in acetone, thus full conversion of starting material cannot be achived at room temperature. Thioacetate exchange efficiency is strongly solvent dependent [30]. Similarly, in present case no reaction was observed in DMF at 60 ºC or with refluxing THF.

Preparation of bisthioacetyl Pc **14** is easier and can be done by stirring the Pc **11** and a four-fold excess of KSAc at room temperature for 4 days. Yield of the target product **14** was 70%. Besides the higher yield this reaction proceeds faster than monothioacetyl synthesis. In fact, after 16 h of stirring the yield of bisthioacetate was as high as 67%.

Formation of tetrathioacetyl phthalocyanine **15** at room temperature is slower. Stirring the mixture of tetrabromo Pc **12** and a two-fold excess of KSAc in acetone for 1 day showed that the reaction was not complete, and heating for 1 day at 60 ºC did not promote the reaction any further. However, when double excess of KSAc was added again and the solution was stirred at 60 ºC for 2 days overall, the tetrathioacetate **15** was obtained with 70% yield after purification.

Preparation of pentafluorophenyl ester-substituted phthalocyanines

Synthesis of pentafluorophenyl ester phthalocyanines **20**-**22** includes three steps. At first succinic acid was attached to hydroxy-substituted Pc (**3**, **6** and **8**), and the *tert*-butyl succinate thus formed was deprotected. In the last step the pentafluorophenyl ester group was added [31].

Monohydroxy Pc **3** and bishydroxy Pc **6** were reacted with mono-*tert*-butyl succinate in CH_2Cl_2, using 1,3-dicyclohexylcarbodiimide (DCC) and 4-dimethylaminopyridine (DMAP) as a catalyst. Both reaction mixtures were stirred at room temperature for 2 days and after chromatographic purifications the *tert*-butyl succinatoxy-substituted products **16** and **17** were obtained with quantitative yields. In the synthesis of tetra-*tert*-butyl succinatoxy-substituted Pc, tetrahydroxy phthalocyanine **8** was first dissolved in THF. Compared to others, the reaction was slow; the reaction mixture was stirred at room temperature for 7 days. The long reaction time is due to the poor solubility of the Pc **8**. However, the intermediate product was obtained with quantitative yield.

The deprotections of phthalocyanines **16**, **17** and the intermediate product tetra-*tert*-butyl succinatoxy were carried out by treatment with trifluoroacetic acid (TFA) in dry CH_2Cl_2 for 3-4 h. After solvent evaporation the yield of monosuccinate **18** was 93%, and the yields of bissuccinate **19** and tetrasuccinate were quantitative. Pentafluorophenyl esters **20** and **21** were prepared by dissolving the compounds **18** and **19** in ethyl acetate and adding DCC and pentafluorophenol. Yield of the target monoester **20** was 55% after 5 days of stirring at room temperature and flash chromatography. The synthesis of bisester **21** was completed after 4 days of stirring at room temperature. Phthalocyanine **21** was obtained as a dark green solid with a yield of 41%. Tetra(pentafluorophenyl ester) **22** was prepared by dissolving the intermediate product tetrasuccinate Pc in ethyl acetate on ultrasonic bath, and after that stirring the reaction mixture of phthalocyanine, DCC and pentafluorophenol in cold for 3 days. After purification by flash chromatography and preparative TLC plate, the product **22** was obtained as dark green solid with a 25% yield.

^{1}H NMR spectra

The structural characterization of phthalocyanines has always been difficult since Pcs have usually poor solubility and a number of regioisomers. We designed our particular chromophores to have good solubility, easy NMR analysis, and a reduced number of regioisomers.

The ^{1}H NMR spectra of the mono-functionalized compounds **3**, **13** and **20** are presented in Figure 1. The spectra show clear aromatic regions where two doublets correspond to the phthalo-protons 25 (δ 9.30 ppm) and 22 (δ 8.90 ppm), and a doublet of doublets originates from the phthalo-proton 24 (δ 7.83 ppm). The multiplet around 7.50 ppm consists of the signals of the rest of β-phthalo protons and the protons from the aryl ring. In the aliphatic region, the signals of alkoxy protons of the butoxy chains at the positions 1 and 18 are shifted upfield compared to other alkoxy protons due to the different environment. Eight alkoxy protons ($OCH_2C_3H_7$) of the butoxy chains, at the positions 4, 8, 11, and 15, are visible as multiplet (δ 4.91-4.81 ppm) whereas the signals of alkoxy protons at the positions 1 and 18 appear as two triplets at 4.70 ppm and 4.61 ppm, respectively. The spectrum of the hydroxy Pc **3** shows a broad singlet at 4.78 ppm, which corresponds to methylene protons between the aryl ring and hydroxy group. In the other spectra this signal is shifted to lower field (δ 5.21 ppm). The shift of this singlet is caused by the substitution with succinic residue, which deshields this CH_2-group. The signals of succinic protons $COCH_2CH_2Br$ and $COCH_2CH_2Br$ in the ^{1}H NMR spectrum of **10** appear as two multiplets at 3.01-2.83 ppm and 3.77-3.52 ppm, respectively (see Supporting information). The same signals for the thioacetate **13** are visible as triplets; for the protons $COCH_2CH_2S$, the triplet is observed at 2.70 ppm and for the protons $COCH_2CH_2S$ it is located at 3.11 ppm. The signal of methyl protons $SCOCH_3$ is found as a singlet (δ 2.22 ppm) overlapping with a multiplet in the spectrum of **13**. The signals of the protons COC_2H_4CO appear as a multiplet in the spectra of the *tert*-butylsuccinate **16** and the succinate **18** (δ 2.70-2.53 ppm) (see Supporting information). The shift of these signals to lower field occurs in the spectrum of the pentafluorophenyl ester

20. For this the signals are divided into two multiplets at 2.97-2.91 ppm and 2.84-2.78 ppm. Characteristic signal of the *tert*-butyl group in the spectrum of **16** is observed at 1.40 ppm, and this singlet disappears from the spectrum of the deprotected compound **18**. The free base Pcs include two protons in the central cavity and those NH-protons are observed as a singlet around 0.10 ppm in each spectrum.

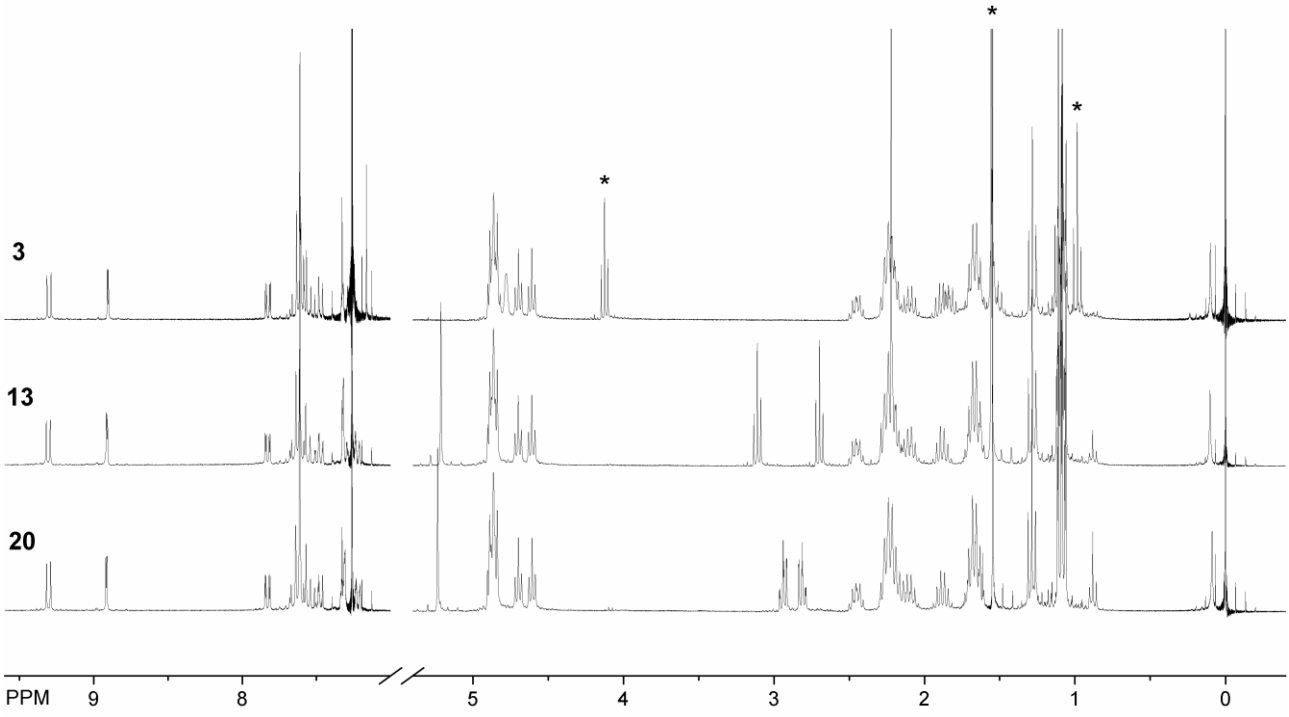

Fig. 1. ^{1}H NMR spectra of monohydroxy **3** (top), monothioacetate **13** (middle) and mono(pentafluorophenyl ester) **20** (bottom) phthalocyanines; signals of residual solvents are marked with asterisk

In the ^{1}H NMR spectra of bishydroxy phthalocyanine **6** and its derivatives (see Supporting information) several multiplets are present due to constitutional isomers. In the aromatic region of the spectrum of **6** three multiplets are visible. Signals of the phthalo-protons 2 and 3 are found as separate multiplet at 6.88-6.07 ppm. In the ^{1}H NMR spectra of bissucinate derivatives **17**, **19** and **21** these signals are shifted to lower field. In the aliphatic region of the spectrum of the bishydroxy compound **6**, the signals of alkoxy protons OCH_2CH$_2$CH_2OH of the hydroxypropyloxy chains at the positions 1 and 4 are visible as broad multiplet (δ 4.65-4.24 ppm). This multiplet is shifted to lower field in all other spectra. The same shift is visible when comparing the multiplet of methylene protons OCH$_2$CH_2CH$_2$O, for example the spectrum of bromopropionate **11** shows the multiplet at 2.71-2.41 ppm, when the spectrum of **6** shows this multiplet at 2.51-2.23 ppm. The signals of the protons COCH_2CH$_2$Br and COCH$_2$CH_2Br of **11** appear both as multiplets at 3.03-2.76 ppm and 3.82-3.49 ppm, respectively. In the spectrum of thioacetate **14**, these multiplets are shifted to higher field. The multiplet at 2.76-2.54 ppm contains also the signals of protons OCH$_2$CH_2CH$_2$O, while the characteristic acetylic protons of **14** are visible as a group of singlets next to it (δ 2.28-2.21 ppm). The signals of the three *tert*-butyl groups at the periphery of Pc are observed in the spectra of bishydroxy, bisbromopropionate, and bisthioacetate **6**, **11**, and **14** as a group of singlets at 1.91-1.68 ppm. Shifting of these signals is observed in ^{1}H NMR spectra of bissuccinates **17**, **19**, and **21** (δ 1.89-1.76 ppm). The characteristic signal of *tert*-butyl ester protons in **17** appears as singlet at 1.44 ppm, and this peak vanishes in the spectrum of the deprotected **19**. NH-protons of bishydroxy Pc **6** are as a multiplet at -2.40 – -2.97 ppm. For bispropionate derivatives these signals are shifted to lower field. Thus for the bisbromopropionate **11** the signals are found at -1.34 – -1.71 ppm, while for the Pc **14** this multiplet is visible at -1.03 – -1.34 ppm. NH-protons signals are visible as multiplet at -0.80 – -1.07 ppm, -1.81 – -2.54 ppm and -1.18 – -1.49 ppm in the spectra of the bissuccinic derivatives **17**, **19** and **21**, respectively.

In the aromatic region of the ^{1}H NMR spectrum of tetra-substituted phthalocyanine **8** (see Supporting information), the signals of 12 phthalo-protons on the Pc periphery are found as a multiplet (δ 8.20-7.38 ppm). Another multiplet in higher field consists of the signals of aryl protons. Similar but broader multiplets are found also in the spectra of tetrabromopropionic and tetrathioacetate Pcs **12** and **15** (see Supporting information). The spectrum of tetra(pentafluorophenyl ester) phthalocyanine **22** shows the most clear signals in the aromatic region (see Supporting information). For example a triplet of β-phthalo-protons is located at 7.81 ppm. A broad triplet at 5.19 ppm with the coupling constant 5.6 Hz corresponds to four hydroxy protons in the spectrum of the compound **8**, and the signals of methylene protons are found as a multiplet at 4.57-4.39 ppm. The group of singlets from the methylene protons is found in much higher field in the spectra of **12**, **15** and **22** (around δ 5.30-5.00 ppm). The signals of protons COCH_2CH$_2$Br and COCH$_2$CH_2Br are observed as multiplets at 3.04-2.68 ppm and 3.80-3.36 ppm in the spectrum of **12**, respectively. For tetrathioacetate Pc **15**, these multiplets are shifted to higher field; signals of protons COCH_2CH$_2$S appear at 2.74-2.51 ppm and signals of protons COCH$_2$CH_2S are found at 3.15-2.91 ppm. In the spectrum of **22**, signals of these protons (COC$_2H_4$CO) overlap and as a result a multiplet is found at 2.99-2.55 ppm. The signals of acetylic protons SCOCH_3 for the compound **15** are visible at 2.33-2.15 ppm as multiplet. Weak signals with negative chemical shift correspond to the NH-protons, and in the spectra of **12**, **15** and **22** these multiplets are found at -1.08 – -1.85 ppm, -1.40 – -2.31 ppm and -1.51 – -2.05 ppm, respectively. Shifting of these signals to lower field is evident when comparing the positions in the spectrum of the Pc **8** (δ -2.03 – -2.62 ppm).

Mass spectra

The structures of the synthesized compound were proved by high resolution ESI-TOF mass spectrometry (see Supporting information). To obtain an accurate value of the mass, a solution of reference compound (Leucine Enkephaline) was infused simultaneously with analyte, and the experimental spectra were processed with peak centering and lock mass TOF correction. In the measurements the solvent was typically a mixture of $CHCl_3$/MeOH 1:1, and positive mode was used.

For monohydroxy-substituted Pc **3** the $[M + H]^+$ peak was observed at *m/z* 1069.5599 (accuracy 4 ppm), along with $[M + Na]^+$ peak at *m/z* 1091.5768. Also aggregated $[2M + H]^+$ and $[2M + Na]^+$ peaks appeared at *m/z* 2138.6091 and 2160.1042, respectively, and the $[3M + 2H]^{2+}$ peak was observed at *m/z* 1603.8296. Molecular ion peak $[M + H]^+$ was observed at *m/z* 1203.4954 (accuracy 3 ppm) for the intermediate product **10**. The $[M + H]^+$ peak was found at *m/z* 1199.5671 (accuracy 2.6 ppm) for the compound **13** and the aggregated peaks $[2M + H]^+$ and $[3M + 2H]^{2+}$ were visible at *m/z* 2398.1262 and 1798.8522, respectively. For phthalocyanine **16**, the $[M + H]^+$, $[2M + H]^+$ and $[3M + 2H]^{2+}$ peaks were observed at *m/z* 1225.6375 (accuracy 3 ppm), 2450.2856 and 1837.9568, respectively. The $[M + H]^+$ peak for **18** was found at *m/z* 1169.5627 (accuracy 7 ppm), and aggregated $[2M + H]^+$ and $[3M + 2H]^{2+}$ peaks were visible at *m/z* 2338.0955 and 1753.8541, respectively. The $[M+H]^+$ peak for the compound **20** was observed at *m/z* 1335.5555 with high accuracy (0.075 ppm). Aggregated $[3M + 2H]^{2+}$ peak was also found at *m/z* 2002.8867 for Pc **20**.

The $[3M + 2H]^{2+}$ peak was visible at *m/z* 1246.6472 (accuracy 0.7 ppm) in the mass spectrum of bishydroxy phthalocyanine **6**, and the $[M + H]^+$ peak was observed at *m/z* 831.4359. Molecular ion peaks $[M]^+$ and $[M + Na]^+$ for the compound **11** were found at *m/z* 1098.3121 (accuracy 10 ppm) and 1121.3079, respectively. In mass spectrum of Pc **14**, the $[M]^+$ peak was observed at *m/z* 1090.4368 (accuracy 7 ppm). The $[M + Na]^+$ and aggregated $[2M + H]^+$, $[2M + Na]^+$ and $[3M + 2H]^{2+}$ peaks were also visible in the spectrum of **14** at *m/z* 1113.4219, 2181.8730, 2203.8757, and 1636.6528, respectively. The spectrum of the compound **17** was measured in positive mode, and aggregated molecular ion peak $[2M + H]^+$ was found at *m/z* 2286.1714 (accuracy 2 ppm). Also the $[M + H]^+$ and $[3M + 2H]^{2+}$ peaks were observed at *m/z* 1143.5874 and 1714.8741, respectively. The mass spectrum of **19** was measured in negative mode and the $[M – H]^-$ peak was visible at *m/z* 1029.4469 (accuracy 4 ppm), and the $[M + Cl]^-$ peak was found next to it (*m/z*

1065.4298). Aggregated $[2M - H]^-$ and $[3M - 2H]^{2-}$ peaks were observed at *m/z* 2059.9153 and 1544.6758, respectively. The $[M + Na]^+$ peak was visible at *m/z* 1385.4221 (accuracy 3.7 ppm) in the measurement of the compound **21**. This spectrum also showed the $[2M + Na]^+$ peak at *m/z* 2747.8450. When the mass measurement was carried out in negative mode for **21**, the $[M - H]^-$ and $[2M - H]^-$ peaks were observed at *m/z* 1361.4127 and 2723.8403, respectively.

The mass measurement of the tetrahydroxy-substituted Pc **8** was carried out in positive mode using MeOH as the solvent. The $[M + H]^+$ peak was observed at *m/z* 1003.3254 (accuracy 5 ppm), while aggregated or sodium adduct peaks were not visible. The $[M + H]^+$ peak was observed at *m/z* 1539.0872 (accuracy 13 ppm) for the compound **12**. The mass spectrum of phthalocyanine **15** showed the high accuracy $[M + H]^+$ peak at *m/z* 1523.3571 (accuracy 0.8 ppm). The structures of intermediate products of compound **22** were proved with mass spectrometry (see Supporting information). Tetra-*tert*-butylsuccinatoxy-substituted Pc was measured using negative mode, and the $[M - H]^-$ and $[2M - H]^-$ peaks were found at *m/z* 1625.6118 and 3252.2451 (accuracy 0.4 ppm), respectively. The $[M + H]^+$ peak was observed at *m/z* 1403.3928 (accuracy 6 ppm) for tetrasuccinate Pc. In the spectrum of the compound **22** the $[M + H]^+$ peak at *m/z* 2067.3279 (accuracy 3 ppm) was visible. Also the $[3M + 2H]^{2+}$ peak was observed at *m/z* 3100.5364 in the spectrum of Pc **22**.

Absorption and emission spectra

In the absorption spectra of the monohydroxy phthalocyanine **3** (Fig. 2) and its derivatives, the Q- and Soret bands are well visible. The Q-band shows two maxima: one is located around 760 nm and another one is found between 734-739 nm, depending on the compound (Table 1, 2). The spectra also show a shoulder between 650-700 nm. The molar absorptivity (ε) of the compound **13** (99600 $M^{-1}.cm^{-1}$) (Fig. 3a) is a bit higher than that of the molecule **3** (89350 $M^{-1}.cm^{-1}$). The highest ε value (154900 $M^{-1}.cm^{-1}$) is found for the Pc **20** (Fig. 4a). The Soret band maximum is located between 335-339 nm, depending on the compound. These wavelengths were used as an excitation wavelength in fluorescence measurements. Emission maximum is situated at 774 nm for Pcs **3** and **13**, while for the compound **20** the maximum peak is shifted a little to shorter wavelength (see Supporting information). All these spectra were measured in $CHCl_3$.

The absorption spectra of the bishydroxy Pc **6** (Fig. 2) and its derivatives show Q-band, which consists of two intense peaks around 700 nm and two lower shoulders between 600-660 nm. The peak around 688 nm is more intense than other maxima at higher wavelength. For the phthalocyanine **6**, these peaks are located at 693 nm and 719 nm, respectively (Table 1). The molar absorptivity of the bisthioacetate Pc **14** (130800 $M^{-1}.cm^{-1}$) is the highest of all of these compounds (Fig. 3a). In the Soret band, all absorptions show one intense broad band as well as one less intense one at roughly 300 nm. The Soret band maximum is located at 340 nm for the compound **6**, while for the molecules **14** and **21** (Fig. 4a) it is found at 343 nm (Table 2). These wavelengths were used as an excitation wavelength in emission measurements. Emission maximum is found at 730 nm for Pc **6** (see Supporting information). In other spectra the emission maximum is shifted by 3 nm to the red. Fluorescence spectra also show broad and weak emission around 810 nm for all the compounds.

Absorption spectra of the tetra-substituted Pcs **8** (Fig. 2), **15** (Fig. 3a) and **22** (Fig. 4a) show two maxima in the Q-bands around 685 nm and 710 nm (Table 1, 2). In the spectra of the tetrahydroxy compound **8** and the tetra(pentafluorophenyl ester) phthalocyanine **22** the intensity of the latter peak is higher, but in the spectrum of **15** this ratio is opposite. In Q-bands a shoulder is found between 600-660 nm, which is also seen in the absorption spectra of bis-functionalized Pcs. Molar absorptivity (ε) of the compound **8** is 155200 $M^{-1}.cm^{-1}$ and for the tetrathioacetate molecule **15** the ε value has reduce a little bit to 97500 $M^{-1}.cm^{-1}$. For tetra(pentafluorophenyl ester) Pc **22** the value of ε is 102800 $M^{-1}.cm^{-1}$. The Soret band maximum is located around 330 nm in the spectra of the compounds **8**, **15** and **22**.

The excitation wavelength of the emission measurements was the Soret band maximum for all compounds. The phthalocyanines **8**, **15** and **22** are emitting at roughly 722 nm, and also at 810 nm a weak emission band is visible (see Supporting information). The spectra of molecules **8** and **15** were measured in DMF, and measurements of Pc **22** were done in $CHCl_3$.

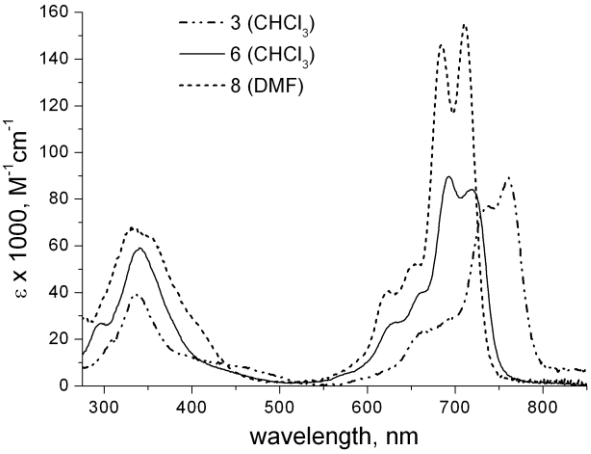

Fig. 2. Absorption spectra of monohydroxy **3**, bishydroxy **6** and tetrahydroxy **8** phthalocyanines

Table 1. Absorption and emission maxima of hydroxy-substituted phthalocyanines **3**, **6** and **8**

Compound	Absorption λ_{max}, nm	Emission λ_{max}, nm
3 ($CHCl_3$)	761, 739, 337	774
6 ($CHCl_3$)	719, 693, 340	730, 810
8 (DMF)	711, 685, 331	722, 810

Table 2. Absorption and emission maxima of thioacetyl-substituted phthalocyanines **13**-**15**, and pentafluorophenyl ester-substituted phthalocyanines **20**-**22**

Compound	Absorption λ_{max}, nm	Emission λ_{max}, nm
13 ($CHCl_3$)	761, 737, 339	774
14 ($CHCl_3$)	715, 688, 344	727, 810
15 (DMF)	713, 688, 332	722, 810
20 ($CHCl_3$)	760, 734, 335	772
21 ($CHCl_3$)	713, 689, 343	727, 810
22 ($CHCl_3$)	716, 684, 337	722, 810

Immobilization on substrates

SAM on gold

It is well known that organosulfur compounds can react with gold. In the case of thioacetyl, an oxidative addition of the S-Ac bond occurs on a gold surface followed by a reductive elimination of acetyl group (Ac) [16]. For spectral measurements, a robust and optically transparent substrate is required, thus, a titanium layer (2 nm) was thermally evaporated on cleaned glass plates first, and on top of this adhesion layer a 3 nm thick gold layer was evaporated. Absorption spectra of the substrates were recorded and used later to calculate the spectra of SAMs. Gold substrates were immersed into solutions of phthalocyanines **13**, **14** and **15** in CH_2Cl_2, where concentration of each solution was 3 mM [32]. The plates were kept at room temperature for 30 min, and after that SAMs on gold surface were rinsed several times with CH_2Cl_2 and $CHCl_3$ to remove unbound Pc molecules.

Absorption spectra of the SAMs **13-15** on gold surfaces show a band between 600-800 nm (Q-band) (Fig. 3b). Compared to the spectra of solutions, the maxima of absorption spectra of SAM **13** and **14** are shifted to shorter wavelengths, even though defining the maxima of the spectra is difficult because of the low absorption of SAMs (Table 3). The shift of the band maxima of SAM **14** on gold is around 40 nm. The spectrum of SAM **15** is red-shifted by 10 nm compared to the spectrum of **15** in DMF. Besides shifting, the Q-bands of the SAM spectra are also broader. No detectable emission of phthalocyanines SAMs was observed.

The absorption maxima of the Q-bands provide a possibility to estimate the mean molecular areas (mma) of phthalocyanines in the SAMs. The mma values calculated assuming the same molar absorption of Pcs in solution and SAMs are presented in Table 3. Comparing the molecular areas of phthalocyanines **13-15** the area increases towards larger chromophore as expected. However, differences in Pc bonding densities are small and the values are larger than what one could expect for tightly packed monolayers. This can be due to a gradual decrease of the molar absorption in SAMs compared to that in solution. Indeed, the Q-bands are 2-3 times broader for films, indicating that the molar absorption can be 2-3 times lower for SAMs. The mean molecular area is better controlled when monolayers are prepared by Langmuir-Blodgett (LB) or Langmuir-Schäfer (LS) methods. It has been shown previously that one LS-monolayer of bishydroxy Pc **6** on quartz plate has an absorbance of *ca.* 0.005, which corresponds to the molecular area of 0.62 nm^2 and can be achieved in the case of vertical orientation of macrocycles in respect to the substrate [33]. In the present case, optical density of one layer on gold is 0.007, but the mma value calculated based on solution molar absorption is 3 nm^2. Therefore the mma values listed in Table 3 present the higher limits for actual mma values, but actual bonding densities of molecules are expected to be 2-3 times greater.

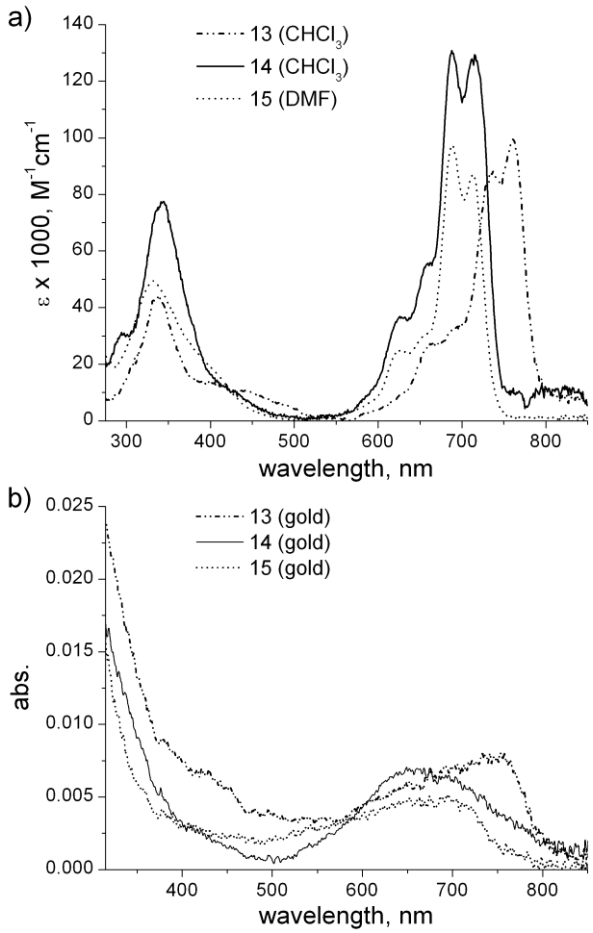

Fig. 3. a) Absorption spectra of monothioacetate **13**, bisthioacetate **14** and tetrathioacetate **15** phthalocyanines, b) absorption spectra of SAMs **13**, **14** and **15** on gold

Table 3. Absorption maxima and mean molecular areas (mma[a]) of SAMs **13**-**15** and **20**-**22** on different substrates

Compound	Absorption λ_{max}, nm	mma, nm^2
13 (gold)	750	2.07
20 (glass)	740, 330	2.06
14 (gold)	650	3.10
21 (glass/ITO)	640, 330	1.61
15 (gold)	695	3.24
22 (glass/ITO)	695, 330	1.90/2.13

[a] mma = ε / ($N_A A$), where ε is molar absorptivity, N_A is Avogadro constant and A is absorbance of the layer

SAM on glass and ITO

Glass and ITO plates were cleaned by sonication in organic solvents before the preparation of SAMs (see Experimental). SAMs were done with a two step process; first the plates were activated with 3-aminopropyltrimethoxysilane in dry toluene at 105 °C for 1h. Phthalocyanines were then covalently attached to the aminopropylsilylated surface by immersing the plates into a solution of compound **20**, **21** or **22** in dry toluene. This was done through amide bond formation between pentafluorophenyl ester group on Pcs and amino group on silylated

substrates (Scheme 4) [34]. This second step was completed in 2 h at 105 °C. Both steps were done under argon. To remove residual physisorbed Pc, the samples were sonicated in toluene and CH_2Cl_2 after the second step. After drying in argon, the UV-vis spectra of the plates with SAMs were measured.

In the absorption spectra of the monolayers on glass and ITO surfaces (Fig. 4b, 4c), one has to take into account that layers are formed on each side of the substrates. Therefore, comparing with absorbances of SAMs on gold surface (Fig. 3b), optical densities of SAMs on glass and ITO are roughly doubled. Absorption spectrum of the SAM **20** on glass substrate shows clear Q- and Soret bands (Table 3). Both are shifted towards shorter wavelengths compared to absorption maxima of the Pc **20** in solution (Table 2). For unknown reasons, the absorption of SAM **20** on ITO is five times smaller than on glass. Results were also the same with an extended reaction time of both steps, so it seems that the molecules bond very weakly onto ITO. This kind of selectivity towards the substrate will be a subject of separate studies. However, the shapes of the absorption spectra of samples **20** on glass and on ITO are the same and very similar to the absorption in solution. In the absorption spectrum of SAM **21** on glass and ITO (Fig. 4b) the Q-band is blue-shifted by almost 50 nm in comparison to the absorption spectrum of **21** in $CHCl_3$ (Table 2). This huge shift is also seen in the spectrum of same molecule on gold. The absorptions of SAM **21** on glass and on ITO are perfectly same on both substrates. The absorption spectra of SAM **22** on glass and ITO (Fig. 4c) are also the same; the absorbance of SAM on ITO is a little smaller than on glass. The spectra show Q-band maxima around 695 nm, which is between the two maxima in the absorption spectrum of compound **22** in $CHCl_3$ (Table 2, 3). Emissions of SAMs **20**, **21** and **22** on glass/ITO substrates were not detectable.

Mean molecular areas (mma) of SAM **20** on glass, **21** and **22** on glass and ITO are very similar (Table 3). Sample **21** on both substrates gives a slightly smaller value than the mono-substituted Pc **20** on glass and the tetra-substituted Pc **22** on glass and on ITO. This difference could be because the molecule **20** has greater side substituents than the *tert*-butyl groups in molecule **21**, while molecule **22** should have preferably flat orientation on surface. Also these results show high mma values and therefore presented results are the higher limits for actual mma values. Bonding density of the compound **20** on glass is the same as the value of SAM **13** on gold. On the other hand, comparing the molecular areas of SAM **14** on gold and SAMs **21** on glass and ITO a difference of 1.5 nm^2 is noticed, which can be attributed to the different tilting angles of the molecules on different substrates. A smaller difference is observed when comparing the SAMs **15** (gold) and **22** (glass/ITO).

As can be seen, the arrangement of different Pcs on gold and on ITO/glass is similar and corresponds to the arrangement of chromophores in LB/LS films. However, the organization of the layer does not depend solely on the number of anchor groups, but is influenced as well by the side substituents and by the interaction of the macrocycle with the substrate surface.

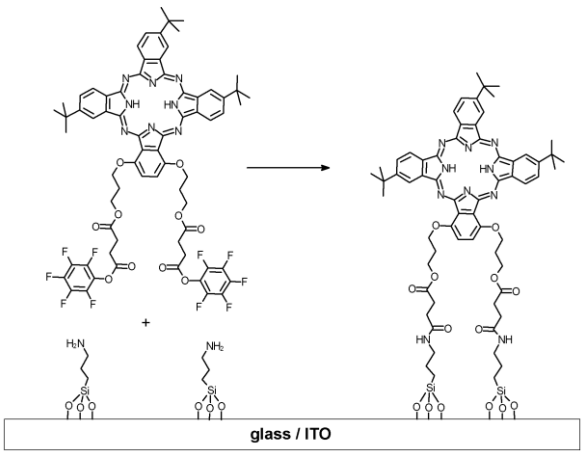

Scheme 4. Covalent attachment of phthalocyanine **21** to activated surface

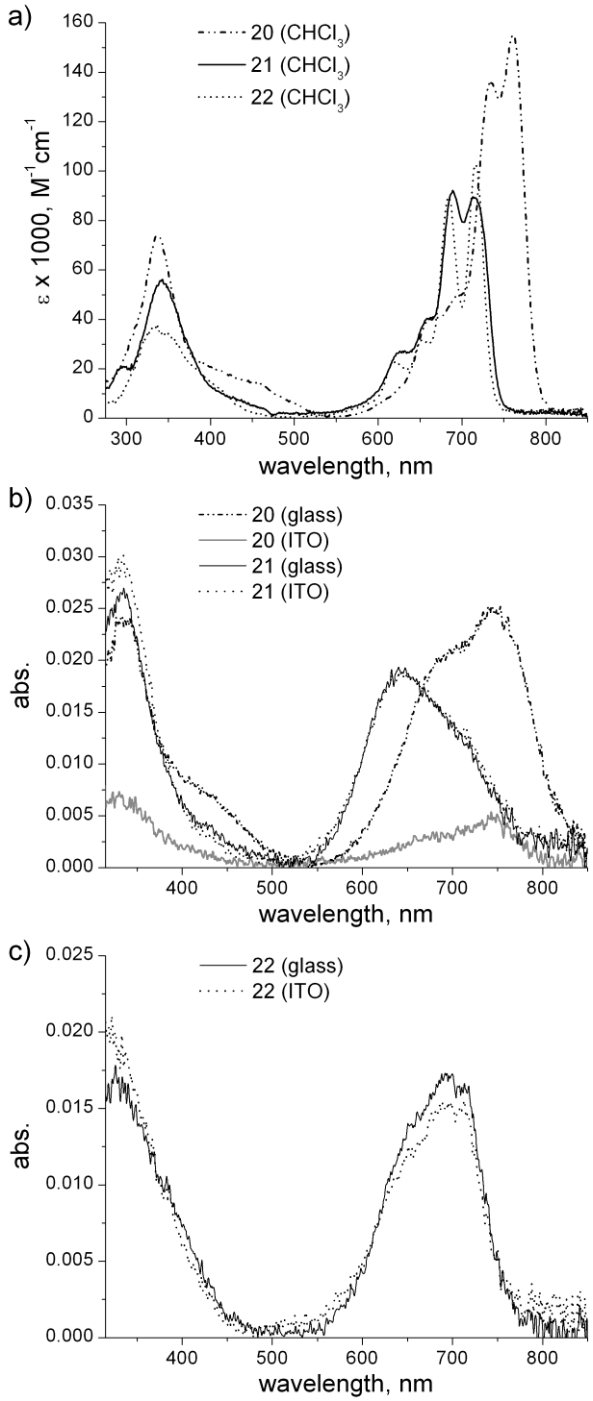

Fig. 4. a) Absorption spectra of mono(pentafluorophenyl ester) **20**, bis(pentafluorophenyl ester) **21** and tetra(pentafluorophenyl ester) **22** phthalocyanines, b) absorption spectra of SAMs **20** and **21** on glass and ITO, c) absorption spectra of SAM **22** on glass and ITO

EXPERIMENTAL

Materials and instrumentations

The solvents of HPLC grade were purchased from Aldrich Chemical Company, Merck, and VWR International. Chemicals were purchased from Acros Organics, Aldrich Chemical Company, or Fluka Chemie. All the materials were used as received without further purification. The monitoring of reactions was carried out by thin layer chromatography

(TLC), employing aluminum sheets precoated with Silica 60 F254 (Merck). The purification and isolation of the products was performed by column chromatography on Silica 60 (mesh size 40 – 63 μm) or Silica 100 (mesh size 63 – 200 μm).

The ^{1}H NMR spectra were measured on Varian Mercury 300 MHz spectrometer (Varian Inc.). All chemical shifts are given in ppm relative to TMS as internal standard. Mass spectra were recorded on ESI-TOF LCT Permier XE mass spectrometer (Waters Corp.). The sample of the analyte was dissolved in an appropriate solvent at concentration *ca.* 0.01 mg.mL^{-1} and infused at a rate of 15 μL.min^{-1}. The reference solution of Leucine Enkephaline (50 pg.mL^{-1}) was infused simultaneously. Original spectra were centered, and lock mass TOF correction was applied. Absorption spectra were measured using Shimadzu UV-2501PC UV-Vis Recording spectrometer, and emission spectra were recorded on Fluorolog Yobin Yvon-SPEX spectrofluorometer.

Synthesis

1,4,8,11,15,18-hexabutoxy-23-[3-(hydroxymethyl)phenoxy]phthalocyanine (3). 3,6-dibutoxyphthalonitrile (**1**) (408 mg, 1.5 mmol), 4-[3-(hydroxymethyl)phenoxy]phthalonitrile (**2**) (75 mg, 0.3 mmol) and lithium (40 mg, 5.8 mmol) were suspended in 1-butanol (12 mL). The reaction mixture was heated at reflux for 4 h under a drying tube. The dark green solution was cooled down to room temperature and $CHCl_3$ (20 mL) was added. The organic phase was washed with water (4 × 100 mL) and the solvent was evaporated under reduced pressure (bath temperature 80 °C). The mixture of the reaction products was purified by column chromatography on Silica 100, eluting with $CHCl_3$. The product was obtained as the second fraction (R_f = 0.55 in $CHCl_3$/EtOH 18:1). The product was crystallized on a watch glass and washed with acetonitrile. Second chromatographic purification was done on Silica 60, eluting with $CHCl_3$. The product **3** was obtained from the second fraction as a dark green solid (78 mg, 24%). UV-vis ($CHCl_3$): λ_{max}, nm (ε, M^{-1}.cm^{-1}) 337 (39167), 739 (77105), 761 (89351). ^{1}H NMR (300 MHz; $CDCl_3$; Me_4Si): δ_H, ppm 9.30 (1H, d, J = 8.3 Hz, 25-phthalo-*H*), 8.90 (1H, d, J = 2.1 Hz, 22-phthalo-*H*), 7.83 (1H, dd, J_1 = 8.3 Hz, J_2 = 2.1 Hz, 24-phthalo-*H*), 7.68-7.12 (10H, m, phthalo-*H*, Ar-*H*), 4.91-4.81 (8H, m, 4,8,11,15-OCH_2C$_3$H$_7$), 4.78 (2H, br s, ArCH_2OH), 4.70 (2H, t, J = 6.4 Hz, 1-OCH_2C$_3$H$_7$), 4.61 (2H, t, J = 6.4 Hz, 18-OCH_2C$_3$H$_7$), 2.51-2.39 (2H, m, 1-OCH$_2$CH_2C$_2$H$_5$), 2.30-2.16 (10H, m, 4,8,11,15,18-OCH$_2$CH_2C$_2$H$_5$), 2.14-2.04 (2H, m, 1-OC$_2$H$_4$CH_2CH$_3$), 1.94-1.78 (2H, m, 18-OC$_2$H$_4$CH_2CH$_3$), 1.72-1.61 (8H, m, 4,8,11,15-OC$_2$H$_4$CH_2CH$_3$), 1.28 (3H, t, J = 7.4 Hz, 1-OC$_3$H$_6$CH_3), 1.14-1.05 (15H, m, 4,8,11,15,18-OC$_3$H$_6$CH_3), 0.10 (2H, s, N*H*), ArCH$_2$O*H* was not resolved. MS (ESI-TOF; CH_2Cl_2/MeOH 1:1): *m/z* 1069.5599 [M + H]$^+$ (calcd. for $C_{63}H_{72}N_8O_8$ 1069.5552).

3-bromopropionyl chloride (9). Oxalyl chloride (0.36 ml, 4.25 mmol) and DMF (5 μL) were added to a solution of 3-bromopropionic acid (500 mg, 3.27 mmol) in CH_2Cl_2 (5 mL). The solution was stirred at room temperature for 16 h. The solvent was evaporated under reduced pressure (bath temperature 40 °C) to yield quantitatively the compound **9**. The residue was redissolved in CH_2Cl_2 (2 mL). Concentration: 1.64 M.

1,4,8,11,15,18-hexabutoxy-23-[3-(3-bromopropanoatemethyl)phenoxy]phthalocyanine (10). Phthalocyanine **3** (20 mg, 18.7 μmol) was dissolved in CH_2Cl_2 (5 mL) and 3-bromopropionyl chloride (**9**) (1.64 M solution in CH_2Cl_2, 68 μL, 112.2 μmol) was added in to the solution. The reaction mixture was stirred at room temperature for 1 day. A few milliliters of $CHCl_3$ were added and the organic layer was washed with saturated $NaHCO_3$ (aq) (13 × 50 mL) and water (2 × 50 mL). The solvent was evaporated under reduced pressure and the crude product was purified three times by column chromatography on Silica 60, eluting with $CHCl_3$. The product was collected as first green fraction (R_f = 0.83 in $CHCl_3$/EtOH 18:1) and was crystallized on a watch glass and washed with n-pentane. The compound **10** was obtained as a dark green solid (17 mg, 77%). UV-vis ($CHCl_3$): λ_{max}, nm (abs.) 339 (0.04963), 735 (0.09788), 761 (0.11309). ^{1}H NMR (300 MHz; $CDCl_3$; Me_4Si): δ_H, ppm 9.31 (1H, d, J = 8.3 Hz, 25-phthalo-*H*), 8.91 (1H, d, J = 2.0 Hz, 22-phthalo-*H*), 7.83 (1H, dd, J_1 = 8.3 Hz, J_2 = 2.1 Hz, 24-phthalo-*H*), 7.69-7.12 (10H, m, phthalo-*H*, Ar-*H*), 5.24 (2H, s, ArCH_2O),

4.91-4.82 (8H, m, 4,8,11,15-OCH_2C$_3$H$_7$), 4.70 (2H, t, J = 6.4 Hz, 1-OCH_2C$_3$H$_7$), 4.61 (2H, t, J = 6.4 Hz, 18-OCH_2C$_3$H$_7$), 3.77-3.52 (2H, m, COCH$_2$CH_2Br), 3.01-2.83 (2H, m, COCH_2CH$_2$Br), 2.51-2.39 (2H, m, 1-OCH$_2$CH_2C$_2$H$_5$), 2.30-2.16 (10H, m, 4,8,11,15,18-OCH$_2$CH_2C$_2$H$_5$), 2.14-2.03 (2H, m, 1-OC$_2$H$_4$CH_2CH$_3$), 1.95-1.82 (2H, m, 18-OC$_2$H$_4$CH_2CH$_3$), 1.73-1.60 (8H, m, 4,8,11,15-OC$_2$H$_4$CH_2CH$_3$), 1.28 (3H, t, J = 7.4 Hz, 1-OC$_3$H$_6$CH_3), 1.13-1.05 (15H, m, 4,8,11,15,18-OC$_3$H$_6$CH_3), 0.10 (2H, s, NH). MS (ESI-TOF; CH$_2$Cl$_2$/MeOH 1:1): *m/z* 1203.4954 [M + H]$^+$ (calcd. for C$_{66}$H$_{75}$N$_8$O$_9$Br 1203.4918).

1,4,8,11,15,18-hexabutoxy-23-[3-(3-acetylsulfonylpropanoatemethyl)phenoxy]phthalocyanine (13). The product **10** (17 mg, 14.1 μmol) was dissolved in acetone (25 mL) and KSAc (3.2 mg, 28.2 μmol) was added. The mixture was heated at reflux under a drying tube for 3 days. After 24 h and 48 h of refluxing, more KSAc (2 mg) and acetone were added. Finally the green solution was cooled down to room temperature and the solvent was evaporated under reduced pressure. The crude product was dissolved in CHCl$_3$, the organic phase was washed with water (5 × 50 mL), and evaporated to dryness under reduced pressure. The product was purified twice by column chromatography on Silica 60, eluting with toluene/EtOAc 5:1, and the compound **13** was collected as second green fraction (R_f = 0.50 in toluene/EtOAc 5:1). The product **13** was obtained as a dark green solid (10 mg, 59%) after crystallizing on a watch glass and washing with n-pentane. UV-vis (CHCl$_3$): λ_{max}, nm (ε, M^{-1}.cm^{-1}) 339 (44056), 737 (88228), 761 (99622). ^{1}H NMR (300 MHz; CDCl$_3$; Me$_4$Si): δ_H, ppm 9.30 (1H, d, J = 8.3 Hz, 25-phthalo-H), 8.91 (1H, d, J = 2.1 Hz, 22-phthalo-H), 7.83 (1H, dd, J_1 = 8.3 Hz, J_2 = 2.1 Hz, 24-phthalo-H), 7.69-7.12 (10H, m, phthalo-H, Ar-H), 5.21 (2H, s, ArCH_2O), 4.91-4.82 (8H, m, 4,8,11,15-OCH_2C$_3$H$_7$), 4.70 (2H, t, J = 6.4 Hz, 1-OCH_2C$_3$H$_7$), 4.61 (2H, t, J = 6.4 Hz, 18-OCH_2C$_3$H$_7$), 3.11 (2H, t, J = 7.0 Hz, COCH$_2$CH_2S), 2.70 (2H, t, J = 7.0 Hz, COCH_2CH$_2$S), 2.51-2.39 (2H, m, 1-OCH$_2$CH_2C$_2$H$_5$), 2.30-2.23 (5H, m, OCH$_2$CH_2C$_2$H$_5$), 2.22 (3H, s, SCOCH_3), 2.21-2.16 (5H, m, OCH$_2$CH_2C$_2$H$_5$), 2.14-2.03 (2H, m, 1-OC$_2$H$_4$CH_2CH$_3$), 1.95-1.81 (2H, m, 18-OC$_2$H$_4$CH_2CH$_3$), 1.74-1.60 (8H, m, 4,8,11,15-OC$_2$H$_4$CH_2CH$_3$), 1.28 (3H, t, J = 7.4 Hz, 1-OC$_3$H$_6$CH_3), 1.13-1.05 (15H, m, 4,8,11,15,18-OC$_3$H$_6$CH_3), 0.10 (2H, s, NH). MS (ESI-TOF; CHCl$_3$/MeOH 1:1): *m/z* 1199.5671 [M + H]$^+$ (calcd. for C$_{68}$H$_{78}$N$_8$O$_{10}$S 1199.5640).

1,4,8,11,15,18-hexabutoxy-23-[3-(*tert*-butylsuccinatoxymethyl)phenoxy]phthalocyanine (16). The compound **3** (50 mg, 46.8 μmol) was dissolved in CH$_2$Cl$_2$ (20 mL) and DCC (14 mg, 70.2 μmol), DMAP (2 mg, 14.0 μmol) and mono-*tert*-butyl succinate (12 mg, 70.2 μmol) were added. The reaction mixture was stirred at room temperature for 2 days. DCC (14 mg) and mono-*tert*-butyl succinate (12 mg) were added more after 1 day of stirring. The solvent was evaporated under reduced pressure, the product was redissolved in a few milliliters of CH$_2$Cl$_2$, and the solution was filtered twice through a cotton plug. Column chromatography was used for purification of the product (Silica 60, eluting with CHCl$_3$). The product was collected as first green fraction (R_f = 0.85 in CHCl$_3$/EtOH 18:1), crystallized on a watch glass, and washed with 2 mL of acetonitrile. The product **16** was obtained as a dark green solid with quantitative yield (57 mg). ^{1}H NMR (300 MHz; CDCl$_3$; Me$_4$Si): δ_H, ppm 9.30 (1H, d, J = 8.3 Hz, 25-phthalo-H), 8.91 (1H, d, J = 2.1 Hz, 22-phthalo-H), 7.82 (1H, dd, J_1 = 8.3 Hz, J_2 = 2.1 Hz, 24-phthalo-H), 7.69-7.12 (10H, m, phthalo-H, Ar-H), 5.22 (2H, s, ArCH_2O), 4.91-4.82 (8H, m, 4,8,11,15-OCH_2C$_3$H$_7$), 4.70 (2H, t, J = 6.4 Hz, 1-OCH_2C$_3$H$_7$), 4.61 (2H, t, J = 6.4 Hz, 18-OCH_2C$_3$H$_7$), 2.70-2.53 (4H, m, COC$_2H_4$CO), 2.51-2.40 (2H, m, 1-OCH$_2$CH_2C$_2$H$_5$), 2.30-2.17 (10H, m, 4,8,11,15,18-OCH$_2$CH_2C$_2$H$_5$), 2.15-2.03 (2H, m, 1-OC$_2$H$_4$CH_2CH$_3$), 1.99-1.76 (2H, m, 18-OC$_2$H$_4$CH_2CH$_3$), 1.74-1.60 (8H, m, 4,8,11,15-OC$_2$H$_4$CH_2CH$_3$), 1.40 (9H, s, OC(CH_3)$_3$), 1.28 (3H, t, J = 7.4 Hz, 1-OC$_3$H$_6$CH_3), 1.14-1.05 (15H, m, 4,8,11,15,18-OC$_3$H$_6$CH_3), 0.10 (2H, s, NH). MS (ESI-TOF; CHCl$_3$/MeOH 1:1): *m/z* 1225.6375 [M + H]$^+$ (calcd. for C$_{71}$H$_{84}$N$_8$O$_{11}$ 1225.6338).

1,4,8,11,15,18-hexabutoxy-23-[3-(succinatoxymethyl)phenoxy]phthalocyanine (18). The product **16** (57 mg, 46.5 μmol) was dissolved in dry CH$_2$Cl$_2$ (2 mL), TFA (2 mL) was added, and the solution was stirred at room temperature for 3 h. More CH$_2$Cl$_2$ was added and the organic phase was washed with water (3 × 50 mL). After evaporating the solvent under reduced pressure, the product was crystallized on a watch glass and washed with n-pentane. The product **18** (R_f =

0.30 in $CHCl_3$/EtOH 9:1) was obtained as dark green solid (50 mg, 93%). UV-vis ($CHCl_3$): λ_{max}, nm (ε, $M^{-1}.cm^{-1}$) 335 (43472), 734 (85217), 761 (98005). ^1H NMR (300 MHz; $CDCl_3$; Me_4Si): δ_H, ppm 9.30 (1H, d, J = 8.3 Hz, 25-phthalo-*H*), 8.85 (1H, d, J = 2.0 Hz, 22-phthalo-*H*), 7.84 (1H, dd, J_1 = 8.3 Hz, J_2 = 2.1 Hz, 24-phthalo-*H*), 7.69-7.12 (10H, m, phthalo-*H*, Ar-*H*), 5.21 (2H, s, ArCH_2O), 4.90-4.81 (8H, m, 4,8,11,15-OCH_2C$_3$H$_7$), 4.69 (2H, t, J = 6.4 Hz, 1-OCH_2C$_3$H$_7$), 4.59 (2H, t, J = 6.4 Hz, 18-OCH_2C$_3$H$_7$), 2.67-2.52 (4H, m, COC$_2H_4$CO), 2.50-2.39 (2H, m, 1-OCH$_2$CH_2C$_2$H$_5$), 2.30-2.18 (10H, m, 4,8,11,15,18-OCH$_2$CH_2C$_2$H$_5$), 2.16-2.03 (2H, m, 1-OC$_2$H$_4$CH_2CH$_3$), 1.97-1.77 (2H, m, 18-OC$_2$H$_4$CH_2CH$_3$), 1.74-1.59 (8H, m, 4,8,11,15-OC$_2$H$_4$CH_2CH$_3$), 1.28 (3H, t, J = 7.4 Hz, 1-OC$_3$H$_6$CH_3), 1.12-1.05 (15H, m, 4,8,11,15,18-OC$_3$H$_6$CH_3), 0.09 (2H, s, N*H*), COO*H* was not resolved. MS (ESI-TOF; MeOH/$CHCl_3$ 10:1): *m/z* 1169.5627 $[M + H]^+$ (calcd. for $C_{67}H_{76}N_8O_{11}$ 1169.5712).

1,4,8,11,15,18-hexabutoxy-23-[3-((pentafluorophenoxy)succinatoxymethyl)phenoxy]phthalocyanine (20). DCC (14 mg, 68.4 μmol) and pentafluorophenol (13 mg, 68.4 μmol) were added to a solution of the compound **18** (40 mg, 34.2 μmol) in EtOAc (10 mL). The mixture of compounds was stirred at room temperature. After 1 day of stirring, DCC (14 mg) and pentafluorophenol (13 mg) were added more. After 5 days the solvent was evaporated under reduced pressure, the product was dissolved in a few milliliters of CH_2Cl_2 and filtered through a cotton plug. Purification was carried out twice by column chromatography on Silica 100 and on Silica 60, eluting both times with $CHCl_3$. The product **20** was collected as first green fraction (R_f = 0.85 in $CHCl_3$/EtOH 18:1) and crystallized on a watch glass. After washing with n-pentane, the compound **20** was obtained as a dark green solid (25 mg, 55%). UV-vis ($CHCl_3$): λ_{max}, nm (ε, $M^{-1}.cm^{-1}$) 335 (73731), 734 (136634), 760 (154889). ^1H NMR (300 MHz; $CDCl_3$; Me_4Si): δ_H, ppm 9.30 (1H, d, J = 8.3 Hz, 25-phthalo-*H*), 8.91 (1H, d, J = 2.1 Hz, 22-phthalo-*H*), 7.83 (1H, dd, J_1 = 8.3 Hz, J_2 = 2.1 Hz, 24-phthalo-*H*), 7.69-7.12 (10H, m, phthalo-*H*, Ar-*H*), 5.23 (2H, s, ArCH_2O), 4.91-4.82 (8H, m, 4,8,11,15-OCH_2C$_3$H$_7$), 4.70 (2H, t, J = 6.4 Hz, 1-OCH_2C$_3$H$_7$), 4.61 (2H, t, J = 6.4 Hz, 18-OCH_2C$_3$H$_7$), 2.97-2.91 (2H, m, COC$_2H_4$CO), 2.84-2.78 (2H, m, COC$_2H_4$CO), 2.51-2.40 (2H, m, 1-OCH$_2$CH_2C$_2$H$_5$), 2.30-2.18 (10H, m, 4,8,11,15,18-OCH$_2$CH_2C$_2$H$_5$), 2.15-2.03 (2H, m, 1-OC$_2$H$_4$CH_2CH$_3$), 1.95-1.81 (2H, m, 18-OC$_2$H$_4$CH_2CH$_3$), 1.74-1.60 (8H, m, 4,8,11,15-OC$_2$H$_4$CH_2CH$_3$), 1.29 (3H, t, J = 7.4 Hz, 1-OC$_3$H$_6$CH_3), 1.12-1.05 (15H, m, 4,8,11,15,18-OC$_3$H$_6$CH_3), 0.09 (2H, s, N*H*). MS (ESI-TOF; MeOH/$CHCl_3$ 10:1): *m/z* 1335.5555 $[M + H]^+$ (calcd. for $C_{73}H_{75}N_8O_{11}F_5$ 1335.5554).

1,4-di[hydroxypropyloxy]-9(10),16(17),23(24)-tri[*tert*-butyl]phthalocyanine (6). Lithium (80 mg, 12 mmol) was dissolved in 1-pentanol (40 mL) under argon atmosphere. 3,6-di(hydroxypropyloxy)phthalonitrile (**4**) (160 mg, 0.58 mmol) and 4-*tert*-butylphthalonitrile (**5**) (641 mg, 3.48 mmol) were added and the reaction mixture was heated at reflux for 2.5 h under argon atmosphere. The solution was cooled down to room temperature and the solvent was evaporated under reduced pressure (bath temperature 80 °C). The product was dissolved in $CHCl_3$, the organic layer was washed with water (2 × 100 mL) and the solvent was evaporated under reduced pressure. The crude product was purified by column chromatography on Silica 100, eluting the first fraction with $CHCl_3$ and the second fraction with $CHCl_3$/EtOH 20:1. The product **6** was obtained from the second fraction (R_f = 0.40 in $CHCl_3$/EtOH 18:1). Second fraction was repurified on Silica 60, eluting as before. The collected product **6** was crystallized on a watch glass, washed with acetonitrile, and obtained as a dark green powder (99 mg, 20%) after drying. UV-vis ($CHCl_3$/EtOH 1:1): λ_{max}, nm (ε, $M^{-1}.cm^{-1}$) 340 (59122), 693 (89631), 719 (84165). ^1H NMR (300 MHz; $CDCl_3$/CD_3OD 10:1; Me_4Si): δ_H, ppm 9.50-8.45 (6H, m, phthalo-*H*), 8.28-8.07 (3H, m, phthalo-*H*), 6.88-6.07 (2H, m, 2,3-phthalo-*H*), 4.65-4.24 (8H, m, OCH_2CH$_2$CH_2OH), 2.51-2.23 (4H, m, OCH$_2$CH_2CH$_2$OH), 1.91-1.68 (27H, m, C(CH_3)$_3$), -2.40 – -2.97 (2H, m, N*H*), CH$_2$O*H* were not resolved. MS (ESI-TOF; $CHCl_3$/MeOH 1:1): *m/z* 831.4359 $[M + H]^+$ (calcd. for $C_{50}H_{54}N_8O_4$ 831.4346).

1,4-di[(3-bromopropanoate)propyloxy]-9(10),16(17),23(24)-tri[*tert*-butyl]phthalocyanine (11). Phthalocyanine **6** (20 mg, 24 μmol) was dissolved in CH_2Cl_2 (5 mL) and 3-bromopropionyl chloride (**9**) (1.64 M solution in CH_2Cl_2, 0.176 ml, 288 μmol) was added in to the sealed vial. The reaction mixture was stirred at room temperature for 3 days. A

little amount of $CHCl_3$ was added, the organic phase was washed with saturated $NaHCO_3$ (aq) (9 × 50 mL) and water (1 × 50 mL), and the solvent was evaporated under reduced pressure. Column chromatography was used for purification of the product (Silica 100, eluting with $CHCl_3$). The target product was collected as first green fraction (R_f = 0.94 in $CHCl_3$/EtOH 18:1). The product **11** was crystallized on a watch glass, washed with n-pentane and it was obtained as a dark green solid (14 mg, 55%). UV-vis ($CHCl_3$/EtOH 1:1): λ_{max}, nm (ε, $M^{-1}.cm^{-1}$) 340 (62352), 689 (94878), 717 (91875). ^1H NMR (300 MHz; $CDCl_3$; Me_4Si): δ_H, ppm 9.49-8.63 (6H, m, phthalo-*H*), 8.35-8.10 (3H, m, phthalo-*H*), 7.15-6.69 (2H, m, 2,3-phthalo-*H*), 4.91-4.33 (8H, m, $OCH_2CH_2CH_2O$), 3.82-3.49 (4H, m, $COCH_2CH_2Br$), 3.03-2.76 (4H, m, $COCH_2CH_2Br$), 2.71-2.41 (4H, m, $OCH_2CH_2CH_2O$), 1.90-1.76 (27H, m, $C(CH_3)_3$), -1.34 – -1.71 (2H, m, N*H*). MS (ESI-TOF; $CHCl_3$/MeOH 1:1): *m/z* 1098.3121 $[M]^+$ (calcd. for $C_{56}H_{60}N_8O_6Br_2$ 1098.3003).

1,4-di[(3-acetylsulfonylpropanoate)propyloxy]-9(10),16(17),23(24)-tri[*tert*-butyl]phthalocyanine (14). The product **11** (19 mg, 17.3 μmol) was dissolved in acetone (7 mL). KSAc (7.9 mg, 69.2 μmol) was added and the reaction mixture was stirred at room temperature for 4 days. The solvent was evaporated under reduced pressure and the dry product was dissolved in $CHCl_3$. The organic phase was washed with water (5 × 50 mL) and then evaporated to dryness under reduced pressure. Purification of the crude product was performed by column chromatography on Silica 100, eluting with toluene/EtOAc 5:1. The target product **14** was collected as second fraction (R_f = 0.27 in toluene/EtOAc 5:1), crystallized on a watch glass, and washed with n-pentane. The compound **14** was obtained as a dark blue-green powder (13 mg, 70%). UV-vis ($CHCl_3$): λ_{max}, nm (ε, $M^{-1}.cm^{-1}$) 344 (77457), 688 (130813), 715 (129384). ^1H NMR (300 MHz; $CDCl_3$; Me_4Si): δ_H, ppm 9.50-8.80 (6H, m, phthalo-*H*), 8.34-8.16 (3H, m, phthalo-*H*), 7.17-6.91 (2H, m, 2,3-phthalo-*H*), 4.91-4.46 (8H, m, $OCH_2CH_2CH_2O$), 3.18-3.04 (4H, m, $COCH_2CH_2S$), 2.76-2.54 (8H, m, $COCH_2CH_2S$, $OCH_2CH_2CH_2O$), 2.28-2.21 (6H, m, $SCOCH_3$), 1.88-1.76 (27H, m, $C(CH_3)_3$), -1.03 – -1.34 (2H, m, N*H*). MS (ESI-TOF; $CHCl_3$/MeOH 1:1): *m/z* 1090.4368 $[M]^+$ (calcd. for $C_{60}H_{66}N_8O_8S_2$ 1090.4445).

1,4-di[*tert*-butylsuccinatoxypropyloxy]-9(10),16(17),23(24)-tri[*tert*-butyl]phthalocyanine (17). The compound **6** (50 mg, 60.2 μmol) was dissolved in CH_2Cl_2 (20 mL). DCC (50 mg, 240.8 μmol), DMAP (6 mg, 48.2 μmol) and mono-*tert*-butyl succinate (42 mg, 240.8 μmol) were added to the solution and the mixture was stirred at room temperature for 2 days. After 1 day, more DCC (25 mg) and mono-*tert*-butyl succinate (21 mg) were added. The solvent was evaporated under reduced pressure. The crude product was dissolved in a few milliliters of CH_2Cl_2 and then filtered through a cotton plug. The product was purified twice by column chromatography on Silica 60, eluting with $CHCl_3$. The compound **17** was collected as first fraction (R_f = 0.88 in $CHCl_3$/EtOH 18:1). The product **17** was obtained as a dark green solid with quantitative yield (68 mg). ^1H NMR (300 MHz; $CDCl_3$; Me_4Si): δ_H, ppm 9.51-8.93 (6H, m, phthalo-*H*), 8.33-8.21 (3H, m, phthalo-*H*), 7.40-7.10 (2H, m, 2,3-phthalo-*H*), 4.92-4.54 (8H, m, $OCH_2CH_2CH_2O$), 2.81-2.49 (12H, m, $OCH_2CH_2CH_2O$, COC_2H_4CO), 1.87-1.76 (27H, m, $C(CH_3)_3$), 1.44 (18H, s, $OC(CH_3)_3$), -0.80 – -1.07 (2H, m, N*H*). MS (ESI-TOF; $CHCl_3$/MeOH 1:1): *m/z* 2286.1714 $[2M + H]^+$ (calcd. for $C_{132}H_{156}N_{16}O_{20}$ 2286.1760).

1,4-di[succinatoxypropyloxy]-9(10),16(17),23(24)-tri[*tert*-butyl]phthalocyanine (19). TFA (2 mL) was added to a solution of the product **17** (68 mg, 59.5 μmol) in dry CH_2Cl_2 (2 mL), and the reaction mixture was stirred at room temperature for 4.5 h. More CH_2Cl_2 was added, and the organic phase was washed with water (4 × 50 mL). The solvent was evaporated under reduced pressure and the compound **19** was crystallized on a watch glass and washed with n-pentane. The product **19** (R_f = 0.44 in $CHCl_3$/EtOH 9:1) was obtained as dark green solid with quantitative yield (61 mg). UV-vis ($CHCl_3$): λ_{max}, nm (ε, $M^{-1}.cm^{-1}$) 343 (45530), 688 (66999), 717 (70093). ^1H NMR (300 MHz; $CDCl_3$; Me_4Si): δ_H, ppm 9.46-7.85 (9H, m, phthalo-*H*), 7.21-6.80 (2H, m, 2,3-phthalo-*H*), 4.91-4.15 (8H, m, $OCH_2CH_2CH_2O$), 2.80-2.42 (12H, m, $OCH_2CH_2CH_2O$, COC_2H_4CO), 1.89-1.74 (27H, m, $C(CH_3)_3$), -1.81 – -2.54 (2H, m, N*H*), COO*H* were not resolved. MS (ESI-TOF; $CHCl_3$/MeOH 1:1): *m/z* 1029.4469 $[M - H]^-$ (calcd. for $C_{58}H_{62}N_8O_{10}$ 1029.4510).

1,4-di[(pentafluorophenoxy)succinatoxypropyloxy]-9(10),16(17),23(24)-tri[*tert*-butyl]phthalocyanine (21). The product **19** (50 mg, 48.5 μmol) was dissolved in EtOAc (10 mL), and DCC (20 mg, 97.0 μmol) and pentafluorophenol

(18 mg, 97.0 μmol) were added. The solution was stirred at room temperature for 4 days. DCC (40 mg) and pentafluorophenol (36 mg) were added more after 1 day of stirring. The solvent was evaporated under reduced pressure and the dry product was dissolved in a few milliliters of CH_2Cl_2 and filtered through a cotton plug. Purification of the crude product was performed twice by column chromatography; first on Silica 100 and second on Silica 60, eluting both times with $CHCl_3$. The product **21** was obtained from the first green fraction (R_f = 0.90 in $CHCl_3$/EtOAc 10:1) and crystallized on a watch glass. After washing with n-pentane, the product **21** was obtained as a dark green solid (27 mg, 41%). UV-vis ($CHCl_3$): λ_{max}, nm (ε, $M^{-1}.cm^{-1}$) 343 (56115), 689 (92162), 713 (89484). ^{1}H NMR (300 MHz; $CDCl_3$; Me_4Si): δ_H, ppm 9.50-8.75 (6H, m, phthalo-*H*), 8.34-8.14 (3H, m, phthalo-*H*), 7.22-6.80 (2H, m, 2,3-phthalo-*H*), 4.93-4.40 (8H, m, $OCH_2CH_2CH_2O$), 2.97-2.48 (12H, m, $OCH_2CH_2CH_2O$, COC_2H_4CO), 1.89-1.76 (27H, m, $C(CH_3)_3$), -1.18 – -1.49 (2H, m, N*H*). MS (ESI-TOF; $CHCl_3$/MeOH 1:1): *m/z* 1385.4221 $[M + Na]^+$ (calcd. for $C_{70}H_{60}N_8O_{10}F_{10}Na$ 1385.4170).

1(4),8(11),15(18),22(25)-tetrakis[3-(hydroxymethyl)phenoxy]phthalocyanine (8). Lithium (200 mg, 29 mmol) was dissolved in 1-octanol (20 mL) under argon atmosphere by heating the solution for 45 min. Thus formed lithium octoxide (20 mL) was added in the solution of 3-[3-(hydroxymethyl)phenoxy]phthalonitrile (**7**) (300 mg, 1.2 mmol) in THF (2 mL). The reaction mixture was stirred at 80 °C under argon atmosphere for 3 days. The dark green solution was cooled down to room temperature, and MeOH/water 1:1 (100 mL) was added. The organic phase was separated and washed two times with water. First obtained water phase was washed with $CHCl_3$, and organic layers were combined and solvents were evaporated. The crude product was poured into hexane (120 mL) and left to precipitate for 1 day. The precipitation was filtered and washed with hexane (2 × 40 mL) and diethyl ether (4 × 40 mL). The product was dissolved in toluene/DMF 2:1 from the filter, and most of the solvent was evaporated under reduced pressure. The dark green product was purified by column chromatography on Silica 100, eluting with toluene/DMF 2:1. The target product was obtained from the first blue-green fraction (R_f = 0.29 in toluene/DMF 4:1). The product was evaporated to dryness under reduced pressure (bath temperature 70 °C), dissolved in MeOH and crystallized on a watch glass. After drying and washing twice with diethyl ether, the compound **8** was obtained as a dark green solid (235 mg, 78%). UV-vis (DMF): λ_{max}, nm (ε, $M^{-1}.cm^{-1}$) 331 (69011), 685 (146151), 711 (155172). ^{1}H NMR (300 MHz; $(CD_3)_2SO$; Me_4Si): δ_H, ppm 8.20-7.38 (12H, m, phthalo-*H*), 7.35-6.91 (16H, m, Ar-*H*), 5.19 (4H, br t, *J* = 5.6 Hz, $ArCH_2OH$), 4.57-4.39 (8H, m, $ArCH_2OH$), -2.03 – -2.62 (2H, m, N*H*). MS (ESI-TOF; MeOH): *m/z* 1003.3254 $[M + H]^+$ (calcd. for $C_{60}H_{42}N_8O_8$ 1003.3204).

1(4),8(11),15(18),22(25)-tetrakis[3-(3-bromopropanoatemethyl)phenoxy]phthalocyanine (12). The compound **8** (100 mg, 0.1 mmol) was dissolved in THF/CH_2Cl_2 1:1 (10 mL) and 3-bromopropionyl chloride (**9**) (1.64 M solution in CH_2Cl_2, 0.6 mL, 1.0 mmol) was added in to the vial. The solution was diluted with CH_2Cl_2 (20 mL) and the reaction mixture was stirred at room temperature for 3 days. After 24 h and 48 h of stirring additionally 0.6 mL of **9** was added. Water (3 mL) was added in the reaction mixture and stirring was continued for 1 day. The organic phase was separated, washed with water (6 × 50 mL), and the solvent was evaporated under reduced pressure. The product was purified by column chromatography on Silica 60, eluting with $CHCl_3$. The product **12** was collected as first fraction (R_f = 0.90 in $CHCl_3$/EtOH 18:1) and crystallized on a watch glass. After washing with n-pentane, the compound **12** was obtained as a dark green tar (73 mg, 47%). UV-vis (DMF): λ_{max}, nm (ε, $M^{-1}.cm^{-1}$) 330 (54185), 688 (104861), 714 (101833). ^{1}H NMR (300 MHz; $CDCl_3$; Me_4Si): δ_H, ppm 8.90-7.75 (12H, br, phthalo-*H*), 7.69-7.03 (16H, m, Ar-*H*), 5.34-5.06 (8H, m, $ArCH_2O$), 3.80-3.36 (8H, m, $COCH_2CH_2Br$), 3.04-2.68 (8H, m, $COCH_2CH_2Br$), -1.08 – -1.85 (2H, m, N*H*). MS (ESI-TOF; $CHCl_3$/MeOH 1:1): *m/z* 1539.0872 $[M + H]^+$ (calcd. for $C_{72}H_{54}N_8O_{12}Br_4$ 1539.0673).

1(4),8(11),15(18),22(25)-tetrakis[3-(3-acetylsulfonylpropanoatemethyl)phenoxy]phthalocyanine (15). The product **12** (50 mg, 32.4 μmol) and KSAc (30 mg, 0.26 mmol) were dissolved in acetone (32 mL). The reaction mixture was stirred at room temperature for 1 day and after that at 60 ºC for 1 day more. More of KSAc (30 mg) was added, and

stirring was continued at 60 ºC of 1 day more. The solution was cooled down and the solvent was evaporated under reduced pressure. The crude product was taken into $CHCl_3$ and the organic layer was washed with water (5 × 100 mL). The solvent was evaporated to dryness under reduced pressure. Purification was performed by column chromatography on Silica 60, eluting with $CHCl_3$. The product was collected as first fraction (R_f = 0.73 in $CHCl_3$/EtOH 18:1), crystallized on a watch glass, and washed with n-pentane. The product **15** was obtained as a dark green tar (35 mg, 70%). UV-vis (DMF): λ_{max}, nm (ε, $M^{-1}.cm^{-1}$) 332 (49416), 688 (97500), 713 (87202). ^1H NMR (300 MHz; $CDCl_3$; Me_4Si): δ_H, ppm 8.83-7.73 (12H, br, phthalo-*H*), 7.67-7.03 (16H, m, Ar-*H*), 5.30-4.99 (8H, m, $ArCH_2O$), 3.15-2.91 (8H, m, $COCH_2CH_2S$), 2.74-2.51 (8H, m, $COCH_2CH_2S$), 2.33-2.15 (12H, m, $SCOCH_3$), -1.40 – -2.31 (2H, m, N*H*). MS (ESI-TOF; $CHCl_3$/MeOH 1:1): *m/z* 1523.3571 $[M + H]^+$ (calcd. for $C_{80}H_{66}N_8O_{16}S_4$ 1523.3558).

1(4),8(11),15(18),22(25)-tetrakis[3-((pentafluorophenoxy)succinatoxymethyl)phenoxy]phthalocyanine (22). The compound **8** (30 mg, 30 μmol) was dissolved in THF (5 mL). CH_2Cl_2 (10 mL), mono-*tert*-butyl succinate (26 mg, 0.15 mmol), DCC (31 mg, 0.15 mmol) and DMAP (catalytic amount) were added to the solution. The reaction mixture was stirred at room temperature overall for 7 days. More DCC (30 mg) and mono-*tert*-butyl succinate (26 mg) were added after 1, 4 and 6 days. The solvent was evaporated under reduced pressure, and the residue was dissolved in EtOAc (3 mL), filtered through a cotton plug and evaporated again. The crude product was purified by column chromatography on Silica 60, eluting first with $CHCl_3$. The intermediate product, 1(4),8(11),15(18),22(25)-tetrakis[3-(*tert*-butylsuccinatoxymethyl)phenoxy]phthalocyanine, was collected after changing the eluent to $CHCl_3$/EtOH 20:1 (R_f = 0.87 in $CHCl_3$/EtOH 18:1). After crystallizing the product on a watch glass, washing it with n-pentane and drying it in exsiccator for few days, the compound was obtained as green solid with quantitative yield (48 mg). MS (ESI-TOF; $CHCl_3$/MeOH 1:1): *m/z* 3252.2451 $[2M - H]^-$ (calcd. for $C_{92}H_{90}N_8O_{20}$ 3252.2463).

The whole amount of 1(4),8(11),15(18),22(25)-tetrakis[3-(*tert*-butylsuccinatoxymethyl)phenoxy]phthalocyanine was dissolved in dry CH_2Cl_2 (2 mL), and TFA (2 mL) was added. The solution was stirred at room temperature for 4.5 h, and after that evaporated under reduced pressure. The residue was dried in exsiccator overnight. The intermediate product, 1(4),8(11),15(18),22(25)-tetrakis[3-(succinatoxymethyl)phenoxy]phthalocyanine, (R_f = 0.05 in $CHCl_3$/EtOH 9:1) was obtained as dark green solid with quantitative yield (41 mg). MS (ESI-TOF; MeOH): *m/z* 1403.3928 $[M + H]^+$ (calcd. for $C_{76}H_{58}N_8O_{20}$ 1403.3845).

The product 1(4),8(11),15(18),22(25)-tetrakis[3-(succinatoxymethyl)phenoxy]phthalocyanine (41 mg, 30 μmol) was dissolved in EtOAc (15 mL) on ultrasonic bath. Pentafluorophenol (44 mg, 0.24 mmol) and DCC (49 mg, 0.24 mmol) were added. The reaction mixture was stirred in ice bath for 2 days and at room temperature for 1 day. After 1 day of stirring in cold, more DCC (49 mg) and pentafluorophenol (44 mg) were added. The solvent was evaporated under reduced pressure and the dry product was dissolved in CH_2Cl_2 (3 mL) and filtered through a cotton plug. The crude product was purified by column chromatography on Silica 60, eluting with $CHCl_3$. The product **22** was obtained from the first green fraction (R_f = 0.94 in $CHCl_3$/EtOAc 18:1) and crystallized on a watch glass. The compound **22** was repurified first by flash chromatography (Silica 60, eluent $CHCl_3$) and finally on preparative TLC plate (Silica gel 60 F_{254}), eluent $CHCl_3$. After solvent removal, the product **22** was crystallized on a watch glass, washed with n-pentane and obtained as a dark green solid (15 mg, 25%). UV-vis ($CHCl_3$): λ_{max}, nm (ε, $M^{-1}.cm^{-1}$) 337 (37420), 684 (89705), 716 (102761). ^1H NMR (300 MHz; $CDCl_3$; Me_4Si): δ_H, ppm 8.79-8.21 (4H, m, α-phthalo-*H*), 7.81 (4H, t, *J* = 7.6 Hz, β-phthalo-*H*), 7.57-7.38 (4H, m, β-phthalo-*H*), 7.38-7.02 (16H, m, Ar-*H*), 5.20-5.01 (8H, m, $ArCH_2O$), 2.99-2.55 (16H, m, COC_2H_4CO), -1.51 – -2.05 (2H, m, N*H*). MS (ESI-TOF; $CHCl_3$/MeOH 1:1): *m/z* 2067.3279 $[M + H]^+$ (calcd. for $C_{100}H_{54}N_8O_{20}F_{20}$ 2067.3213).

Immobilization

Glass plates were cleaned first manually with a cotton stick and $CHCl_3$, and then by sonication in $CHCl_3$, acetone, chromosulfuric acid and NaOH (aq) (0.001 M), 30 min in each solvent. After sonication in acetone, acid and NaOH, the plates were washed several times with MilliQ water. The cleaned glass plates were dried in oven at 150 °C. Glass plates with ITO layer on one side were cleaned by sonication in acetone/water 1:1, 2-propanol and CH_2Cl_2, 5 min in each solvent, and dried in oven at 150 °C.

The gold substrates were prepared by thermal evaporation under vacuum of a layer of gold onto cleaned glass plates that had been precoated with a titanium adhesion layer. Titanium and gold layers were 2 nm and 3 nm thick, respectively. Phthalocyanine SAMs were prepared by immersing the gold-coated glass plates in the Pc **13**, **14** and **15** solutions in CH_2Cl_2 (3 mM) for 30 min at room temperature [32]. After that the plates were rinsed with CH_2Cl_2 and $CHCl_3$, altogether ten times, and dried in air.

A reaction vessel, which was cooled down after being in oven (150 °C), was charged with dry toluene (20 mL), isopropyl amine (0.4 mL) and 3-aminopropyltrimethoxysilane (2 mL) under argon flow [34]. The plates (glass and ITO) were immersed in the solution, the reaction vessel was filled with argon and heated at 105 °C for 1h. The activated plates were cleaned right from the reactor by 15 s sonication in toluene and toluene/acetone 1:1 mixture. The plates were dried in argon flow (30 min), and used for further Pc immobilization immediately. Phthalocyanine (2 mg) was dissolved in dry toluene (20 mL) and loaded in the reaction vessel with argon. Concentration of **20** was 75 µM, concentration of **21** was 73 µM, and concentration of **22** was 48 µM. The dried activated plates were immersed in the solution, and reaction vessel was filled again with argon and heated at 105 °C. After 2h the plates were sonicated twice in toluene and once in CH_2Cl_2, 15 s in each solvent, and the samples were dried in argon flow (30 min).

CONCLUSION

We have developed a set of basic phthalocyanine structures, which can be easily fuctionalized to produce the monomolecular layers on gold, glass and ITO. We have demonstrated that the organization of the layer does not depend on the number of anchor groups only, but is influenced as well by the interaction of the macrocycle and the side substituents with the substrate surface. Research studies on the application of the synthesized Pcs in optical fiber sensors, organic solar cells, and chromophore-functionalized gold nanoparticles and SPR-sensors are under way and will be published in due time.

Acknowledgements

We thank Optoelectronics Research Centre (ORC Tampere, Finland) for preparation of gold plates. Academy of Finland and Tekes (the Finnish Funding Agency for Technology and Innovation) are greatly acknowledged for financial support.

Supporting information

Mass spectra of all synthesized Pcs (**3**, **6**, **8** and **10**-**22**), NMR spectra of the Pcs **6**, **8**, **10**-**12**, **14**-**19**, **21** and **22**, and emission spectra of Pcs **3**, **6**, **8**, **13**-**15** and **20**-**22** are given in the supplementary material. This material is available at http://www.u-bourgogne.fr/jpp/.

REFERENCES

1. Herbst W and Hunger K. *Industrial Organic Pigments: Production, Properties, Applications* (3rd edn). Wiley-VCH: Weinheim, 2004; 422-452.
2. Gregory P. *J. Porphyrins Phthalocyanines* 2000; **4**: 432-437.
3. Thomas AL. *Phthalocyanine Research and Applications*. CRC Press: Boca Raton, 1990; 43-52.
4. De la Torre G, Claessens CG and Torres T. *Chem. Commun.* 2007; **20**: 2000-2015.
5. Cook MJ. *Pure Appl. Chem.* 1999; **71**: 2145-2151.
6. Armstrong NR, Wang W, Alloway DM, Placencia D, Ratcliff E and Brumbach M. *Macromol. Rapid Commun.* 2009; **30**: 717-731.
7. Nyokong T and Bedioui F. *J. Porphyrins Phthalocyanines* 2006; **10**: 1101-1115.
8. Muzikante I, Parra V, Dobulans R, Fonavs E, Latvels J and Bouvet M. *Sensors* 2007; **7**: 2984-2996.
9. Gryko DT, Clausen C and Lindsey JS. *J. Org. Chem.* 1999; **64**: 8635-8647.
10. Ohyama J, Hitomi Y, Higuchi Y, Shinagawa M, Mukai H, Kodera M, Teramura K, Shishido T and Tanaka T. *Chem. Commun.* 2008; **47**: 6300-6302.
11. Huang X, Liu Y, Wang S, Zhou S and Zhu D. *Chem. Eur. J.* 2002; **8**: 4179-4184.
12. DiBenedetto SA, Facchetti A, Ratner MA and Marks TJ. *Adv. Mater.* 2009; **21**: 1407-1433.
13. Cid J-J, García-Iglesias M, Yum J-H, Forneli A, Albero J, Martínez-Ferrero E, Vázquez P, Grätzel M, Nazeeruddin MK, Palomares E and Torres T. *Chem. Eur. J.* 2009; **15**: 5130-5137.
14. Metzger RM. *Chem. Rev.* 2003; **103**: 3803-3834.
15. Würthner F. *Supramolecular dye chemistry.* Springer: Berlin, 2005; 257-313.
16. Ulman A. *Chem. Rev.* 1996; **96**: 1533-1554.
17. Imahori H, Norieda H, Yamada H, Nishimura Y, Yamazaki I, Sakata Y and Fukuzumi S. *J. Am. Chem. Soc.* 2001; **123**: 100-110.
18. Guo C-C, Ren T-G, Song J-X, Liu Q, Luo K, Lin W-Y and Jiang G-F. *J. Porphyrins Phthalocyanines* 2005; **9**: 830-834.
19. Andersson M, Holmberg M, Lundström I, Lloyd-Spetz A, Mårtensson P, Paolesse R, Falconi C, Proietti E, Di Natale C and D'Amico A. *Sens. Actuators, B* 2001; **77**: 567-571.
20. Amao Y, Asai K, Miyakawa K and Okura I. *J. Porphyrins Phthalocyanines* 2000; **4**: 19-22.
21. Hoppe H and Sariciftci NS. *J. Mater. Res.* 2004; **19**: 1924-1945.
22. Uchida S, Xue J, Rand BP and Forrest SR. *Appl. Phys. Lett.* 2004; **84**: 4218-4220.
23. Loi MA, Denk P, Hoppe H, Neugebauer H, Winder C, Meissner D, Brabec C, Sariciftci NS, Gouloumis A, Vázquez P and Torres T. *J. Mater. Chem.* 2003; **13**: 700-704.
24. Vivo P, Ojala M, Chukharev V, Efimov A and Lemmetyinen H. *J. Photochem. Photobiol., A* 2009; **203**: 125-130.
25. El-Khouly ME, Ito O, Smith PM and D'Souza F. *J. Photochem. Photobiol., C* 2004; **5**: 79-104.
26. De la Torre G, Claessens CG and Torres T. *Eur. J. Org. Chem.* 2000; **2000**: 2821-2830.
27. Isosomppi M, Tkachenko NV, Efimov A, Vahasalo H, Jukola J, Vainiotalo P and Lemmetyinen H. *Chem. Phys. Lett.* 2006; **430**: 36-40.
28. Cook MJ, Dunn AJ, Howe SD, Thomson AJ and Harrison KJ. *J. Chem. Soc., Perkin Trans. 1* 1988; 2453-2458.
29. Tercel M, Stribbling SM, Sheppard H, Siim BG, Wu K, Pullen SM, Botting KJ, Wilson WR and Denny WA. *J. Med. Chem.* 2003; **46**: 2132-2151.
30. Zheng T-C, Burkart M and Richardson DE. *Tetrahedron Lett.* 1999; **40**: 603-606.

31. Isosomppi M, Tkachenko NV, Efimov A, Kaunisto K, Hosomizu K, Imahori H and Lemmetyinen H. *J. Mater. Chem.* 2005; **15**: 4546-4554.
32. Yasseri AA, Syomin D, Malinovskii VL, Loewe RS, Lindsey JS, Zaera F and Bocian DF. *J. Am. Chem. Soc.* 2004; **126**: 11944-11953.
33. Lehtivuori H, Kumpulainen T, Hietala M, Efimov A, Lemmetyinen H, Kira A, Imahori H and Tkachenko NV. *J. Phys. Chem. C* 2009; **113**: 1984-1992.
34. McCallien DWJ, Burn PL and Anderson HL. *J. Chem. Soc., Perkin Trans. 1* 1997; 2581-2586.

Paper II

Synthesis of porphyrinoids with silane anchors and their covalent self-assembling and metallation on solid surface

Essi Sariola-Leikas, Matti Hietala, Alexey Veselov, Oleg Okhotnikov, Sergei L. Semjonov, Nikolai V. Tkachenko, Helge Lemmetyinen and Alexander Efimov

J. Colloid Interface Sci. **2012**, *369*, 58-70.

Journal of Colloid and Interface Science 369 (2012) 58–70

Contents lists available at SciVerse ScienceDirect

Journal of Colloid and Interface Science

www.elsevier.com/locate/jcis

Synthesis of porphyrinoids with silane anchors and their covalent self-assembling and metallation on solid surface

Essi Sariola-Leikas [a,*], Matti Hietala [a], Alexey Veselov [a], Oleg Okhotnikov [b], Sergei L. Semjonov [c], Nikolai V. Tkachenko [a], Helge Lemmetyinen [a], Alexander Efimov [a,*]

[a] Department of Chemistry and Bioengineering, Tampere University of Technology, P.O. Box 541, 33101 Tampere, Finland
[b] Optoelectronics Research Centre, Tampere University of Technology, P.O. Box 692, 33101 Tampere, Finland
[c] Fiber Optics Research Center of Russian Academy of Sciences, 38, Vavilov Street, Moscow 119333, Russia

ARTICLE INFO

Article history:
Received 29 August 2011
Accepted 15 December 2011
Available online 28 December 2011

Keywords:
Hydrosilylation
Metallation
Photonic crystal fiber
Phthalocyanine
Porphyrin
Self-assembled monolayer
Silane anchor

ABSTRACT

We have synthesized a set of porphyrin and phthalocyanine compounds with two different silane anchors. Syntheses of the anchor-substituted chromophores have been carried out via hydrosilylation of alkene derivatives, catalyzed by platinum complexes. The reduction side-process was suppressed using specific anchor/catalyst pairs, and the silane-containing compounds were successfully isolated from hydrogenated by-products in pure form with good yields. The target porphyrinoids having stable reactive silane anchors possess the ability to self-assemble on metal oxides and quartz surfaces and optical fibers. Covalent attachment is done in one-step, which makes the bonding process fast and easy. Immobilized chromophores were further converted by on-surface reactions into Zn(II) and Mg(II) metal complexes. The metallation time was found to be as fast as 1 min for Zn ion. Bonding densities calculated from the absorbances of the deposited layers give rough estimations for packing of the molecules on various substrates and evidence for monomolecular layers formation.

1. Introduction

Porphyrins and phthalocyanines (Pcs) have been recently employed for advanced applications like sensors and organic solar cells (OSCs), where these chromophores are organized in thin film structures [1–3]. Therefore, a considerable part of the modern research has been concentrated to develop anchor containing molecules, which could be attached to solid surfaces [4–7]. The deposition of the molecules can be either one-step direct adsorption of the functional component that carries surface-active group (*e.g.,* thiol) or two-step procedure, where the functional components are bonded to preform ω-functionalized (*e.g.,* —COOH, —NH_2) tails, which are covalently attached to the solid surface [8].

Definitely, there is a need for mechanically and chemically stable layers for, *e.g.,* OSCs and optical sensor applications. The anchoring of molecules onto a surface as self-assembled monolayers (SAMs) is often used for this purpose [9,10]. The film preparation by SAM technique is an established and well documented technology, which is reasonably fast, easy, and reliable. Among many available methods, the two-step SAM procedure is the most widely used, though it requires longer synthetic path and two subsequent SAM procedures, and can be difficult to accomplish [11,12]. One-step SAMs from trialkoxysilane- or chlorodimethylsilane-containing compounds represent a good alternative but are less studied. The main problems associated with such compounds are difficulties in the synthesis and rather poor shelf life. Hydrosilylation step is usually the most challenging part, as the opening of a terminal double bond and silane formation is often accompanied by reduction of the starting alkene into alkane. Separation of the two usually cannot be accomplished by chromatography since the silane component is prone to decomposition and irreversible sorption during chromatographic purification [13–16]. To the best of our knowledge, there are no examples of chromophores with silane anchors isolated in pure form, and the compounds used for immobilization are usually mixtures with the side products [14–17].

In the present work, we have developed a method of synthesis of A_3B type porphyrins and phthalocyanines containing stable yet reactive silane anchors. Syntheses of the anchor-substituted chromophores have been carried out via hydrosilylation in the presence of platinum complexes (Speier or Karstedt catalysts) [18,19], and the silane-containing compounds were successfully isolated in pure form. We have demonstrated that by choosing suitable anchor/catalyst pairs, it is possible to suppress the reduction side-process and improve the yields of the target compounds.

The anchor residues used in this work differ by chain length and terminal silane derivatives and are suitable for the attachment of

* Corresponding authors. Fax: +358 3 3115 2869.
E-mail addresses: essi.sariola-leikas@tut.fi (E. Sariola-Leikas), alexandre.efimov@tut.fi (A. Efimov).

0021-9797/$ - see front matter © 2011 Elsevier Inc. All rights reserved.
doi:10.1016/j.jcis.2011.12.044

the chromophores to solid surfaces. Covalent attachment was done in one-step, which made the bonding process efficient and fast. The target chromophores were assembled on metal oxide (ITO, ZnO) and quartz surfaces as monomolecular layers, as evidenced by absorption measurements. Immobilized chromophores were further converted by on-surface reactions into corresponding metal complexes. Proposed on-surface metallation of the free base porphyrinoids has several advantages over preparation and immobilization of individual metal chelates. This includes possibility to obtain sensitive complexes (*e.g.,* Mg(II)), easy diversity creation, and the synthetic pathways optimized for particular chromophore/anchor pair. In future need, metallation could allow to fine-tune analyte binding ability of the chromophores in sensors, or photochemical properties in solar cell applications.

In recent years, there is an instant growth in the development of optical chemical sensors based on organic molecules, which change their photophysical properties upon interaction with analytes. For example, porphyrins deposited on a flat glass plate can be used for gas detection [20]. The performance of sensing system can be improved if the light interaction with the sensing molecules is increased by depositing the molecules on tapered optical fibers, which simultaneously can be used to deliver excitation light and collect photoresponse of the molecules [21]. Furthermore, the photoactive molecules can be immobilized on the walls of the channels of photonic crystal fibers providing even better light-organic layer interaction. In the present work, the porphyrinoid chromophores were immobilized on optical fibers to demonstrate the potential of proposed method.

2. Experimental

2.1. Materials and instrumentations

Solvents of HPLC grade were purchased from Aldrich Chemical Company, Merck, and VWR International. Chloroform was distilled over K_2CO_3 and toluene over sodium shots. Triethylamine was distilled over KOH and tetrahydrofurane over $LiAlH_4$. Chemicals were purchased from Acros Organics, Aldrich Chemical Company, or Fluka Chemie and were used as received unless otherwise mentioned. ITO plates were purchased from Solems.

The catalyst solutions were prepared as follows:

Speier catalyst – stock solution (Cat1): Hexachloroplatinic(IV) acid hydrate ($H_2PtCl_6 \cdot nH_2O$, Fluka) (43 mg) was dissolved in dry THF (2 mL). The vial was filled with argon. Concentration: 0.05 mol/L.

Speier catalyst – stock solution (Cat2): Hexachloroplatinic(IV) acid hydrate ($H_2PtCl_6 \cdot nH_2O$, Fluka) (32 mg) was dried in a vacuum oven (150 °C) for 4 h. The melted catalyst was dissolved in 2-propanol (1.5 mL) on ultrasonic bath. The vial was filled with argon. Concentration: 0.05 mol/L.

Karstedt catalyst – stock solution (Cat3): Platinum(0)-1,3-divinyl-1,1,3,3-tetramethyldisiloxane complex solution (Pt ~2%) in xylene (Aldrich) (33 μL) was diluted with distilled toluene (1.5 mL). *Concentration*: 0.05 mol/L.

The monitoring of reactions was carried out by thin layer chromatography (TLC), employing aluminum sheets precoated with Silica 60 F254 (Merck). The purification and isolation of the products was performed by column chromatography on Silica 60 (mesh size 40–63 μm). The compounds **7**, **9**, **12,** and **13** were purified by flash chromatography using CombiFlash Companion (Teledyne ISCO).

The ^{1}H NMR spectra were measured on Varian Mercury 300 MHz spectrometer (Varian Inc.). All chemical shifts are given in ppm relative to TMS as internal standard. Mass spectra were recorded on high resolution ESI–TOF LCT Permier XE mass spectrometer (Waters Corp.). The sample of an analyte was dissolved in appropriate solvent at concentration *ca.* 0.01 mg/mL and infused at 15 μL/min rate. The reference solution of Leucine Enkephaline (50 pg/mL) was infused simultaneously. Original spectra were centered, and lock mass TOF correction was applied. Absorption spectra were measured using Shimadzu UV-2501PC UV–Vis Recording spectrometer, and emission spectra were recorded by Fluorolog Yobin Yvon-SPEX spectrofluorometer. Fluorescence lifetime microscope (FLM) images and lifetimes were measured with MicroTime 200 FLM with spatial resolution down to 0.3 μm.

Immobilization of chromophores inside photonic crystal fibers was monitored by FLM instrument as described in [22]. Solid-core photonic crystal fiber (SCPCF) was obtained from the Fiber Optics Research Center of Russian Academy of Sciences. SCPCF has core and hole diameters 28 μm, and the used length was 125 mm. A pressure cell (PC) was used to pump the required solutions through SCPCFs. The emission studies of the deposited molecular layers on SCPCFs were carried out as described earlier [22].

2.2. Synthesis

2.2.1. 29H,31H-phthalocyanine-1(4),8(11),15(18),22(25)-tetrayltetrakis(oxy-3,1-phenylenemethylene) tetrakisacrylate (2)

3-Bromopropanoic acid (1.0 g, 6.54 mmol) was dissolved in CH_2Cl_2 (10 mL), and oxalyl dichloride (0.72 mL, 8.5 mmol) and DMF (10 μL) were added. The reaction mixture was stirred at room temperature for 1 day. The solution was evaporated under reduced pressure, and the remained yellow liquid was diluted in CH_2Cl_2 (3 mL). The solution of 3-bromopropanoyl chloride (2.18 mol/L) thus obtained was stored in refrigerator. Tetrahydroxy phthalocyanine **1** [[29*H*,31*H*-phthalocyanine-1(4),8(11),15(18),22(25)-tetrayltetrakis(oxy-3,1-phenylene)]tetramethanol] [7] (80 mg, 80 μmol) was dissolved in THF (10 mL). Solution of 3-bromopropanoyl chloride (0.37 mL, 0.8 mmol) and triethylamine (0.22 mL, 1.6 mmol) were added, and the reaction mixture was kept on ultrasonic bath at room temperature. After 2.5 h more of 3-bromopropanoyl chloride solution (0.37 mL) and THF (5 mL) were added, and the mixture was stirred at room temperature for another 3.5 h. More CH_2Cl_2 (15 mL) and triethylamine (0.44 mL) were added, and stirring was continued for 1 day. The solution was washed with water (3 × 100 mL), and organic phase was evaporated under reduced pressure. The product was purified by column chromatography on Silica 60, eluting with $CHCl_3$. Compound **2** was collected as the second fraction (R_f = 0.1 in $CHCl_3$). Product **2** was crystallized on a watch glass and obtained as a dark green solid (40 mg, 41%). UV–vis ($CHCl_3$): λ_{max}, nm (ε, $M^{-1}\,cm^{-1}$) 333 (66,100), 683 (141,930), 716 (162,250). ^{1}H NMR (300 MHz; $CDCl_3$; Me_4Si): δ_H, ppm 8.49–8.33 (m, 4H, phthalo-*H*), 7.92–7.75 (m, 4H, phthalo-H), 7.59–7.50 (m, 4H, phthalo-*H*), 7.45 (br s, 4H, aryl-*H*), 6.32 (dd, J_1 = 1.32 Hz, J_2 = 17.4 Hz, 4H, *trans*-COCHC*H*$_2$), 6.07 (dd, J_1 = 10.22 Hz, J_2 = 17.14 Hz, 4H, COC*H*CH$_2$), 5.70 (dd, J_1 = 1.32 Hz, J_2 = 10.22 Hz, 4H, *cis*-COCHC*H*$_2$), 5.28–5.19 (m, 8H, OC*H*$_2$Ar), −1.28 (br s, 1H, N*H*), and −1.67 (br s, 1H, N*H*). MS (ESI–TOF; $CHCl_3$/MeOH 10:15): *m/z* 1219.3607 $[M + H]^+$ (calcd. for $C_{76}H_{58}N_8O_{12}$ 1219.3627).

2.2.2. 2-{3-[10,15,20-Tris(3,5-di-tert-butylphenyl)porphyrin-5-yl]phenoxy}ethanol (5)

3,5-Di-*tert*-butylbenzaldehyde (928 mg, 4.25 mmol), 3-(2-hydroxyethoxy)benzaldehyde (706 mg, 4.25 mmol) and pyrrole (0.59 mL, 8.5 mmol) were dissolved in freshly distilled $CHCl_3$ (850 mL). The reaction flask was purged with argon and protected from light. After 10 min of stirring, boron trifluoride etherate (0.52 mL, 4.25 mmol) was added and the reaction was stirred further for 3 h in the dark. Then, *p*-chloranil (2.09 g, 8.5 mmol) was added, and the reaction mixture was refluxed for 2 h. The solution was distilled to 30 mL volume, filtered, and evaporated under reduced

pressure. The mixture of porphyrins was separated by column chromatography on Silica 60, eluting with $CHCl_3$. The target product was obtained as the second fraction (R_f = 0.7 in $CHCl_3$/EtOH 18:1). The product was filtered through a cotton plug and subjected to the second column (Silica 60, eluent: $CHCl_3$). Product **5** was crystallized on a watch glass and obtained as a dark red solid (158 mg, 7.3%). ^{1}H NMR (300 MHz; $CDCl_3$; Me_4Si): δ_H, ppm 8.93–8.84 (m, 8H, *β-H*), 8.10–8.06 (m, 6H, phenyl-*H*), 7.89–7.84 (m, 1H, phenyl-*H*), 7.83–7.80 (m, 1H, phenyl-*H*), 7.80–7.77 (m, 3H, phenyl-*H*), 7.64 (t, *J* = 7.9 Hz, 1H, phenyl-*H*), 7.37–7.32 (m, 1H, phenyl-*H*), 4.28 (t, *J* = 4.4 Hz, 2H, OCH_2CH_2OH), 4.08–4.00 (m, 2H, OCH_2CH_2OH), 2.10 (t, *J* = 6.3 Hz, 1H, O*H*), 1.52 (br, 54H, *tert*-butyl-*H*), and -2.72 (s, 2H, N*H*).

2.2.3. 2-{3-[10,15,20-Tris(3,5-di-tert-butylphenyl)porphyrin-5-yl]phenoxy}ethyl but-3-enoate (6a)

Compound **5** (80 mg, 79 μmol) was dissolved in CH_2Cl_2 (10 mL). DCC (33 mg, 158 μmol), DMAP (4 mg, 32 μmol), and 3-butenoic acid (13.5 μL, 158 μmol) were added to the solution, and the mixture was stirred at room temperature for 3 days. The solvent was evaporated under reduced pressure. The crude product was dissolved in a few milliliters of EtOAc, the flask was frozen under cold water and filtered through a cotton plug. This procedure was done twice. The product was purified by column chromatography on Silica 60, eluting with $CHCl_3$. Compound **6a** was collected as the first fraction (R_f = 0.9 in $CHCl_3$/EtOH 18:1). Product **6a** was crystallized on a watch glass and obtained as a dark red solid (71 mg, 83%). ^{1}H NMR (300 MHz; $CDCl_3$; Me_4Si): δ_H, ppm 8.95–8.85 (m, 8H, *β-H*), 8.13–8.07 (m, 6H, phenyl-*H*), 7.90–7.85 (m, 1H, phenyl-*H*), 7.83–7.78 (m, 4H, phenyl-*H*), 7.63 (t, *J* = 7.9 Hz, 1H, phenyl-*H*), 7.33–7.28 (m, 1H, phenyl-*H*), 6.00–5.85 (m, 1H, $COCH_2CH{=}CH_2$), 5.19–5.11 (m, 2H, $COCH_2CH{=}CH_2$), 4.54–4.48 (m, 2H, OCH_2CH_2OCO), 4.37–4.31 (m, 2H, OCH_2CH_2OCO), 3.15 (dt, J_1 = 6.9 Hz, J_2 = 1.4 Hz, 2H, $COCH_2CH{=}CH_2$), 1.53 (br, 54H, *tert*-butyl-*H*), and -2.69 (s, 2H, N*H*). MS (ESI-TOF; $CHCl_3$/MeOH 10:15): *m/z* 1079.6752 $[M+H]^+$ (calcd. for $C_{74}H_{86}N_4O_3$ 1079.6779).

2.2.4. 2-{3-[10,15,20-Tris(3,5-di-tert-butylphenyl)porphyrin-5-yl]phenoxy}ethyl 4-(triethoxysilyl)butanoate (7a)

All the glassware was dried in oven (150 °C, 3 h) before use. The reaction flask was sealed with septum, placed on ice bath, and kept under constant argon flow. Compound **6a** (10 mg, 9.3 μmol) was dissolved in distilled toluene (1 mL) and added to the flask. Triethoxysilane (0.5 mL, 2.8 mmol) and **Cat2** (0.05 mol/L solution in 2-propanol, 10 μL, 0.5 μmol) were added, and the mixture was stirred in cold under argon. After 10 min, the stirring was continued at room temperature without constant argon flow for 2 h. The crude product was evaporated under reduced pressure using mechanical vacuum pump. Purification was done on Combiflash chromatograph using 12 g Silica 60 column (purged with argon) and CH_2Cl_2/MeOH gradient as eluent (flow rate: 18 mL/min; CH_2Cl_2 (0.5 min), CH_2Cl_2/MeOH 20:1 (3 min)). Product **7a** was obtained as the second fraction (R_f = 0.8 in CH_2Cl_2/MeOH 20:1) as a dark red solid (4.5 mg, 39%). ^{1}H NMR (300 MHz; $CDCl_3$; Me_4Si): δ_H, ppm 8.93–8.82 (m, 8H, *β-H*), 8.10–8.04 (m, 6H, phenyl-*H*), 7.88–7.83 (m, 1H, phenyl-*H*), 7.81–7.76 (m, 4H, phenyl-*H*), 7.64 (t, *J* = 7.9 Hz, 1H, phenyl-*H*), 7.36–7.31 (m, 1H, phenyl-*H*), 4.53–4.47 (m, 2H, OCH_2CH_2OCO), 4.38–4.32 (m, 2H, OCH_2CH_2OCO), 3.77 (q, *J* = 7.0 Hz, 6H, $Si(OCH_2CH_3)_3$), 2.43 (t, *J* = 7.3 Hz, 2H, $COCH_2C_2H_4Si$), 1.84–1.71 (m, 2H, $COCH_2CH_2CH_2Si$), 1.52 (br, 54H, *tert*-butyl-*H*), 1.17 (t, *J* = 7.0 Hz, 9H, $Si(OCH_2CH_3)_3$), 0.72–0.61 (m, 2H, $COC_2H_4CH_2Si$), and -2.72 (s, 2H, N*H*). MS (ESI-TOF; CH_3CN/acetone 1:1): *m/z* 1243.7650 $[M+H]^+$ (calcd. for $C_{80}H_{102}N_4O_6Si$ 1243.7646).

2.2.5 2-{3-[10,15,20-Tris(3,5-di-tert-butylphenyl)porphyrin-5-yl]phenoxy}ethyl pent-4-enoate (6b)

The synthesis and purification were carried out as described for porphyrin **6a** from compound **5** (27 mg, 27 μmol), which was dissolved in CH_2Cl_2 (5 mL), DCC (11 mg, 53 μmol), DMAP (1.3 mg, 11 μmol), and 4-pentenoic acid (5.5 μL, 53 μmol). Product **6b** was collected as the first fraction (R_f = 0.9 in $CHCl_3$/EtOH 18:1), crystallized on a watch glass and obtained as a dark red solid (25 mg, 86%). UV–vis ($CHCl_3$): λ_{max}, nm (ε, M^{-1} cm^{-1}) 421 (356,290), 518 (12,340), 553 (6460), 589 (3940), 647 (3550). ^{1}H NMR (300 MHz; $CDCl_3$; Me_4Si): δ_H, ppm 8.94–8.84 (m, 8H, *β-H*), 8.12–8.06 (m, 6H, phenyl-*H*), 7.90–7.85 (m, 1H, phenyl-*H*), 7.83–7.77 (m, 4H, phenyl-*H*), 7.64 (t, *J* = 7.9 Hz, 1H, phenyl-*H*), 7.35–7.29 (m, 1H, phenyl-*H*), 5.87–5.72 (m, 1H, $COC_2H_4CH{=}CH_2$), 5.08–4.93 (m, 2H, $COC_2H_4CH{=}CH_2$), 4.54–4.48 (m, 2H, OCH_2CH_2OCO), 4.38–4.32 (m, 2H, OCH_2CH_2OCO), 2.52–2.33 (m, 4H, $COC_2H_4CH{=}CH_2$), 1.53 (br, 54H, *tert*-butyl-*H*), and -2.70 (s, 2H, N*H*). MS (ESI-TOF; $CHCl_3$/MeOH 10:15): *m/z* 1093.6981 $[M+H]^+$ (calcd. for $C_{75}H_{88}N_4O_3$ 1093.6935).

2.2.6. 2-{3-[10,15,20-Tris(3,5-di-tert-butylphenyl)porphyrin-5-yl]phenoxy}ethyl 5-(triethoxysilyl)pentanoate (7b)

Compound **7b** was prepared using a similar method as described for porphyrin **7a**, starting from compound **6b** (11 mg, 10.1 μmol), which was dissolved in distilled toluene (1 mL), triethoxysilane (0.45 mL, 2.5 mmol), and **Cat3** (0.05 mol/L solution in distilled toluene, 8 μL, 0.4 μmol). The crude product was purified on Combiflash chromatograph using 12 g Silica 60 column (purged with argon) eluting with CH_2Cl_2/EtOH gradient (flow rate: 30 mL/min; CH_2Cl_2 (0.5 min), CH_2Cl_2/EtOH 20:1 (3 min)). Product **7b** was obtained as the second fraction (R_f = 0.8 in $CHCl_3$/EtOH 18:1) as a dark red solid (8 mg, 67%). ^{1}H NMR (300 MHz; $CDCl_3$; Me_4Si): δ_H, ppm 8.92–8.85 (m, 8H, *β-H*), 8.10–8.06 (m, 6H, phenyl-*H*), 7.88–7.83 (m, 1H, phenyl-*H*), 7.81–7.77 (m, 4H, phenyl-*H*), 7.64 (t, *J* = 7.9 Hz, 1H, phenyl-*H*), 7.36–7.31 (m, 1H, phenyl-*H*), 4.52–4.47 (m, 2H, OCH_2CH_2OCO), 4.38–4.32 (m, 2H, OCH_2CH_2OCO), 3.76 (q, *J* = 7.0 Hz, 6H, $Si(OCH_2CH_3)_3$), 2.38 (t, *J* = 7.5 Hz, 2H, $COCH_2C_3H_6Si$), 1.75–1.63 (m, 4H, $COCH_2C_2H_4CH_2Si$), 1.52 (br, 54H, *tert*-butyl-*H*), 1.17 (t, *J* = 7.0 Hz, 9H, $Si(OCH_2CH_3)_3$), 0.65–0.58 (m, 2H, $COC_3H_6CH_2Si$), and −2.71 (s, 2H, N*H*). MS (ESI–TOF; $CHCl_3$/EtOH 10:15): *m/z* 1257.7825 $[M+H]^+$ (calcd. for $C_{81}H_{104}N_4O_6Si$ 1257.7804).

2.2.7. 2-{3-[10,15,20-Tris(3,5-di-tert-butylphenyl)porphyrin-5-yl]phenoxy}ethyl 5-[methoxy(dimethyl)silyl]pentanoate (9)

The synthesis was carried out as described for porphyrin **7a** from compound **6b** (11 mg, 10.1 μmol), which was dissolved in distilled toluene (1 mL), chlorodimethylsilane (0.5 mL, 4.6 mmol), and **Cat2** (0.05 mol/L solution in 2-propanol, 10 μL, 0.5 μmol). Dry product was dissolved in MeOH (1 mL), and dry Et_3N (1 mL) was added. The reaction mixture was stirred at room temperature for 2 h. The crude product was purified on Combiflash chromatograph using 12 g Silica 60 column (purged with argon) and CH_2Cl_2/MeOH gradient as eluent (flow rate: 30 mL/min; CH_2Cl_2 (1 min), CH_2Cl_2/MeOH 20:1 (3 min)). Product **9** was obtained as the second fraction (R_f = 0.3 in CH_2Cl_2) as a dark red solid (6.7 mg, 56%). ^{1}H NMR (300 MHz; $CDCl_3$; Me_4Si): δ_H, ppm 8.93–8.85 (m, 8H, *β-H*), 8.11–8.05 (m, 6H, phenyl-*H*), 7.89–7.84 (m, 1H, phenyl-*H*), 7.82–7.77 (m, 4H, phenyl-*H*), 7.64 (t, *J* = 7.9 Hz, 1H, phenyl-*H*), 7.36–7.31 (m, 1H, phenyl-*H*), 4.53–4.47 (m, 2H, OCH_2CH_2OCO), 4.38–4.32 (m, 2H, OCH_2CH_2OCO), 3.36 (s, 3H, $SiOCH_3$), 2.38 (t, *J* = 7.5 Hz, 2H, $COCH_2C_3H_6Si$), 1.74–1.61 (m, 2H, $COCH_2CH_2C_2H_4Si$), 1.52 (br, 54H, *tert*-butyl-*H*), 1.43–1.27 (m, 2H, $COC_2H_4CH_2CH_2Si$), 0.62–0.54 (m, 2H, $COC_3H_6CH_2Si$), 0.04 (s, 6H, $Si(CH_3)_2$), and -2.72 (s, 2H, N*H*). MS (ESI-TOF; $CHCl_3$/MeOH

10:15): *m/z* 2367.4949 $[2\,M + H]^+$ (calcd. for $C_{156}H_{196}N_8O_8Si_2$ 2367.4824).

2.2.8. 3-{3-[1,15,22-Tris(3,5-di-tert-butylphenyl)-29H,31H-phthalocyanin-8-yl]phenyl}propyl pent-4-enoate (11)

Monohydroxy phthalocyanine **10** [3-{3-[1,15,22-tris(3,5-di-*tert*-butylphenyl)-29*H*,31*H*-phthalocyanin-8-yl]phenyl}propan-1-ol] [23] (40 mg, 33 μmol) was dissolved in CH_2Cl_2 (10 mL). DCC (14 mg, 66 μmol), DMAP (1.6 mg, 13 μmol), and 4-pentenoic acid (6.7 μL, 66 μmol) were added to the solution, and the mixture was stirred at room temperature for 1 day. After 3 h, DCC (14 mg) and pentenoic acid (6.7 μL) were added more, and DCC (14 mg) were added even more after 19 h. The solvent was evaporated under reduced pressure. The crude product was dissolved in CH_2Cl_2 (3 mL) and filtered through a cotton plug. The product was purified twice by column chromatography on Silica 60, eluting with CH_2Cl_2. Compound **11** was collected as the first fraction (R_f = 0.9 in $CHCl_3$/EtOH 18:1). Product **11** was crystallized on a watch glass, scrubbed under water, and obtained as a dark green solid (29 mg, 67%). UV–vis ($CHCl_3$): λ_{max}, nm (ε, $M^{-1}\,cm^{-1}$) 341 (41,860), 676 (72,830), 709 (87,450). ^1H NMR (300 MHz; $CDCl_3$; Me_4Si): δ_H, ppm 8.66 (dd, J_1 = 5.4 Hz, J_2 = 3.2 Hz, 1H, 4-phthalo-*H*), 8.44–8.36 (m, 3H, 11,18,25-phthalo-*H*), 8.15–8.10 (m, 1H, 1-Ar-*H*), 8.09–7.94 (m, 12H, Ar-*H*, phthalo-*H*), 7.90–7.85 (m, 6H, 8,15,22-Ar-*H*), 7.78 (t, *J* = 7.6 Hz, 1H, 1-Ar-*H*), 7.70–7.65 (m, 1H, 1-Ar-*H*), 5.82–5.67 (m, 1H, $COC_2H_4CH{=}CH_2$), 5.03–4.87 (m, 2H, $COC_2H_4CH{=}CH_2$), 4.20 (t, *J* = 6.5 Hz, 2H, $C_2H_4CH_2O$), 3.02 (t, *J* = 7.7 Hz, 2H, $CH_2C_2H_4O$), 2.41–2.27 (m, 4H, $COC_2H_4CH{=}CH_2$), 2.22–2.11 (m, 2H, $CH_2CH_2CH_2O$), 1.51 (br s, 36H, 8,22-*tert*-butyl-*H*), 1.50 (s, 18H, 15-*tert*-butyl-*H*), and −0.29 (s, 2H, N*H*). MS (ESI-TOF; $CHCl_3$/MeOH 10:15): *m/z* 1295.7588 $[M + H]^+$ (calcd. for $C_{88}H_{94}N_8O_2$ 1295.7578).

2.2.9. 3-{3-[1,15,22-Tris(3,5-di-tert-butylphenyl)-29H,31H-phthalocyanin-8-yl]phenyl}propyl 5-(triethoxysilyl)pentanoate (12)

Compound **12** was prepared using a similar method as described for porphyrin **7a**, starting from compound **11** (13 mg, 10 μmol), which was dissolved in distilled toluene (1 mL), triethoxysilane (0.45 mL, 2.5 mmol), and **Cat3** (0.05 mol/L solution in distilled toluene, 8 μL, 0.4 μmol). Purification was done on Combiflash chromatograph using 12 g Silica 60 column (purged with argon) and CH_2Cl_2/EtOH gradient as eluent (flow rate: 30 mL/min; CH_2Cl_2 (0.5 min), CH_2Cl_2/EtOH 20:1 (2 min), CH_2Cl_2/EtOH 10:1 (4 min)). Product **12** was obtained as the first fraction (R_f = 0.8 in $CHCl_3$/EtOH 18:1) as a dark green solid (10 mg, 70%). ^1H NMR (300 MHz; $CDCl_3$; Me_4Si): δ_H, ppm 8.66 (dd, J_1 = 5.4 Hz, J_2 = 3.2 Hz, 1H, 4-phthalo-*H*), 8.44–8.36 (m, 3H, 11,18,25-phthalo-*H*), 8.16–8.11 (m, 1H, 1-Ar-*H*), 8.09–7.94 (m, 12H, Ar-*H*, phthalo-*H*), 7.90–7.86 (m, 6H, 8,15,22-Ar-*H*), 7.78 (t, *J* = 7.6 Hz, 1H, 1-Ar-*H*), 7.70–7.65 (m, 1H, 1-Ar-*H*), 4.19 (t, *J* = 6.5 Hz, 2H, $C_2H_4CH_2O$), 3.75 (q, *J* = 7.0 Hz, 6H, $Si(OCH_2CH_3)_3$), 3.02 (t, *J* = 7.7 Hz, 2H, $CH_2C_2H_4O$), 2.56 (t, *J* = 7.5 Hz, 2H, $COCH_2C_3H_6Si$), 2.22–2.10 (m, 2H, $CH_2CH_2CH_2O$), 1.87–1.60 (m, 4H, $COCH_2C_2H_4CH_2Si$), 1.51 (d, *J* = 0.9 Hz, 36H, 8,22-*tert*-butyl-*H*), 1.50 (s, 18H, 15-*tert*-butyl-*H*), 1.17 (t, *J* = 7.0 Hz, 9H, $Si(OCH_2CH_3)_3$), 0.64–0.57 (m, 2H, $COC_3H_6CH_2Si$), and −0.30 (s, 2H, N*H*). MS (ESI–TOF; $CHCl_3$/EtOH 10:15): *m/z* 1459.8472 $[M + H]^+$ (calcd. for $C_{94}H_{110}N_8O_5Si$ 1459.8447).

2.2.10. 3-{3-[1,15,22-Tris(3,5-di-tert-butylphenyl)-29H,31H-phthalocyanin-8-yl]phenyl}propyl 5-[methoxy(dimethyl)silyl]-pentanoate (13)

The synthesis was started same way as described for porphyrin 7a from compound 11 (13 mg, 10 μmol), which was dissolved in distilled toluene (1 mL), chlorodimethylsilane (0.5 mL, 4.6 mmol), and Cat2 (0.05 mol/L solution in 2-propanol, 20 μL, 1 μmol). The reaction mixture was stirred at 80 °C for 6 h. Dry product was dissolved in distilled toluene (1 mL), and MeOH (1 mL) and dry Et_3N (1 mL) were added. The reaction mixture was stirred at room temperature for 1 h. The crude product was purified on Combiflash chromatograph using 12 g Silica 60 column (purged with argon) and CH_2Cl_2/MeOH gradient as eluent (flow rate: 30 mL/min; CH_2Cl_2 (1 min), CH_2Cl_2/MeOH 20:1 (3 min)). Product 13 was obtained as the second fraction (R_f = 0.5 in $CHCl_3$/EtOH 18:1) as a dark green solid (2.1 mg, 15%). ^1H NMR (300 MHz; $CDCl_3$; Me_4Si): δ_H, ppm 8.66 (dd, J_1 = 5.4 Hz, J_2 = 3.2 Hz, 1H, 4-phthalo-*H*), 8.43–8.37 (m, 3H, 11,18,25-phthalo-*H*), 8.15–8.10 (m, 1H, 1-Ar-*H*), 8.09–7.94 (m, 12H, Ar-*H*, phthalo-*H*), 7.89–7.85 (m, 6H, 8,15,22-Ar-*H*), 7.78 (t, *J* = 7.6 Hz, 1H, 1-Ar-*H*), 7.70–7.65 (m, 1H, 1-Ar-*H*), 4.19 (t, *J* = 6.5 Hz, 2H, $C_2H_4CH_2O$), 3.45–3.33 (m, 3H, $SiOCH_3$), 3.01 (t, *J* = 7.7 Hz, 2H, $CH_2C_2H_4O$), 2.56 (t, *J* = 7.5 Hz, 2H, $COCH_2C_3H_6Si$), 2.22–2.07 (m, 2H, $CH_2CH_2CH_2O$), 1.86–1.59 (m, 4H, $COCH_2C_2H_4CH_2Si$), 1.50 (d, *J* = 0.9 Hz, 36H, 8,22-*tert*-butyl-*H*), 1.49 (s, 18H, 15-*tert*-butyl-*H*), 0.59–0.51 (m, 2H, $COC_3H_6CH_2Si$), 0.02 (s, 6H, $Si(CH_3)_2$), and −0.30 (s, 2H, N*H*). MS (ESI-TOF; $CHCl_3$/MeOH 10:15): *m/z* 1384.8033 $[M]^+$ (calcd. for $C_{91}H_{104}N_8O_3S$ 1384.8000).

2.3. Immobilization and metallation

Quartz plates were prewashed manually using a cotton stick and $CHCl_3$ and washed with concentrated HNO_3, NaOH (aq) (0.001 M), and EtOH. After that the plates were rinsed with $CHCl_3$ and cleaned by sonication in $CHCl_3$ and chromosulfuric acid, 2 h in each solvent. After washing several times with MilliQ water, the plates were kept overnight in NaOH (aq) (0.001 M) solution and afterward washed with MilliQ water. The cleaned quartz plates were dried in oven at 150 °C. Glass plates with ITO layer on one side were cleaned by sonication in acetone/water 1:1, 2-propanol, and CH_2Cl_2, 5 min in each solvent, and dried in oven at 150 °C. Glass plates with aluminum doped ZnO (AZO) layer on one side were prepared as described in [24] and were used next day after layer deposition by atomic layer deposition (ALD) (at 150 °C). Size of the all plates was approximately 2 × 1 cm.

Reaction vessel (40 ml, screw-cap glass vial 95 × 27.5 mm from VWR) was dried in the oven (2 h, 150 °C) and cooled down. Chromophore (2 mg) was dissolved in distilled toluene (20 mL) and loaded in the reaction vessel under argon. Isopropyl amine (0.4 mL) was added, and the cleaned plates (quartz, ITO and AZO) were immersed in the solution. The reaction vessel was filled with argon and heated at 105 °C for 2 h. After appropriate time, the plates were sonicated twice in toluene and once in CH_2Cl_2, 15 s in each solvent, and finally dried in argon flow (30 min).

Optical fibers were precleaned before the SAM procedure. $CHCl_3$, acetone, MilliQ water, NaOH (aq) (0.001 M), and MilliQ water were successively pumped through the fiber for 30 min each. The fibers were kept under an absolute pressure 3 bar of pure nitrogen flow. A part of fiber was heated by placing into a glass vial filled with glycerol at 100 °C.

The solution of chromophore (2 mg) and isopropylamine (0.4 mL) in dry toluene (20 mL) was injected into the fibers via pressure cell [22] and was pumped through the fiber by nitrogen pressure for 2 h. After that the fiber was washed with toluene, toluene/acetone 1:1 and CH_2Cl_2 for 10 min, each step. Finally, the fiber was purged with nitrogen for 15 min.

Metallation of the porphyrin SAMs was done by immersing the samples into solutions with corresponding metal ions. *Zn-solution*: Dihydrate zinc acetate (0.2 g, 0.9 mmol) was dissolved in MeOH (20 mL) by sonication for 10 min. *Mg-solution*: Anhydrous magnesium iodide (70 mg, 0.25 mmol) was dissolved in CH_2Cl_2 (20 mL), and DIEA (87 μL, 0.5 mmol) was added. The vial was filled with argon and sonicated for 45 min. The plates with SAMs were immersed in the salt solution and kept there for 1–4 h. After appropriate time,

the plates were washed with MeOH, and the samples were dried in argon flow.

3. Results and discussion

3.1. Synthesis

Ideally, orientation of the molecules on surface is determined by the number and relative position of the anchors. Porphyrinoids may easily accommodate from one to four anchor groups, thus favouring the orientation from edge-to-surface to plane-to-surface with different tilting angles. Tetra-anchored molecules are arguably the best option, considering the ease of preparation of symmetrical chromophores with four identical functional units. On the other hand, four anchors of the same molecule might self-condensate during immobilization steps, and in addition to that the reaction of all four functional groups with a surface is difficult to ensure. That is, while mono-anchored chromophores are more elaborated in synthesis, their immobilization is somewhat simpler than that of the tetra-functionalized compounds.

Apart from the number of surface-reactive groups, there is a question of method flexibility. Görlach et al. [25] describes phthalocyanine with four siloxane groups linked to the macrocycle by alkylic chains. In that case, the enyloxyphthalonitrile precursors were synthesized first, tetramerized into phthalocyanine, and finally hydrosilylated. The length of linkers is determined at the step of phthalonitrile preparation and thus is not variable afterward. Another option is to prepare a chromophore with reactive sites first and attach the linkers of various length to it later, which is sometimes a more convenient approach [7].

For initial experiments, we selected tetrahydroxy phthalocyanine ***1*** [7], which was acylated with bromopropionic acid and dehydrobrominated by treatment with triethylamine (Scheme 1). Phthalocyanine tetraacrylate **2** thus obtained was hydrosilylated with ***Cat1*** and triethoxysilane [25]. Unfortunately, the reaction product was a mixture of partly silylated and reduced compounds (***3***), as revealed by mass-spectrometry and NMR. The mixture was not possible to separate, and the target tetrasilane phthalocyanine ***4*** was never isolated in pure form.

Evidently, the problem required a different approach. Firstly, acrylic acid was replaced with next shortest possible linkers, 3-butenoic and 4-pentenoic acids. Secondly, in the further work, only mono-anchored compounds were used, and the reaction conditions were optimized using monohydroxy porphyrin as a basic structure. Porphyrin was selected because of simple synthesis, ease of separation, and good solubility that greatly facilitated the purification and analysis. After optimizing the hydrosilylation with porphyrin, the same reaction conditions were applied to prepare the phthalocyanine derivatives.

2-{3-[10,15,20-Tris(3,5-di-*tert*-butylphenyl)porphyrin-5-yl] phenoxy}ethanol (**5**) was synthesized by mixed aldehyde condensation as described previously [26]. Target monohydroxy product **5** was obtained with 7.3% yield. Porphyrins **6a** and **6b** with terminal double bond were synthesized starting from compound **5** and either 3-butenoic acid or 4-pentenoic acid, respectively, by DCC-DMAP method (Scheme 2). After 3 days of stirring at room temperature, the dicyclohexylurea and unreacted DCC were removed by filtering the cold solution of reaction products in ethyl acetate, and the compounds **6a** and **6b** were purified by column chromatography on Silica 60 (eluent $CHCl_3$). 2-{3-[10,15,20-Tris(3,5-di-*tert*-butylphenyl) porphyrin-5-yl]phenoxy}ethyl but-3-enoate (**6a**) and 2-{3-[10,15,20-tris(3,5-di-*tert*-butylphenyl)porphyrin-5-yl]phenoxy} ethyl pent-4-enoate (**6b**) were obtained with good yields, 83% and 86%, respectively.

Monohydroxy phthalocyanine **10** was prepared by already described method [23]. Acylation with 4-pentenoic acids was done the same way as for porphyrin **6b**. Reaction time of 1 day was enough, but the reaction required larger excess of DCC and acid. Purification was accomplished by two subsequent flash columns using Silica 60 and CH_2Cl_2 as eluent. First, green fraction was collected, and compound, 3-{3-[1,15,22-tris(3,5-di-*tert*-butylphenyl)-29*H*,31*H*-phthalocyanin-8-yl]phenyl}propyl pent-4-enoate (**11**), was obtained as a dark green solid with 67% yield (Scheme 3).

3.1.1. Preparation of stock solutions of catalysts

It is evident from the literature that catalyst plays a crucial role in hydrosilylations. Many publications do not specify the catalyst used; however it mostly concerns simple substrates. In those cases reduction of double bonds does not occur or at least is not reported. However, when some large organic chromophores are involved in hydrosilylation, the side hydrogenation reaction becomes a complication, which sometimes can be solved by the proper treatment of catalyst. Thus, as reported by Behr et al. [27], the formation of hydrogenated by-products can be suppressed using the recycled hexachloroplatinic acid catalyst. In our experiments, when Speier catalyst (hexachloroplatinic(IV) acid hydrate, $H_2PtCl_6 \cdot nH_2O$, Fluka) was used without pretreatment, the reaction product was mostly the reduced compound (**8**).

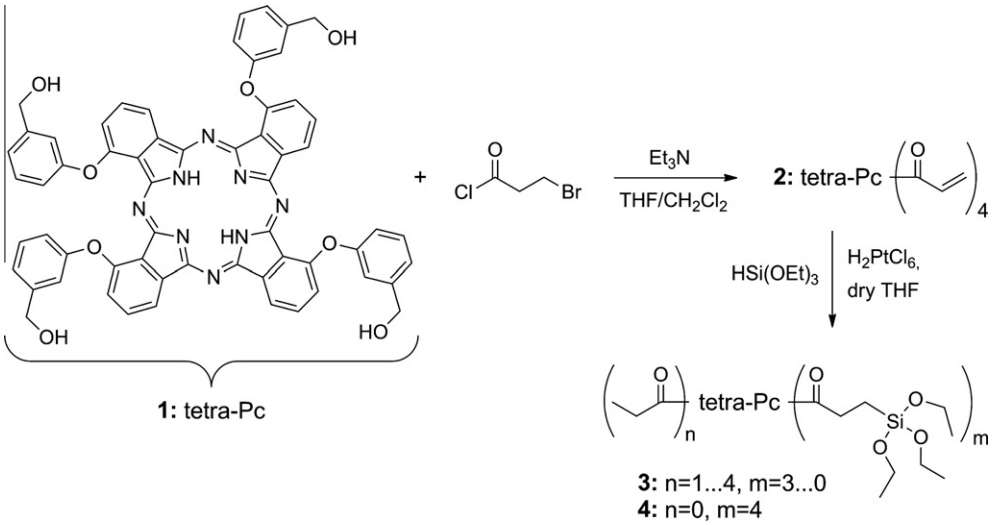

Scheme 1. Synthetic route to tetra(triethoxysilane) phthalocyanine **4** and its by-products **3**. Only one of four possible regioisomers of Pc **1** is shown for simplicity.

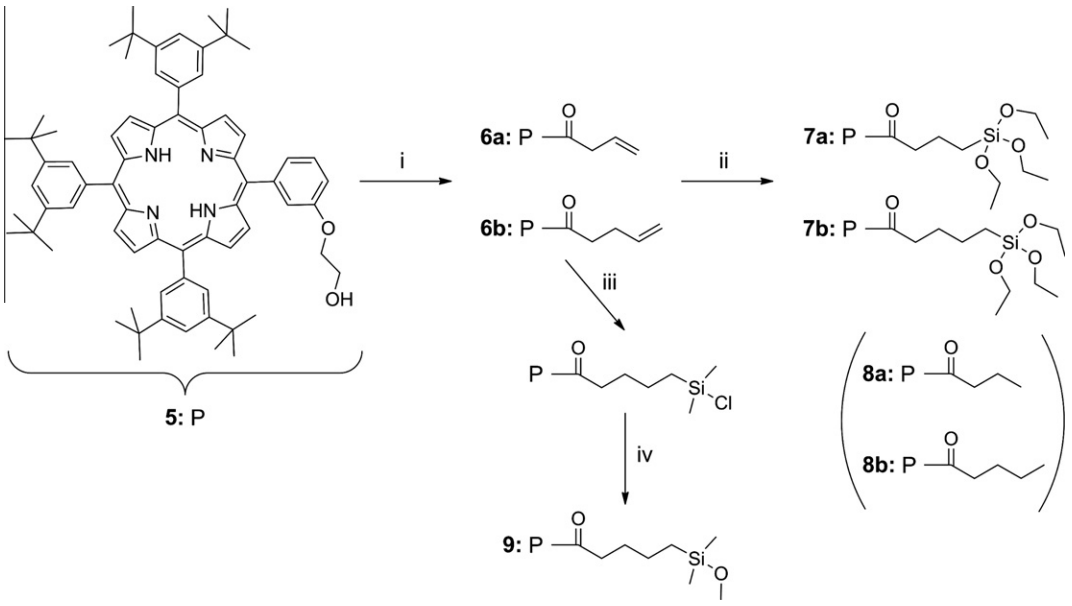

Scheme 2. Synthetic route to mono(triethoxysilane) porphyrins **7a** and **7b**, their by-products **8a** and **8b**, and mono(dimethylmethoxysilane) porphyrin **9**. *Reagents and conditions*: (i) 3-butenoic acid/4-pentenoic acid, DCC, DMAP, CH_2Cl_2, rt, 72 h; (ii) triethoxysilane, **Cat2**/**Cat3**, dist. toluene, Ar, 0 °C/rt, 2 h; (iii) chlorodimethylsilane, **Cat2**, dist. toluene, Ar, 0 °C/rt, 2 h; (iv) MeOH, dry Et_3N, rt, 2 h.

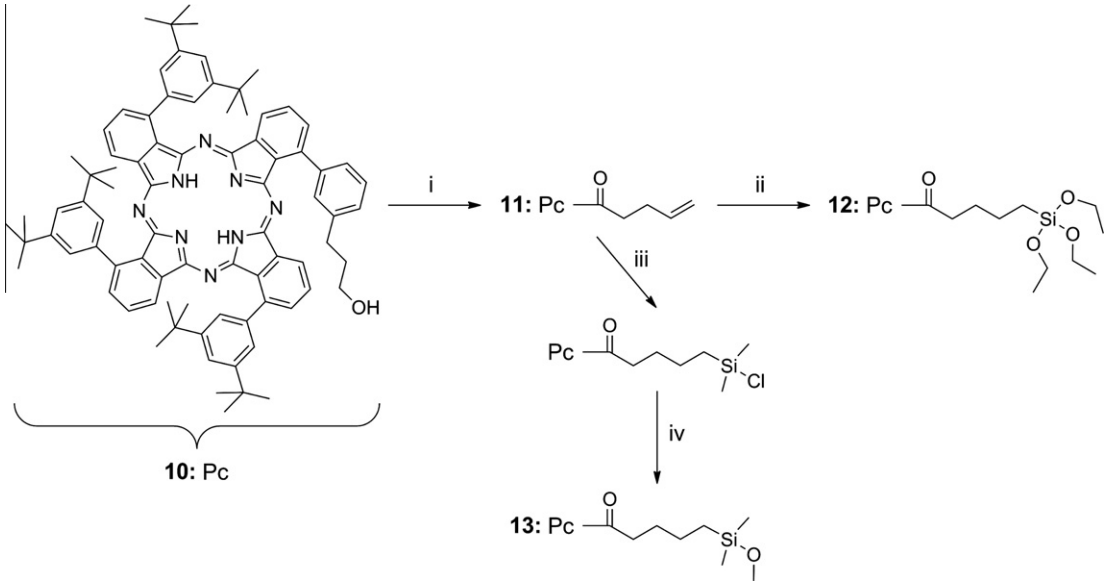

Scheme 3. Synthetic route to mono(triethoxysilane) phthalocyanine **12**, and mono(dimethylmethoxysilane) phthalocyanine **13**. *Reagents and conditions*: (i) 4-pentenoic acid, DCC, DMAP, CH_2Cl_2, rt, 24 h; (ii) triethoxysilane, **Cat3**, dist. toluene, Ar, 0 °C/rt, 2 h; (iii) chlorodimethylsilane, **Cat2**, dist. toluene, Ar, 80 °C, 6 h; (iv) dist. toluene, MeOH, dry Et_3N, rt, 1 h.

In the present work, three catalysts were employed. **Cat1** was commercial Speier catalyst ($H_2PtCl_6 \cdot nH_2O$, Fluka), which was dissolved in dry THF to 0.05 M concentration and used without any further treatment in the initial experiments. **Cat2** was same commercial Speier catalyst, which was dried in a vacuum oven at 150 °C for 4 h before use. After drying, the catalyst was dissolved in 2-propanol at 0.05 M concentration and sealed under argon. **Cat3** was commercial Karstedt catalyst (platinum(0)-1,3-divinyl-1,1,3,3-tetramethyldisiloxane complex solution (Pt ~2%) in xylene, Aldrich), which was diluted with distilled toluene to 0.05 M concentration. The solution was stored under argon. Same stock solution of dried Speier catalyst (**Cat2**) was used in all syntheses, but a new solution of Karstedt catalyst (**Cat3**) was prepared every time just before the reaction.

3.1.2. Hydrosilylation

As it was mentioned before, hydrogenation is a serious obstacle in the synthesis of silane-anchored macrocycles. Another difficulty is due to residual starting silane, which is barely possible to completely remove from reaction mixture by evaporation. The traces of a free silane in the reaction products not only hinder the analysis, but also shorten the shelf life of the product because of self-condensation. Chromatographic purification could be the best option [25,28] but might lead to significant losses of silylated products on the column. Considering the balance between reactivity and stability, two hydrosilanes were selected for experiments, namely triethoxysilane and chlorodimethylsilane. Chromatographic purification of trialkoxysilanes is described, but chlorodimethylsilane is far too reactive for separation on Silica. Therefore,

chlorodimethylsilane anchor was converted into dimethylmethoxysilane group, thus making it suitable for purification by conventional methods.

Hydrosilylation reactions were done in dried flask under argon. In a typical procedure, the flask was precooled on ice bath. The solution of porphyrin in distilled toluene, neat triethoxysilane, and catalyst solution were injected subsequently via septum, and the mixture was stirred for 2 h. Solvent/silane ratio was approximately 2:1 v/v. The solvent and excess of silane were removed by rotary evaporation at 40 °C under membrane pump vacuum. The solid residue of unpurified product was additionally dried in vacuum exsiccator and stored under argon.

Initial experiments were conducted with porphyrin **6a** and catalyst **Cat1**. Unfortunately, the reaction led to the efficient formation of "reduced" butanoate **8a** with only trace amount of the target silane-porphyrin (Scheme 2). The product ratio was estimated by ESI mass-spectrometry, which showed an intense peak of the product **8a** at 1081.7 *m/z* accompanied by a very small signal of the compound **7a**. Additional proofs were gained from TLC analysis (even though the silane-porphyrins tend to stack on Silica irreversibly, the process is slow enough for a plate to run). Thus, in CH_2Cl_2, the starting compound has R_f 0.75 and the side product is very close to it with R_f 0.7, while the silane-porphyrin is much slower with R_f 0.1. In the system $CHCl_3$/EtOH 18:1, all three compounds have similar mobilities and cannot be clearly distinguished. The components were identified by mass-spectrometry of the extracts of the corresponding spots from TLC plate. One-dimensional ^{1}H NMR analysis was not enough in identifying the reaction products. Indeed, disappearance of the double bond signal was a good sign of the reaction being completed, but distinguishing between "reduced" and silylated porphyrins was not easy. The residual silane hindered the region around 1 ppm, and the three-protons triplet of a terminal methyl (compound **8a**) or the two-protons triplet of the α-silicon-methylene (compound **7a**) could not be reliably differentiated. Much more information was gained from the two-dimensional gHSQC spectrum with multiplicity editing. Showing CH and CH_3 signals as positive and CH_2 as negative peaks, it revealed the same fact that the main product of the reaction was reduced porphyrin **8a**. Though frustrating, the initial experiments provided a couple of useful conclusions, such as (1) the molecules with silanes are stable enough to survive fast chromatographic analysis and (2) even before purification, the reaction products can be distinguished by gHSQC NMR with multiplicity editing and by ESI MS.

Evidently, the parameter to vary was the catalyst. Compound **6a** and **Cat2** were used to prepare 2-{3-[10,15,20-tris(3,5-di-*tert*-butylphenyl)porphyrin-5-yl]phenoxy}ethyl 4-(triethoxysilyl)butanoate (**7a**), and compound **6b** and **Cat3** were used to produce product 2-{3-[10,15,20-tris(3,5-di-*tert*-butylphenyl)porphyrin-5-yl]phenoxy}ethyl 5-(triethoxysilyl)pentanoate (**7b**). Hydrogenated products (**8a** and **8b**) were still observed in reactions, but in minor amounts. Products **7a** and **7b** were isolated with 39% and 67% yields, respectively. These results indicated that Karstedt catalyst (**Cat3**) works better with triethoxysilane, and phthalocyanine **12** was therefore prepared using a similar method as described for porphyrin **7b**, starting from compound **11** (Scheme 3). Product **12** was obtained as a dark green solid with 70% yield. Conditions of hydrosilylation reactions are listed in Table 1.

As mentioned earlier, chlorodimethylsilane residue was converted into dimethylmethoxysilane moiety [29]. In the first stage, chlorodimethylsilane anchor was attached on terminal double bond of the porphyrin. Chlorine in the anchor was converted into methoxy group in the second step. Substitution of chlorine was necessary because porphyrin containing the chloride anchor cannot be purified with usual methods. Also important, the methoxy product is easier to handle and it is more stable. Synthesis of porphyrin **9** was carried out as described for compound **7a** starting from porphyrin **6b**, chlorodimethylsilane, and **Cat2**. Addition of silane caused protonation of porphyrin, which was observed as color change from red to green. After 2 h of stirring, the reaction mixture was evaporated and the crude product was redissolved in MeOH. Dry triethylamine (Et_3N) was added in proportion to MeOH (1:1), and color changed back to red. Again, hydrogenated compound (**8b**) was found in the product, but it could be separated chromatographically, and the target product 2-{3-[10,15,20-tris(3,5-di-*tert*-butylphenyl)porphyrin-5-yl]phenoxy}ethyl 5-[methoxy (dimethyl)silyl]pentanoate (**9**) was obtained with 56% yield. Same reaction was also done using **Cat3**. After 2 h of stirring at room temperature, starting material was still left. Reaction time was extended to 3 days, but full conversion of the starting material was not achieved. After methanol/triethylamine treatment, the obtained product was a mixture of unreacted starting material **6b** and hydrogenated compound **8b**.

Table 1
Conditions and yields of hydrosilylation reactions.

Starting compound	Catalyst	Silane	Product	Yield%
6a	Cat1	$HSi(OEt)_3$	**8a**	–
6a	Cat2	$HSi(OEt)_3$	**7a**	39
6b	Cat3	$HSi(OEt)_3$	**7b**	67
11	Cat3	$HSi(OEt)_3$	**12**	70
6b	Cat2	$(CH_3)_2SiHCl$	**9**	56
6b	Cat3	$(CH_3)_2SiHCl$	**6b + 8b**	–
11	Cat2	$(CH_3)_2SiHCl$	**13**	15

Karstedt catalyst (**Cat3**) was best option for hydrosilylation reaction with triethoxysilane but did not work well in the reaction with chlorodimethylsilane. That is, dimethylmethoxysilane porphyrin could only be prepared using dried Speier catalyst (**Cat2**). From results obtained with porphyrin synthesis, Pc **13** was prepared as described for porphyrin **9**. At room temperature reaction did not work, only starting material was recovered. Therefore, the reaction mixture was stirred at 80 °C for 6 h. Second step of the synthesis was over after 1 h. Product **13**, 3-{3-[1,15,22-tris(3,5-di-*tert*-butylphenyl)-29*H*,31*H*-phthalocyanin-8-yl]phenyl}propyl 5-[methoxy(dimethyl)silyl]pentanoate, was obtained as a dark green solid with 15% yield.

Purification of the reaction products and selecting the proper eluent system are another important aspects of hydrosilylation reaction. Even though the mobilities of silane-modified chromophores on normal phase Silica are high, the compounds tend to adsorb irreversibly during separation. Therefore, a considerably polar eluent at high flow rate is needed to prevent the excessive losses of the target compound during separation. On the other hand, separation of the by-products requires the eluent of low polarity; thus, the chromatographic run should consist of an isocratic hold of unpolar solvent followed by gradient elution with more polar composition. Conventional flash columns are unsuitable in this case, and automated low-pressure Combiflash chromatograph was used. The packed columns were flushed with argon right before separation as an extra care measure. Initially, methanol was used as a polar additive to the main eluent component, dichloromethane. However, when the crude product of compound **7a** was eluted using CH_2Cl_2/MeOH gradient, the ethoxy groups of silane anchor were partly replaced with methoxyls, as evidenced by MS. Thus, in addition to the main peak with *m/z* 1243.7, two more peaks were visible, with the masses −14 and −28 Da, corresponding to $Si(OEt)_2OMe$ and $SiOEt(OMe)_2$ anchors, respectively. Also, the peak of higher mass (+134 Da) was visible, corresponding to siloxane olygomerization (—$Si(OEt)_2$—O—$Si(OEt)_3$). Nevertheless, the target compound was successfully isolated from the by-products.

In further work, compounds **7b** and **12** were purified using CH_2Cl_2/EtOH gradient, thus preventing a change in triethoxysilane anchor. Crude products **9** and **13** were purified using CH_2Cl_2/MeOH gradient, as there was no danger of silane exchange. With the above described purification methods, the target compounds could be separated from the hydrogenated products in all cases.

3.2. ^{1}H NMR spectra

The structural characterization of molecules was done with NMR (see Supporting information). All the products had good solubility allowing the measurements of highly concentrated samples in $CDCl_3$. Signal assignments are based on two-dimensional NMR spectroscopy, mostly the heteronuclear single quantum coherence (gHSQC) with multiplicity editing. The NMR spectra of porphyrinoids are informative though crowded; thus, full assignment of the peaks for the starting materials is needed for correct interpretation of the spectra of the final compounds.

3.2.1. Porphyrins

The ^{1}H NMR spectrum of compound **5** shows clear aromatic region, where signals of β- and phenyl protons are located. β-Protons signals are found as a multiplet around 8.90 ppm, and signals of phenyl protons are visible between 8.10–7.30 ppm. In the aliphatic region, protons of CH_2 group which are closer to phenyl ring produce a triplet at 4.28 ppm, and signal of other CH_2 protons is in higher field (δ 4.08–4.00 ppm). Signal of a hydroxy proton is observed as a triplet at 2.10 ppm, and signals of *tert*-butyl groups are visible as a group of singlets around 1.52 ppm. The free base porphyrin includes two protons in the central cavity and those NH protons are found as a singlet at −2.72 ppm in the spectrum.

The spectra of acylated porphyrins with terminal double bonds **6a** and **6b** show similar aromatic region as the spectrum of compound **5**. Multiplets of protons OC_2H_4OCO are shifted to lower field (around 4.45 ppm) in both spectra when compared to the spectrum of compound **5** (around 4.10 ppm). Another signal of CH_2 groups protons is visible as doublet of triplets in the spectrum of compound **6a** and as a multiplet in the spectrum of product **6b** at 3.15 ppm and 2.52–2.33 ppm, respectively. Signals of *tert*-butyl groups protons and NH protons are found as same singlets as it is shown in the spectrum of porphyrin **5**. Signals of protons of the double bond are located between 6.00–5.10 ppm as two groups of multiplets in the spectrum of compound **6a**. In the spectrum of porphyrin **6b,** these groups are shifted a little to higher field (δ 5.87–4.93 ppm).

The ^{1}H NMR spectra of hydrosilylation products **7a** and **7b** have similar aromatic region as other compounds with minor shifts of the signals. In aliphatic part, signals of protons OC_2H_4OCO are found at same places as they are in the spectra of compounds **6a** and **6b** as well as the signals of *tert*-butyl groups protons and NH. The characteristic signals of ethoxy protons are visible as a quartet ($Si(OCH_2CH_3)_3$) (negative in gHSQC) and a triplet ($Si(OCH_2CH_3)_3$) (positive in gHSQC) at 3.77 ppm and 1.17 ppm in the both spectra of products **7a** and **7b**, respectively. Coupling constant in all signals is 7.0 Hz. Signal of protons $COCH_2C_2H_4Si$ is visible as triplet at 2.43 ppm in the spectrum of **7a** and this signal is shifted to higher field compared with the spectrum of double bond compound **6a** (δ 3.15 ppm). Middle CH_2 group is observed as multiplet (δ 1.84–1.71 ppm), and signal of $COC_2H_4CH_2Si$ protons is shielded at 0.72–0.61 ppm as a multiplet in the spectrum of product **7a**. In the spectrum of porphyrin **7b**, signal of CH_2 group protons next to carboxy group is found as triplet at 2.38 ppm, and in higher field, signals of $COCH_2C_2H_4CH_2Si$ protons are located as multiplet (δ 1.75–1.63 ppm). Protons of CH_2 next to silane are observed at 0.65–0.58 ppm as multiplet (negative in gHSQC).

Signals of hydrogenated product protons **8a** and **8b** can be distinguished from signals of silane-anchored compounds protons using the two-dimensional gHSQC spectrum with multiplicity editing. In NMR spectrum of compound **7a** (crude product), protons (CH_2 and CH_3 groups) of reduced product **8a** are visible. Triplet at 2.36 ppm corresponds to CH_2 protons next to carboxy group, multiplet around 1.67 ppm originates from $COCH_2CH_2CH_3$ protons, and signal of CH_3 protons is observed as triplet at 0.93 ppm. In spectrum of porphyrin **7b** (crude product), amount of hydrogenated product is small and signals are overlapping with the target compound signals.

Aromatic region of the NMR spectrum of product **9** is similar as described for compound **5**. When NMR spectrum was measured from mid-product, 2-{3-[10,15,20-tris(3,5-di-*tert*-butylphenyl)porphyrin-5-yl]phenoxy}ethyl 5-[chloro(dimethyl)silyl]pentanoate, partly protonated porphyrin was observed. Protonation was visible in aromatic region as new signals and lack of the signals of NH protons. Aliphatic region of compound **9** shows two multiplets at 4.53–4.47 ppm and 4.38–4.32 ppm, which correspond to OCH_2CH_2OCO and OCH_2CH_2OCO protons, respectively. Signal of methoxy group is found as a singlet at 3.36 ppm (positive in gHSQC), and a triplet nearest to it (δ 2.38 ppm) contains $COCH_2C_3H_6Si$ protons (negative in gHSQC). Other signals from CH_2 protons are observed between 1.74–0.54 ppm, and this range shows also signals from *tert*-butyl protons as group of singlets at 1.52 ppm. Signals of two methyl groups and NH protons are found as singlets at 0.04 ppm and −2.72 ppm, respectively.

3.2.2. Phthalocyanines

Phthalocyanines show the changes in NMR spectra very similar to those described for porphyrins. Mostly, the linker signals are affected by hydrosilylation/hydrogenation, while other peaks remain unaffected. The ^{1}H NMR spectrum of compound **11** shows in aromatic region a doublet of doublets at 8.66 ppm, which corresponds to phthalo-proton 4. The signal indicates that only one isomer is present in the sample [23]. Signals of phthalo-protons 11, 18 and 25 are found as a multiplet at 8.44–8.36 ppm, and next to this a multiplet is visible, which contains one of the aryl group (position 1) protons at 8.15–8.10 ppm. A triplet and multiplet from protons of same aryl ring are found at 7.78 ppm and 7.70–7.65 ppm, respectively. The spectrum shows signals of protons of aryl rings (positions 8, 15 and 22) as multiplet (δ 7.90–7.85 ppm). Rest of the signals of phthalo- and aryl-protons are located at 8.09–7.94 ppm. Aliphatic region of spectrum of Pc **11** shows protons of the double bond as multiplets at 5.82–5.67 ppm ($COC_2H_4CH{=}CH_2$) and 5.03–4.87 ppm ($COC_2H_4CH{=}CH_2$). A triplet at 4.20 ppm contains $C_2H_4CH_2O$ protons and another triplet at 3.02 ppm belongs to $CH_2C_2H_4O$ protons. Signals of $COC_2H_4CH{=}CH_2$ protons are overlapping (δ 2.41–2.27 ppm), and next to this multiplet in lower frequency signals of $CH_2CH_2CH_2O$, protons are located as multiplet (δ 2.22–2.11 ppm). Two singlets around 1.50 ppm are signals from *tert*-butyl protons, and signals of NH protons are found as singlet at higher field (δ −0.29 ppm).

The spectra of Pcs **12** and **13** show similar aromatic region as compound **11**. Also, in aliphatic region, both spectra of **12** and **13** show signals of $C_2H_4CH_2O$ and $CH_2C_2H_4O$ protons as triplets at same position as in spectrum of Pc **11**. Compared to spectrum of **11**, signal of $COCH_2C_3H_6Si$ protons is shifted to lower field (δ 2.56 ppm), but same multiplet containing signals of $CH_2CH_2CH_2O$ is visible at 2.22–2.10 ppm in both spectra of Pcs **12** and **13**. Signal from $COCH_2C_2H_4CH_2Si$ protons is found as a multiplet at 1.87–1.60 ppm in both spectra (negative in gHSQC). Signals of $COC_3H_6CH_2Si$ protons are found as multiplet at 0.64–0.57 ppm in spectrum of Pc **12** and at 0.59–0.51 ppm in spectrum of Pc **13**. The characteristic signals of $Si(OCH_2CH_3)_3$ (negative in gHSQC) and $Si(OCH_2CH_3)_3$ (positive in gHSQC) are located at 3.75 ppm

and 1.17 ppm as quartet and triplet in the spectrum of **12**, respectively. Coupling constant in both signals is 7.0 Hz. In the spectrum of **13**, $SiOCH_3$ protons are found at 3.45–3.33 ppm as multiplet, and a singlet at 0.02 ppm contains signal of $Si(CH_3)_2$ protons. Signals of *tert*-butyl protons are found as doublet and singlet around 1.50 ppm, and NH protons are visible as singlet at −0.30 ppm in both spectra of Pcs **12** and **13**.

3.3. Immobilization and metallation

3.3.1. Immobilization on quartz, ITO, and AZO plates

Quartz and ITO plates were cleaned in a set of solvents on ultrasonic bath before preparation of SAMs (see Section 2). Glass plates with aluminum doped ZnO (AZO) layer on one side were used as received after atomic layer deposition (ALD) [24]. SAMs were done with a one-step process, where the reaction vessel was loaded with a solution of chromophore in distilled toluene and isopropyl amine under argon. The cleaned plates were immersed in the solution, and the reaction vessel was heated at 105 °C for 2 h. After appropriate time, the plates were sonicated twice in toluene and once in CH_2Cl_2 to remove residual physisorbed compound. After drying in argon, the absorption and emission spectra of the plates with SAMs were measured. Absorption of SAM was obtained by subtracting absorption of clean substrate from absorption of plate with SAM.

Considering the absorption spectra of the monolayers on quartz, ITO, and AZO surfaces, one has to take into account that layers are formed on both sides of the substrates. To estimate the absorbances of single layers, the optical densities in Figs. 1, 2 and 5 thus should be divided by two. Absorption of free base porphyrin in solution shows usually a narrow Soret band and four small Q bands. Absorption of SAM of porphyrin **7a** (SAM **7a**) on quartz has the Soret band at 426 nm and two well visible Q bands at 514 nm and 553 nm (Fig. 1a, Table 2). Two other Q bands are also present but not well resolved due to spectrophotometer sensitivity limit. The Soret band is red shifted by 5 nm compared to compound **6b** in $CHCl_3$. Less difference is seen in the Q bands positions, but the Soret and the Q bands of SAM **7a** are broader than porphyrin **6b** bands. Absorption of SAM **7b** on quartz and ITO corresponds well to absorption spectrum of porphyrin **6b** in $CHCl_3$. SAM **7b** on quartz and ITO have the Soret band at 422 nm and two of the Q bands around 520 nm and 550 nm. SAM **7b** on AZO has the Soret band at 424 nm. Broadening of the bands is visible on spectra of SAMs. Surprisingly, SAM **9** with dimethylmethoxysilyl anchor has almost 10 times lower absorbance than SAM **7b**. Even though absorbances are low, the Soret band is clearly distinguishable in spectra of SAM **9** around 420 nm (Fig. 1b).

Absorption spectra of SAMs of triethoxysilane–phthalocyanine **12** (SAM **12**) on quartz, ITO, and AZO have similar shape as phthalocyanine (Pc) **11** in $CHCl_3$ (Fig. 2). SAM **12** on quartz has two Q band maxima at 713 nm and 679 nm (Table 2). In solution, these bands positions are at few nanometers lower wavelength, and the spectrum also shows a shoulder between 600–650 nm. The Soret band is found in both spectra close to 340 nm. SAM **12** on ITO and AZO shows quite same maxima of the Q bands as in absorption spectrum of SAM **12** on quartz. Absorption of SAM of Pc **13** is so low that it is not visible from the noise, which correlates with the result gained from porphyrins. Difference in the absorbances of triethoxysilyl-porphyrin SAM and that of dimethylmethoxysilane-anchored SAMs was a 10-fold decrease and, if the case is the same phthalocyanines, absorption of SAM **13** would be too small to be observed.

The absorption maximum of the Soret band provides a possibility to estimate the mean molecular area (mma) of porphyrins in the SAM. The mma values were calculated assuming the same molar absorptivity (ε) of compounds in solution and SAMs. This is true only if molecules are randomly oriented on the surface and if

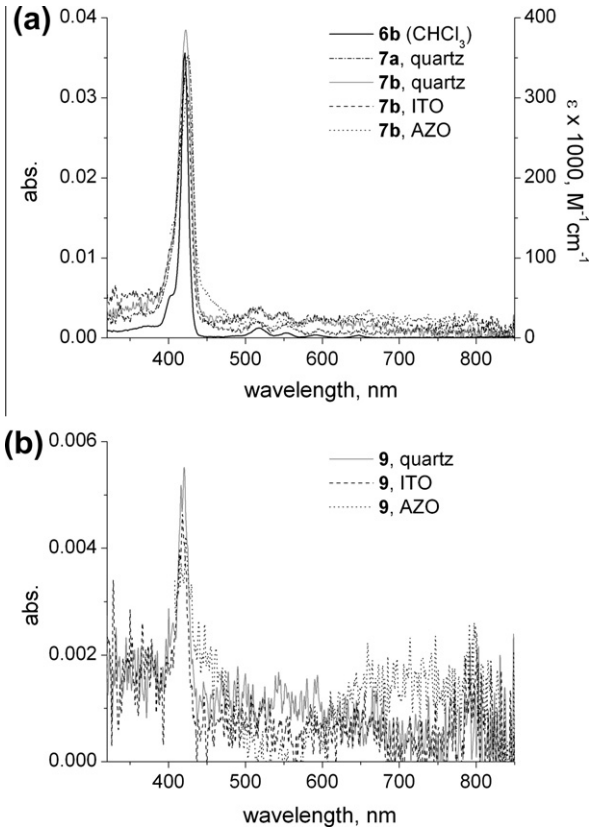

Fig. 1. Absorption spectra of (a) porphyrin **6b** on molar absorptivity (ε) scale, and porphyrin SAMs **7a** and **7b** on different substrates, (b) porphyrin SAM **9** on different substrates. The spectrum of SAM **7b** on AZO (Fig. 1a) is plotted only till 400 nm because at lower wavelength ZnO layer starts to absorb.

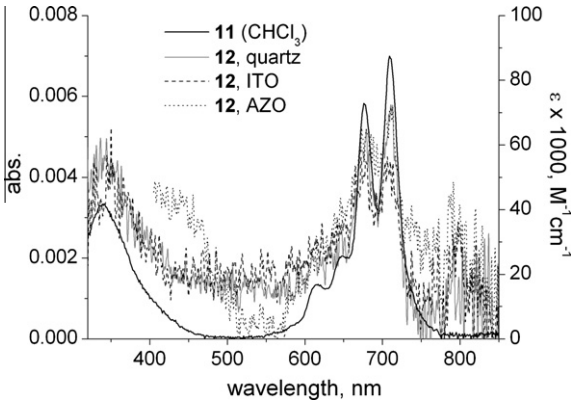

Fig. 2. Absorption spectra of phthalocyanine **11** on molar absorptivity (ε) scale and phthalocyanine SAM **12** on different substrates.

chromophore–chromophore or chromophore–surface interactions are disregarded [30]. As shown in Table 2, the molecular areas of porphyrins **7a** and **7b** on quartz are relatively the same, as expected. Also, the mma values of SAM **7b** on ITO and AZO are below 4 nm^2. The values are larger than what one could expect for tightly packed monolayers and that might be due to the changes in the spectra of immobilized compounds compared to those in solutions. Indeed, the Soret bands are two times broader for films, thus making the apparent optical densities for SAMs two times lower. The calculated mma values present the higher limits for actual area per molecule, but the real bonding densities of molecules are expected to be greater. The mma values for porphyrin SAM **9** on

Table 2
Absorption and emission maxima of samples and mean molecular areas (mma[a]) of SAMs on different substrates.

Sample	Solvent/ substrate	Absorption, λ_{max} (nm)	Emission, λ_{max} (nm)	mma (nm^2)
6b	$CHCl_3$	421, 518, 553	652, 720	
SAM 7a	Quartz	426, 514, 553	654, 721	3.3
SAM 7b	Quartz	422, 520, 549	652, 718	3.1
	ITO	422, 518, 550	652, 719	3.5
	AZO	424, 510, 550		3.9
SAM 9	Quartz	420	652, 719	20
	ITO	418	652, 718	25
	AZO	422		27
11	$CHCl_3$	341, 676, 709	716, 800	
SAM 12	Quartz	344, 679, 713	716	4.8
	ITO	350, 673, 706	–	5.8
	AZO	673, 713		4.8
SAM 13	Quartz	–	691, 711	–

[a] mma = $\varepsilon/(N_A A)$, where ε is molar absorptivity, N_A is Avogadro constant and A is absorbance of the layer.

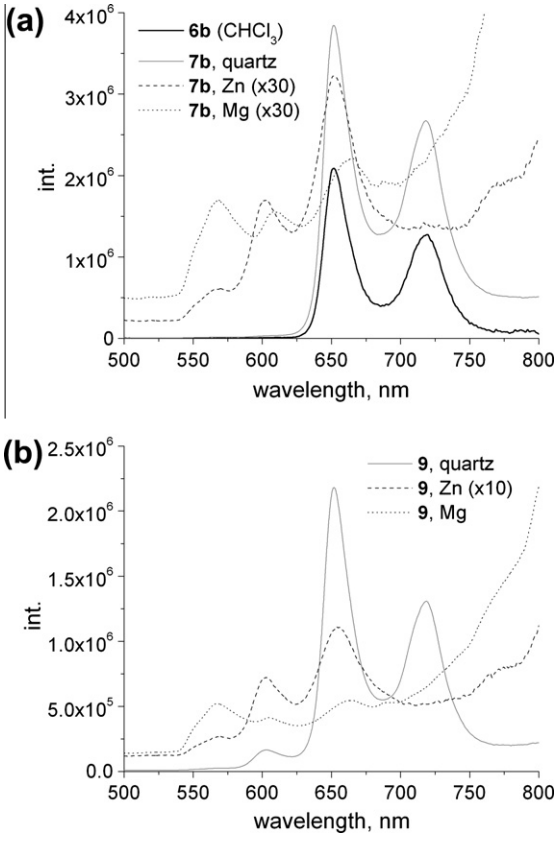

Fig. 3. Emission spectra of (a) porphyrin **6b** (slits 1), porphyrin SAM **7b** and metallated SAMs on quartz (slits 5), and (b) porphyrin SAM **9** and metallated SAMs on quartz (slits 5).

different substrates are over 20 nm^2, which are evidences for loosely packing of the molecules with dimethylmethoxysilane anchor on surface.

Comparing the molecular areas of porphyrins and phthalocyanines, the area increases toward larger chromophore, phthalocyanine, as expected. However, differences in bonding densities are quite small. The mma values for Pc SAM **12** are calculated from maximum of the Q band, and the molecular areas are around 5 nm^2. The area per molecule for dimethylmethoxysilyl-Pc SAM **13** cannot be calculated reliably because of too low absorbance of the sample.

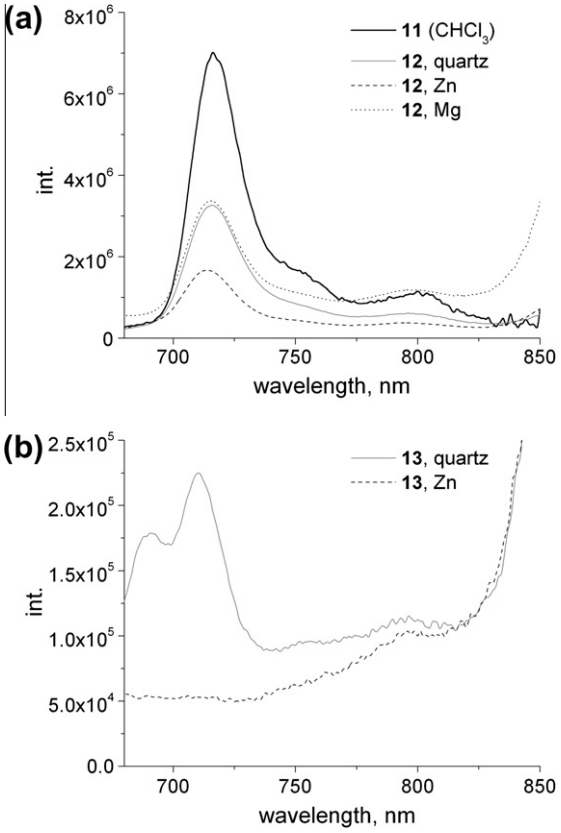

Fig. 4. Emission spectra of (a) phthalocyanine **11** (slits 1), phthalocyanine SAM **12** and metallated SAMs on quartz (slits 5), and (b) phthalocyanine SAM **13** and metallated SAM on quartz (slits 5).

Aggregation of porphyrins is usual, and the phenomenon is typically observed as quenching of fluorescence. Wavelengths of absorption maxima were used as the excitation wavelengths in emission measurements (for porphyrins λ_{Exc} = 420 nm and for phthalocyanine λ_{Exc} = 330 nm). Emission maxima are at 652 nm and 720 nm both for porphyrin **6b** in $CHCl_3$ and for SAMs **7a**, **7b** and **9** (Fig. 3, Table 2). It should be noted that despite 10 times greater absorbance, the emission of SAM **7b** on quartz is only two times higher than emission of SAM **9** on quartz. This can be explained by more efficient fluorescent quenching in more tightly packed molecular layers. Fluorescence lifetime microscope (FLM) studies also support these results (see Supporting information), showing even and smooth coverage of the substrate with chromophore's film, as well.

Phthalocyanine **11** in $CHCl_3$ has emission maximum at 716 nm (Fig. 4a, Table 2). A weak emission band is also visible around 800 nm. SAM **12** on quartz has similar emission spectrum, but on ITO it is hidden under the stronger emission of ITO substrate. Despite negligible absorbance, the emission spectrum of dimethylmethoxysilane-anchored SAM **13** on quartz clearly shows two maxima at 691 nm and 711 nm (Fig. 4b).

3.3.2. Metallation on flat surfaces

Immobilized free base chromophores were further converted by on-surface reactions into Zn(II) and Mg(II) metal complexes. Quartz plates with monolayers on top where immersed into salt solutions for 1–4 h, and the reaction was controlled by absorption and emission measurements. Absorption and emission maxima of

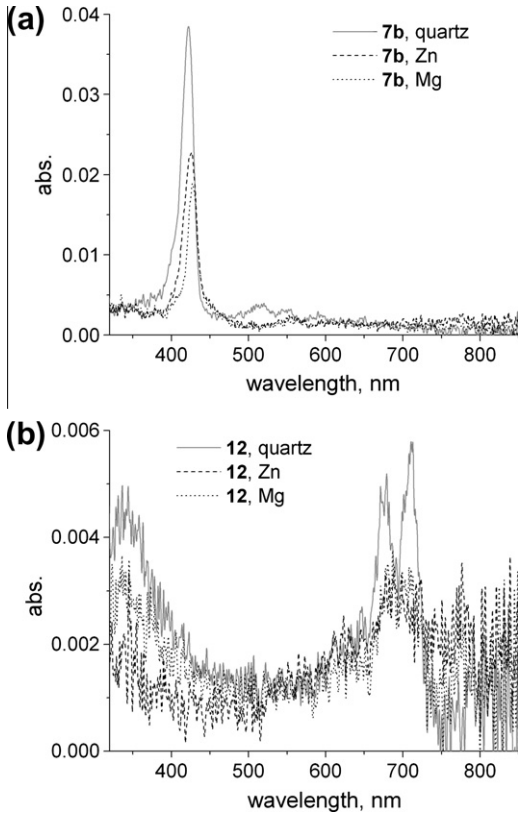

Fig. 5. Absorption spectra of (a) porphyrin SAM **7b** on quartz and on-surface metallated SAMs and (b) phthalocyanine SAM **12** on quartz and on-surface metallated SAMs.

metallated SAMs are collected in Table 3. Metallation of porphyrins is clearly observed. Comparing to free base, the Soret band position shifts to the longer wavelengths, and the first Q band disappears. For metal complexes of SAMs **7b** and **9,** the Soret band is red shifted by 3–5 nm, and the Q band of SAM **7b** at 520 nm is vanished (Fig. 5a). Emission spectra show metallation process even better. The metal ion chelated in porphyrinoid cavity alters the fluorescence properties. The emission band of porphyrin at 720 nm disappears, while a new band around 600 nm is formed (Fig. 3). Disappearance of the emission band at 720 nm gives a good way to monitor the reaction course. For Zn complex, no free base left (no band at 720 nm) after 1 h incubation in zinc acetate solution, but insertion of Mg requires longer time, up to 4 h. It should be noted that the band around 570 nm and the rise from 700 nm in the spectra of SAMs **7b** and **9** is a background emission, which is visible also for clean quartz plates.

Metallation of phthalocyanine is more difficult to detect, as the changes in absorbances are not as pronounced as for porphyrins, and emission of immobilized phthalocyanines is weak. Absorption spectra of both Zn and Mg metallated SAMs **12** show one broad peak around 700 nm instead of two bands of a free base (Fig. 5b). For the SAM **12** treated with zinc acetate solution, the emission intensity is quenched twofolds, but the emission spectrum has the same shape as free base Pc SAM on quartz (Fig. 4a), which is a good indication of successful formation of Zn(II) phthalocyanine complex. However, the emission of Pc **12** layer treated with MgI is even bit higher than that of the free base, which does not allow to conclude that Mg(II) complex was obtained. All of the fluorescence of Pc SAM **13** was quenched (Fig. 4b), which gives good grounds to state that the formation of Zn complex was successful.

Table 3
Absorption and emission maxima of on-surface metallated (Zn and Mg) SAMs.

Sample	Substrate	Metal	Absorption, λ_{max} (nm)	Emission, λ_{max} (nm)
SAM **7b**	Quartz	Zn	426	603, 651
		Mg	427	608, 666
SAM **9**	Quartz	Zn	423	603, 656
		Mg	423	604, 662
SAM **12**	Quartz	Zn	690	714
		Mg	690	715
SAM **13**	Quartz	Zn	–	–

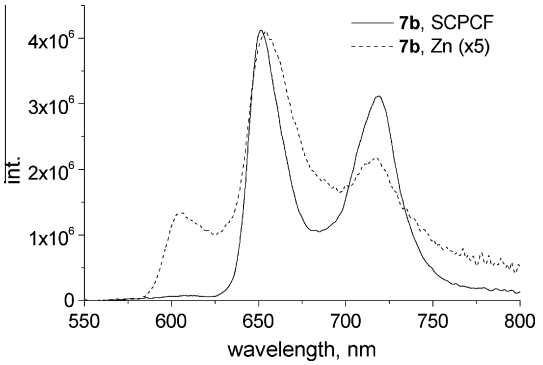

Fig. 6. Emission spectra of porphyrin **7b** deposited inside SCPCF (solid line) and after 1 min of metallation by Zn(II) is shown by dashed line.

3.3.3. Immobilization and metallation inside the channels of SCPCF

An advantage of the self-assembling by covalent bonding is that the layers can be formed on surfaces with complex morphologies, if such surfaces are accessible to the reaction solution. To demonstrate the potential of the newly synthesized compounds, the SAMs were assembled inside the channels of SCPCF. The practical outcome of optical fibers functionalized with photoactive compounds may be found, for example in optical sensor applications, benefiting from enhanced light interactions with SAM since the layers are deposited right on the light guiding channels and availability of advanced fiber optic tools to deliver excitation light to the sensing layer and to collect the photo response.

Emission spectrum of porphyrins deposited inside SCPCF is shown in Fig. 6. It is in good agreement with emission spectra measured from the SAMs deposited on flat quartz surfaces (Fig. 3) and with previously SAMs on tapered optical fiber [21]. It is worth mentioning that in the case of SCPCF much smaller surface area has to be covered with SAM to obtain reasonably strong and accurate emission spectra of samples as compared to that of the flat quartz plates, though direct comparison of the emission intensities in Figs. 3a and 6 is not possible since different method and instruments were used for the measurements.

Similarly to SAMs on flat quartz plates, the porphyrin layers inside channels of SCPCF can be metallated by pumping zinc acetate solutions through the channels. In all cases, just 1 min reaction time was found to be sufficient for the completion of the reaction. The resulting emission spectrum after zinc insertion is presented in Fig. 6. The characteristic zinc porphyrin band can be seen at 605 nm, but the free base porphyrin band at 720 nm did not disappear completely. To study the reason for remaining free base porphyrin emission fluorescence lifetime microscopy (FLM) was used. Images were taken from the top of the fiber (fiber cross-section mode as presented in Fig. 7b) and along the fiber (Fig. 7a). In the latter case, the fiber was placed into immersion oil, which allowed to observe longitudinal sections of the fiber. A typical FLM image taken from the top of the modified SCPCF is shown in Fig. 8. As it

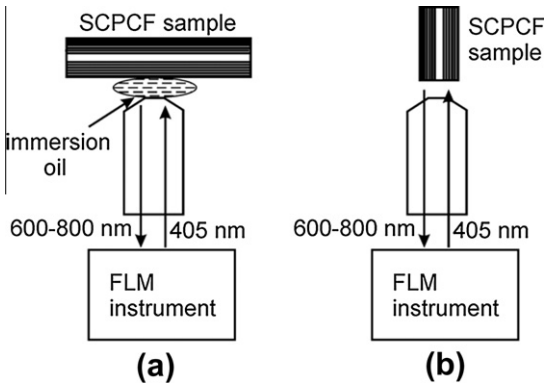

Fig. 7. Setup used to measure (a) FLM images along the SCPCF and (b) cross-sectional FLM images of the SCPCF.

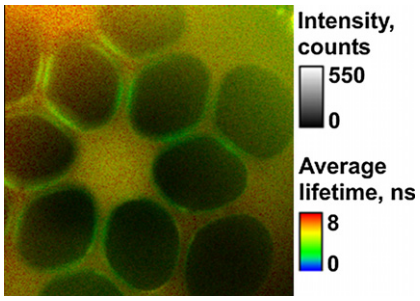

Fig. 8. A typical cross-sectional FLM image of modified SCPCF after the metallation procedure.

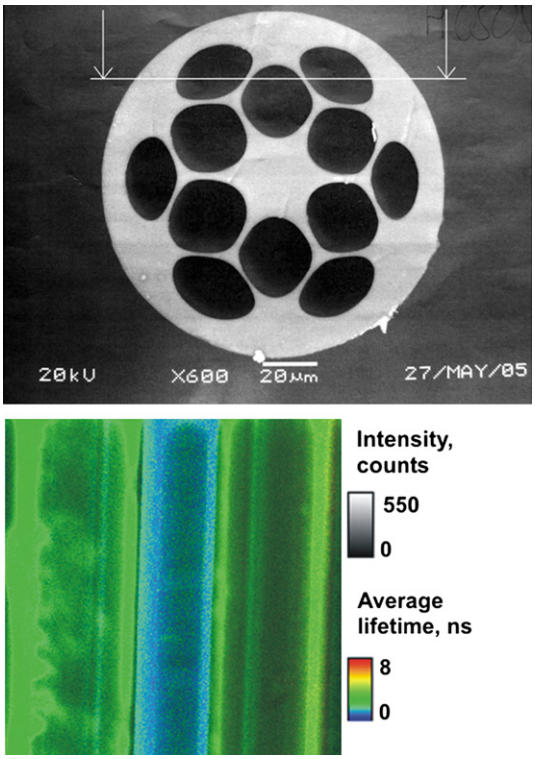

Fig. 9. The scheme showing the position of the cross-section scan from SCPCF cross-section image obtained with SEM (upper figure) and a typical longitudinal FLM image of modified SCPCF after the metallation procedure (lower figure).

is clearly seen, most of the channel walls are covered with SAM (green stripes in Fig. 8).

A representative longitudinal FLM image of modified SCPCF is shown in Fig. 9 (the lower figure) together with the line marking the scan cross-section of the microscope (Fig. 9, the upper figure). The cross-section was selected in such way that three channels can be seen in the image. The colors in the images correspond to average lifetimes with color-lifetime scale shown on the right side of the image. The colors of the channels are different, and the corresponding average lifetimes are 0.87 ± 0.03 ns for the left channel, 0.46 ± 0.01 ns for the central channel, and 1.1 ± 0.04 ns for the right channel. The fluorescence lifetime of zinc porphyrin SAM is shorter than that of free base porphyrin SAM, and one can conclude that the central channel in covered by the Zn porphyrin SAM, while the two other by the free base one. The most probable reason for this is that the left and right channels were blocked by, *e.g.,* dust particles during the metallation of the SAM, as these channels are narrower and easier to block. The fact that not all the channels were available for metallation explains remaining emission band of free base porphyrin in Fig. 6.

Overall, the presented results show that the single step self-assembling is versatile method to form molecular films not only on flat surfaces but also on surfaces with complex morphologies. In particular, the tiny channels of photonic crystal fibers can be functionalized by photoactive and environmental sensitive compounds for their further utilization in fluorescence molecular sensor application.

4. Conclusions

We have elaborated the alkene-terminated anchors, which can be attached to virtually any —OH containing chromophore. Synthesis shows that both butenyl and pentenyl fragments are good short anchors with equal reactivity. Specific reaction conditions are found for hydrosilylation reaction with triethoxysilane, yielding up to 70% of the target silane porphyrinoids, which can be isolated, purified, and characterized. We found that monomethoxy derivative can be prepared with good yield as well but requires different conditions.

The silane-anchored porphyrinoids can be assembled by an easy procedure on quartz, ITO, and ZnO plates, and even on sapphire crystals or inside photonic crystal fibers. We demonstrated that the layers are stable enough to be metallated by Zn and Mg ions. It should be noted that Mg(II) complexes are not accessible on surface by any other way. The metallation time was found to be about 1 min with Zn ion.

The silane-containing compounds have good stability and shelf life, which simplifies their use in SAM films preparation. With calculated mean molecular areas, we observed more difference in bonding densities depending on anchor nature, and less difference depending on surface nature.

Acknowledgments

Graduate School of Tampere University of Technology and Tekes (the Finnish Funding Agency for Technology and Innovation) are greatly acknowledged for financial support.

Appendix A. Supplementary material

Supplementary data associated with this article can be found, in the online version, at doi:10.1016/j.jcis.2011.12.044.

References

[1] M.J. Cook, Pure Appl. Chem. 71 (1999) 2145.
[2] N.R. Armstrong, W. Wang, D.M. Alloway, D. Placencia, E. Ratcliff, M. Brumbach, Macromol. Rapid Commun. 30 (2009) 717.

[3] R. Buntem, A. Intasiri, W. Lueangchaichaweng, J. Colloid Interface Sci. 347 (2010) 8.
[4] D.T. Gryko, C. Clausen, J.S. Lindsey, J. Org. Chem. 64 (1999) 8635.
[5] S.A. DiBenedetto, A. Facchetti, M.A. Ratner, T.J. Marks, Adv. Mater. 21 (2009) 1407.
[6] J.-J. Cid, M. García-Iglesias, J.-H. Yum, A. Forneli, J. Albero, E. Martínez-Ferrero, P. Vázquez, M. Grätzel, M.K. Nazeeruddin, E. Palomares, T. Torres, Chem. Eur. J. 15 (2009) 5130.
[7] E. Sariola, A. Kotiaho, N.V. Tkachenko, H. Lemmetyinen, A. Efimov, J. Porphyrins Phthalocyanines 5 (2010) 397.
[8] V. Kriegisch, C. Lambert, Top. Curr. Chem. 258 (2005) 257.
[9] A. Ulman, Chem. Rev. 96 (1996) 1533.
[10] R.K. Smith, P.A. Lewis, P.S. Weiss, Prog. Surf. Sci. 75 (2004) 1.
[11] D.W.J. McCallien, P.L. Burn, H.L. Anderson, J. Chem. Soc., Perkin Trans. 1 (1997) 2581.
[12] X. Li, W. Xu, H. Jia, X. Wang, B. Zhao, B. Li, Y. Ozaki, J. Colloid Interface Sci. 274 (2004) 9.
[13] P. Stegmaier, J.M. Alonso, A. del Campo, Langmuir 24 (2008) 11872.
[14] I.E. Markó, S. Stérin, O. Buisine, G. Mignani, P. Branlard, B. Tinant, J.-P. Declercq, Science 298 (2002) 204.
[15] E.C.P. Smits, S.G.J. Mathijssen, P.A. van Hal, S. Setayesh, T.C.T. Geuns, K.A.H.A. Mutsaers, E. Cantatore, H.J. Wondergem, O. Werzer, R. Resel, M. Kemerink, S. Kirchmeyer, A.M. Muzafarov, S.A. Ponomarenko, B. de Boer, P.W.M. Blom, D.M. de Leeuw, Nature 455 (2008) 956.
[16] S. Petersen, J.M. Alonso, A. Specht, P. Duodu, M. Goeldner, A. Del Campo, Angew. Chem., Int. Ed. 47 (2008) 3192.
[17] M.J. Cook, R. Hersans, J. McMurdo, D.A. Russell, J. Mater. Chem. 6 (1996) 149.
[18] B. Marciniec, Silicon Chem. 1 (2002) 155.
[19] H. Brunner, Angew. Chem., Int. Ed. 43 (2004) 2749.
[20] S.O. Korposh, N. Takahara, J.J. Ramsden, S.-W. Lee, T. Kunitake, JBPC 6 (2006) 125.
[21] A. Veselov, C. Thür, A. Efimov, M. Guina, H. Lemmetyinen, N.V. Tkachenko, Meas. Sci. Technol. 21 (2010) 115205.
[22] A.A. Veselov, C. Thür, A. Efimov, M. Guina, H. Lemmetyinen, N.V. Tkachenko, Phys. Status Solidi A 208 (2011) 1858.
[23] J. Ranta, T. Kumpulainen, H. Lemmetyinen, A. Efimov, J. Org. Chem. 75 (2010) 5178.
[24] H. Saarenpää, T. Niemi, A. Tukiainen, H. Lemmetyinen, N. Tkachenko, Sol. Energy Mater. Sol. Cells 94 (2010) 1379.
[25] B. Görlach, C. Hellriegel, S. Steinbrecher, H. Yüksel, K. Albert, E. Plies, M. Hanack, J. Mater. Chem. 11 (2001) 3317.
[26] A. Efimov, P. Vainiotalo, N.V. Tkachenko, H. Lemmetyinen, J. Porphyrins Phthalocyanines 7 (2003) 610.
[27] A. Behr, F. Naendrup, D. Obst, Adv. Synth. Catal. 344 (2002) 1142.
[28] J.M. Alonso, A. Reichel, J. Piehler, A. del Campo, Langmuir 24 (2008) 448.
[29] M. Kamieth, U. Burkert, P.S. Corbin, S.J. Dell, S.C. Zimmerman, F.-G. Klärner, Eur. J. Org. Chem. 1999 (1999) 2741.
[30] A.L. Bramblett, M.S. Boeckl, K.D. Hauch, B.D. Ratner, T. Sasaki, J.W. Rogers Jr., Surf. Interface Anal. 33 (2002) 506.

Paper III

Supramolecular assemblies of *bay*-substituted perylene diimides in solution and on a solid substrate

Essi Sariola-Leikas, Marja Niemi, Helge Lemmetyinen and Alexander Efimov

Org. Biomol. Chem. **2013**, *11*, 6397-6406.

Organic & Biomolecular Chemistry

RSC Publishing

PAPER

Supramolecular assemblies of *bay*-substituted perylene diimides in solution and on a solid substrate†

Cite this: *Org. Biomol. Chem.*, 2013, **11**, 6397

Essi Sariola-Leikas,* Marja Niemi, Helge Lemmetyinen and Alexander Efimov

Received 22nd May 2013,
Accepted 30th July 2013

DOI: 10.1039/c3ob41058g

www.rsc.org/obc

Perylene diimides (PDIs) substituted with a terpyridine moiety at the *bay*-region have been synthesized. These building blocks were used to construct supramolecular complexes in chloroform. A dimer and a trimer were built *via* the *bay*-region complexation with zinc. The PDI compounds were further modified to have silane anchors and PDI self-assembled monolayers (SAMs) were prepared on a quartz substrate. Complexation of metal ions was also done on the surface, and this was observed clearly in the absorption spectrum. These studies on the surface show possible progress in the study of supramolecular multilayer structures.

Introduction

In recent years, considerable attention has been focused on surface modification of solid substrates by forming highly ordered organic films. One of the approaches to form ultrathin films on the surface is immersing the substrate into a diluted solution of an anchor-containing organic compound. The formed films are referred to as self-assembled monolayers (SAMs).[1] Silanes are one of the anchor group types, which form a strong and stable covalent bond between the molecule and the oxide surface.[2] Siloxane-containing compounds are rather difficult to synthesize but they enable creating SAMs in a fast and easy manner.[3,4]

The use of a chelating ligand, such as a terpyridine, supports the formation of supramolecular assemblies. Terpyridine ligands are highly attractive terminal groups to be incorporated into SAMs, since they can coordinate to a broad range of metals and be substituted with many different functionalities.[5] The three nitrogen donors on each 2,2′:6′2″-terpyridine (tpy) interact strongly with the metal ion. The most commonly used metals for this purpose are zinc(II)[6,7] and ruthenium(III)/(II).[8] The terpyridine moieties are widely used in metallo-supramolecular polymers, where their role is significant.[9]

Perylene diimides (PDIs) are a unique class of chromophores, which exhibit outstanding optical, electronic and physical properties. Typically, PDIs are functionalized at the imide ring, which restricts the interactions between chromophores and their successive layers.[10] On the other hand, introducing functional groups in the *bay*-region (1,6,7,12-positions) modifies the electronic and optical properties of PDIs and allows their fine tuning.[11,12] These dyes combined with the tpy units are powerful building blocks for supramolecular organization and because of their photoactive properties these units can be used for optoelectronic applications.[13,14]

In this paper we report syntheses of PDIs substituted with the terpyridine moiety at the *bay*-region. Terpyridine moieties at the *bay*-region in PDIs are extremely rare.[15] We have also synthesized PDIs with a silane anchor and prepared PDI SAMs on a solid substrate (quartz). Siloxane anchors on PDIs are also uncommon and, to the best of our knowledge, no PDIs with a silane anchor at the *bay*-region have been published before.[16] Covalent attachment to the substrate was done in one step and monomolecular layer formation was proved by absorption measurements. Coordination with zinc(II) is a promising option for the layer-by-layer formation of supramolecular assemblies of photoactive compounds.[17] A supramolecular dimer and a trimer were constructed in solution. Such tpy-PDI complexes, which are connected through the *bay*-region, were prepared for the first time. Furthermore, energy transfer from the middle PDI to the side PDIs was observed in the PDI trimer with quantum yield close to unity, even though the distance between the donor and the acceptor is quite long.

Department of Chemistry and Bioengineering, Tampere University of Technology, P.O. Box 541, 33101 Tampere, Finland. E-mail: essi.sariola-leikas@tut.fi; Fax: +358 3 364 1392; Tel: +358 40 198 1124

†Electronic supplementary information (ESI) available: Fluorescence decays of PDI **8** and PDI **3**. ^{1}H NMR, ^{13}C NMR and gHSQC NMR spectra of compounds **1**, **3–6**, **8**, **10** and **11**. ^{1}H NMR spectra of complexes **Zn-3**, **Zn-8**, **3-Zn-3a**, **3-Zn-3b** and **3-Zn-8**. Mass spectra of complexes **3-Zn-3b** and **3-Zn-8**. See DOI: 10.1039/c3ob41058g

Results and discussion

Synthesis

Borylation of bromophenylterpyridine was done according to Scheme 1 with a moderate yield of 50% of tpy **1**. Attempts to improve the reaction efficiency by changing the base to NaOAc and by using the catalyst $PdCl_2$ and the ligand [dppf = 1,1′-bis-

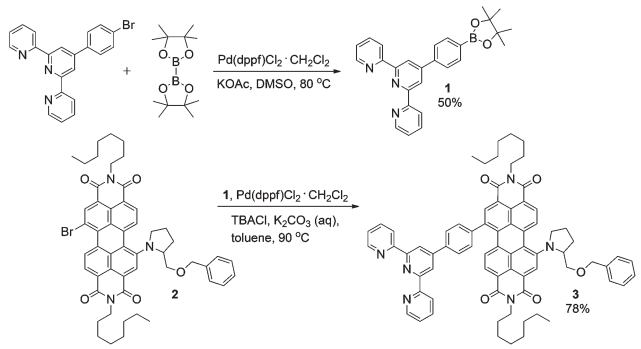

Scheme 1 Borylation of tpy **1** and Suzuki coupling reaction of tpy-PDI **3**.

(diphenylphosphanyl)ferrocene] as separate reagents did not increase the yield. Tpy **1** was used in a Suzuki coupling reaction with 2-(benzyloxymethyl)pyrrolidine substituted PDI **2**. The synthesis of PDI **2** was done according to a procedure reported earlier.[18]

Building block tpy-PDI **3** was synthesized from regioisomerically pure 1,7-PDI **2** (Scheme 1).[11] The reaction was done in a toluene–water biphasic system with Pd catalyst. Product **3** was purified using automated low-pressure Combiflash chromatography on an alumina column. Silica columns could not be used for the purification because of their excessive sorption of terpyridyl-containing compounds.

Deprotection of tpy-PDI **3** was performed using boron tribromide (Scheme 2). The thus received PDI **4** was further modified to have a siloxane anchor. The hydrosilylation procedure was similar to the one published earlier for other chromophores.[4] Compounds **4**, **5** and **6** were obtained with relatively high yields as indicated in Scheme 2.

Bis(substituted) tpy-PDI **8** (Scheme 3) was synthesized from dibromo-PDI **7**, which was a pure 1,7-regioisomer.[11] The reaction conditions were similar to those described for PDI **3**. However, purification was not straightforward because of the minor amount of mono-tpy-substituted PDI. Column separation did not provide enough resolution, and complete separation was achieved only using preparative alumina TLC plates.

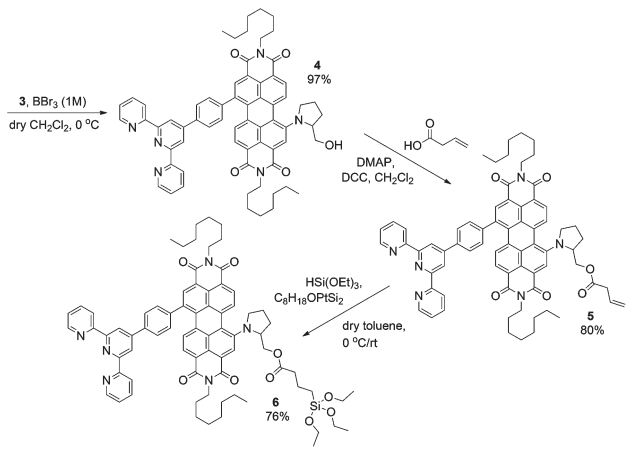

Scheme 2 Synthetic route to tpy-PDI-Si(OEt)$_3$ **6**.

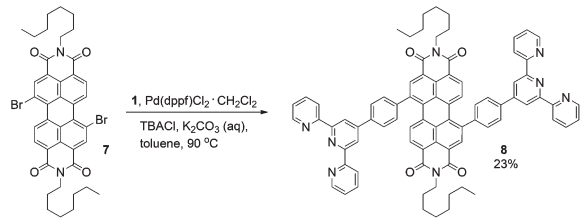

Scheme 3 Synthesis of bis(substituted) tpy-PDI **8**.

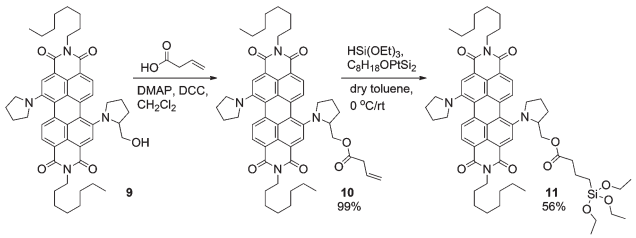

Scheme 4 Synthetic route to pyr-PDI-Si(OEt)$_3$ **11**.

Bis-pyrrolidine PDI **11** with a siloxane anchor was also prepared to compare the bonding densities of PDIs with different substituents. Hydroxy-PDI **9** was prepared according to a literature procedure.[18] Syntheses of allyl PDI **10** and siloxane PDI **11** were similar to that of the terpyridine PDIs. Purification of all these compounds could be efficiently performed using silica gel. The synthetic route is presented in Scheme 4.

Solution studies

PDIs **3** and **8** were used to construct supramolecular complexes in solution. According to the literature, the zinc ion forms complexes with terpyridine under very mild conditions and the complexation can be detected from their absorption spectra.[7,13] In our experiments, zinc acetate did not give stable complexes. Therefore, the counter ion was changed and zinc triflate ($Zn(OTf)_2$) was chosen. The complexes were prepared by dissolving PDI (**3** or **8**) in $CHCl_3$–CH_3CN and adding zinc triflate stock solution into the mixture. The reaction solution was stirred at room temperature for 1 h. Structures of the formed zinc complexes **Zn-3** and **Zn-8** are presented in Fig. 1.

A dimer (**3-Zn-3**) and a trimer (**3-Zn-8**) were also prepared (Fig. 1). The dimer was produced either from monomers **Zn-3** and **3** (**3-Zn-3a**) or directly from PDI **3** (**3-Zn-3b**). Trimer **3-Zn-8** was assembled in DMF because the solubility of **Zn-8** in chloroform-based solvents was poor.

Steady-state absorption was used as a quick method to prove the formation of the complexes. Characteristic absorption bands of tpy-PDI **3** appear between 550–750 nm and 400–500 nm (Fig. 2). Both the PDI core and the tpy unit absorb also at wavelengths below 350 nm. The 650 nm centered band is characteristic for pyrrolidine substituted PDI.[19] Distinct changes in absorption were observed after complexation with zinc: an increase of the absorption intensity between 300 and 350 nm and a decrease and sharpening around 270 nm. These

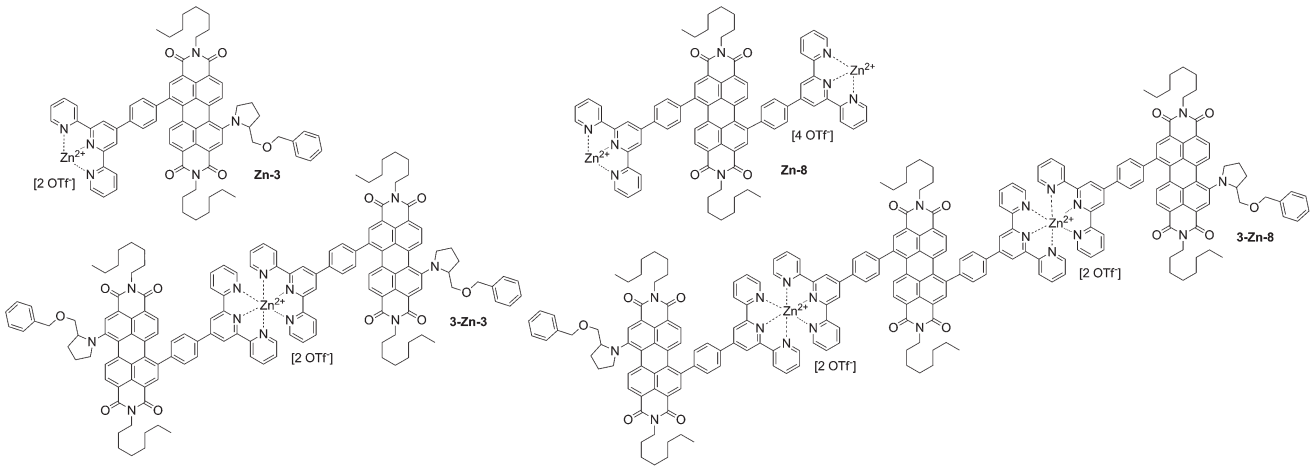

Fig. 1 Supramolecular complexes.

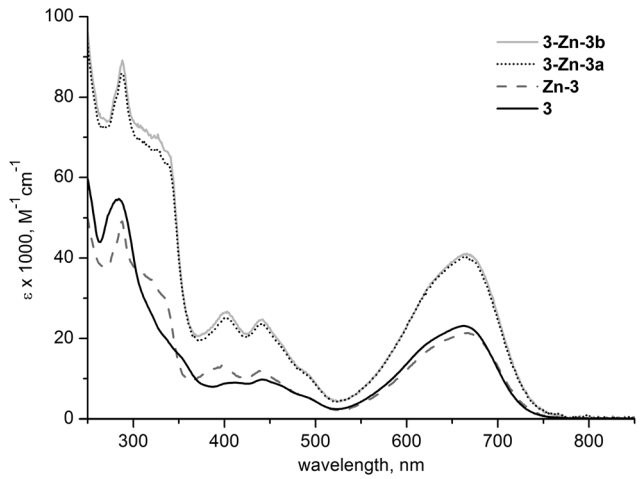

Fig. 2 Absorption spectra of tpy-PDI **3** and its zinc complexes in $CHCl_3$.

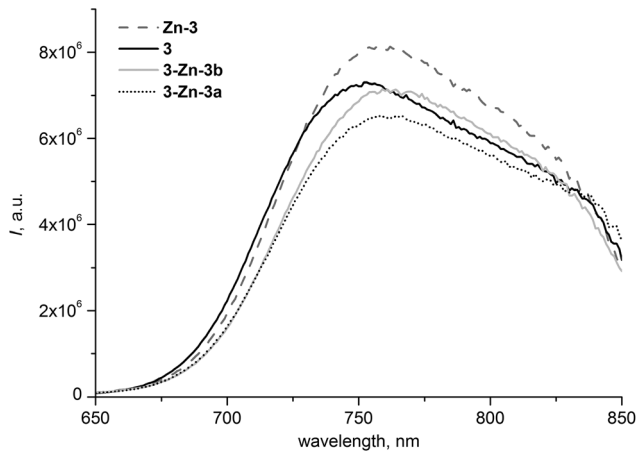

Fig. 3 Emission spectra of tpy-PDI **3** and its zinc complexes in $CHCl_3$ (Exc: 630 nm).

correspond to the changes in the tpy unit absorption and thus indicate the formation of the zinc complex.[13]

A small red-shift of the absorption maximum of the PDI unit from 662 nm to 666 nm was observed during the complexation. Also in the emission spectra a small shift of the maximum was noticed (Fig. 3). A two-fold increase in the molar absorptivities (ϵ) was observed for the dimers (**3-Zn-3a** and **3-Zn-3b**). As expected, the dimers formed *via* different routes give identical absorption spectra (Fig. 2). Table 1 presents absorption and emission maxima of compounds **3** and **8** and their complexes in solution.

Zn-complexation of compound **8** showed similar changes in the absorption spectrum as that of compound **3**, *i.e.* an increase of the absorption around 340 nm and a sharpening below 300 nm, which are due to the formation of zinc tpy (**Zn-8**, Fig. 4). A remarkable blue shift was observed for the PDI band from around 660 nm of **3** and **Zn-3** to around 555 nm of **8** and **Zn-8**. Such a shift was expected for PDI **8** where there is no pyrrolidine substituent. The low molar absorptivity of **Zn-8** in Fig. 4 cannot be considered accurate because of the low solubility and aggregation of the complex in $CHCl_3$. When trimer **3-Zn-8** was formed, bands similar to those for **3** and **Zn-3** were spotted and the absorption maxima match well with the zinc complexes of PDI **3** and **8** (Table 1). Evidently the shoulder at about 570 nm corresponds to the PDI moiety between the two tpy units (**8**), and the maximum at about 665 nm to the PDI complexed with only one tpy moiety (**3**).

Table 1 Absorption and emission maxima of compounds **3** and **8** and their zinc complexes in $CHCl_3$

Compound	Absorption, λ_{max} (nm)	Emission, λ_{max} (nm)
3	284, 442, 662	753
Zn-3	288, 397, 438, 663	757
3-Zn-3a	288, 402, 439, 666	758
3-Zn-3b	288, 403, 442, 666	759
8	284, 556	619
Zn-8	288, 338, 553	607
3-Zn-8	288, 389, 439, 666	603, 755

The emission spectra of bis(substituted) tpy-PDI **8** and its zinc complexes are presented in Fig. 5. As expected, the

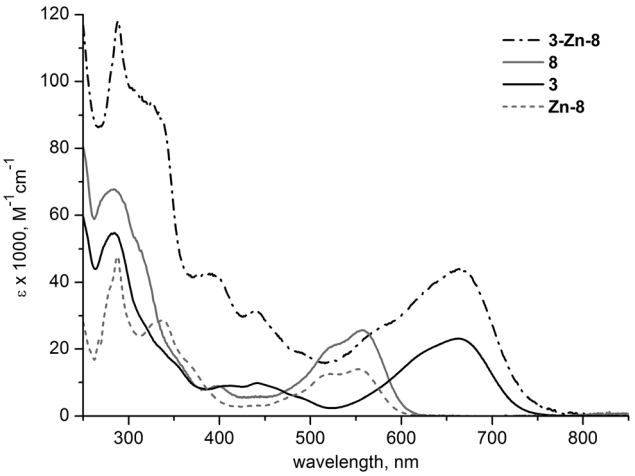

Fig. 4 Absorption spectra of bis(substituted) tpy-PDI **8** and its zinc complexes in $CHCl_3$. The absorption spectrum of tpy-PDI **3** is shown for comparison.

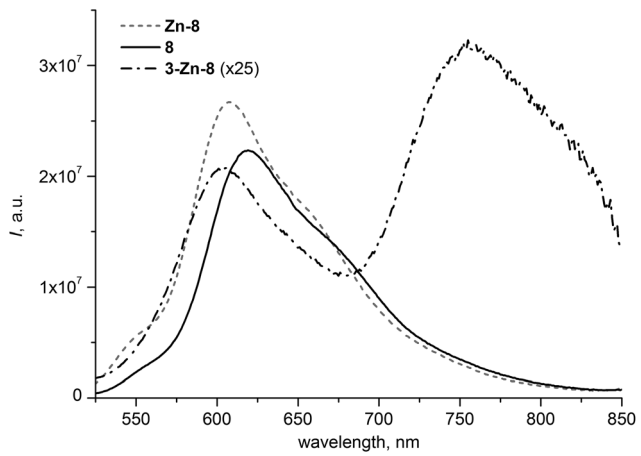

Fig. 5 Emission spectra of bis(substituted) tpy-PDI **8** and its zinc complexes in $CHCl_3$ (Exc: 505 nm).

spectrum of trimer **3-Zn-8** has two emission maxima at 603 nm and 755 nm, which correspond to PDI **8** and PDI **3**, respectively. Quenching of the fluorescence bands around 600 nm and 760 nm are seen in the trimer, whose emission spectrum is multiplied by 25 for comparison with the references. At the excitation wavelength of 505 nm, the absorbance of PDI **3** is rather weak in comparison to that of PDI **8**, but still a relatively strong emission around 750 nm is observed for the trimer. This indicates that the energy transfer from the middle PDI to one of the side PDIs is the reason for the quenching in the trimer.

Energy transfer from the middle PDI to the side PDI was confirmed by time-resolved fluorescence measurements with the time-correlated single photon counting method. Lifetimes of the first singlet excited state of reference compounds PDI **8** and PDI **3** were determined as 8.3 ns and 1.57 ns, respectively (see ESI†). To distinguish between the different emitting species in **3-Zn-8**, fluorescence decay was collected with a constant accumulation time (180 s) in the range 580–840 nm with

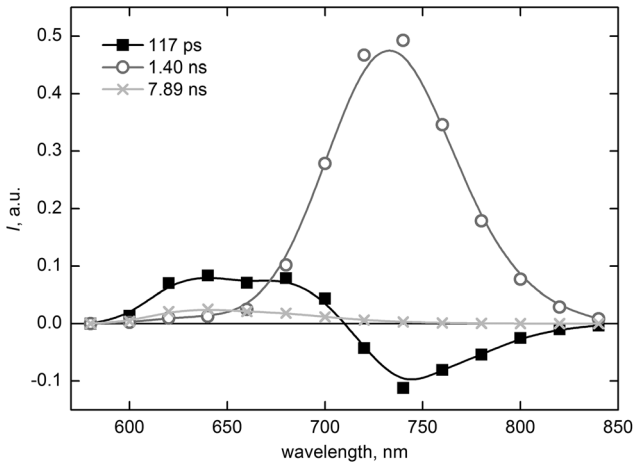

Fig. 6 Fluorescence decay-associated spectra of trimer **3-Zn-8** in $CHCl_3$ (Exc: 405 nm).

20 nm steps. The obtained decay curves were fitted globally to obtain fluorescence decay component spectra (Fig. 6). Three exponents were needed for a reasonable fit quality. The fastest component (117 ps) follows the shape and position of the fluorescence spectrum of PDI **8** at 600–700 nm. The negative amplitude around 750 nm indicates the formation of fluorescence and thus corresponds to energy transfer from the middle PDI to the side PDI. The formed component shows clearly the spectrum of PDI **3** (see Fig. 6) centered at 750 nm and the lifetime (1.40 ns) is in agreement with the one measured for reference PDI **3** (1.57 ns). The final component with a lifetime of 7.89 ns is weak in amplitude, but shows clearly the spectrum of PDI **8**. The lifetime is similar to that measured for reference PDI **8** and this component can be assigned to a small amount of free PDI **8** in the solution due to dissociation of the trimer.

The rate constant of energy transfer, k_{enT}, in the trimer can be calculated as $k_{enT} = k_1 - k_{fl}$, where k_1 is the rate constant of the fastest process in the trimer (8.55×10^9 s^{-1}) and k_{fl} is the rate constant of the fluorescence, which is obtained from the measurement of PDI **8** (1.2×10^8 s^{-1}). The calculated k_{enT} = 8.43×10^9 s^{-1} and the quantum yield of energy transfer can be estimated from $\phi_{enT} = k_{enT}/(k_{enT} + k_{fl})$ as 0.99. Considering the highly efficient energy transfer, it seems unreasonable that there is significant emission around 600 nm in the steady state fluorescence spectrum of the trimer (Fig. 5). This can be explained by the presence of *ca.* 4% (as derived from the fluorescence quenching) of the highly emissive longer oligomers,[13] residual **3-Zn-3** and trimer dissociated to its components. Even a small amount of free PDI **8** will cause a strong signal in the steady state spectrum due to the relatively long lifetime of its singlet excited state.

NMR characterization

The synthesized compounds were fully characterized by mass spectrometry (see the Experimental section) and NMR spectroscopy (see ESI†). All the products had good solubility

allowing the NMR measurements in $CDCl_3$. The signal assignments are based on two-dimensional NMR spectroscopy, the heteronuclear single-quantum coherence (gHSQC) with multiplicity editing and the homonuclear correlation spectroscopy (COSY).

The assignment of ^{1}H NMR peaks is complicated due to the overlapping of the peaks and crowded aromatic and aliphatic regions. Thus most of the signals are visible as multiplets. However, assignment for all the proton signals was successfully done. When comparing the aromatic regions of compounds **3**, **4**, **5** and **6**, some small changes of peak positions are observed in the perylene core proton signals (7, 11, 14) and in the signals of phenylene protons. In the spectrum of PDI **4** these signals are distinguished better. In the spectra of PDIs **5** and **6**, the signal from proton 13 is shifted to lower field compared to the other spectra. The aliphatic regions in the spectra are quite consistent. In the spectrum of PDI **4**, the signal from proton d is moved to higher field when compared to the other spectra. In the spectra of PDIs **5** and **6**, the signal from proton e is deshielded (δ 4.66–4.41 ppm), which is due to changes in the anchor group. All the characteristic proton signals such as hydroxyl group, terminal double bond and silane protons are observed easily from the spectra of PDIs **4**, **5** and **6**, respectively. The positions of these signals correspond well with the values of previously studied chromophores.[4]

The symmetric structure of PDI **8** makes its spectrum quite straightforward to resolve. Also the spectra of PDIs **10** and **11** are simpler than those of the other PDIs because of the uncomplicated substituent. Comparing ^{1}H NMR spectra of compounds **10** and **11**, all the peaks in the aromatic region have shifted a bit downfield in the spectrum of PDI **11**. In the aliphatic region, the signals from the terminal double bond have vanished and the silane signals are visible in the spectrum of PDI **11**. The signal positions match well with the signals in the spectrum of PDI **6**.

Resolving the spectra of complexes (**Zn-3**, **3-Zn-3**, **Zn-8**, and **3-Zn-8**) is complicated but possible. The signals in the aliphatic region correlate nicely with the uncomplexed ones, though the aromatic region signals are shifted. When comparing the spectra of PDI **3** and complex **Zn-3**, it is clear that complexation has occurred (Fig. 7). Nearly all the peaks in the aromatic region have moved in the spectrum of **Zn-3**. The closest protons to the nitrogen atoms in the terpyridine moiety (5″-H and 6″-H) are shifted to lower field from 7.35 and 8.75 ppm to 7.80 and 8.90 ppm, respectively. When comparing the spectra of **Zn-3** and dimer **3-Zn-3**, an extreme high-field shift of protons 6″-H is observed (marked with * in Fig. 7). The signal from protons 5″-H is shifted back to its old position (around 7.40 ppm) in the spectrum of the dimer. These observations are similar to the results found previously for a PDI with terpyridines at the imide region.[13]

Complex **Zn-8** was the only one measured in deuterated methanol because of its low solubility in $CDCl_3$. However, a similar shifting of signals from protons 5″-H and 6″-H is observed when the spectra of bis(substituted) tpy-PDI **8** and **Zn-8** are compared. The signal of protons 6″-H is deshielded from 8.70 to 8.95 ppm, and the signal of protons 5″-H is shifted from 7.40 to 7.95 ppm. Assignment of the aromatic region protons in the spectrum of trimer **3-Zn-8** is too complex. The region is nearly one big multiplet. Nevertheless, the integrals match well with the number of protons.

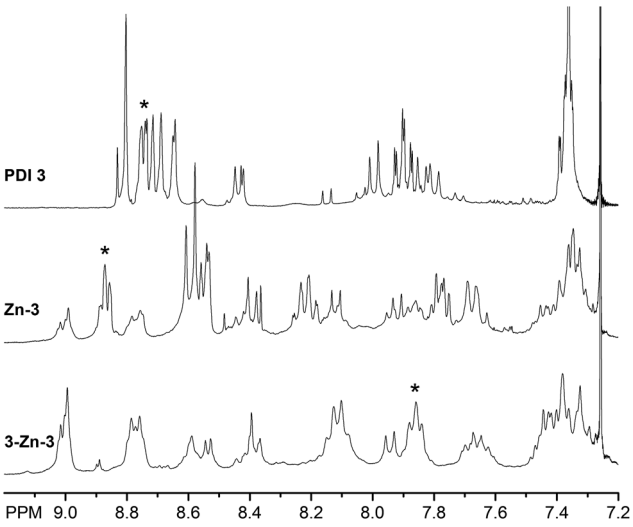

Fig. 7 The aromatic regions of ^{1}H NMR spectra of tpy-PDI **3**, **Zn-3** and **3-Zn-3**. The marked signal (*) corresponds to protons 6′′-H, the closest protons to nitrogen atoms in terpyridine.

Immobilization and complexation

SAMs were prepared in a one-step process, where the reaction vessel was loaded with a solution of siloxane PDI **6** or **11** in distilled toluene and isopropyl amine under argon. Quartz plates were precleaned according to a previously reported method.[4] The cleaned plates were immersed in the solution, and the reaction vessel was heated at 105 °C. After 2 h, the plates were sonicated on an ultrasonic bath to remove the residual physisorbed compound. Absorption spectra of the SAMs were obtained by subtracting the absorbance of the clean substrate from the absorbance of the plate with the SAM. Considering the absorption spectrum of the monolayer on the surface, the optical densities in Fig. 8 and 9 should be divided by two, because layers are formed on both sides of the substrate.

The absorption spectrum of SAM **6** shows a similar shape as PDI **5** in solution (Fig. 8). Even though absorptions of the SAMs are low, the complexation with zinc triflate is nicely observed from the spectrum of the plate. Complexation on the surface was done by immersing the substrate with the SAM in the salt solution for 1 h. The same changes in the absorption spectrum are seen as with complexation in chloroform: an increase of absorption between 300 and 350 nm and a decrease around 270 nm. An expected increase at 400 nm and 440 nm is also noticeable as these bands are more intense in the complex form of PDI (absorption spectrum of **Zn-3**). The PDI band of SAMs around 640 nm is slightly red-shifted upon complexation as was visible also in the solution studies. The absorption maxima are presented in Table 2.

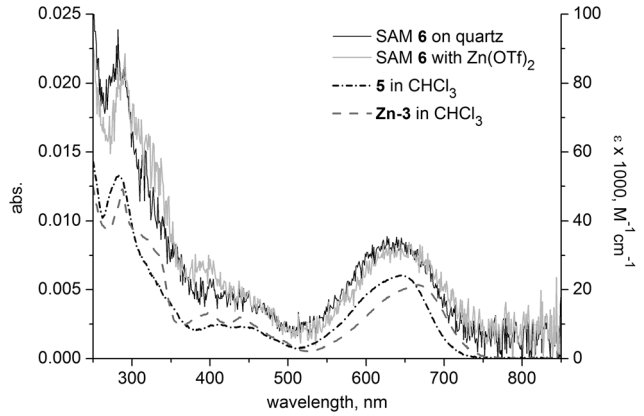

Fig. 8 Absorption spectra of tpy-PDI **5** and complex **Zn-3** on the molar absorptivity (ε) scale and PDI SAM **6** on the quartz surface.

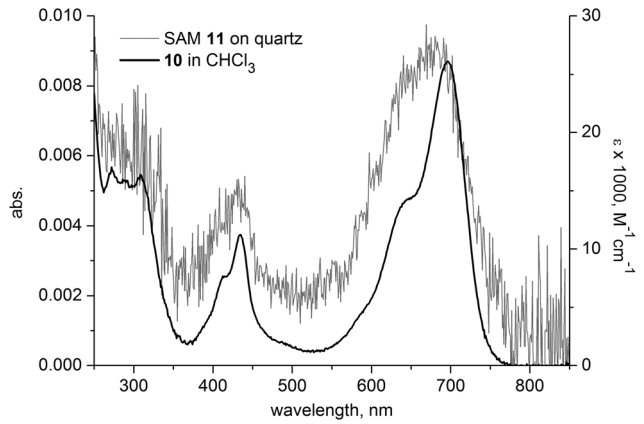

Fig. 9 Absorption spectra of pyr-PDI **10** on the molar absorptivity (ε) scale and PDI SAM **11** on the quartz surface.

Table 2 Absorption maxima and mean molecular areas (mma) of samples

Sample	Solvent/substrate	Absorption, λ_{max} (nm)	mma[a] (nm^2)
PDI 5	$CHCl_3$	283, 412, 647	
SAM 6	Quartz	282, 640	1.01
SAM 6, Zn	Quartz	291, 645	0.89
PDI 10	$CHCl_3$	272, 434, 696	
SAM 11	Quartz	432, 680	0.96

[a] mma = $\varepsilon/(N_A A)$, where ε is the molar absorptivity, N_A is the Avogadro constant and A is absorbance of the layer.

Bis-pyrrolidine PDI **11** was also attached on the surface. The absorption spectrum of SAM **11** imitates nicely the absorption of pyr-PDI **10** (Fig. 9). The absorption bands are broader in the spectrum of the SAM but the band maxima correspond quite well with pyr-PDI **10** in solution (Table 2).

The absorption maximum provides a possibility to estimate the mean molecular area (mma) of the PDI in the SAM. The mma values were calculated assuming the same molar absorptivity (ε) of compounds in SAMs as in solution (Table 2). This is true only if the molecules are randomly oriented on the surface and if the chromophore–chromophore or chromophore–surface interactions are disregarded.[20] The mma values are smaller than what one could expect for perfect monolayers. This might be due to the long linker, which allows chromophores to stack one over another instead of forming an ideal monomolecular film. This hypothesis is supported by the complete fluorescence quenching of the films, which is due to the aggregation of the PDI units. Evidently, a more rigid tether is needed to improve the orientation of the molecules in films, and research on this is currently under way.

Experimental

Materials and instrumentation

All reagents and solvents (HPLC grade) were purchased from Sigma-Aldrich Co., Tokyo Chemical Industry Co. or VWR International. Unless otherwise mentioned, chemicals were used as received. Dichloromethane was distilled over P_2O_5 and toluene over sodium shots. Quartz plates were purchased from Finnish Specialglass.

The monitoring of the reactions was carried out by thin layer chromatography (TLC), employing aluminum sheets precoated with silica gel 60 F_{254} or aluminium oxide 60 F_{254} neutral (Merck). The purification and isolation of the products were performed by column chromatography on Silica 60 (mesh size 40–63 μm) or by flash chromatography using CombiFlash Companion (Teledyne ISCO).

The ^{1}H NMR spectra were measured using a Varian Mercury 300 MHz spectrometer (Varian Inc.). All chemical shifts are given in ppm relative to TMS as an internal standard and the coupling constants, J, are given in Hz. Mass spectra were recorded using a high resolution ESI-TOF LCT Premier XE mass spectrometer (Waters Corp.). The sample of an analyte was dissolved in appropriate solvent at a concentration of *ca.* 0.01 mg mL^{-1} and infused at a 15 μL min^{-1} rate. The reference solution of Leucine Enkephalin (50 pg mL^{-1}) was infused simultaneously. The original spectra were centred, and lock mass TOF correction was applied. Absorption spectra were measured using a Shimadzu UV-2501PC UV-Vis Recording spectrometer and emission spectra were recorded using a Fluorolog Yobin Yvon-SPEX spectrofluorometer.

Fluorescence decay of the samples in the nanosecond and sub-nanosecond time scales was measured using a time-correlated single photon counting (TCSPC) system (PicoQuant GmbH) consisting of a PicoHarp 300 controller and a PDL 800-B driver. The samples were excited with the pulsed diode laser head LDH-P-C-405B at 404 nm and fluorescence decay was measured at the wavelength of maximum emission (620 nm and 750 nm for PDI **8** and PDI **3**, respectively). The signals were detected with a micro channel plate photomultiplier tube (Hamamatsu R2809U). The time resolution of the TCSPC measurements was about 80 ps (FWHM of the instrument response function). For trimer **3-Zn-8** the fluorescence decay was measured in the wavelength range of 580–840 nm with 20 nm steps and a constant accumulation

time of 180 s. The decay at different wavelengths was fitted globally to obtain decay-associated spectra.

4′-(4-(4,4,5,5-Tetramethyl-1,3,2-dioxaborolan-2-yl)phenyl)-2,2′:6′,2″-terpyridine (1).[21] 4′-(4-Bromophenyl)-2,2′:6′,2″-terpyridine (100 mg, 0.26 mmol) and KOAc (76 mg, 0.77 mmol) were dissolved in DMSO (5 mL) on an ultrasonic bath. Bis(pinacolato)diboron (78 mg, 0.31 mmol) and Pd(dppf)Cl_2·CH_2Cl_2 (10 mg, 0.013 mmol) were added and the reaction mixture was stirred at 80 °C under argon for 45 min. The solution was diluted with $CHCl_3$ and washed with a saturated solution of EDTA (3 × 80 mL). The organic phase was evaporated under reduced pressure. The crude product was purified on a Combiflash chromatograph using an alumina column (12 g) eluting with a hexane–EtOAc gradient (flow rate: 30 mL min^{-1}; hexane (1 min), hexane to hexane–EtOAc 10 : 3.5 (5 min), hexane–EtOAc 10 : 3.5 (3 min)). Product **1** was isolated as a white solid (56 mg, 50%). δ_H (300 MHz; $CDCl_3$; Me_4Si): 1.39 (12H, s, Me), 7.33–7.40 (2H, m, 5″-H), 7.89 (2H, td, *J* 7.8, 1.8, 4″-H), 7.92–7.98 (4H, m, phenylene-H), 8.68 (2H, d, *J* 7.9, 3″-H), 8.74 (2H, d, *J* 3.8, 6″-H), 8.75 (2H, s, 3′-H). δ_C (75 MHz; $CDCl_3$; Me_4Si): 25.1 (CH_3), 84.2 (C-dioxaborolane), 119.1 (C-3′), 121.6 (C-3″), 124.1 (C-5″), 126.8 (C^o-phenylene), 135.6 (C^m-phenylene), 137.1 (C-4″), 141.2 (C^i-phenylene), 149.4 (C-6″), 150.3 (C-4′), 156.2 (C-2′), 156.4 (C-2″); C^p-phenylene signal was not observed. MS (ESI-TOF, CH_3CN): *m*/*z* = 435.2223 $[M + H]^+$ (calcd for $C_{27}H_{26}BN_3O_2$ 435.2233).

5-(4-([2,2′:6′,2″-Terpyridin]-4′-yl)phenyl)-12-(2-((benzyloxy)methyl)pyrrolidin-1-yl)-2,9-dioctylanthra[*2,1,9-def:6,5,10-d′e′f′*]diisoquinoline-1,3,8,10(2*H*,9*H*)-tetraone (3). Monobromo-PDI **2** [5-(2-((benzyloxy)methyl)pyrrolidin-1-yl)-12-bromo-2,9-dioctylanthra[2,1,9-def:6,5,10-d′e′f′]diisoquinoline-1,3,8,10(2*H*,9*H*)-tetraone][18] (110 mg, 0.12 mmol), compound **1** (60 mg, 0.14 mmol), tetrabutylammonium chloride (7 mg, 0.025 mmol) and Pd(dppf)Cl_2·CH_2Cl_2 (10 mg, 0.012 mmol) were dissolved in a two-phase mixture of toluene (5 mL) and 1 M K_2CO_3 (aq.) (5 mL). The reaction mixture was stirred at 90 °C for 19 h. The organic phase was separated and washed with water (2 × 40 mL). The aqueous phase was extracted with toluene (2 × 10 mL) and the organic layers were combined and evaporated under reduced pressure. The product was purified on a Combiflash chromatograph using an alumina column (12 g) eluting with a $CHCl_3$–hexane gradient (flow rate: 30 mL min^{-1}; $CHCl_3$–hexane 1 : 1 (6 min)). Product **3** was crystallized on a watch glass and obtained as a dark green solid (108 mg, 78%). UV-vis λ_{max} ($CHCl_3$)/nm 284 (ε/dm^3 mol^{-1} cm^{-1} 54 740), 442 (9800) and 662 (23 120). δ_H (300 MHz; $CDCl_3$; Me_4Si): 0.81–0.93 (6H, m, 22-H), 1.18–1.54 (20H, m, 17–21-H), 1.65–1.86 (4H, m, 16-H), 1.95–2.15 (2H, m, b-H), 2.16–2.41 (2H, m, c-H), 3.43–3.77 (2H, m, a-H), 3.77–4.11 (2H, m, e-H), 4.12–4.30 (4H, m, 15-H), 4.59–4.69 (2H, m, f-H), 4.69–4.80 (1H, m, d-H), 7.32–7.41 (7H, m, 5″-H, g-H), 7.80 (1H, d, *J* 8.5, 13-H), 7.82–7.95 (5H, m, 4″-H, phenylene-H), 8.00 (2H, d, *J* 8.2, 6-H, phenylene-H), 8.39–8.48 (1H, m, 14-H), 8.62–8.67 (2H, m, 7-H, 11-H), 8.70 (2H, d, *J* 7.9, 3″-H), 8.73–8.77 (2H, m, 6″-H), 8.80 (2H, s, 3′-H), 8.83 (1H, s, 4-H). MS (ESI-TOF, CH_3CN): *m*/*z* = 1111.5450 $[M + H]^+$ (calcd for $C_{73}H_{70}N_6O_5$ 1111.5486).

5-(4-([2,2′:6′,2″-Terpyridin]-4′-yl)phenyl)-12-(2-(hydroxymethyl)-pyrrolidin-1-yl)-2,9-dioctylanthra[*2,1,9-def:6,5,10-d′e′f′*]diisoquinoline-1,3,8,10(2*H*,9*H*)-tetraone (4). Compound **3** (98 mg, 0.09 mmol) was dissolved in dry CH_2Cl_2 (5 mL) and stirred in an ice bath under a drying tube for 1 h. BBr_3 (1 M solution in CH_2Cl_2; 105 μL, 0.105 mmol) was added in five different portions with an interval of 30 min. The progress of the reaction was closely monitored by TLC analysis. After complete consumption of the starting material (4 h), the reaction was quenched by the addition of MeOH (10 mL). The reaction mixture was washed with water (3 × 40 mL) and the organic phase was evaporated under reduced pressure. The crude product was purified on a Combiflash chromatograph using an alumina column (12 g) eluting with $CHCl_3$ (flow rate: 30 mL min^{-1}). Product **4** was isolated as a dark green solid (87 mg, 97%). δ_H (300 MHz; $CDCl_3$; Me_4Si): 0.78–0.94 (6H, m, 22-H), 1.17–1.52 (20H, m, 17–21-H), 1.69–1.82 (4H, m, 16-H), 1.83–2.06 (2H, m, b-H), 2.06–2.42 (2H, m, c-H), 2.89 (1H, br s, OH), 3.42–3.68 (2H, m, a-H), 3.78–4.08 (2H, m, e-H), 4.09–4.32 (4H, m, 15-H), 4.47–4.66 (1H, m, d-H), 7.32–7.41 (2H, m, 5″-H), 7.54 (1H, d, *J* 7.9, 13-H), 7.62–7.71 (2H, m, phenylene-H), 7.85–7.94 (3H, m, 4″-H, phenylene-H), 7.99 (2H, d, *J* 8.2, 6-H, phenylene-H), 8.33–8.39 (1H, m, 7-H), 8.48 (1H, s, 11-H), 8.54 (1H, d, *J* 7.9, 14-H), 8.65–8.70 (2H, m, 3″-H), 8.70–8.75 (2H, m, 6″-H), 8.77 (2H, s, 3′-H), 8.81 (1H, s, 4-H). MS (ESI-TOF, CH_3CN): *m*/*z* = 1021.5068 $[M + H]^+$ (calcd for $C_{66}H_{64}N_6O_5$ 1021.5016).

(1-(12-(4-([2,2′:6′,2″-Terpyridin]-4′-yl)phenyl)-2,9-dioctyl-1,3,8,10-tetraoxo-1,2,3,8,9,10-hexahydroanthra[*2,1,9-def:6,5,10-d′e′f′*]diisoquinolin-5-yl)pyrrolidin-2-yl)methyl but-3-enoate (5). Compound **4** (75 mg, 0.073 mmol) was dissolved in CH_2Cl_2 (5 mL). DCC (30 mg, 0.15 mmol), DMAP (4 mg, 0.03 mmol) and 3-butenoic acid (12.5 μL, 0.15 mmol) were added to the solution, and the mixture was stirred at room temperature for 3.5 h. The solvent was evaporated under reduced pressure. The crude product was dissolved in a few milliliters of EtOAc, the flask was frozen under cold water and filtered through a cotton plug. This procedure was done twice. The product was purified on a Combiflash chromatograph using an alumina column (12 g) eluting with $CHCl_3$ (flow rate: 30 mL min^{-1}) and a second purification using a $CHCl_3$–CH_2Cl_2 gradient ($CHCl_3$–CH_2Cl_2 1 : 1 to $CHCl_3$ (6 min)). Product **5** was crystallized on a watch glass and obtained as a dark green solid (64 mg, 80%). UV-vis λ_{max} ($CHCl_3$)/nm 283 (ε/dm^3 mol^{-1} cm^{-1} 53 130), 412 (9870) and 647 (24 310). δ_H (300 MHz; $CDCl_3$; Me_4Si): 0.80–0.94 (6H, m, 22-H), 1.19–1.52 (20H, m, 17–21-H), 1.62–1.85 (4H, m, 16-H), 1.86–2.11 (2H, m, b-H), 2.12–2.46 (2H, m, c-H), 3.22 (2H, d, *J* 6.7, $COCH_2$), 3.40–3.75 (2H, m, a-H), 4.06–4.33 (4H, m, 15-H), 4.48–4.66 (2H, m, e-H), 5.14–5.28 (2H, m, CH═CH_2), 5.86–6.05 (1H, m, C*H*═CH_2), 4.75 (1H, br s, d-H), 7.32–7.41 (2H, m, 5″-H), 7.77–7.84 (1H, m, phenylene-H), 7.85–7.93 (5H, m, 4″-H, 13-H, phenylene-H), 7.98 (2H, d, *J* 8.2, 6-H, phenylene-H), 8.50–8.71 (5H, m, 3″-H, 7-H, 11-H, 14-H), 8.71–8.76 (2H, m, 6″-H), 8.78 (2H, s, 3′-H), 8.81 (1H, s, 4-H). MS (ESI-TOF, CH_3CN): *m*/*z* = 1088.5270 $[M]^+$ (calcd for $C_{70}H_{68}N_6O_6$ 1088.5200).

(1-(12-(4-([2,2′:6′,2″-Terpyridin]-4′-yl)phenyl)-2,9-dioctyl-1,3,8,10-tetraoxo-1,2,3,8,9,10-hexahydroanthra[*2,1,9-def:6,5,10-d′e′f′*]diisoquinolin-5-yl)pyrrolidin-2-yl)methyl 4-(triethoxysilyl)-butanoate (6). All the glassware was dried in an oven (150 °C, 2 h) before use. The reaction flask was sealed with a septum, placed on an ice bath, and kept under constant argon flow. Compound **5** (15 mg, 0.014 mmol) was dissolved in distilled toluene (1 mL) and added to the flask. Triethoxysilane (0.46 mL, 2.5 mmol) and Karstedt catalyst (platinum(0)-1,3-divinyl-1,1,3,3-tetramethyldisiloxane complex solution (Pt ~2%) in xylene; 17.2 μL, 2.07 μmol) were added, and the mixture was stirred in the cold under argon. After 10 min, argon was removed and after 1 h the stirring was continued at room temperature for 3 h more. The crude product was evaporated under reduced pressure using a mechanical vacuum pump. Purification was done on a Combiflash chromatograph using an alumina column (12 g, purged with argon) eluting with a $CHCl_3$–EtOH gradient (flow rate: 30 mL min^{-1}; $CHCl_3$ (0.5 min), $CHCl_3$–EtOH 10 : 1 (2 min)). Product **6** was obtained as a dark green solid (13 mg, 76%). δ_H (300 MHz; $CDCl_3$; Me_4Si): 0.51–0.71 (2H, m, $COC_2H_4CH_2Si$), 0.82–0.92 (6H, m, 22-H), 1.13–1.49 (29H, m, 17–21-H, $Si(OCH_2CH_3)_3$), 1.65–1.86 (6H, m, 16-H, $COCH_2CH_2CH_2Si$), 1.88–2.31 (4H, m, c-H, b-H), 2.33–2.53 (2H, m, $COCH_2C_2H_4Si$), 3.64–3.91 (8H, m, $Si(OCH_2CH_3)_3$, a-H), 4.11–4.31 (4H, m, 15-H), 4.41–4.64 (2H, m, e-H), 4.77 (1H, br s, d-H), 7.34–7.41 (2H, m, 5″-H), 7.78–7.83 (1H, m, phenylene-H), 7.85–7.98 (5H, m, 4″-H, 13-H, phenylene-H), 8.03 (2H, d, *J* 8.2, 6-H, phenylene-H), 8.52–8.72 (5H, m, 3″-H, 7-H, 11-H, 14-H), 8.72–8.77 (2H, m, 6″-H), 8.80 (2H, s, 3′-H), 8.83 (1H, s, 4-H). MS (ESI-TOF, CH_3CN): *m*/*z* = 1253.6212 $[M + H]^+$ (calcd for $C_{76}H_{84}N_6O_9Si$ 1253.6147).

5,12-Bis(4-([2,2′:6′,2″-terpyridin]-4′-yl)phenyl)-2,9-dioctylanthra[*2,1,9-def:6,5,10-d′e′f′*]diisoquinoline-1,3,8,10(2*H*,9*H*)-tetraone (8). 1,7-Dibromo-PDI **7** [5,12-dibromo-2,9-dioctylanthra[*2,1,9-def:6,5,10-d′e′f′*]diisoquinoline-1,3,8,10(2*H*,9*H*)-tetraone][11,19] (50 mg, 0.06 mmol), compound **1** (62 mg, 0.14 mmol), tetrabutylammonium chloride (4 mg, 0.013 mmol) and $Pd(dppf)Cl_2{\cdot}CH_2Cl_2$ (11 mg, 0.013 mmol) were dissolved in a two-phase mixture of toluene (5 mL) and 1 M K_2CO_3 (aq.) (5 mL). The reaction mixture was stirred at 90 °C for 18 h. The organic phase was separated and washed with water (2 × 30 mL). The aqueous phase was extracted with toluene (2 × 10 mL) and the organic layers were combined and evaporated under reduced pressure. The product was purified on a preparative TLC plate (aluminium oxide), eluent CH_2Cl_2–$CHCl_3$ 2 : 1. Product **8** was obtained as the second fraction (R_f = 0.4 in CH_2Cl_2–$CHCl_3$ 2 : 1) as a dark red solid (19 mg, 23%). UV-vis λ_{max} ($CHCl_3$)/nm 284 (ε/dm^3 mol^{-1} cm^{-1} 67 790) and 556 (25 610). δ_H (300 MHz; $CDCl_3$; Me_4Si): 0.78–0.95 (6H, m, 22-H), 1.16–1.50 (20H, m, 17–21-H), 1.65–1.85 (4H, m, 16-H), 4.02–4.29 (4H, m, 15-H), 7.33–7.45 (4H, m, 5″-H), 7.62 (2H, d, *J* 7.3, phenylene-H), 7.74 (2H, d, *J* 7.3, phenylene-H), 7.86–7.98 (6H, m, 4″-H, 6-H, 13-H), 8.01–8.11 (4H, m, phenylene-H), 8.15–8.26 (2H, m, 7-H, 14-H), 8.65–8.79 (10H, m, 3″-H, 6″-H, 4-H, 11-H), 8.80–8.87 (4H, m, 3′-H). MS (ESI-TOF, $CHCl_3$–MeOH 10 : 15): *m*/*z* = 1229.5481 $[M + H]^+$ (calcd for $C_{82}H_{68}N_8O_4$ 1229.5442).

(1-(2,9-Dioctyl-1,3,8,10-tetraoxo-12-(pyrrolidin-1-yl)-1,2,3,8,9,10-hexahydroanthra[*2,1,9-def:6,5,10-d′e′f′*]diisoquinolin-5-yl)pyrrolidin-2-yl)methyl but-3-enoate (10). Pyrrolidine-PDI **9** [5-(2-(hydroxymethyl)pyrrolidin-1-yl)-2,9-dioctyl-12-(pyrrolidin-1-yl)-anthra[*2,1,9-def:6,5,10-d′e′f′*]diisoquinoline-1,3,8,10(2*H*,9*H*)-tetraone][18] (30 mg, 0.04 mmol) was dissolved in CH_2Cl_2 (5 mL). DCC (16 mg, 0.08 mmol), DMAP (2 mg, 0.015 mmol) and 3-butenoic acid (6.5 μL, 0.08 mmol) were added to the solution, and the mixture was stirred at room temperature for 20 h. The solvent was evaporated under reduced pressure. The crude product was dissolved in a few milliliters of EtOAc, the flask was frozen under cold water and filtered through a cotton plug. This procedure was done twice. The product was purified by column chromatography on Silica 60, eluting with $CHCl_3$. Product **10** was obtained as a dark green solid (32 mg, 99%). UV-vis λ_{max} ($CHCl_3$)/nm 272 (ε/dm^3 mol^{-1} cm^{-1} 17 040), 434 (11 230) and 696 (26 120). δ_H (300 MHz; $CDCl_3$; Me_4Si): 0.77–0.90 (6H, m, 22-H), 1.15–1.48 (20H, m, 17–21-H), 1.59–1.78 (4H, m, 16-H), 1.88–2.37 (8H, m, c-H, b-H, i-H, j-H), 3.19 (2H, d, *J* 6.2, $COCH_2$), 3.48–3.98 (6H, m, a-H, h-H, k-H), 4.17 (4H, t, *J* 7.3, 15-H), 4.41–4.69 (3H, m, d-H, e-H), 5.07–5.25 (2H, m, $CH{=}CH_2$), 5.80–6.03 (1H, m, $CH{=}CH_2$), 7.44–7.57 (1H, m, 13-H), 8.10 (1H, d, *J* 8.2, 6-*H*), 8.16–8.44 (3H, m, 4-H, 7-H, 14-H), 8.58 (1H, s, 11-H). MS (ESI-TOF, $CHCl_3$–MeOH 10 : 15): *m*/*z* = 850.4658 $[M]^+$ (calcd for $C_{53}H_{62}N_4O_6$ 850.4669).

(1-(2,9-Dioctyl-1,3,8,10-tetraoxo-12-(pyrrolidin-1-yl)-1,2,3,8,9,10-hexahydroanthra[*2,1,9-def:6,5,10-d′e′f′*]diisoquinolin-5-yl)pyrrolidin-2-yl)methyl 4-(triethoxysilyl)butanoate (11). All the glassware was dried in an oven (150 °C, 2 h) before use. The reaction flask was sealed with a septum, placed on an ice bath, and kept under constant argon flow. Compound **10** (15 mg, 0.018 mmol) was dissolved in distilled toluene (1 mL) and added to the flask. Triethoxysilane (0.46 mL, 2.5 mmol) and Karstedt catalyst (platinum(0)-1,3-divinyl-1,1,3,3-tetramethyldisiloxane complex solution (Pt ~2%) in xylene; 7.3 μL, 0.88 μmol) were added, and the mixture was stirred in the cold under argon. After 10 min, the stirring was continued at room temperature without constant argon flow for 2 h. The crude product was evaporated under reduced pressure using a mechanical vacuum pump. Purification was done on a Combiflash chromatograph using an alumina column (12 g, purged with argon) eluting with a $CHCl_3$–EtOH gradient (flow rate: 30 mL min^{-1}; $CHCl_3$ (0.5 min), $CHCl_3$–EtOH 20 : 1 (2 min)). Product **11** was obtained as a dark green solid (10 mg, 56%). δ_H (300 MHz; $CDCl_3$; Me_4Si): 0.51–0.72 (2H, m, $COC_2H_4CH_2Si$), 0.81–0.92 (6H, m, 22-H), 1.12–1.50 (29H, m, 17–21-H, $Si(OCH_2CH_3)_3$), 1.65–1.84 (6H, m, 16-H, $COCH_2CH_2CH_2Si$), 1.86–2.41 (8H, m, c-H, b-H, i-H, j-H), 2.41–2.58 (2H, m, $COCH_2C_2H_4Si$), 3.53–3.96 (12H, m, $Si(OCH_2CH_3)_3$, a-H, h-H, k-H), 4.21 (4H, t, *J* 7.5, 15-H), 4.36–4.77 (3H, m, d-H, e-H), 7.66 (1H, d, *J* 7.9, 13-H), 8.12–8.27 (1H, m, 6-H), 8.31–8.55 (3H, m, 4-H, 7-H, 14-H), 8.59–8.72 (1H, m, 11-H). MS (ESI-TOF, CH_3CN): *m*/*z* = 1014.5597 $[M]^+$ (calcd for $C_{59}H_{78}N_4O_9Si$ 1014.5538).

Complexes

$Zn(OTf)_2$ solution: zinc(II) trifluoromethanesulfonate (36 mg, 0.1 mmol) was dissolved in $CHCl_3$–CH_3CN 4 : 1 (10 mL) by sonication.

Complex Zn-3. Compound **3** (10 mg, 0.009 mmol) was dissolved in $CHCl_3$–CH_3CN 4 : 1 (5 mL), and a $Zn(OTf)_2$ solution (0.9 mL, 0.009 mmol) was added. The reaction mixture was stirred at room temperature for 1 h. The solvent was evaporated under reduced pressure. Product **Zn-3** was obtained as a dark green solid with quantitative yield (13 mg). UV-vis λ_{max} ($CHCl_3$)/nm 288 (ε/dm^3 mol^{-1} cm^{-1} 49 120), 397 (13 250), 438 (11 950) and 663 (21 460). δ_H (300 MHz; $CDCl_3$; Me_4Si): 0.76–0.95 (6H, m, 22-H), 1.19–1.51 (20H, m, 17–21-H), 1.63–1.83 (4H, m, 16-*H*), 1.95–2.08 (2H, m, b-H), 2.12–2.38 (2H, m, c-H), 3.41–3.69 (2H, m, a-H), 3.74–4.10 (2H, m, e-H), 4.10–4.33 (4H, m, 15-H), 4.55–4.82 (3H, m, d-H, f-H), 7.28–7.50 (5H, m, g-H), 7.62–7.73 (2H, m, 13-H, phenylene-H), 7.74–7.82 (2H, m, 5″-H), 7.83–7.98 (2H, m, 6-H, phenylene-H), 8.07–8.29 (4H, m, 4″-H, phenylene-H), 8.35–8.49 (2H, m, 7-H, 14-H), 8.51–8.64 (4H, m, 3′-H, 3″-H, 4-H, 11-H), 8.72–8.81 (1H, m, 3″-H), 8.83–8.92 (2H, m, 6″-H), 8.96–9.05 (1H, m, 3′-H). MS (ESI-TOF, CH_3CN): m/z = 1323.4382 $[M - OTf]^+$ (calcd for $C_{74}H_{70}F_3N_6O_8SZn$ 1323.4220).

Complex 3-Zn-3a. Compound **3** (10 mg, 0.009 mmol) was dissolved in $CHCl_3$–CH_3CN 4 : 1 (5 mL), and complex **Zn-3** (13 mg, 0.009 mmol) was added. The reaction mixture was stirred at room temperature for 1 h. The solvent was evaporated under reduced pressure. Product **3-Zn-3a** was obtained as a dark green solid with quantitative yield (23 mg). UV-vis λ_{max} ($CHCl_3$)/nm 288 (ε/dm^3 mol^{-1} cm^{-1} 85 990), 402 (25 290), 439 (23 650) and 666 (40 230). δ_H (300 MHz; $CDCl_3$; Me_4Si): 0.75–0.92 (12H, m, 22-H), 1.17–1.50 (40H, m, 17–21-H), 1.61–1.82 (8H, m, 16-H), 1.91–2.07 (4H, m, b-H), 2.10–2.38 (4H, m, c-H), 3.38–3.67 (4H, m, a-H), 3.72–4.35 (12H, m, 15-H, e-H), 4.53–4.83 (6H, m, d-H, f-H), 7.30–7.51 (14H, m, 5″-H, g-H), 7.54–7.71 (4H, m, 13-H, phenylene-H), 7.77–7.98 (8H, m, 6-H, 6″-H, phenylene-H), 8.00–8.20 (8H, m, 4″-H, phenylene-H), 8.29–8.45 (4H, m, 7-H, 14-H), 8.46–8.64 (4H, m, 4-H, 11-H), 8.71–8.85 (4H, m, 3″-H), 8.94–9.08 (4H, m, 3′-H). MS (ESI-TOF, CH_3CN): m/z = 2433.9680 $[M - OTf]^+$ (calcd for $C_{147}H_{140}F_3N_{12}O_{13}SZn$ 2433.9626).

Complex 3-Zn-3b. Compound **3** (10 mg, 0.009 mmol) was dissolved in $CHCl_3$–CH_3CN 4 : 1 (5 mL), and a $Zn(OTf)_2$ solution (0.45 mL, 0.0045 mmol) was added. The reaction mixture was stirred at room temperature for 1 h. The solvent was evaporated under reduced pressure. Product **3-Zn-3b** was obtained as a dark green solid with quantitative yield (12 mg). UV-vis λ_{max} ($CHCl_3$)/nm 288 (ε/dm^3 mol^{-1} cm^{-1} 89 130), 403 (26 730), 442 (24 770) and 666 (41 100). δ_H (300 MHz; $CDCl_3$; Me_4Si): 0.77–0.90 (12H, m, 22-H), 1.16–1.50 (40H, m, 17–21-H), 1.62–1.83 (8H, m, 16-H), 1.94–2.08 (4H, m, b-H), 2.11–2.39 (4H, m, c-H), 3.40–3.68 (4H, m, a-H), 3.73–4.30 (12H, m, 15-H, e-H), 4.54–4.80 (6H, m, d-H, f-H), 7.28–7.51 (14H, m, 5″-H, g-H), 7.58–7.73 (4H, m, 13-H, phenylene-H), 7.79–8.00 (8H, m, 6-H, 6″-H, phenylene-H), 8.01–8.24 (8H, m, 4″-H, phenylene-H), 8.33–8.46 (4H, m, 7-H, 14-H), 8.50–8.64 (4H, m, 4-H, 11-H), 8.72–8.83 (4H, m, 3″-H), 8.96–9.07 (4H, m, 3′-H). MS (ESI-TOF, CH_3CN): m/z = 2433.9766 $[M - OTf]^+$ (calcd for $C_{147}H_{140}F_3N_{12}O_{13}SZn$ 2433.9626).

Complex Zn-8. Compound **8** (10 mg, 0.008 mmol) was dissolved in $CHCl_3$–CH_3CN 4 : 1 (5 mL), and a $Zn(OTf)_2$ solution (1.6 mL, 0.016 mmol) was added. The reaction mixture was stirred at room temperature for 1 h. The solvent was evaporated under reduced pressure. Product **Zn-8** was obtained as a dark red solid with quantitative yield (16 mg). UV-vis λ_{max} ($CHCl_3$)/nm 288 (ε/dm^3 mol^{-1} cm^{-1} 47 680), 338 (28 780) and 553 (13 980). δ_H (300 MHz; $CDCl_3$; Me_4Si): 0.84–0.92 (6H, m, 22-H), 1.25–1.48 (20H, m, 17–21-H), 1.70–1.88 (4H, m, 16-H), 3.97–4.36 (4H, m, 15-H), 7.70–7.89 (5H, m, phenylene-H), 7.92–8.03 (5H, m, 5″-H, phenylene-H), 8.18–8.49 (12H, m, 4″-H, 4-H, 6-H, 7-H, 11-H, 13-H, 14-H, phenylene-H), 8.88–9.02 (8H, m, 3″-H, 6″-H), 9.11 (4H, s, 3′-H). MS (ESI-TOF, CH_3CN): m/z = 1803.2660 $[M - OTf]^+$ (calcd for $C_{85}H_{68}F_9N_8O_{13}S_3Zn_2$ 1803.2507).

Complex 3-Zn-8. Complex **Zn-8** (16 mg, 0.008 mmol) and compound **3** (20 mg, 0.018 mmol) were dissolved in DMF (7 mL). The reaction mixture was stirred at room temperature for 2 h. The solvent was evaporated under reduced pressure using a mechanical vacuum pump. Product **3-Zn-8** was obtained as a dark green solid with quantitative yield (34 mg). UV-vis λ_{max} ($CHCl_3$)/nm 288 (ε/dm^3 mol^{-1} cm^{-1} 118 050), 389 (42 710), 439 (31 690) and 666 (48 620). δ_H (300 MHz; $CDCl_3$; Me_4Si): 0.76–0.95 (18H, m, 22-H), 1.15–1.52 (60H, m, 17–21-H), 1.62–1.83 (12H, m, 16-H), 1.93–2.08 (4H, m, b-H), 2.13–2.30 (4H, m, c-H), 3.41–3.68 (4H, m, a-H), 3.76–4.37 (16H, m, 15-H, e-H), 4.55–4.86 (6H, m, d-H, f-H), 7.29–7.51 (17H, m), 7.54–7.80 (11H, m), 7.82–8.00 (11H, m), 8.02–8.28 (15H, m), 8.31–8.67 (15H, m), 8.70–8.94 (9H, m), 8.96–9.27 (6H, m). MS (ESI-TOF, CH_3CN): m/z = 1937.6973 $[M - 2(OTf)]^{2+}$ (calcd for $C_{230}H_{206}F_6N_{20}O_{20}S_2Zn_2$ 1937.6901).

Immobilization and complexation

Quartz plates were cleaned according to a process reported earlier.[4] The reaction vessel was cooled down after heating in an oven (2 h, 150 °C). Siloxane compound (**6**, **11**) (2 mg) was dissolved in distilled toluene (20 mL) and loaded in the reaction vessel under argon. Isopropyl amine (0.4 mL) was added and the cleaned plates were immersed in the solution. The reaction vessel was filled with argon and heated at 105 °C for 2 h. After an appropriate time the plates were sonicated twice in toluene and once in CH_2Cl_2, 15 s in each solvent, and the samples were dried under argon flow (30 min).

Complexation of the SAM of tpy-PDI **6** was done by immersing the samples into solutions of the corresponding metal ions. *Zn-solution*: zinc(II) trifluoromethanesulfonate (36 mg, 0.1 mmol) was dissolved in $CHCl_3$–CH_3CN 4 : 1 (10 mL) by sonication. For complexation the stock solution (3.6 mL) was diluted with $CHCl_3$–CH_3CN 4 : 1 (20 mL). The plates with SAMs were immersed in the salt solution and kept there for 1 h.

After an appropriate time, the plates were washed with $CHCl_3$–CH_3CN 4 : 1, and the samples were dried under argon flow.

Conclusions

We have synthesized PDIs with terpyridine groups and silane anchors at the *bay*-region. Both of these groups are rarely found in this position of PDIs. Supramolecular dimer and trimer structures were constructed from the monomers *via* the terpyridine moieties and zinc ions. A trimer complex showed efficient energy transfer from the middle PDI to the side PDIs. The silane-containing PDIs were attached on the quartz substrate and coordination of zinc was also done on the surface. Formation of the complex was observed clearly in steady-state absorption measurements. The molecular films were not obtained as perfect monolayers, but demonstrate the potential to construct supramolecular assemblies of PDI directly on a solid substrate. This implies that attention should be paid to the surface–PDI tether, and these studies are currently under way.

Acknowledgements

The Graduate School of Tampere University of Technology and the Academy of Finland are greatly acknowledged for financial support.

Notes and references

1 A. Ulman, *Chem. Rev.*, 1996, **96**, 1533; E. Sariola, A. Kotiaho, N. V. Tkachenko, H. Lemmetyinen and A. Efimov, *J. Porphyrins Phthalocyanines*, 2010, **14**, 397.
2 J. Sagiv, *J. Am. Chem. Soc.*, 1980, **102**, 92; Y. Yang, A. M. Bittner, S. Baldelli and K. Kern, *Thin Solid Films*, 2008, **516**, 3948.
3 C. Baik, D. Kim, M.-S. Kang, S. O. Kang, J. Ko, M. K. Nazeeruddin and M. Grätzel, *J. Photochem. Photobiol., A*, 2009, **201**, 168.
4 E. Sariola-Leikas, M. Hietala, A. Veselov, O. Okhotnikov, S. L. Semjonov, N. V. Tkachenko, H. Lemmetyinen and A. Efimov, *J. Colloid Interface Sci.*, 2012, **369**, 58.
5 M. Chiper, R. Hoogenboom and U. S. Schubert, *Macromol. Rapid Commun.*, 2009, **30**, 565; A. Winter, S. Hoeppener, G. R. Newkome and U. S. Schubert, *Adv. Mater.*, 2011, **23**, 3484.
6 Y.-Y. Chen, Y.-T. Tao and H.-C. Lin, *Macromolecules*, 2006, **39**, 8559.
7 A. R. Rabindranath, A. Maier, M. Schäfer and B. Tieke, *Macromol. Chem. Phys.*, 2009, **210**, 659.
8 T.-Y. Dong, M.-C. Lin, M. Y.-N. Chiang and J.-Y. Wu, *Organometallics*, 2004, **23**, 3921; H. Wolpher, S. Sinha, J. Pan, A. Johansson, M. J. Lundqvist, P. Persson, R. Lomoth, J. Bergquist, L. Sun, V. Sundström, B. Åkermark and T. Polívka, *Inorg. Chem.*, 2007, **46**, 638.
9 H. Hofmeier, J. Pahnke, C. H. Weidl and U. S. Schubert, *Biomacromolecules*, 2004, **5**, 2055; P. D. Vellis, J. A. Mikroyannidis, C.-N. Lo and C.-S. Hsu, *J. Polym. Sci., Part A: Polym. Chem.*, 2008, **46**, 7702; K. W. Cheng, C. S. C. Mak, W. K. Chan, A. M. C. Ng and A. B. Djurišić, *J. Polym. Sci., Part A: Polym. Chem.*, 2008, **46**, 1305.
10 F. Würthner, *Chem. Commun.*, 2004, 1564; C. Huang, S. Barlow and S. R. Marder, *J. Org. Chem.*, 2011, **76**, 2386.
11 F. Würthner, V. Stepanenko, Z. Chen, C. R. Saha-Möller, N. Kocher and D. Stalke, *J. Org. Chem.*, 2004, **69**, 7933.
12 D. Wang, Y. Shi, C. Zhao, B. Liang and X. Li, *J. Mol. Struct.*, 2009, **938**, 245; M. Queste, C. Cadiou, B. Pagoaga, L. Giraudet and N. Hoffmann, *New J. Chem.*, 2010, **34**, 2537; V. L. Gunderson, E. Krieg, M. T. Vagnini, M. A. Iron, B. Rybtchinski and M. R. Wasielewski, *J. Phys. Chem. B*, 2011, **115**, 7533; S. Dey, A. Efimov and H. Lemmetyinen, *Eur. J. Org. Chem.*, 2012, 2367.
13 R. Dobrawa, M. Lysetska, P. Ballester, M. Grüne and F. Würthner, *Macromolecules*, 2005, **38**, 1315.
14 V. Stepanenko, M. Stocker, P. Müller, M. Büchner and F. Würthner, *J. Mater. Chem.*, 2009, **19**, 6816; M. T. Rawls, J. Johnson and B. A. Gregg, *J. Electroanal. Chem.*, 2010, **650**, 10.
15 G. Golubkov, H. Weissman, E. Shirman, S. G. Wolf, I. Pinkas and B. Rybtchinski, *Angew. Chem., Int. Ed.*, 2009, **48**, 926.
16 T. van der Boom, G. Evmenenko, P. Dutta and M. R. Wasielewski, *Chem. Mater.*, 2003, **15**, 4068; N. Mizoshita, T. Tani and S. Inagaki, *Adv. Funct. Mater.*, 2011, **21**, 3291; H. Rathnayake, J. Binion, A. McKee, D. J. Scardino and N. I. Hammer, *Nanoscale*, 2012, **4**, 4631; N. Mizoshita, T. Tani and S. Inagaki, *Adv. Mater.*, 2012, **24**, 3350.
17 N. Tuccitto, I. Delfanti, V. Torrisi, F. Scandola, C. Chiorboli, V. Stepanenko, F. Würthner and A. Licciardello, *Phys. Chem. Chem. Phys.*, 2009, **11**, 4033; M. L. Hassan, C. M. Moorefield, H. S. Elbatal, G. R. Newkome, D. A. Modarelli and N. C. Romano, *Mater. Sci. Eng., B*, 2012, **177**, 350.
18 R. K. Dubey, M. Niemi, K. Kaunisto, A. Efimov, N. V. Tkachenko and H. Lemmetyinen, *Chem.–Eur. J.*, 2013, **19**, 6791.
19 R. K. Dubey, A. Efimov and H. Lemmetyinen, *Chem. Mater.*, 2011, **23**, 778.
20 A. L. Bramblett, M. S. Boeckl, K. D. Hauch, B. D. Ratner, T. Sasaki and J. W. Rogers Jr., *Surf. Interface Anal.*, 2002, **33**, 506.
21 M. Vrábel, M. Hocek, L. Havran, M. Fojta, I. Votruba, B. Klepetářová, R. Pohl, L. Rulíšek, L. Zendlová, P. Hobza, I.-H. Shih, E. Mabery and R. Mackman, *Eur. J. Org. Chem.*, 2007, 1752.

Paper IV

Color bricks: building of highly organized and strongly absorbing multi-component arrays of terpyridyl-perylenes on metal oxide surfaces

Essi Sariola-Leikas, Zafar Ahmed, Paola Vivo, Anniina Ojanperä, Kimmo Lahtonen, Jesse Saari, Mika Valden, Helge Lemmetyinen and Alexander Efimov

Chem. Eur. J. **2015**, submitted

Tampereen teknillinen yliopisto
PL 527
33101 Tampere

Tampere University of Technology
P.O.B. 527
FI-33101 Tampere, Finland

ISBN 978-952-15-3600-7
ISSN 1459-2045